CHALMERS

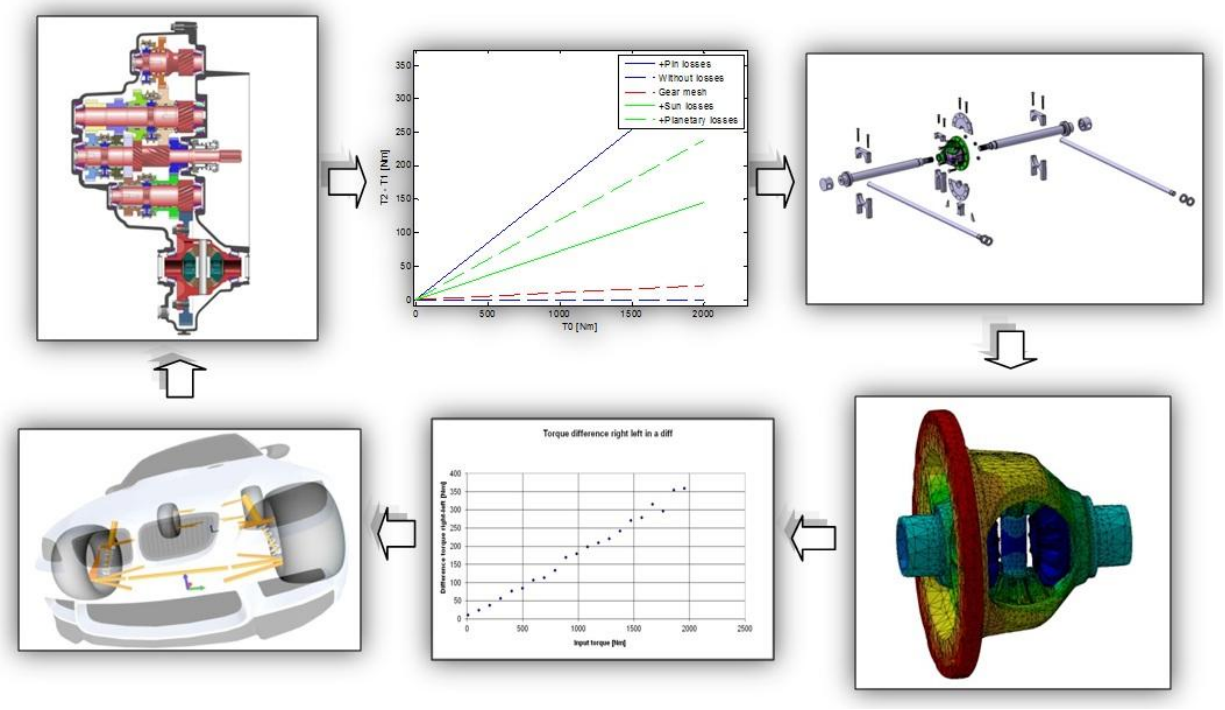

Torque split between left and right drive shaft over a front wheel drive differential

Mechanical and Automotive Engineering

Master's Thesis in the Mechanical and Automotive Engineering Msc

MARC OLLÉ BERNADES

Department of Applied Mechanics
Division of Vehicle Dynamics and Autonomous Systems
Vehicle Dynamics Group
CHALMERS UNIVERSITY OF TECHNOLOGY
Göteborg, Sweden 2012
Master's thesis 2012:21

MASTER'S THESIS IN VEHICLE DYNAMICS AND AUTONOMOUS SYSTEMS

Torque split between left and right drive shaft over a front wheel drive differential

MARC OLLÉ BERNADES

Department of Applied Mechanics
Vehicle Dynamics and Autonomous Systems
Vehicle Dynamics Group
CHALMERS UNIVERSITY OF TECHNOLOGY
Göteborg, Sweden 2012

Torque split between left and right drive shaft over a front wheel drive differential
MARC OLLÉ BERNADES

© MARC OLLÉ BERNADES 2012

Master's Thesis 2012:21
ISSN 1652-8557
Department of Applied Mechanics
Division of Vehicle Dynamics and Autonomous Systems
Vehicle Dynamics Group
Chalmers University of Technology
SE-412 96 Göteborg
Sweden
Telephone: + 46 (0)31-772 1000

Cover:
There is shown a brief representation, starting from the differential design, of all the steps that are followed (Modelling, Rig design, FEM analysis, Rig Test and Dynamic simulations) during this Thesis Work.

Chalmers University of Technology / Department of Applied Mechanics
Göteborg, Sweden 2012

Torque split between left and right drive shaft over a front wheel drive differential
Master's Thesis in Mechanical Engineering
MARC OLLÉ BERNADES
Department of Applied Mechanics
Division of Vehicle Dynamics and Autonomous system
Chalmers University of Technology

ABSTRACT

Steering feel and vehicle steering motion is affected by wheel torques from propulsion, especially for front wheel drive cars. Often these problems are referred to as "torque steer". Many systems interact to cause these problems: propulsion, steering and suspension.

Torque steer contributors are not only the differential (friction, self locking effect, Torsen differential), but also the input from the ground and car geometry such as road conditions (friction and surface), the vehicle state (cornering, rolling, acceleration) and weight distribution (loading). In addition, the suspension design contributes as well, like the suspension geometry (kingpin offset, camber, caster, tolerances), the tire quality (conicity, wear, profile) and wheel geometry (size, uniformity, wheel offset). Finally, regarding the transmission contributors, the engine (torque, alignment) and drive shafts (alignment, length, symmetry) are contributors as well.

Particularly, within the propulsion system, it is partly the asymmetry in differential and drive-shafts that could cause torque steer. In fact, the friction of the gear meshing and bearings, and mainly the contact with the housing (carrier) during slippery and static conditions or the housing stiffness itself might be causes of this torque steer problem.

Hence, the losses over the differential can explain the torque steer effect due to the torque difference between left and right driveshaft. This fact affects the behaviour of the vehicle.

This is the reason why Volvo Cars Corporation (VCC) is interested in studying the friction in a differential to use it in further simulations (vehicle dynamics purposes) or understand which parts of the design may be modified or changed in order to reduce or increase (depending on the goal, either getting as close as possible an open or a limited slip differential behaviour) the overall friction.

The motivation of the thesis work comes from this problem. The thesis derives a model for an open differential in order to qualify and quantify the difference of torque between left and right side.

In addition, to be able to test the differential, a rig is designed and machined outhouse. Moreover, during testing the model is updated and the parameters are changed according to the statistic experiment plan and the results from the FEM analysis carried out.

Finally, not only all the conclusions and results are written down, but also some vehicle dynamics simulations to show the effect of the differential in the behaviour of the car.

Contents

Preface

In this study, differential tests have been done in order to get a suitable model for the internal losses in a differential and to get knowledge of how much it might affect in the torque steer contribution. The tests have been carried out from January 2012 to June 2012. The work is a part of a research project concerning the difference of output torque between left and right drive shaft due to the losses in a bevel gear differential of a front wheel drive car. The project is carried out at the Department of Manual Transmission at Volvo Car Corporation, as well as the Department of Applied Mechanics, in Division of Vehicle Dynamics and Autonomous Systems, Chalmers University of Technology, Sweden. The project is mainly financed through Volvo Car Corporation.

This part of the project has been carried out with Marc Ollé Bernades as a researcher and Professor Bengt Jacobson as supervisor and examiner at Chalmers University of Technology. But also, Magnus Karlsson as a supervisor at Volvo Car Corporation. All tests have been carried out in the laboratory of the Department of Transmission at Volvo Car Corporation. My co-worker during FEM analysis, Christian Lönnqvist is highly appreciated for his help. I would also like to thank Mikel Törmänen, Raoul Rinaldo, Mikel Bigert and Jan Christian Holmström from VCC for their co-operation and involvement.

Finally, it should be noted that the tests could never have been conducted without the sense of high quality and professionalism of the laboratory and workshop staff, both Chalmers University of Technology and Volvo Car Corporation.

Göteborg June 2012

Marc Ollé Bernades

Notations

Notation	Unit	Description
Roman upper case letters		
B	*m*	Tooth length
C	*kN*	Dynamic load capacity of the bearing
C_w	$N/_{slip}$	Tire stiffness in both wheels expressed in unitary slip (slope of F_x/slip curve)
D	*m*	Rod diameter
E	*MPa*	Young modulus of the steel rod
F	*N*	Applied load in the rig
F_1	*N*	Reaction force between Pin and top housing (due to transmission torque)
F_{1w}	*N*	Longitudinal (traction) force in wheel 1
F_2	*N*	Reaction force between Pin and bottom housing (due to transmission torque)
F_{2w}	*N*	Longitudinal (traction) force in wheel 2
F_{fl}	*N*	Friction force due to the normal contact force Nfl
F_{fr}	*N*	Friction force due to the normal contact force N_{fr}
F_{max}	*N*	Maximum force on the arm (of the rig)
F_{Mmax}	*N*	Maximum mounting force of the bolt
F_{Mmin}	*N*	Maximum mounting force of the bolt limited by the lubrication and tool used.
F'_{Mmin}	*N*	Maximum mounting force once the sitting force has been taken into account
F_{pf1}	*N*	Friction force due to the normal contact force N_{pf1}
F_{n1}	*N*	Normal transmission force between left Sun (1) and Planetary teeth
F_{n2}	*N*	Normal transmission force between left Sun (2) and Planetary teeth
$F_{p'}$	*N*	Remaining force after removing the separation force
F_{p1}	*N*	Friction force due to the reaction R_1 between Pin and Planetary
F_s	*N*	Separation force
F_t	*N*	Tangential force on the housing due to the input torque (applied on the bolt pattern)
F_{t1}	*N*	Tangential transmission force between Sun 1 and Planetary teeth
F_{t2}	*N*	Tangential transmission force between Sun 1 and Planetary teeth
F_{yf}	*N*	Lateral force in front axle (vehicle simulation 2)
F_{yr}	*N*	Lateral force in rear axle (vehicle simulation 2)
G	N/mm^2	Modulus of rigidity

I_p	N/m^2	Inertia in the torsional axis
I_{zz}	N/m^2	Rod inertia along z-axis (longitudinal)
J	$kg \cdot m^2$	Inertia of the car in vehicle simulation 2
$K_{assembly}$	*Nm/rad*	Stiffness of the whole differential assembly
K_c	*N/mm*	Stiffness of the bolt
$K_{housing}$	*Nm/rad*	Stiffness of the housing
$K_{gear\ set}$	*Nm/rad*	Stiffness of the gear set
K_p	*N/mm*	Stiffness of the clamping part
L	*m*	Distance between welding and bearing support on the drive shaft
L	*m*	Distance between front and rear axle of the car in vehicle simulation 2
L’	*m*	Rod length after deformation
L_1	*m*	Distance between welding support and bearing
L_2	*m*	Length of the driveshaft (between welding support and housing contact)
L_t	-	Life of the bearing in turns
M_{max}	*Nm*	Maximum moment (z-axis) on the arm (of the rig)
M_v	*Nm*	Torsional moment applied on each part (housing and gear set) to calculate the torsional stiffness
M_x	*Nm*	Moment along the rod in x-axis (perpendicular to the rod)
N	*N*	Normal clamping force needed between housing and support
N_{fl}	*N*	Normal contact force between Sun 1 and the housing
N_{fr}	*N*	Normal contact force between Sun 2 and the housing
N_{pf1}	*N*	Normal contact force between Planetary and housing
P_b	*N*	Applied total load on the bearing
P_{eq}	N/m^2	Equivalent contact pressure
P_i	N/m^2	Contact pressure on node *i*
P_{rel}	*W*	Relative power in the differential in vehicle dynamic simulation 8.2
Q	*N/m*	Weight of the road
R_1	*m*	Reaction force between Pin and top Planetary (transmission torque force)
R_2	*m*	Reaction force between Pin and bottom Planetary (transmission torque force)
R_A	*N*	Reaction force on the bearing contact and driveshaft
R_B	*N*	Reaction force on the housing contact and driveshaft
R_{eq}	*mm*	Equivalent radius on the washers where the equivalent pressure is applied
R_h	*m*	Inner radius of the housing
R_i	*mm*	Radius value corresponding to node i

R_w	*m*	Wheel radius in vehicle simulation 2
S_{ratio}	-	Steering ratio
SWA	*rad*	Steering wheel angle
SWA_{ampl}	*deg*	Steering wheel angle amplitude
SWA_{deg}	*deg*	Steering wheel angle in degrees
SWT	*Nm*	Difference torque T_1-T_2 proportional to the steering wheel torque
T	*Nm*	Torque applied on the housing (surface in contact with the rig support in the left side)
T_0	*Nm*	Input torque (output transmission torque). Used for Loss Model, Rig Test Results and Vehicle Simulations
T_{0_param}	*Nm*	Constant input torque in vehicle dynamic simulation 8.2
T_{01}	*Nm*	Left drive shaft torque (without shaft friction)
T_{02}	*Nm*	Right drive shaft torque (without shaft friction)
T_1	*Nm*	Left drive shaft torque (output in rig conditions). Used in vehicle simulation 2 as well
T_2	*Nm*	Right drive shaft torque (output in rig conditions). Used in vehicle simulation 2 as well
T_{ratio}	-	Torque ratio value during vehicle dynamic simulation 8.2
Roman lower case letters		
a_y	m/s^2	Lateral car acceleration in vehicle dynamic simulation 8.2
b_w	*m*	Thickness of the washer between gears and housing (bushing width)
c	-	Compressive relationship
c’	-	Compressive relationship adjusted
c_{hp}	*m*	Chamfer in the pinion gear on the pinion hole (in radial direction)
c_{hs}	*m*	Chamfer in the side gear on the shaft hole (in radial direction)
d_g	*mm*	Outer diameter of the gear set
d_h	*mm*	Outer diameter of the ring of the housing
dx	*mm*	Differential of translational deformation for each part (housing and gear set) used for the stiffness calculations
f	*m*	Contact mesh offset (Gear mesh losses)
f	*Hz*	Frequency of the steering wheel angle input in vehicle simulation 2
gap	*m*	Gap between the teeth and the inner sphere of the housing
i	-	Gear ratio between planetary and side gear
i	-	Factor of action level of the separation force
k	-	Factor for the vehicle dynamics simulation (steering wheel released) to adjust the hyperbolic tangent step
l	*m*	Rod length
l_0	*mm*	Characteristic longitude for the stiffness calculations

		(substituted for d_h and d_g)
loss	-	Quotient of the torque for the vehicle dynamic simulation (steering wheel released)
$lossfactor_0$	-	Breakaway torque ratio in vehicle dynamic simulation 8.2
$lossfactor_1$	-	Sliding (dynamic) torque ratio in vehicle dynamic simulation 8.2
m	*kg*	Mass of the car in vehicle simulation 2
n	-	Number of bolts
r	*mm*	Radius in the bolt pattern of the housing
r_0	*m*	Effective reaction force (F_1, F_2) radius from the centre Pin
r_{01}	*m*	Effective Sun 1 tooth contact force radius (without contact mesh losses)
r_1	*m*	Effective Sun 1 tooth contact force radius (with contact mesh offset)
r_{02}	*m*	Effective Sun 2 tooth contact force radius (without contact mesh losses)
r_2	*m*	Effective Sun 2 tooth contact force radius (with contact mesh offset)
r_{fl}	*m*	Effective Sun 1 friction left radius (housing-sun 1)
r_{fr}	*m*	Effective Sun 2 friction right radius (housing-sun 2)
r_p	*m*	Pin reaction (R_1, R_2) distance from centre Pin (torque transmission)
r_{p01}	*m*	Effective Planetary 1 tooth contact force radius (without contact mesh losses)
r_{p1}	*m*	Effective Planetary 1 tooth contact force radius (with contact mesh offset)
r_{p02}	*m*	Effective Planetary 2 tooth contact force radius (without contact mesh losses)
r_{p2}	*m*	Effective Planetary 2 tooth contact force radius (with contact mesh offset)
r_{pf1}	*m*	Effective top Planetary friction radius (housing-planetary)
r_{pin}	*m*	Pin radius
r_{si}	*m*	Nominal radius of the shaft (part in contact with the side gear)
s_N	*Kg*	Standard deviation (calculated from results of the rig)
s_{x1}	-	Slip wheel 1
s_{x1}		Slip wheel 2
tw	*m*	Track width considered in vehicle dynamic simulation 8.2
v_x	*m/s*	Longitudinal vehicle speed in vehicle dynamic simulation 8.2
v_{x_param}	*m/s*	Constant speed value of v_x
v_y	*m/s*	Vehicle lateral speed in vehicle dynamic simulation 8.2
v_{1v}	*m/s*	Longitudinal speed of the hub 1 in x-axis
v_{2v}	*m/s*	Longitudinal speed of the hub 2 in x-axis
v_{1w}	*m/s*	Longitudinal speed of the wheel 1 (along its longitudinal axis)

v_{2w}	*m/s*	Longitudinal speed of the wheel 2 (along its longitudinal axis)
w_p	*m*	Surface width (in radial direction) in contact between side gear and its washer
w_s	*m*	Surface width (in radial direction) in contact between pinion gear and its washer
x_i	*mm*	x coordinate of the washers nodes
$\overline{x}$	*Kg*	Average of each Extra load column from the rig results
z_i	*mm*	z coordinate of the washers nodes
z_p	-	Number of teeth of the planetary gear (pinion gear)
z_s	-	Number of teeth of the sun gear (side gear)
Greek case letters		
ΔF_M	*N*	Sitting force
α	*deg*	Pressure angle teeth (forces angle)
β	*deg*	Angle of the tangency in the Sun effective friction radius
β	*rad*	(body) side slip angle in vehicle simulation 2
δ	*rad*	Front wheel angle respect longitudinal axis x of the vehicle
δ_{max}	*mm*	Maximum deflection of the rod for a given load
δ_{total}	μm	Sitting strain
δ_{xj}	μm	Sitting strain due to the joint
δ_{xr}	μm	Sitting strain due to the fillet
θ	*deg*	Angle of the tangency in the Planetary effective friction planetary radius
θ_d	*rad*	Angle displacement
θ'	*rad*	Rod deflection for an applied load
φ_e	*rad*	Angle displacement
φ_z	*rad/s*	Heading angle in vehicle dynamic simulation 8.2
μ	-	Friction coefficient for the bushing material in wet conditions
μ_G	-	Friction coefficient for the bolts for attaching the housing
μ_H	-	Friction coefficient between housing and its support.
σ	*MPa*	Traction strength
σ_{adm}	*MPa*	Maximum traction strength allowed (for steel)
ω_1	*rad/s*	Left wheel speed
$\omega_{1Noslip}$	*rad/s*	Left wheel speed without considering slip
ω_2	*rad/s*	Right wheel speed
$\omega_{2Noslip}$	*rad/s*	Right wheel speed without considering slip
ω_z	*rad/s*	Rotational speed of the vehicle around z axis
ϕ	*deg*	Angle of the bevel teeth respect the gear axis

1 Introduction

1.1 Problem motivating the work

Steering feel and vehicle steering motion is affected by wheel torques from propulsion, especially for front wheel drive cars. Often these problems are referred to as "torque steer". Many systems interact to cause these problems: propulsion, steering and suspension.

According to some surveys (*see* [23] and [32]) the torque steer contributors are not only the differential (friction, self locking effect, Torsen differential), but also the input from the ground and car geometry such as road conditions (friction and surface), the vehicle state (cornering, rolling, acceleration) and weight distribution (loading). In addition, the suspension design contributes as well, like the suspension geometry (kingpin offset, camber, caster, tolerances), the tire quality (conicity, wear, profile) and wheel geometry (size, uniformity, wheel offset). Finally, regarding the transmission contributors, the engine (torque, alignment) and drive shafts (alignment, length, symmetry) are contributors as well.

Particularly, within the propulsion system, it is partly the asymmetry in differential and drive-shafts that could cause torque steer. In fact, the friction of the gear meshing and bearings, and mainly the contact with the housing (carrier) during slippery and static conditions or the housing stiffness itself might be causes of this torque steer problem.

Hence, the losses over the differential can explained the torque steer effect due to the torque difference between left and right driveshaft. This fact affects the behaviour of the vehicle since the losses over the differential affect the final torque in each wheel.

This is the reason why Volvo Cars Corporation (VCC) is interested in studying the friction in a differential to use it in further simulations (vehicle dynamics purposes) or understand which parts of the design may be modified or changed in order to reduce or increase (depending on the goal, either getting as close as possible an open or a limited slip differential behaviour) the overall friction.

1.2 Scope/Research question

The aim of this study is being able to understand, quantify and qualify the torque split left/right over a front wheel driven open differential M66 currently used in VCC.

It will begin doing a research of the differential concept so as to understand how the differential works from a mechanical point of view, the different possible solutions and the influence of the parameters to the overall friction in the differential system.

Thus, the analysis and modelling of the differential is carried out so as to understand how important the effects in each friction surface are as well as to qualify the behaviour of these losses according to the input torque.

So as to corroborate this, a rig will be designed in order to be able to test the differential physically. Then, a test planning will be created not only to check the original design but also to make some changes in some parameters and check the effect of these parameters to the overall torque split.

Furthermore, a FEM analysis will be carried out to give the technical understanding of the behaviour of the differential once this is loaded.

Finally, the results will be checked with log data got from a car test so as to compare what has been got in the rig and what it really is in the car (difference between the breakaway and sliding friction).

Additionally, the influence of the uneven torque split will be studied in a limited number of vehicle manoeuvres so that some examples of the effect of not having a symmetric torque distribution between shafts show the vehicle dynamics behaviour.

1.3 Limitations

Once it was decided the need of testing the differential, the rig was designed. Nevertheless the rig has the limitation: the housing (carrier) is clamped on the bench, restricting then its degree of freedom. Thus, the inertia and centripetal acceleration are neglected. But also, as the housing is totally fixed, the working parameters differ from the real car, the oil film thickness is not set, the temperature is not the optimal and also the friction is higher since a static (or quasi-static) study of the friction of the differential is done. A solution would be running the whole transmission with such a rig which allowed the driveshaft turning in different speed so as to check the behaviour of the differential when it starting differentiating the rotational speed between shafts, or doing a test with the whole car analysing, then, all the parameters that may affect the torque split left/right over the driveline.

As a consequence of having the limitation of this static differential test, the Nedox coating washers have just been tested in this static rig. It might be that if they were tested in a dynamical rig, the friction difference between the Nedox coating washers and the original material would increase, i.e these heat treated washers might be designed to have a higher reduction in dynamic rather than in static conditions.

On the other hand, there is the limitation of the gear mesh, since it is a static test, depending on the gear mesh which is used the results may differ. Thus, in case the test is done in a running rig, the results will be already got within the band where all the different values of force are, due to the sinusoidal shape that the force distribution has depending on the rotational angle in each instant of time (the running test will take all this values into account). However, it also affects the FEM analysis, since the gear mesh study could be a thesis work itself, just studying the effect of the possible different contact tooth mesh and the different effect in the deformation and pressure distribution of the differential parts.

The studies on vehicle level in this thesis do not intend to study and solve any explicit vehicle level problems. They rather are examples of how the differential model could be used in a vehicle model. As it has not been got the real problem formulation of the torque steer (with some logged data), the work could have been much more focused on what to model and simulate on vehicle level.

For the first simulation using the VDL libraries, the differential has been assumed to be in the same working state during the simulation period, thus it might be that it has transient changes from locking to semi locking as it has been shown in the second driving case. Thus, it was tried to study a driving scenario that allowed assuming as a constant torque ratio as soon as there was a difference in relative speed.

On the other hand, for the second simulation, the model has been simplified in order to try to figure out the phenomena. The next step would be trying to get or do some vehicle test to see how the torque steer effect is and then update the model as much as it is needed.

However, the effect of the differential in a particular driving condition using the complete vehicle model has been carried out and some steering feeling phenomena has been figured out in a driving situation due to the effect of the differential to the overall torque distribution.

1.4 Conceptual design solutions of differentials

There are several solution used in mostly all the commercial cars such as a bevel gear differential with four or six gear wheels (two sun gears and either two or four planetary gears). There are also solutions using worm gears and a planetary spur gear differential, whereas all of them belong to the open differential group. This kind of differential allows the drive wheels to turn in different speeds.

For instance, in the Figure 1.1 below it is possible to see a sketch of the bevel gear differential (with four wheels; two side gears and two pinion gears) and spur gear differential.

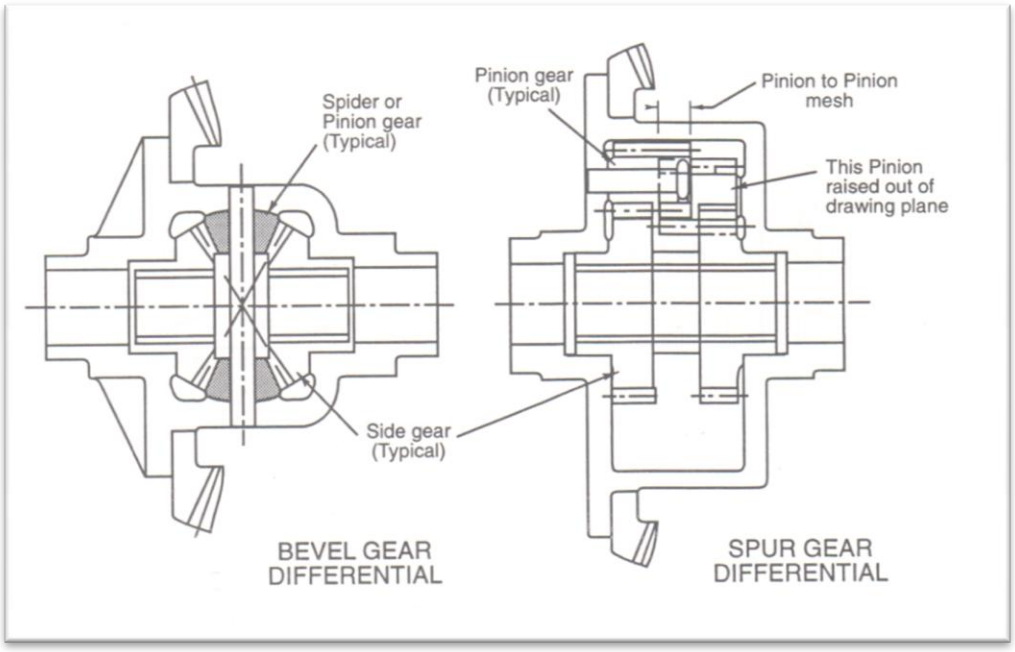

Figure 1.1. Bevel and spur gear differential.

Before the brief description of the possible causes of the internal friction in the differential, some technical information about the differential itself is described in order to know why there is the need of using it and which the goal is, focusing in general types of differential, open and limited slip differential.

1.4.1 Accelerating in a curve

When accelerating out of a corner the drive wheels are unevenly loaded and traction on the inside wheel is limited to a lower value than the outside wheel. Different types

of device are available which may help in this situation. Ideally, both drive wheels would be fitted with an anti-spin device that would apply the maximum propulsion force to each tire, given the vertical and slip angle of operation.

1.4.2 Turning without longitudinal wheel force

When negotiating a curve without demands neither on acceleration nor deceleration the inside wheel should be at a lower rotational speed (less load and smaller radius of travel) than the outer. The best concept of differentials in this situation is the standard open differential (driving conditions where it is worth reducing friction as much as possible); it will allow the inside wheel to spin up and the outer wheel decrease the speed and limit the driving torque on each wheel to that of the spinning wheel.

1.4.3 Straight line driving

For independent suspensions the differential is less critical for straight line acceleration. Loads on the tires are even (independent suspensions) and the same torque is applied to each shaft. If the two are locked together, the shaft torques can be different due to small differences in tire size may, and it can, steer the car. This acceleration-torque-steer is found primarily on front wheel drive (FWDs) cars due to compliance and asymmetry in the steering and suspension.

For solid axle suspension, the wheel loads are uneven on acceleration unless some torque reaction device is used. A limited slip differential (increasing friction) or even a spool certainly helps in this case.

1.4.4 Decelerating in a curve

When throttle is dropped in a turn, the front tires are loaded up and they can produce more side force (destabilizing) than they did when the power was on. An open differential has probably the least effect in this situation; the driving torque and the motoring torque are split evenly between the drive wheels. If the drive wheels are locked (or partially locked) under power (by limited slip differential), and they unlock when the power is removed (a characteristic of certain differentials), relatively more side force will suddenly be available. A differential that remains locked with the throttle dropped will add "yaw damping".

While braking in a turn it is most desirable to have anti-lock. Barring the differential keeps both wheels turning at the same speed (regardless of braking) will help prevent lockup one of them. This would be one of the fixed preload types of limited slip.

For best rough road traction (and probably directional control) some sort of antilock differential will keep an unloaded wheel from spinning up and then disturbing the car when it lands.

As far as a differential for the FWDs is concerned, a limited slip may be some help in rough cornering. On the minus side a differential that is locking and unlocking the front axle will make steering difficult. Ideally, the limited slip differential would be smooth in operation.

1.4.5 Influence on steering system

Finally, for FWDs, any type of differential that dynamically changes the torque on the two wheels will give a steering reaction. This reaction will add to any torque reaction caused by angularity of the driveshafts due to steer angle or other misalignment such as that caused by ride travel. Hence, the differential in a FWD car are the devices that

will be studied. The study will focus in the devices situated on the front axle since VCC produces FWD cars with high torque.

1.5 Differential overview

Moreover, the four bevel gear opened differential is studied. A representative working view of the differential assembly which will be analysed in this thesis work is represented in the Figure 1.2 below as an example of a four bevel gear differential:

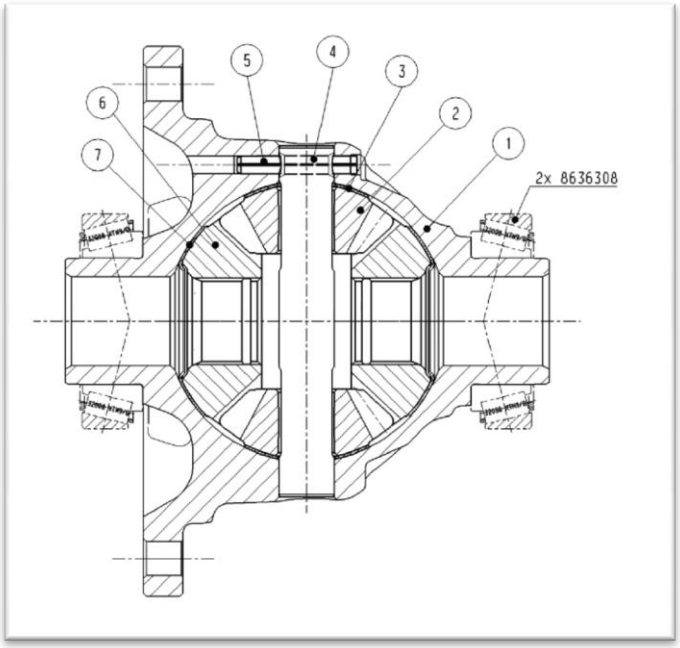

Figure 1.2. Overview of the four bevel gears M66 FWD differential studied.

Currently, it is the most used in the commercial vehicles due to its simplicity, low cost and reliability.

The differential mechanism is built into the centre portion of the final drive crown wheel. It usually consists of a cast malleable iron cage housing which incorporates the bevel differential gears. The bevel gear train may be considered to form a closed loop or ring in which there are two bevel side-gears generally called sun gears and between them are two or four bevel pinion gears known as planetary gears which indirectly link the sun gears together, depending if it is a four or six wheels differential.

The sun gears have extended sleeve shoulders which are externally machined and polished to provide bearing surfaces to support these gears in bosses formed in the differential cage. The hollow centres of these gears are splined so that they can engage and support the inner ends of the drive shafts.

Furthermore, the cross-pin is situated in the centre of the differential and at right angles to the sun-gear axis and it provides the axis for the planet gears. This pin is a force fit in the cage casting, but additionally secured by a small location pin.

The differential cage is generally made in two halves so that gears can be assembled, but a single housing may be used for light-duty purposes, although the gear's assembly becomes more complex. The inside of the cage is spherical-shaped to provide an effective bearing reaction surface for the sun and planet gear end-thrust.

But, some other shapes can be taken into account to reduce the thrust and friction on these surfaces. Externally, the cage has a machined flange to locate and support the crown wheel.

Whereas, a worm gear differential might be used, but it has a huge disadvantage which is the low efficiency that it has, around 30 or 50%, due to the sliding contact thread leadscrew. This sliding contact friction limits the efficiency. However, the use of involutes tooth profile can increase the efficiency, but not high enough to become more useful and reliable. Mostly, worm gear differentials are used only on non-steered (rear) axle or on vehicles where the kingpin offset (lever for torque steer effect) is very small or torque steer can be controlled away with electric steering assistance and VCC are none of these.

However, an advantage is that a worm gear is self-locking for opposed power direction (not backdrivable), so it does not need a brake or any external power to hold a load.

On the other hand, there is the possibility to use a single spur planetary differential even spurteeth or helical teeth. The concept is still the same but it has a better packaging, even though the space that the differential takes in a front wheel driven and front mounted engine is no so important because it is down the transmission and the space that the steering wheels have is not affected by the differential mounting.

Another advantage might be that as the planetary goes between the sun and the crown there is no slipper contact surfaces and no need to use bushes. Thus, it saves the friction between these contact surfaces.

Hence, the conventional bevel gear set differential requires that the spider gears rotate between side gears of equal size and this precludes the unequal lever arm design. There are, however, many other configurations of gears that give differential action. For example, planetary gear set differential which allow the two output lever lengths to be unequal. This is the basis for the uneven torque split differentials that may be found as central differential (third differential) of AWD cars with differential between axles.

In this project, the bevel gear differential will be studied since it is the one which is used by Volvo Car Corporation nowadays. Some modifications in this design will be taken into account in order to reach the best design possible minimizing the friction.

1.5.1 Boundary between open and limited slip differential

In a real open differential there is friction (Coulumb friction) in all the gear meshes and bearings and a small amount of hydraulic damping (proportional to velocity or velocity squared) due to oil churning. Thus, an open differential is not perfect considering the equal distribution left/right.

This is shown in the Figure 1.3 which shows a small step in Δtorque at the point of fast-slow wheel reversal (due to the friction), and a very gradual increase in Δtorque with increase in ΔRPM. The result of the friction is to slightly "lock" the two output shafts to each other. This gives a small offset and slope to the theoretically even torque split. The wheel that gets more torque is always the slower wheel (*see* [35]).

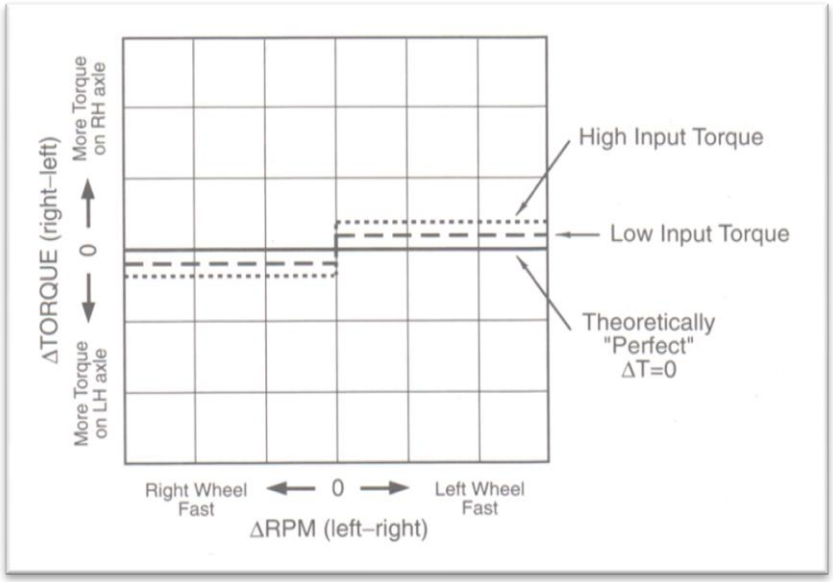

Figure 1.3. Open differential characteristics.

It can be split up in two curves for high and low engine input torque. The difference between these two curves depends on the design of the differential; an increase in friction may increase with an increase in torque. One possible mechanism for this effect is distortion of the differential case with high torque, resulting in binding of the bearings.

Hence, a disadvantage of open differentials is that with high power and/or low traction, the drive force at the road is limited by the tire with less traction, the drive force at the road is limited by the tire with less traction. For low-speed operation in low friction coefficient such as snow or mud conditions, a simple solution is to partially apply some brake on the drive axle.

Another solution to the lack of traction with an open differential is to partially lock the two axles by increasing internal friction, perhaps by preloading some of the journal bearings (typically the spider gears). Now, the slow wheel receives more torque and the fast wheel less torque. Referring back to the Figure 1.3, extra friction will increase the size of the step in torque at the fast-slow wheel reversal point. This increase in friction will generate excess heat when the wheel speeds differ (in cornering) and some means of cooling may be required for heavy-duty usage.

In racing, for example, various tricks have been used to good advantage when open differentials are mandated. Of course, the tech inspectors have caught on and will check that the wheels counter-rotate freely with the drive wheels jacked off the ground.

The open differential, with or without some added friction, is likely to be used for many more years. Its strengths are in situations where rolling resistance is important (high-speed turning) and either high torque, low gear or wheel spin are not problems.

Open differentials probably have the least effect on handling of any of the various types because they cannot contribute yaw moments (from left-right thrust imbalance) to the vehicle under any circumstances, either power-on or power-off. In situations where traction is broken, the inside wheel acts as a "safety valve" when it spins up. Under these circumstances, the outside wheel maintains some lateral force capability.

1.5.2 Effects of the differential in chassis set-up

1.5.2.1 The effect of a differential type on acceleration out of a corner

With an open differential the lightly loaded inside wheel is free to spin up under power if enough torque is available. This limits the available acceleration. Limited slip differentials, for instance, have been used with varying success. It is unlikely that the simple addition such a differential will be successful. As with any major change, a period of development must be gone through to make the new set-up work. The type of limited slip differential chosen will be very important. Undesirable jerkiness occurs with many types and research (*see* [35]) has shown this to be undesirable for combined acceleration and turning.

The locked rear end or spool is another common solution to the problem of wheel spin because the locked axle has high resistance to yaw, more front cornering power may be required to keep the car neutral. If all the turns are the same directions, stagger (differential tire circumference) may be used to "split the difference" between low drag when straight running and when turning.

1.5.2.2 The effect of differential type on straight line acceleration

If both tires are on similar coefficient pavement at similar vertical load, the differential type should not affect straight line acceleration capability (wheel spin limited). This is true of most independent suspensions and some torque tube solid axles. With solid rear axles this is not true since the wheel loads differ on acceleration.

With the differential partially locked, small differences in tire size may cause the car to pull on acceleration (especially true on some front drives). This can be diagnosed by swapping the tires; if it pulls the other way, the wheels are being locked to the same speed by the differential and the tires differ in circumference.

1.5.2.3 The effect of differential type on dropped throttle in a turn

An open differential that distributes the torque evenly will probably have the least effect on dropped throttle behaviour. A differential that remains locked (possibly due to some preload) when throttle is dropped produces a stabilizing yawing moment or "yaw damping" moment. Some limited slip differentials may put shock loads into the drivetrain when they lock and unlock. This can have effects that are hard to predict.

1.5.2.4 The effect of differentials on steering kickback

This effect occurs stronger using limited slip differentials rather than open differential and just when it is in the steering wheels side, usually on the front.

If any limited slip differential is fitted that locks-up or unlocks suddenly, it will be reflected to the steering. If there is any scrub radius, the change in drive torque will produce a torque about the kingpin which will be noticed at the steering wheel. Event with centerpoint steering a change in engine torque will change the tire self-aligning torque and this will change the steering force in a turn.

All these causes happen in an open differential but in a lower dimension. Due to the small friction inside the differential, the torque steer might be affected by the friction. Mostly in production cars whose customers should not have any steering feel. The car should become as perfect and soft as the supply can.

1.6 Influencing parameters

The theoretical study of the different parameters that could affect the friction inside the differential and, hence, the torque difference between left and right shaft, is listed below:

1.6.1 Gear meshing

Gear meshing: This depends upon the tooth design, the lubricant, the speed and the resulting coefficient of friction.

Using different teeth angle the losses in the meshing change. Thus, taking into account first the cylindrical gears, it can be said that the spur gears the efficiency of the gears may differ between 98 and 99% per each mesh (*see* [32]). This difference could be an input to maximize the efficiency. If the teeth are helical the efficiency can rise slightly, moreover the noise is reduced, but a new axial load appears.

The coefficient of friction is influenced by the surface roughness, but primarily the relative radius of curvature and velocities of the surfaces, and by the thickness and mean viscosity of the oil-film.

The temperature also affects to the efficiency, the overall efficiency has a maximum in an interval of temperatures. It decreases in cold or too hot conditions. In fact, it is due to the change of properties of the lubrication which is optimum in a certain interval.

Regarding the bevel gears, the losses are higher than the spur gears, but it changes perpendicularly the direction of the input and output shafts.

1.6.2 Contact surfaces

It is affecting the bevel gear differential since there is a contact between the planetary and the housing itself by means of a bushing that tries to reduce the friction. This contact may be crucial since its high slippery all the time that the housing and planetary are not turning as one solid part. However, the planetary gear is not just having contact on the housing but also on the pin. When the vehicle turns, there is a relative speed between the pinion pin and the planetary so that some friction torque appears on this surface.

Moreover, a contact between the sun gears and the housing also exists. Different concepts of surfaces can be taken into account for this contact. Those could be either flat or spherical. Currently, the spherical is been used but the flat used to be used as well (actually, it might be the future differential generation design in VCC). Hence, a different concept solution for the shape is not taking into account in the model and simulation, since just the current differential M66 from VCC is modelled.

Finally, another slippery surface, likely not as critical as the former contact surfaces, exists between the drive shaft and the housing. The drive shaft is holding on both the housing and the internal splines of the sun so that between a slight friction exists between the housing shoulder and the drivesahft. In fact, some modifications can be pointed out before beginning the model and the simulation, such as using a bearing between the shaft and the housing or machining the shaft to have less contact surface (although the pressure will increase). Further study will be done in the following chapters to quantify this effect.

1.6.3 Bearing losses

Rolling bearings involve rolling friction (typically proportional to radial load on bearings) together with an added oil-drag loss in the lubricant within bearings, but the total is less than the tooth-friction loss. When plain bearings are used, the bearing friction greatly exceeds the tooth-friction losses.

It cannot be changed since they are supplied but some different concepts of bearings may be studied to check how the friction changes, if this friction is relevant compared to the overall.

1.6.4 Lubrication

The efficiency of gears with a high sliding percentage, worm and hypoid gears, for instance, may increase up to 15 percent if synthetic oil is used instead of a mineral oil. Even in the case of spur, helical and bevel gears (which have a naturally high gear efficiency), it is possible to increase gear efficiency of up to one percent by using a synthetic gear oil. This may not seem like much at first, but it may result in considerable cost savings depending on the nominal output of the gear unit, especially in the case where several gears are deployed. The most important parameters to take into account in the used oil are the viscosity and the oil film thickness.

Even though, there are different kinds of oil, this parameter cannot be modified since it is an input for the differential. The whole transmission (engine, gearbox and differential) has already been designed using a particularly kind of oil which has given the best results in optimum working conditions. Thus, the model will not include the viscosity effects in order to minimize the time consuming. Even though, the lubrication will affect the static test since the differential will not work in optimum conditions regarding oil film thickness and temperature, for instance.

1.6.5 Stiffness of the housing

Finally, one of the other possible parameters to adjust in the differential itself could be the stiffness of the housing. It might contribute in the overall torque split slightly, since it also contributes in the stiffness chassis.

2 Differential Loss Model

In order to explain the test results with theoretical mechanic equations, a model is set up. Such a model also makes possible to explain how significant parameters affect the torque difference. This model might also be taken into account in dynamic simulations with the whole car system or front driveline subsystem in order to check the dynamic behaviour of the car without taking over a theoretic perfect open differential.

The basic model is got after the literary survey and the understanding of the differential. In particular, with the current M66 open differential used in front wheel drive cars at VCC.

Moreover, by means of the Rig Test (see Chapter 4 and Chapter 6) and FEM analysis (Chapter 5), the Loss Model will be able to be developed and checked in parallel until it fits as best as possible with these results. Thus, both the Rig Test and the FEM Analysis will be used as well to give some feedback to this Loss Model, such as slope and shape of the curve (linear or non-linear), friction coefficient, contact points (equivalent friction torque radius). In the *Appendix A*, it can be found more in detail the development of the model. From the first assumptions and analysis until the last check with the Rig Test Resuls.

As far as the assumptions are concerned, with a compromising reliability and time consuming, it was decided to consider a rigid system and no effects of the oil viscosity. As the Rig Test is done in static conditions, the centripetal acceleration and mass of the components is neglected. Finally, the Coloumb model was used for the friction forces on the contact surfaces.

2.1 Description of the basic model

The differential consists in four bevel gear wheels: two side gears (or sun gears), two pinion gears (or planetary gears), the housing and the pinion pin.

Note that the housing and the pinion pin are fastened so that can be considered as the carrier of this planetary drivetrain.

Furthermore, to study this planetary bevel gear differential, the free body diagram of each part is done and using the equilibrium and the Coloumb friction model, it is possible to get a reliable system of equations to be solved.

As far as the friction is concerned, it was decided to take over, *a priori*, the following parameters: the friction between the planetary gear and the housing, the sun gear and the housing, the pinion and the planetary and the gear meshes losses of the side and pinion gears. Thus, it was decided to neglect the gear mesh losses of the splines between the drive shaft and the side gear and also, the contact losses between the driveshaft and the housing itself, which are sliding when the driveshafts turn relatively to the housing (carrier).

On the other hand, it was decided to not study the effect of the bearing losses, since they might be neglected compared to the contact friction in the other components and also the effect of the lubrication (oil film thickness, working temperature and variable sliding friction) in order to minimize the time consuming in this static analysis.

Consecutively, the model is created and developed using the following equations, considering the differential in static working conditions (or quasistatic), taking over the first order effects. As it is said, further modifications will be included as soon as the Rig Test and FEM analysis are done.

- For the left sun gear and drive shaft:

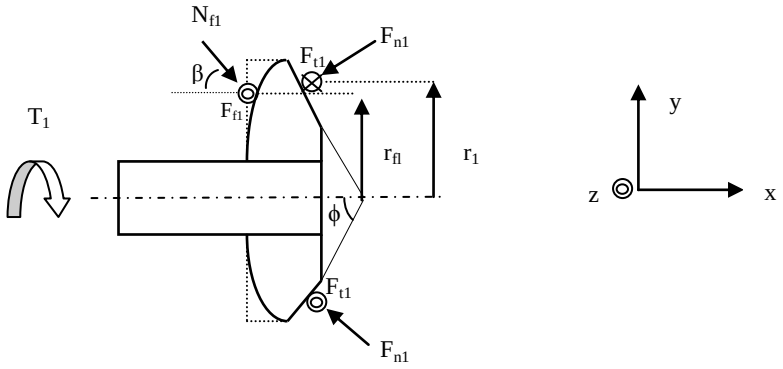

Figure 2.1. Free body diagram of the left sun gear and drive shaft.

$$\sum F_x = 0 \rightarrow \quad N_{fl}\cos(\beta) = F_{n1}\sin(\phi) \tag{2.1}$$

$$\sum M_x = 0 \rightarrow \quad T_1 = F_{t1}r_1 - F_{fl}r_{fl} \tag{2.2}$$

Observation: Note that there are six equations in the 3-Dimensional space, but the relevant are the ones which are written.

Moreover, note that it has been considered ideal differential when the forces are symetrical. Thus, the forces acting due to the reactions of each planetary are the same (if all the equations are considered, then the results show so).

Finally, the normal force due to the contact with the housing has just been shown in one side, but it is evenly constant along all the contact line circumeferncially. Whereas, the friction force is shown just in one side, but it is all the way. Basically just know that it creates a torque in x-direction equal to $F_{fl}{\cdot}r_{fl.}$

- For the top planetary gear:

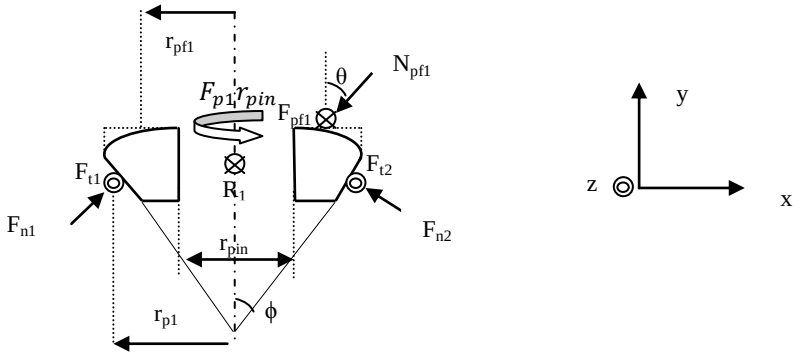

Figure 2.2. Free body diagram of the top planetary gear.

$$\sum F_x = 0 \rightarrow \quad F_{n1} - F_{n2} = 0 \tag{2.3}$$

$$\sum F_y = 0 \rightarrow \quad N_{pf1}\cos(\theta) - F_{n1}\cos(\phi) - F_{n2}\cos(\phi) = 0 \tag{2.4}$$

$$\sum F_z = 0 \rightarrow \quad F_{t1} + F_{t2} = R_1 \tag{2.5}$$

$$\sum M_y = 0 \rightarrow \quad F_{t2} r_{p2} = F_{t1} r_{p1} + F_{pf1} r_{pf1} + F_{p1} r_{pin} \tag{2.6}$$

- For the bottom planetary gear:

The free body diagram is still the same as the top (symmetry). Thus, the equations got from this part are not used for the whole model since if they are used, the system will become over constraint (indeterminate). Actually, the effect of having two planetary gears is already considered since the forces in the gear mesh in the sun are doubled (top and bottom gear teeth contact assumed just in contact thanks to the symmetry).

Thus, the friction force is considered to be set just through one planetary. As just first order effects are assumed, the fact of splitting the force in two planetary gears will give the same amount of friction torque in both: contact between pinion gear and housing and contact between pinion gear and pin.

In terms of the results, considering two symmetric planetary taking the half of the torque yields to the same results as if one planetary is considered, taking over all the forces and friction torque along it.

- For the right sun gear and drive shaft:

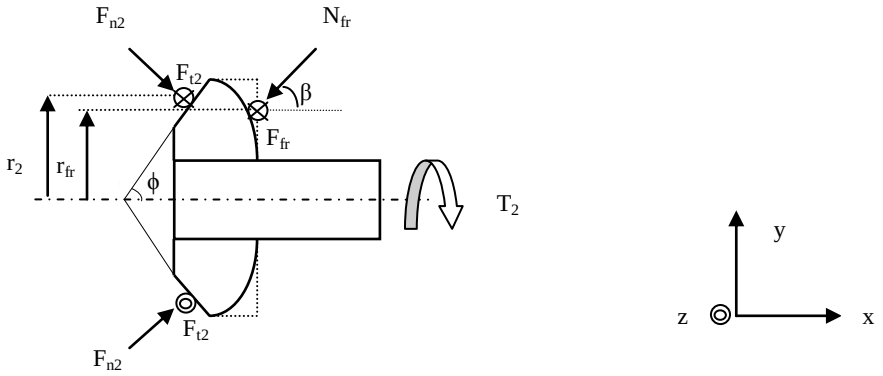

Figure 2.3. Free body diagram of the right sun gear and drive shaft.

$$\sum F_x = 0 \rightarrow \quad N_{fr}\cos(\beta) = F_{n2}\sin(\phi) \tag{2.7}$$

$$\sum M_x = 0 \rightarrow \quad T_2 = F_{t2} r_2 + F_{fr} r_{fr} \tag{2.8}$$

- For the whole differential:

$$T_1 + T_2 = T_0 \tag{2.9}$$

Observation: It is a balancing of the whole differential analysis for the balance of torques. The input torque T_0 is the sum of the output torques.

- Angle of the forces on the teeth:

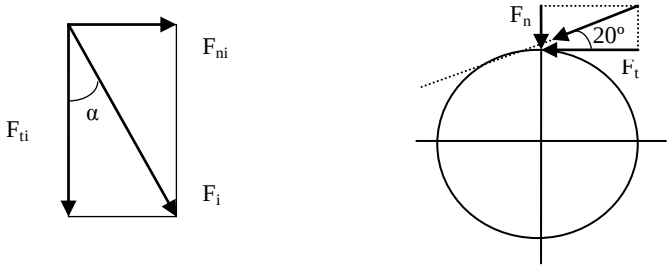

Figure 2.4. Sketch of the forces on the contact mesh.

$$\frac{F_{n1}}{F_{t1}} = \tan(\alpha) \tag{2.10}$$

$$\frac{F_{n2}}{F_{t2}} = \tan(\alpha) \tag{2.11}$$

- Friction's forces (Coulomb's friction):

$$F_{fl} = \mu\, N_{fl} \tag{2.12}$$

$$F_{fr} = \mu\, N_{fr} \tag{2.13}$$

$$F_{pf1} = \mu\, N_{pf1} \tag{2.14}$$

$$F_{p1} = \mu\, R_1 \tag{2.15}$$

2.2 Definition of parameters

Using the data of the current differential M66, all the data was set as it can be seen below. Some assumptions were done such as considering that the friction radius is in the middle point (in radial direction between inner and outer edge) through all the width in contact with the gears and the washers housing. In addition, the gear mesh was set on the middle point of the teeth (*see* [24]) and also considering that it is just one tooth in contact for wheel at the same time.

Hence, the dimensions of this differential are:

$r_{01}=26 \cdot 10^{-3}$ m
$r_{02}=26 \cdot 10^{-3}$ m
$r_{p01}=17 \cdot 10^{-3}$ m
$r_{p02}=17 \cdot 10^{-3}$ m
$\phi=54.28º$
$\alpha = 20º$
$r_{fl} = 25 \cdot 10^{-3}$ m
$r_{fr} = 25 \cdot 10^{-3}$ m
$r_{pf1} = 15 \cdot 10^{-3}$ m
$\mu = 0.20$
$r_{pin} = 4.37 \cdot 10^{-3}$ m

$\beta = \sin^{-1}(r_{fr} / (R_h - b_w))$ rad
$\theta = \sin^{-1}(r_{pf1} / (R_h - b_w))$ rad
T_{0_vec} = [0, 10, 20, ..., 2000] Nm
f = 0.15
Instead of making the model more complex adding the efficiency of the gear mesh (and hence, adding 4 more variable and equations). These losses can be taken into account as well like a pole offset of the application point of force in both sides (in the direction of the power flow). The gear mesh will yield to a efficiency value around 99%.
$r_1 = r_{01} - f \cdot \cos(\phi) \cdot 10^{-3}$ m
$r_2 = r_{01} + f \cdot \cos(\phi) \cdot 10^{-3}$ m
$r_{p1} = r_{p01} + f \cdot \sin(\phi) \cdot 10^{-3}$ m
$r_{p2} = r_{p02} - f \cdot \sin(\phi) \cdot 10^{-3}$ m

Furthermore, it has been assumed an overall friction coefficient of 0,20 so as to be able to get the first outcome from the simulation.

2.3 Results

In the following Figure 2.5 and Figure 2.6, the results are shown once the determinate system of equations explained above is solved.

The *x*-axis represents the input torque in the differential (would represent the output of the transmission) and the *y*-axis represents the torque split left/right over the differential. In this first plot, the effect of each contributor is summed until the overall is reached, starting from gear mesh, every parameter has been added consecutively.

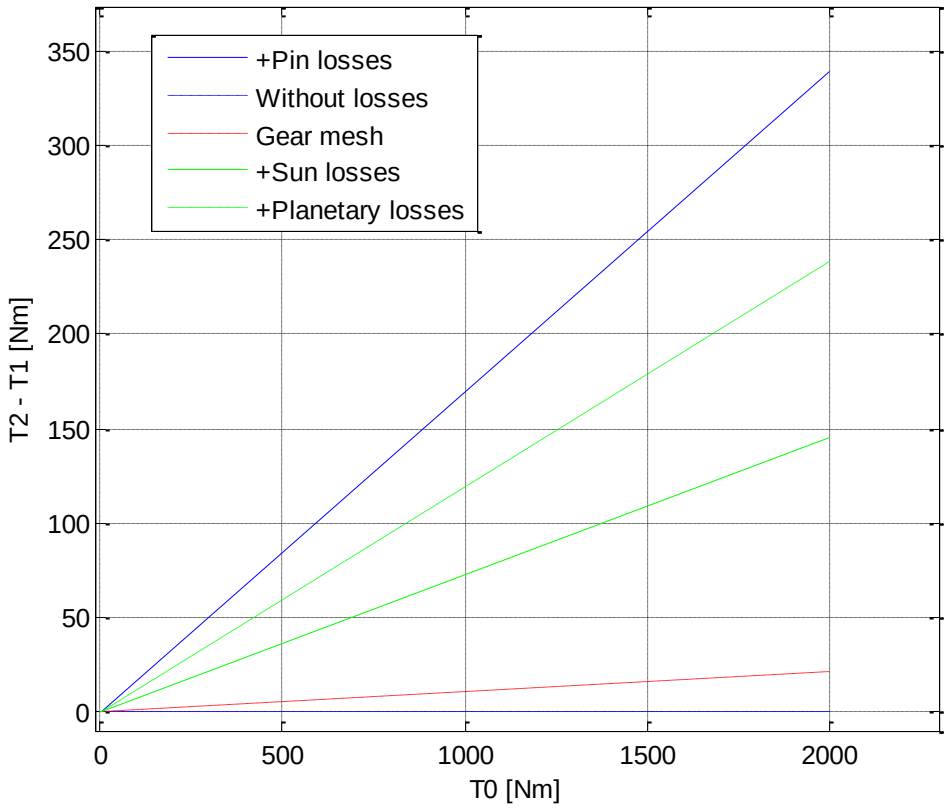

Figure 2.5. Output torque difference right-left vs. Input torque (summed contributions).

Whereas, if instead of studying the sum of the consecutively losses, the individual study is one so as to show clearly how much every parameter contributes to the final torque difference the Figure 2.6 is got.

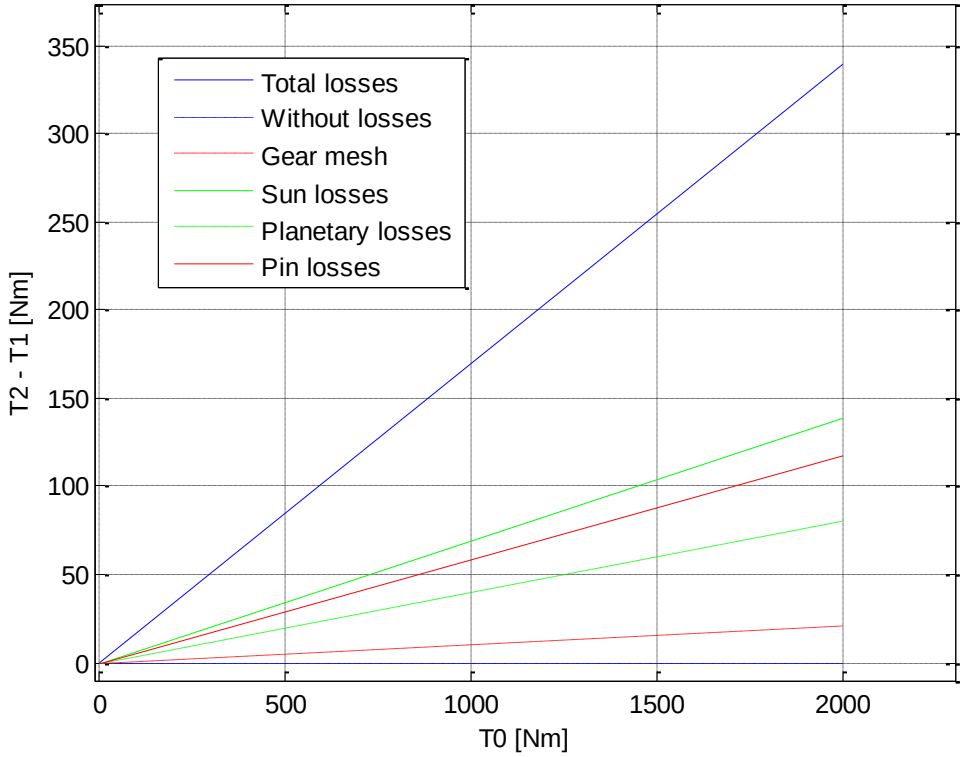

Figure 2.6. Output torque difference right-left vs. Input torque (individual contributions).

Hence, the output torque is lineally dependent of the input torque in the differential because of the lack of second order effects. The difference of torque between left and right driveshaft represents a 17% of the total input during the wide range of values (when the input torque is 2000 Nm, the output becomes 339.8 Nm).
Furthermore, so as to quantify the amount of contribution for each parameter, the input and output torque are taken and compared to the total amount. Thus, this yields to the table below:

Table 2.1. Contribution of each parameter to the overall torque split.

Parameter *(i)*	**Contribution** $\left[\frac{(T2-T1)_i}{(T2-T1)_{Total}} x100\right]$
Gear mesh	6.20 %
Contact in the sun gear	40.76 %
Contact in the planetary gear	23.50 %
Contact in the pinion pin	34.46 %
TOTAL (product)	≃100%

Note that the sum does not reach the 100%, it is due to internal numerical difference in the solver explained in the *Appendix A* (some small error is added one it is approximated with 2 significant numeric figures).
Thus, in the Table 2.1 it has been checked how much every parameter may contribute to the final difference torque between axles.

Actually, it is worth pointing out that the friction torque that appears between the contact of the sun (side) gear and the side washer represents a high percentage that although the model is not defined yet, it may represent already the quality of the real contribution of each friction torque to the overall torque split.
In addition, it is seen how the friction between the pinion pin and the planetary (pinion) gear represents also an important amount of the total value. Whereas, the gear mesh loss is really low (it seems a good assumption since the gear mesh efficiencies are usually really high, and in particularly also with bevel gears) and the friction torque between the planetary gear and its washer does not contribute as much as it was thought *a priori*. The friction torque in this model is lower not only due to the equivalent radius that is smaller and then the friction torque becomes lower than the side gear as well, but also due to the force that pushes the gear to the housing and the geometry that make the total normal contact force smaller.
Note here as well, that the sliding between the gears and the washers has been considered instead of considered the sliding between the housing and the washer. After some investigations, it was set like that and finally it was proved and checked in the Rig Test. Basically, this assumption affects just the radius of the housing, which becomes smaller than the housing radius if the sliding is considered between the washers and the gears.
As far as some extracted conclusions from this model are concerned, it is not possible to claim right now that the difference torque between shafts has a linear dependence on the input torque. It will be after the Rig Test is done that the model will be able to be judged by checking how both the experimental and the model fit. The conclusions and modifications to this simulation model will take place after having studied the Chapter 4, 5 and 6.
The model may be or may not be full linear following the same relation between input and output all the wide range of torque. In addition the hypothesis assumed for the equivalent radius and the contact point of the gear teeth mesh may be not true, it has just been assumed so far.
Then, the next step will be studying the deflection of the housing, pin axle, side and pinion gears for being able to know the pressure distributions and the real contact gear mesh points and effective radius friction by FEM analysis By this way, the simulation Matlab model will be able to be edited so as to include the results got from these analysis, regarding equivalent friction torque radius and linearity.
On the other hand, another study of the effects of each parameter is done in order to get an overview of how much changing the dimension of each contributor would modify the torque difference between shafts (see Figure 2.7). In order to not have three variables depending system, the input torque has become constant, so it has set to 1500 Nm for instance, it will not affect the quality since in the y-axis is plotted the quotient between the torque difference left/right and the input torque.
Then, the swept is done to get an overview and to understand the effect of each one independently. It is said, how it affects (qualitatively) but not how much it does (quantitatively).

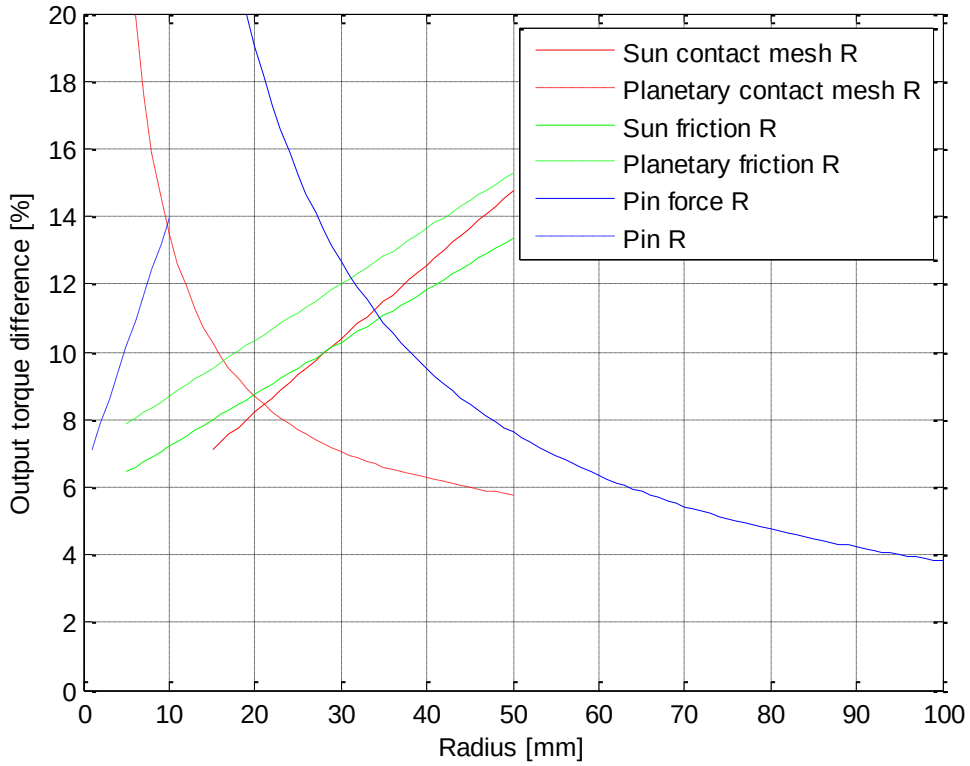

Figure 2.7. Output torque difference right-left vs. Parameters dimensions (individual change).

The effects that have been considered are:
- The radius where the force on the contact tooth in the sun (side) gear is. It shows that as bigger the radius is as higher difference between right and left torque appears.
- The radius where the force on the contact tooth in the planetary (pinion) gear is. This behaves the other way round, as higher the radius respect the revolution axis is as lower difference on torque. This is due to the fact that the forces that push the pinion gear towards the housing are lower as smaller the gear ratio is, keeping the same radius in the side gear.
Actually, these two parameters should be studied together since if one increases the other does is as well.
- Effective radius where the equivalent friction torque is applied on the side gear. As higher the radius is, for the same force the friction torque increases, and the difference torque between shafts does it as well.
- Effective radius where the equivalent friction torque is applied on the pinion gear. The conclusions are analogously as before, but the curve is above the one of the side gear. According to what it has been checked before, in the Figure 2.5 and 2.6, the side gear friction torque is higher than in the pinion gear. But here, no strong conclusions can be extracted since these parameters cannot be changed independently.
- Pin radius force is the distance between the centre of the pin and the place where the contact with the pinion gear is in longitudinal direction. In the sketch below it can be seen the parameter. Basically, the Equation (2.9) has been replaced for the following expressions so as to be able to check the effect of the length of the pinion pin (relationship between the input torque and the forces in the pin).

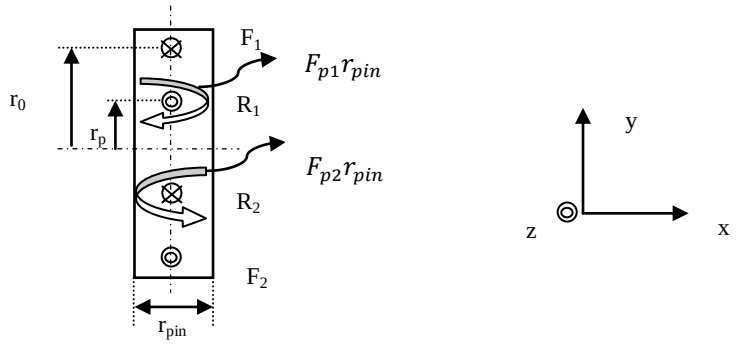

Figure 2.8. Sketch of the pinion pin.

$$\sum F_x = 0 \rightarrow \quad F_{p1} - F_{p2} = 0 \tag{2.16}$$

$$\sum F_z = 0 \rightarrow \quad R_1 - F_1 - R_2 + F_2 = 0 \rightarrow R_1 = R_2 \tag{2.17}$$

$$\sum M_x = 0 \rightarrow \quad F_1 r_0 2 = R_1 r_p 2 \rightarrow R_1 = \frac{T_0}{2r_p} \tag{2.18}$$

Observation: The forces F_{p1} and F_{p2} are not in the plane of the drawing (they are contained on the plane y-z). These are the friction forces created due to the contact reaction to transmit the engine torque. They are considered to be on one point.
The forces F_1 and F_2 are the actions that come from the housing (transmitting the input torque thanks to the fastened connection between housing and pin).

$$F_1 = F_2 \tag{2.19}$$

$$F_1 + F_2 = \frac{T_0}{r_0} \tag{2.20}$$

Finally, the equation (2.18) is multiplied per 2 in the model in order to consider the symmetry effects of the bottom planetary gear.

So, once the equations are replaced, the parameter r_p can be analysed. It is seen that as longer it is, as less torque difference between shafts exists. This is because the length of the pinion reduces the reaction force which transmits the torque to the rest of the system (R_1), and the direct effect is that the friction between the pinion gear and the pinion pin is reduced since it is proportional to the normal force R_1. Besides, the forces of the contact mesh as well as the normal forces on the gears are reduced so that the friction torque in these places is reduced.
These last three parameters cannot be changed independently; basically they should be studied together since they are limited by the inner diameter of the housing, from a manufacturing point of view.
So, the parameters to study must be those which can be changed by being manufactured in the workshop. Otherwise it can be physically impossible or at least, not real conclusions can be got.
They have been split up in three groups:
- Firstly, the inner diameter of the differential housing. From a manufacturing and assembling point of view, it affects three variables. These are the length of the pinion axle, the radius of the transmission force of the sun gear and the planetary gear (in the

gear mesh). Thus, a relationship between all these variables with the housing diameter is found in order to make the swept that affects all of them.
- Secondly, the width of the contact surfaces between the sun gear and the washer and the planetary gear and its washer as well (independently one from the other).
The width is the total radial distance in contact between the gear and its washer. It is related with the friction torque if it is still taken over that the equivalent friction radius keeps always in the middle of this width parameter.
- Finally, the diameter of the pinion axle. It is a controllable parameter because it affects just the pinion itself (the radius is just affected by itself and is proportional to the friction torque between pinion gear and pin).
Thus, these are the parameters that have been figured out in order to be able to control them by the manufacturing process.
Below, there are the equations related on the geometry of the parts that have allowed sweeping the parameters for the whole range of dimension.
First of all, for the equivalent radius where the friction force is applied, the swept is made with the parameter w_s and w_p that means the width in contact with the washer in the side and pinion gear respectively.

$$r_{fr} = r_{si} + \frac{w_s}{2} + ch_s \tag{2.21}$$
$$r_{fl} = r_{si} + \frac{w_s}{2} + ch_s \tag{2.22}$$
$$r_{pf1} = r_{pin} + \frac{w_p}{2} + ch_p \tag{2.23}$$

Then, for the equivalent radius in the contact gear mesh (if it is still considered in the middle of the gear tooth) the equations are:

$$r_{01} = (R_h - b_w - gap - \frac{B}{2}) \cdot \sin(\phi) \tag{2.24}$$
$$r_{02} = (R_h - b_w - gap - \frac{B}{2}) \cdot \sin(\phi) \tag{2.25}$$
$$r_{p01} = (R_h - b_w - gap - \frac{B}{2}) \cdot \cos(\phi) \tag{2.26}$$
$$r_{p02} = (R_h - b_w - gap - \frac{B}{2}) \cdot \cos(\phi) \tag{2.27}$$

where the gap is the free space between the end of the tooth and the inner housing radius.
Here it can be checked if the geometric equations are close to the gear ratio. As the pinion has 9 teeth and the side gear has 14 teeth, the gear ratio can be defined as:

$$i = \frac{z_s}{z_p} = \frac{14}{9} = 1{,}5 \tag{2.28}$$

Now, if it is gear ratio is defined using the equivalent radius where the transmitted force is applied, the gear ratio should be pretty similar:

$$i = \frac{r_{01}}{r_{p01}} = \frac{(R_h - b_w - gap - \frac{B}{2}) \cdot \sin(\phi)}{(R_h - b_w - gap - \frac{B}{2}) \cdot \cos(\phi)} = 1{,}4 \tag{2.29}$$

Thus, the gear ratio fits quite well, although there is a slight difference between them due to the calculation of the radius according to the geometry of the gears and the approximations done.

Hence, if these equations are written in the simulation the swept of the parameters can be done. So, after modifying the simulation program and adapt it to be able to get and check all these variations, the following plot is got:

Note that in order to make the simulation easier and simple the surface of the gears in contact with the housing (by means of the washers) has been considered flat. The effect is that the normal force does not depend on any angle (either β or θ). Then, when the swept is done, it is not affected by the normal angle which changes for each value.

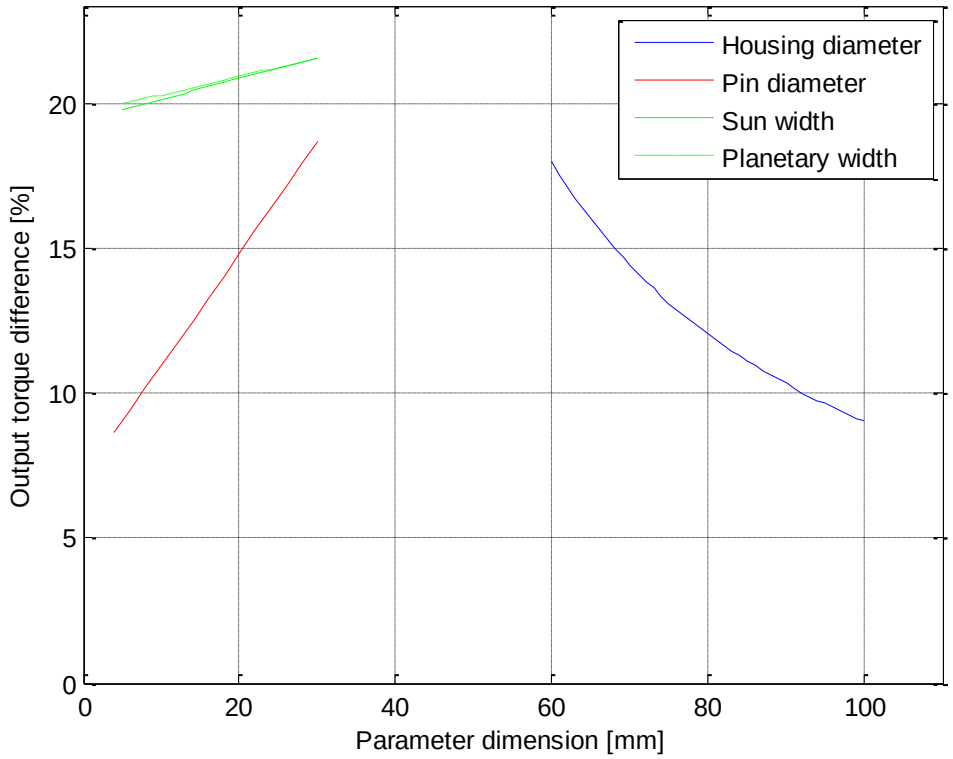

Figure 2.9. Output torque difference right-left vs. Parameters dimensions.

It can be seen that the dependence of the width of the pinion and side gear is lineally constant and the output difference is higher as long as the width increases. In addition, the effect is stronger with the side gear width than the pinion width. However, in the analytical analysis of the contribution of each parameter, it was shown that the friction between the side gear and the washer represented around the 40% of the total amount of difference torque, but here, the side gear value due to the change of the surface in contact does not represent as much due to not having considered the spherical shape of the gear. So, it might be claimed that having a flat surface in side gears would help reducing the friction in this contact area.

Furthermore, a large pin diameter increases the losses in the output torque and also, the proportional dependence is bigger, it is said, for smaller changes in the diameter, the output torque notices a stronger variation. This is due to the fact that the pin reactions with the planetary are really heavy; they are the forces which transmit the total torque so that the friction forces are really big, and just a small change of radius, corresponds to a big change of the friction torque.

Finally, the blue curve represents the dependence between the housing inner dimension and the output torque difference. As it is seen, the dependence is not linear and for big housings the amount of torque difference between axles is reduced. It is a multiple affect with the parameters explained before.

On the other hand, if an independently swept of the friction coefficient value is done, the plot below is got. It has considered, as well as it has been done in the modelling, that the friction coefficient is equal in all the contacts. Besides, it has been the same study setting different coefficients for each contact and sweeping one each time keeping the other to the predefined value of 0.2.

Note that to make this study, the normal force applied on the surface in contact between gears and washers has been considered again as the original equations with the spherical shape, so that the angles β and θ are taken into account.

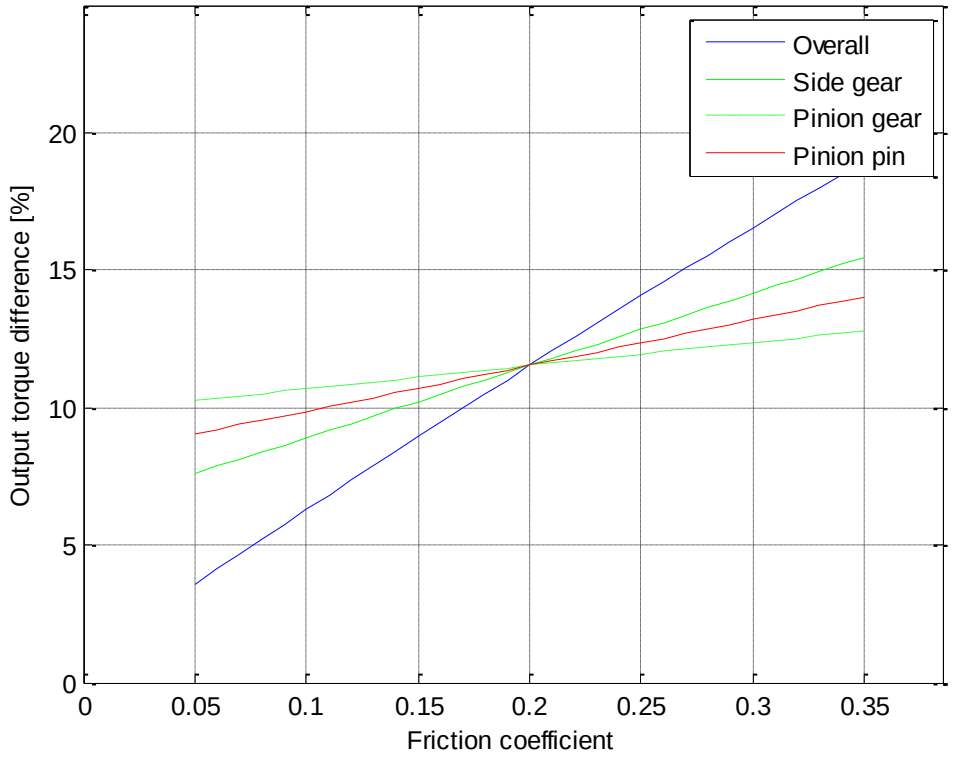

Figure 2.10. Output torque difference right-left vs. Friction coefficient.

As it was expected, the effect is totally linear, as bigger the coefficient is, as more difference torque between shafts is got.

Moreover, it is observed that all the curves are meeting in one point that belongs to the friction coefficient of 0.2 which has been set to every contact when the sweeping for each was doing.

It is seen how important the friction in each side is. It corroborates the results already got for the contribution of each loss in the Figure 2.5 and 2.6. The side gear is the one whose effect is the biggest. For low friction coefficients, makes the whole system reducing the difference of torque between shafts. Whereas, the pinion gear friction is the one which contributes the least.

3 Rig Test Design

Testing the real differential in the workshop is done not only to get the Loss Model fitting the real behaviour, but also to check results of the model thanks to results taken from the rig.

This test consists on an evaluation of the difference of output torque in each side of the differential. Such a test is done fixing the housing on a bench so that allows loading both drive shafts equally and after adding extra load in one of them until motion starts. Once this motion is seen (the driveshafts start turning in different directions), the extra load that have been put in one of these axles will be quantified as the losses (torque difference between left and right) that correspond to this input load.

A priori, the test will be carried out according to an experiment plan (see Chapter 3.2). Particularly, six different experiments will be done based on statistic dependence of parameters so as to be as efficient as possible. Finally, the statistical dependence of these parameters will be studied using Minitab software in order to check the correlation between each experiment. Nevertheless, before starting the experiment plan a test with the original differential in order to check how the model differs from the test in order to edit it.

3.1 Rig design

Testing means also an extra design to be done. Thus, parallel to the model building stage, the design of the complete rig is done.

In the *Appendix C*, the steps done for the design can be checked more carefully.

However, in the following Figure 3.1 it can be seen an overview of the rig assembly:

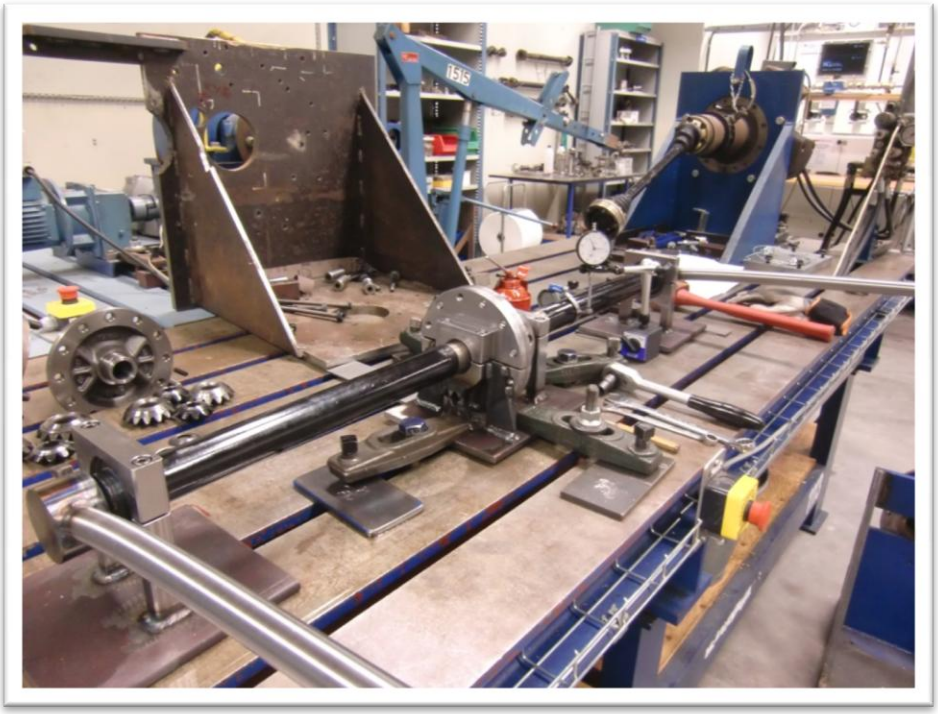

Figure 3.1. Rig overview.

3.2 Experiment planning

To be efficient, a statistic experiment planning had to be done. This planning reduces the amount of experiments in order not to prove all the possible combinations of the parameters that can be changed in the workshop.

First of all, one experiment with the current differential without changing anything is done so as to check the model and to feel comfortable with the rig (check if it works properly or some modifications must be taken into account). Once this is done successfully, the model will be updated in case it is necessary and afterwards it will be proceeded with all the possible changes in the design.

From all the wide range of possible parameters to analyse, not all of them can be changed in the workshop since some involve a totally new differential design, for instance, changing the inner diameter of the housing or the pin axle diameter.

But some other parameters can be changed, such us the material of the bushings (it affects the friction coefficient), either using the current steel bushing or testing with the Nedox coating, which VCC has been looking into, that are supposed to have a lower friction coefficient.

On the other hand, still taking over the equivalent radius of the friction torque is always in the middle radial distance of the contact surface, the width can be machined in order to see the effects of increasing (supposedly higher torque) or decreasing the equivalent radius. This last change is made machining the width of the gear in contact with its washer. If it is taken into account (and it has been in the model) that the effective radius is in the midpoint of the total width, then machining downwards will make the radius bigger (the contact surface with the housing will be further from the axis) and vice versa. This is an assumption done *a priori* that will be proved by the results and also by the FEM analysis.

Hence, in the following table can be seen the parameters that can be studied in order to check how much they contribute to the overall torque split over the differential. In addition, this will give a general idea about the dependence of all this parameters.

Table 3.1. Possible parameter changes.

PARAMETER	**OPTIONS (CHANGES)**		
Washer material	Ordinary	Nedox + Ordinary (combination)	Nedox
Width of the sun gear	Current dimensions	Bigger effective friction radius	Smaller effective friction radius
Width of the planetary gear	Current dimensions	Bigger effective friction radius	Smaller effective friction radius

There are 3 parameters (material of the washer, width of the sun gear and width of the planetary gear). So, it would mean that in order to get all the combinations between them 2 x 2 x 2 experiments should be done (taking into account that every parameter has three levels (+, - and 0) and the midpoint is neglected). But, if the relation and interaction between the parameters is not taken into account, and the individual effect

to the result is the relevant relation that is wished, the test planning can be reduced to 4 combinations, taking the orthogonal points between them (neglecting the mid level of each parameter).

Four of the six experiments are orthogonal between them. Then, a midpoint will be added in order to get further information about the relation between the values and the result, and finally there is the current combination.

Actually, doing all the possible combinations is not physically possible due to the time that each one takes, so according to the statistical design of experiments the amount of experiments is reduced to six.

All this combination can be seen in the Table 3.2 below:

Table 3.2. Test planning.

TEST PLANNING		
Planetary Width A	**Sun Width B**	**Washer material C**
Min	Min	Nedox
Max	Min	Original
Min	Max	Original
Max	Max	Nedox
Original	Original	Nedox just in Sun
Original	Original	Original

In the end of the experiment stage (Chapter 4) the statistic study will be carried out in order to get the results of the dependence between parameters. It is done using Microsoft Excel Minitab and Microsoft Excel software where after writing down all the results it is possible to see the combination and effects of each independent test.

This would be just valid in case the assumptions done so far are right and the real equivalent radius moves in such a way that remains in the mid point in radial direction on the contact surface once this contact surface is machined.

3.3 Rig outcome

In the *Appendix C*, the measurement limitations, test measurements, comparisons between a new and used differential and a finally checking between the first results and the Loss Model can be checked in more detail.

4 Rig Test Results

4.1 Test results

After carrying out the first tests using the current M66 differential (*Appendix C*), it was possible to know the limitations of the rig and try to proceed in such a way to avoid the possible effects that might be got from the testing results. As it is explained in this *Appendix C*, each test will be done three times for each input load and the average will be taken, using finally a totally new M66 differential.

In the *Appendix B*, it can be seen the results from the Rig Test.

4.1.1 First Test: Original differential

Once the three experiments are done, the average is taken and then the results can be analysed. In this first test it has seen how the real behaviour is. It seems as in the beginning, for small torques, the effect is totally linear as the previous model got. But, as soon as the torque increases it seems as if the difference between left and right increases in a non-linear way. However, it might be approximated as a two linear models with different slopes as it has been shown in the *Appendix C* or even with a fully linear curve. The conclusion will be extracted after having studied the FEM analysis, since there is no clue yet if the variation is due to the behaviour of the differential or if it is just due to the measurements.

In the Figure 4.1, the results for the original design are shown:

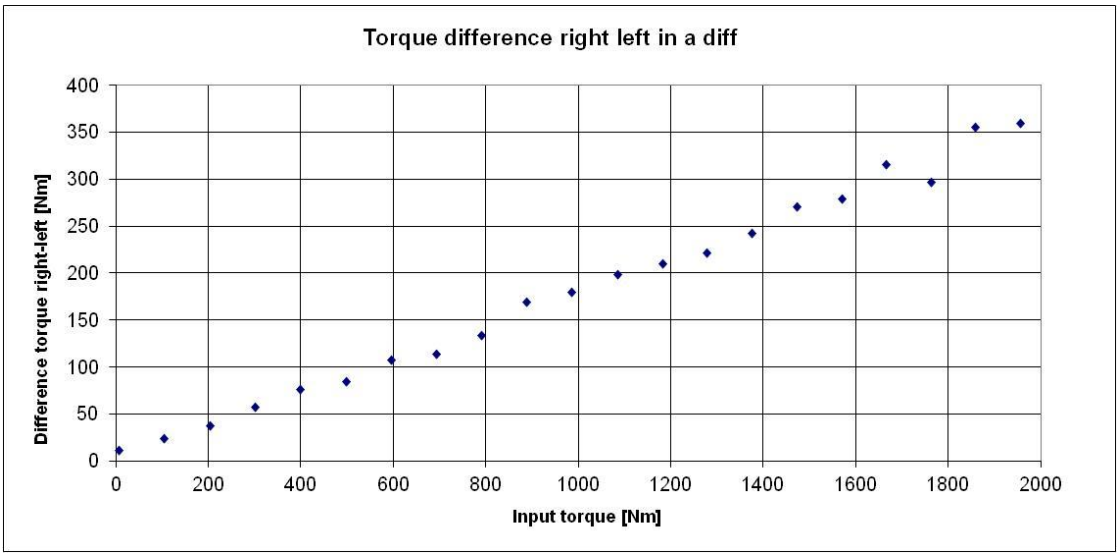

Figure 4.1. Test 1 results.

4.1.2 Second Test

The second experiment is done using the pinion gear with the surface machined inside, so having the contact surface with the washer moved towards the outer (it would mean having bigger equivalent friction torque radius).

On the other hand, the side gear is machined the vice versa, keeping contact with the surface close to the shaft (smaller equivalent radius).

The results of this test are shown below:

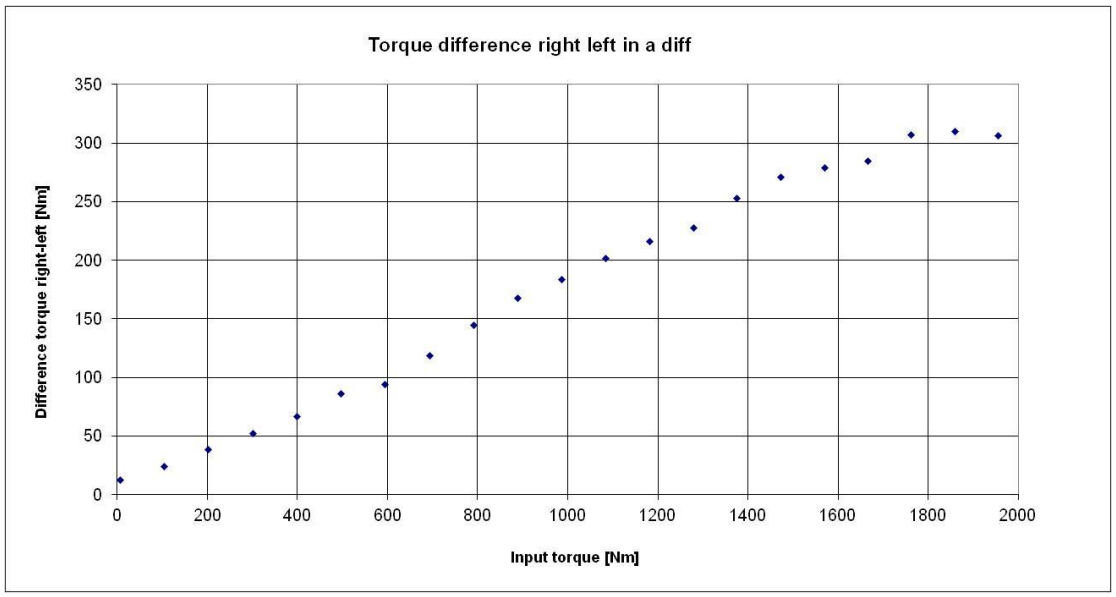

Figure 4.2. Test 2 results.

It is seen how the behaviour is more or less equal than the original differential. If the assumptions are done, the difference should be lower. Indeed, it is lower than before. However, if the equivalent radius of the side gear has been reduced but in the pinion gear has been increased, the effects should be cancelled. But, as well as it has been seen in the Chapter 2 (Loss Model), the side gear has stronger effect in the overall friction torque. Then, it may be claimed that the quality of the results looks more roughly reasonable according to the assumptions done so far. But, it is not possible to get any conclusions regarding the quantity yet.

4.1.3 Third Test

This test is the totally opposite side compared from the one explained above. The gears are switched having the side gear with the maximum diameter and the pinion one with the minimum diameter.

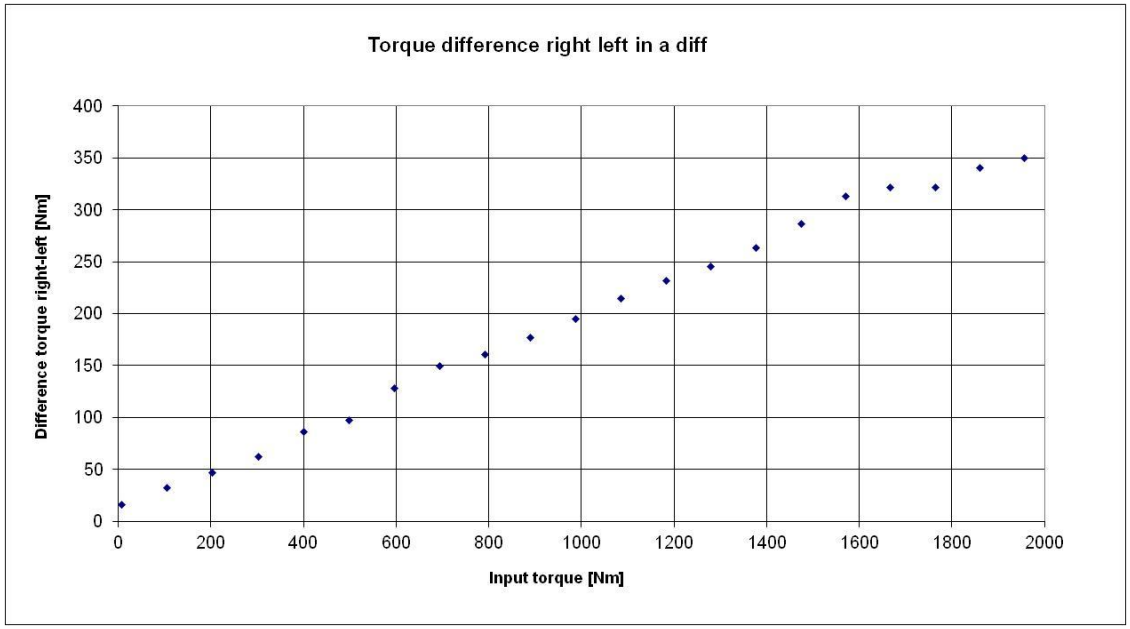

Figure 4.3. Test 3 results.

In this case, the results look quite similar to the original differential, or even lower losses. If the assumptions taken in the Chapter 2 were true, the losses should be even higher since the equivalent friction radius of the pinion pin has been reduced and in the side gear has been increased. But, the effects are stronger in this last contact than the contact between the washer and the pinion gear. Thus, the torque split should have increased slightly.

It could be said either that these results may not be reliable or that the assumptions were wrong and basically, there is no reason to claim now which the real effect of machining the surface of the gears is to the overall friction loss.

Thus, it was decided to stop the test planning and just to check, for instance, testing such a combination that allowed observing its effect, in spite of not having included it in the test planning. This is analysed in the following Subchapter 4.1.4.

4.1.4 Extra Test

In this experiment, the contribution of the pinion is shown; the setting was just changing the pinion gear, machined in order to have a bigger radius.

The rig results show something that was not expected, according to the model, the difference of torques should be higher but, here it is seen how it is lower than the original differential.

However, it is seen how the slope is higher for low torques, it would mean that perhaps the effective equivalent radius might have increased just for low torques (during the linear behaviour) and a nonlinear effect shows up for higher torques.

Actually, it was decided to fully stop the test planning and analyse all the results got, to see not only if there is any dependence between them (if it is really what it was expected according to the assumptions done in the Chapter 2), but also if there was

any other effect due to the measurements, such as the spread was bigger than the real change of the parameter done. This is summarized in the following subchapter.

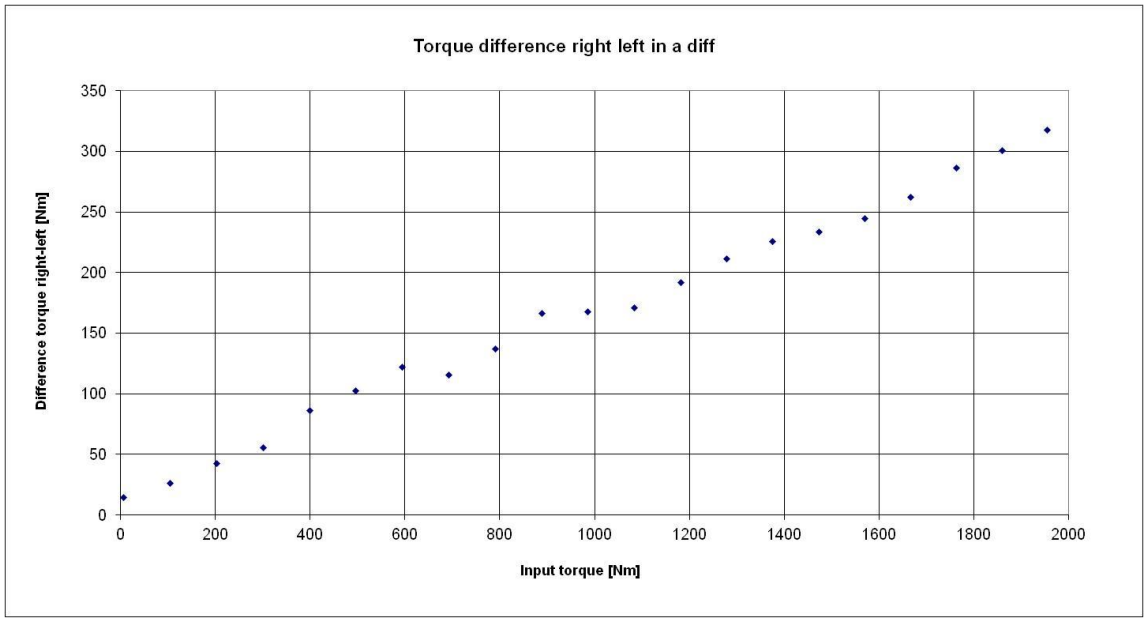

Figure 4.4. Test Extra results.

4.2 Statistics results of parameters dependence

Once all the results are studied. The results show how indeed there is no relationship and difference between the combinations.

If the quotient between the standard deviation s_N and the average $\overline{x}$ is calculated for each input load for all the experiment of the first (original differential design), second (side minimum radius and pinion maximum) and third (side maximum radius and pinion minimum) tests and it is divided by the average of all the experiments, the Table 4.1 is got.

The standard deviation can be expressed as:

$$s_N = \sqrt{\frac{1}{N}\sum_{i=1}^{N}(x_i - \overline{x})^2} \qquad (4.1)$$

Then, for the first three columns (2,3 and 4), the standard deviation is calculated for the corresponding output (Extra load column, see from Table B.15 to B.26 in *Appendix B*) of each input load.

So, for each input load, in the rig three different measurements were done (Extra load measurement [Kg]) which represents the losses that the differential has for each input.

Thus, the standard deviation is calculated for each input load and it is compared to the average of these three measurements done for this input.

On the other hand, the values of the last three columns (5, 6 and 7), the comparison between the tests is done.

It has been proceeded analogously to the previous calculations. But, the standard deviation is done using the average value of the three measurements done for one test

and the average of the three measurements done for the same input load for the other test (Original differential (First test), Second or Third Test), and finally it is compared with the average of these two values ($\overline{x}$ value in the table).

To do so, all the possible combinations of comparisons have been considered. The Original Test with the Second test, the Original Test with the Third Test and the Second with the Third Test.

Table 4.1. Statistic analysis of the rig results.

1	2	3	4	5	6	7
Input load (*i*) [kg]	**Original diff (O)** $\frac{s_N}{\overline{x}_i}$	**Second test (C2)** $\frac{s_N}{\overline{x}_i}$	**Third test (C3)** $\frac{s_N}{\overline{x}_i}$	**O_C2** $\frac{s_N}{\overline{x}}$	**O_C3** $\frac{s_N}{\overline{x}}$	**C2_C3** $\frac{s_N}{\overline{x}}$
0	0,25	0,43	0,17	0,09	0,25	0,16
5	0,00	0,00	0,09	0,00	0,20	0,20
10	0,08	0,13	0,16	0,03	0,16	0,13
15	0,13	0,11	0,11	0,06	0,07	0,13
20	0,10	0,11	0,13	0,10	0,08	0,18
25	0,09	0,09	0,10	0,01	0,10	0,09
30	0,08	0,08	0,08	0,09	0,13	0,22
35	0,05	0,06	0,02	0,03	0,19	0,16
40	0,08	0,08	0,03	0,06	0,13	0,08
45	0,03	0,06	0,02	0,01	0,03	0,04
50	0,02	0,02	0,00	0,02	0,06	0,04
55	0,06	0,03	0,00	0,01	0,06	0,04
60	0,02	0,01	0,03	0,02	0,07	0,05
65	0,09	0,03	0,01	0,02	0,07	0,05
70	0,06	0,00	0,04	0,03	0,06	0,03
75	0,04	0,01	0,05	0,00	0,04	0,04
80	0,04	0,01	0,03	0,00	0,08	0,08
85	0,07	0,05	0,04	0,07	0,01	0,09
90	0,04	0,07	0,07	0,02	0,06	0,03
95	0,06	0,03	0,02	0,10	0,03	0,07
100	0,05	0,02	0,09	0,11	0,02	0,09
Average	0,069	0,070	0,060	**0,039**	**0,095**	**0,096**

Finally, in the last row, the average of all the values of every column is done. Here it is seen how the difference between the first three values is really small, so the relationship between the different tests might be meaningless.

Then, when the average of the comparison between experiments is got (bolt numbers), it can be checked how the value does not differ quite much compared to the average value of each independent test. It means that it might not exist any correlation between the different tests. In fact, it is not possible to claim that there is a relevant difference that defines a change of behaviour in the output (Extra load) so that there is no correlation between the original combination and the two other combinations.

Moreover, if a study of random regression is done using Minitab to compare the original configuration and the second test (C2), the results are found below in the Figure 4.5.

The study is done taking the final results for each test, i.e using the average of the three experiments for each input load.

It is seen how the variation between the two different tests corresponds to a 0.6%, this means that as it is below the 5%, taking into account a confidence level of the 95%, no correlation between the original combination and the second test exists.

Hence, the test planning had to be modified since using this first proposal the results have not shown reliable conclusions. Actually, it might be that the assumptions done with the equivalent radius situated in the middle of the contact were wrong and there is no knowledge to claim how the output would behave if the parameters were changed as they have been. Later on, in the Chapter 5, the FEM analysis of the differential will be done and it would be possible to check if the assumption done setting the parameters was really wrong.

In addition, in the following Chapter 4.3, a new test planning will be considered using the material of the washer as the only parameter controllable, after having checked that the first test planning set was not showing any correlation between the combinations.

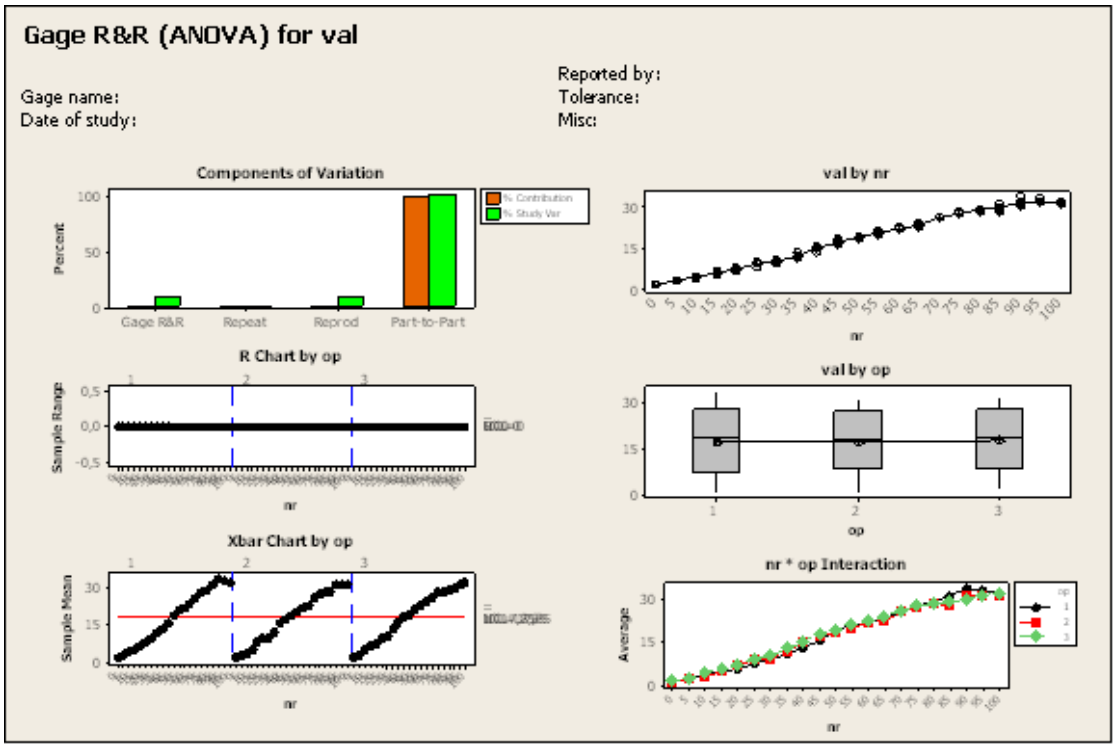

Figure 4.5. Statistic random regression study.

4.3 Testing conclusions

So, finally, since basically it is not possible to claim that the equivalent radius moves through the surface in contact with the washer as it was assumed (either the assumption was wrong or the spread due to the measurements was too big to see the real effects). By this way, it was decided to edit and do another test planning in order to get reliable results, or at least the user knew already the effect of the parameter, i.e changing washer with a lower friction material.

Thus, it has been reduced to one parameter which is the material of the washers keeping the gears as they were initially. The Nedox treatment which should have a

lower friction coefficient (the Nedox treatment from Bodycote is a coating with Niquel and Teflon so as to reduce the friction and also make the part harder).

Then, since there is just one parameter to analyse, all the possible combinations can be done (3 combinations plus the combination using the original differential which has already been done). So, the test planning will be changed to the one shown in the table below:

Table 4.2. Final test planning.

FINAL TEST PLANNING		
TEST NUMBER	**SIDE GEAR WASHER**	**PINION GEAR WASHER**
0	Original	Original
1	Nedox	Nedox
2	Nedox	Original
3	Original	Nedox

Before starting the Final test planning, the FEM analysis will be carried out in order to get the understanding of the overall behaviour of the differential when is loaded regarding the deformation, pressure distribution and contact pattern. As soon as the FEM analysis is done, the Final test planning will be able to be carried out.

5 Finite Element Modelling and Analysis

5.1 Introduction

A quasi static Finite Element Analysis of the differential is carried out in order to study the potential influence of deformable bodies on the kinematics of the differential. Particularly, the deformation of the pinion pin and its consequence on the differential kinematics, the influence of asymmetric gear mesh on axial settlement of the diff gears and the contribution of each part of the assembly to the deformation behaviour of the whole assembly.

CATIA V5R18 is used as CAE software tool by means of the linear Elfini solver so as to make all the simulation and analysis of the results obtained.

Basically, the main target of this analysis is being able to check if there are effects in the behaviour of the differential (the outcome difference torque between both shafts) which are due to the deformation of the housing respect the whole gear set (gear mesh and pinion pin) and to quantify and qualify these effects. This will be done analysing, for different input torques, the contact pressure distribution in the interference of those parts which are affected by the friction torque (mostly the contact between the washers and gears) in order to know where regions of high contact pressure are.

Furthermore, the pressure distributions of sections of the washers and pinion pin will be got in order to get the understanding of the modelling and corroborate the results from the former deflection study of the differential kinematics.

Finally, a study of the torsional stiffness of each part will be done by studying the rotational displacement contribution, due to the input torque, of the assembly parts. By this way, it will be known how important the contributions of each part are. Not only the stiffness, but also the strain results will be extracted in order to study where most of the local deformation/straining of the material take place.

Apart from that, there were some initial hypotheses that have been considered so far.

Thus, the intent of the FEM model is to either confirm or discard these:

Firstly, in the Loss Model, the effective radius was considered to be in the middle point between the inner and outer radius.

Secondly, the pressure distribution in the washers was considered to be even through the entire circumference and similar for each radial section.

Thirdly, the housing had the most contribution of the deformation since it is not the stiffest compared to the gear set assembly.

5.2 FEM analysis

5.2.1 Modelling set-up

The first step is setting up a simplified model without detail, like contacts, to gain confidence in the overall functioning of the assembly. Firstly, all the contacts were neglected so as to make it easier and reduce the running time.

Once, the simplified model was already working, all the constraints were defined.

Firstly, the rotation of the side gears were fixed at the spline interface of the drive shafts, by this way the system became with one degree of freedom (as it is interesting to know the maximum torque difference just when it starts turning, moment where the friction torque gets the highest value possible).

Then, the contacts were put between the four washers and its respective gear, as well as between the pinion pin and the pinion gears. Whereas, as theoretically the washer should be stuck on the housing and the most of the sliding should be between the washer and the housing, the constraint regarding the contact between washer and housing was decided to be just normal sliding contact, hence only restraining movement in normal direction.

Moreover, the general other contact constraints (allowing also separation) were set to the contact mesh.

Finally, the housing was constrained in order not to allow it to move in the 3D space and just allow the rotational movement according the *y-axis* (axial axis), an sliding constraint was put at the bearings shoulders and an axial constraint. Besides, the load was put in the surface where the ring is attached and the torque is transmitted on this face. In the following picture, it can be seen an overview of all the constraints:

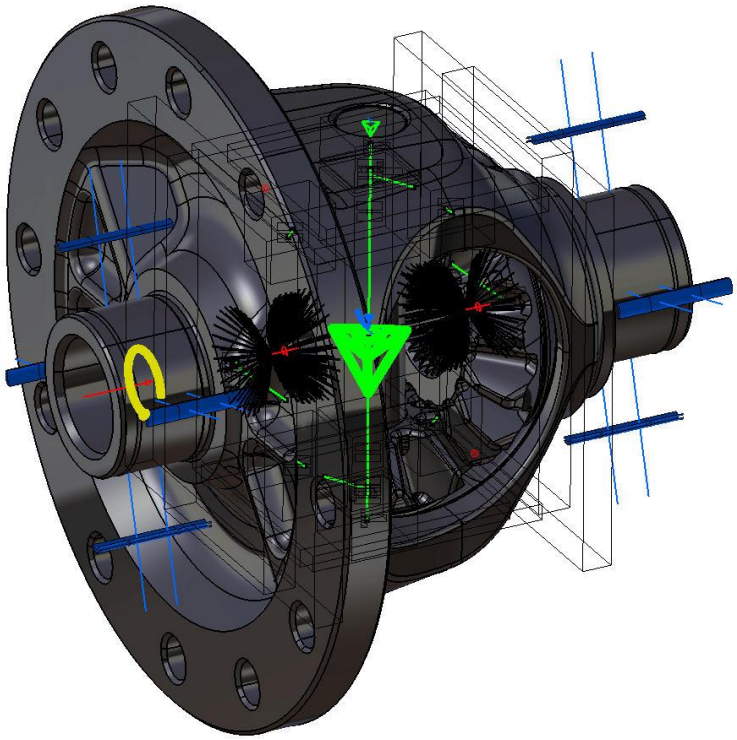

Figure 5.1. Definitive constraints setting.

Once the simulation has been run, the results are possible to be observed. In order to get a clear understanding of the behaviour during the wide range of input torque, four different simulations were done with 100 Nm, 500 Nm, 1000 Nm and 2000 Nm.

5.2.2 Analysis outcome

In the following figures can be seen the most reliable results for one load, for instance for 500 Nm, for the other input loads, the results can be found in the *Appendix D* (the conclusions are analogously). These results are the total deformation of all the system,

the deformation of the pin and the pressure distribution in all the contact parts for the input torques of 500 Nm, 1000 Nm and 2000 Nm.

The Figure 5.2 shows the total translational deformation, here it is seen that once the housing is loaded and the shafts are being fixed, the maximum translational should be out on the ring. The maximum value is 0,449 mm.

The side gears seem quite stiff, they are standing still because they are fixed, just the force is applied through the contact mesh, but not big enough to see some displacement on these gears.

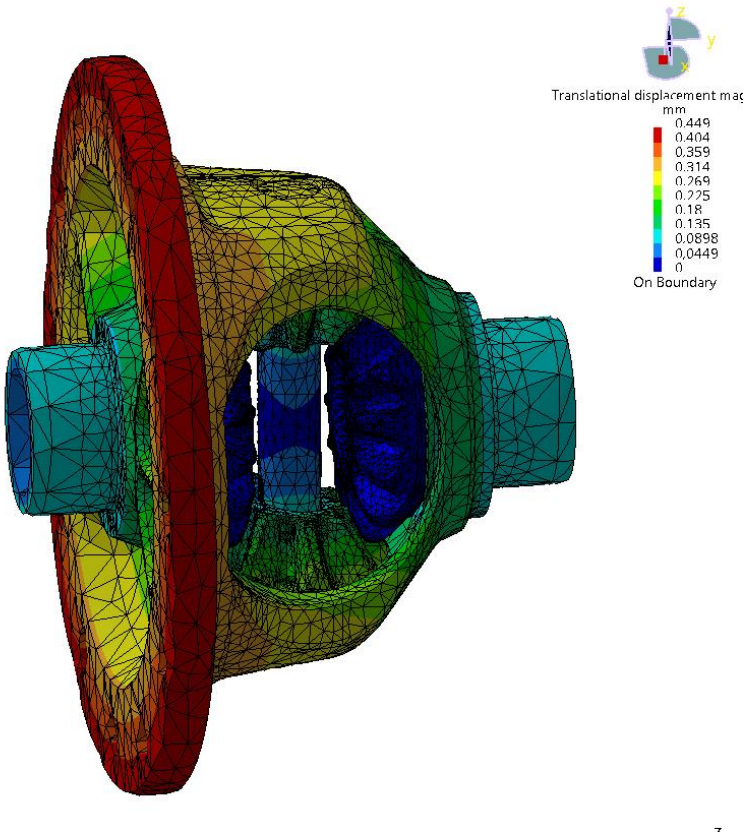

Figure 5.2. Total translation deformation of the whole assembly.

On the other hand, in the Figure 5.3 can be seen the shape that the pinion pin has once it is loaded. It has a kind of "S" shape, that is due to the fact that the forces are transferred from the housing to the pin mainly by shear and bending, which transmit the whole torque to the gear set, have one direction (action torque), and then the reaction forces where the pinion gears are set try to react to the pin in order to not allow it to turn (action-reaction force since the side gears are fixed).

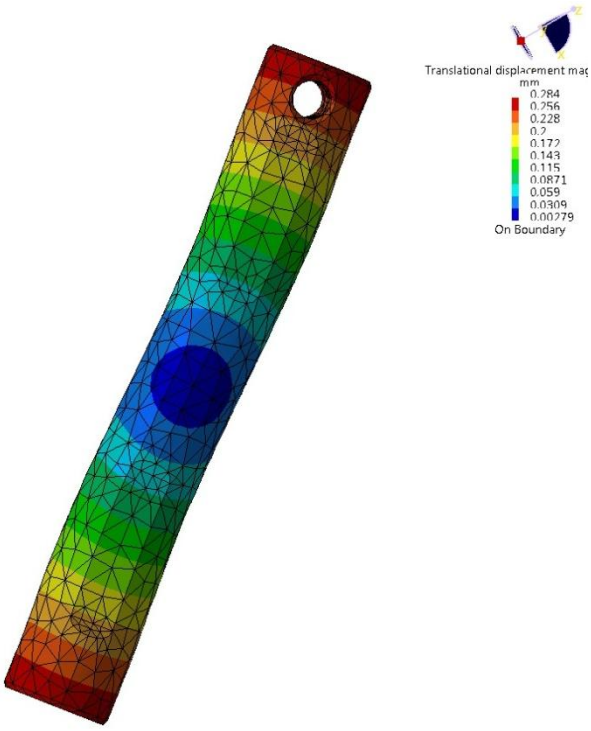

Figure 5.3. Total translation deformation of pinion pin.

Furthermore, the following Figure 5.4 shows the effect of the nodal contact pressure distribution, where the maximum values are on the contact mesh. It is seen that the values and distribution is not symmetrical. Actually, that has been and will be the major problem of the reliability and variance of the results depending on the gear mesh chosen (which influences the directional vector of the resultant reaction force acting on the gear teeth flanks), not only in the simulation but also in the test results. It is not possible to constraint the gear mesh in such a way that the results are symmetrical in all the directions. In the real case with the differential set in the end of the transmission of a car, once it is running, the force depends on the instant of time and has a sinusoidal shape during the entire interval. In this project, it can be just studied the static effect and then the gear mesh is not possible to control. So, it was just tried to keep it as centred as it was possible, but the results will be affected by this asymmetric.

As far as gear mesh is concerned, in the following figures the contact pressure distribution is seen so that it can be observed how the peak of the pressure is on the contact mesh. The pressure due to the forces on the teeth is situated on the middle of the tooth itself, by this way, supposing the contact mesh more or less in the middle point of the teeth has been a realistic assumption during the simulation in the Chapter 2.

However, the asymmetrical forces applied in each contact mesh will affect the quality of the results. Once the model was set, it was not possible to constraint symmetrically all the gear meshes so that the forces and pressure distributions in each tooth was the same. That will affect, basically, the deformation and contact pressure between left and right side for the contact between side gears and washers, which will not be even.

The values of the pressure for the contact mesh are so high compared to the other pressure that getting results for the other contact zones becomes difficult to be

understood with the current contact pressure plot (Figure 5.3), this is the reason why the pressure nodal value has been limited in the Figures 5.5 and 5.6 to be able to see the effect on the washers and pins.

If it is sum up with a table the maximum pressure nodal value for all the contacts in order to compare with the gear tooth contact mesh pressure value, it yields with the Table 5.1. It shows the maximum pressure for the input load of 500 Nm due to the contact mesh force is around 20 times bigger than all the other maximum pressure nodal values from the other contact pressures.

Table 5.1. Comparison of maximum nodal pressure values.

Contact	Maximum nodal pressure [N/m^2]	$\frac{\text{Maximum contact mesh pressure}}{\text{Maximum contact}_i \text{ pressure}}$
Contact mesh	$5{,}72 \cdot 10^8$	1
Side gear washer	$2{,}7 \cdot 10^7$	21,18
Pinion gear washer	$3{,}2 \cdot 10^7$	17,86
Pinion pin	$3{,}06 \cdot 10^7$	18,69

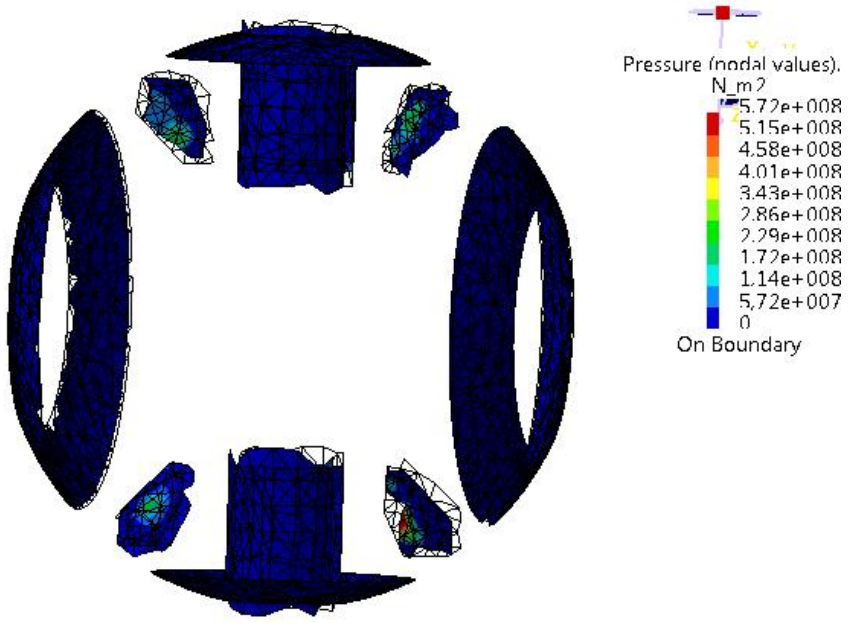

Figure 5.4. Contact pressure distribution.

Moreover, when the differential is loaded, the teeth are bended and the contact pressure on the bushings is not even through the entire circumference. This fact is possible to be seen in the following figures.

In the Figure 5.5 and 5.6 it is observed how the pressure in the washers and the pin is. The whole gear set is bended so that basically there are two main zones of contact in

the side gear washers. The reaction forces on the teeth have two components, one which transmits the torque and the other one which pushes the gear to the housing. This is the force responsible of the contact pressure between the gear and the washer.

Thus, the contact pressure should be higher close to the gear mesh than to some other place of the washer and gear contact. Indeed, the left contact distribution behaves like that. Due to the deformation of all the gear set, mostly all the contact between the washer and side gear just appears close to the gear mesh since the push force comes from it. As far as it goes from here, the pressure is reduced until it becomes neglected (without contact) in the opposite 90º sides from the zone where the contact is.

However, the right washer has more than one contact zone. This might be explained due to the asymmetrical gear mesh, the right part of the gear set is bended differently and some other contacts appear, in fact, the forces towards the right side are bigger (the maximum value seen in the Figure 4.4 belongs to the right contact mesh).

So, clearly, that might be the main reason why this side has another pressure distribution compared to the left one. The other explanation might be that the input torque is no applied in the middle of the housing and by this way the housing might be deformed unequally in both sides. However, it is not possible to claim it right now that will be checked in the Chapter 5.5 during the deformation contribution and stiffness test.

Anyway, the left side pressure distribution seems to be more symmetrical to the y-axis and the main contact is close from the contact of the gear mesh. This force is the one that pushes the gear to the washer.

On the other hand, it is seen that in the pinion gears, the pressure looks more or less even in both, and it is acting just in one zone for each washer (opposite sides for the top and bottom one). This is due to the deformation shape of the pinion pin, one washer is bended in on direction and the other in the opposite, due to the whole bending of the gear set plus housing. So, the cause of the contact force is still the reaction force component of the gear mesh. But, the difference between the side and pinion gear contact is that in the pinion the contact is affected by the deformation of an "S" shape of the pinion pin, then all the contact pressure sits around a half of the circumference of the washer between both contact meshes, so that roughly the other half of the washer is lifted up and the other half of the circumference contact between pinion gear and washer is zero. Whereas, in the side gear the contact is more or less through the entire circumference, although the main pressure is close to the gear meshes.

In these washers (pinion gear ones), the pressure distribution is opposite (in the opposite sides of the washer) but very similar in both, because the effect of the asymmetric gear mesh does not influence. Thus, the forces in the pin due to the input load should be quite similar in both sides. In these figures it can be observed that it is like that, but in the Chapter 5.4, the pressure distribution will be analysed and it will be possible to check if there is any difference or not in the radial pressure distribution between the top and bottom pinion gear contacts.

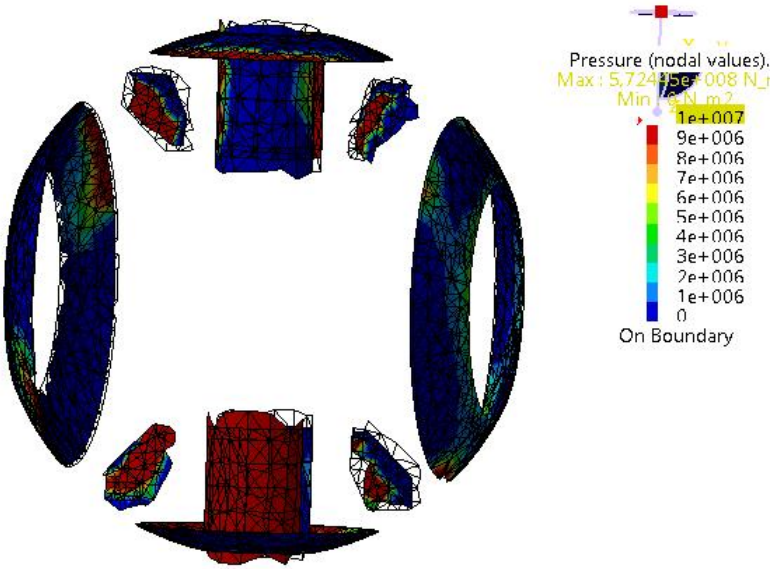

Figure 5.5. Contact pressure distribution (scale restricted view 1).

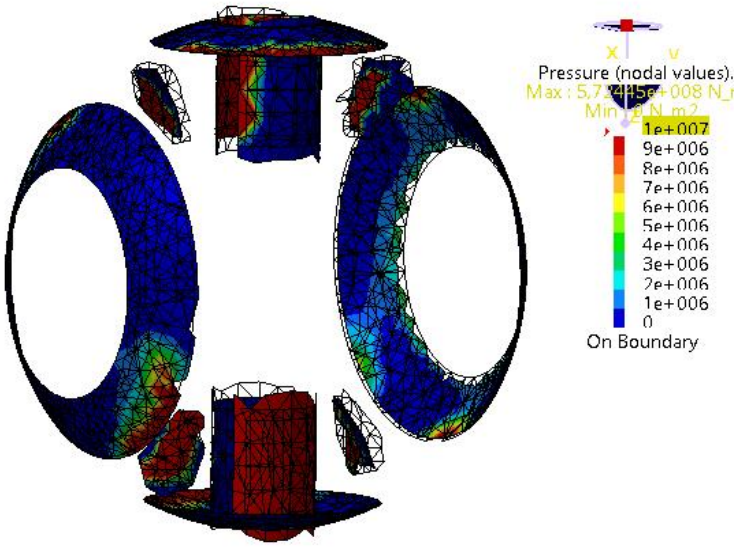

Figure 5.6. Contact pressure distribution (scale restricted view 2).

5.2.3 Analysis conclusions

To sum up, as soon as the simulation analysis is done, it has been checked when the differential is loaded the effective radius is not on the middle radius of the bushing, it is displaced to the outer part due to the deflection of the whole assembly and the way how the torque is transmitted between the housing and the gear set. This probably movement of the effective radius to the outer edge will be studied in the following Chapter 5.3, in order to quantify the values.

Regarding the gear mesh, it has not only been checked how big the values of pressure are compared to the pressure in the pin and washers, but also the asymmetrically of the contact mesh which affects the behaviour of the side gear and washers contact pressure.

Furthermore, it is seen how the pin axle is bended due to the transmitted torque. That affects the contact equivalent point force distribution compared to the one supposed in the rigid Matlab model. It was supposed having an even pressure with the result force applied in the centre of the pin, but due to this deflection the friction force will have an offset from the centre. Basically, the effect of this deflection makes the gear and pin axle tilting and then the surfaces in contact change. However, it will not affect the simulation Matlab model, in terms of results, since the force will be still there and the friction radius will be calculated using the friction force times the radius of the pin which is still the same.

5.3 Deformation effects on the output torque

What may be the cause and explanation of the non-linear (or change of slope curve in the measurement output) is the change of the contact pressure points on the washers due to the deformation. This study will check, since it is not possible to claim it before carrying it out just the results from the Chapter 5.2 qualitatively, if there is any parameter that causes this non linear behaviour of the M66 differential.

Thus, all the contact pressure distributions of all the washers will be studied in order to check how big the equivalent radius is. Actually, an assumption must be done to allow studying this. This is that the friction force is proportional to the contact pressure. It has been already supposed in the Chapter 2, using the Coulomb model, the friction pressure is equivalent to the contact pressure times the friction coefficient. Thus, getting results from the contact pressure means getting results from the friction pressure distribution.

To do such a study, all the values for every node will be needed. CATIA allows the data to be exported.

Nevertheless, a new coordinate system has to be create in order to know the exactly radius of each node. As it can be seen in the Figure 5.7 and 5.8, the y-axis is the revolution axis of the washer and the minimum square distance between x and z axis represents the radius to the y-axis (the same is created for the pinion gear washer).

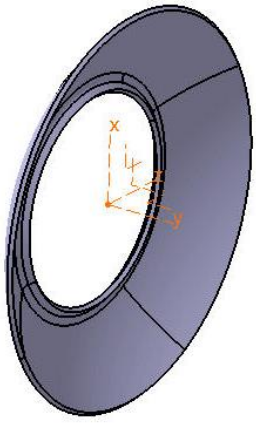

Figure 5.7. Coordinate system of the side gear washer.

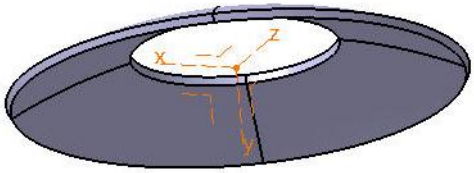

Figure 5.8. Coordinate system of the pinion gear washer.

By this way, when all the coordinates of the 1024 nodes of each side gear washer and the 268 nodes of each pinion gear washer are got, the radius for each node to the y axis can be calculated as the square root of the sum of the x square distance and z square distance. So, every node has the radius coordinate respect the y-axis and it is:

$$R_i = \sqrt{{x_i}^2 + {z_i}^2} \tag{5.1}$$

In order to calculate the equivalent radius, which is defined as the radius where can be claimed that the equivalent pressure is applied, the following operation must be done so as to consider the weight that every pressure node does to the y-axis:

$$R_{eq} = \frac{\sum_{i=1}^{n} R_i P_i}{\sum_{i=1}^{n} P_i} \tag{5.2}$$

And thus, the equivalent pressure, which is that pressure that is applied to the equivalent radius and has the same implication to the overall system as the pressure distribution of each node for each radius, can be calculated as:

$$P_{eq} = \frac{\sum_{i=1}^{n} R_i P_i}{R_{eq}} \tag{5.3}$$

Once that is done for different load cases through all the range of input torque, the results obtained are sum up in the Table 5.2 below:

Table 5.2. Outcome of equivalent radius of the contacts on washers for each load.

Equivalent radius [mm]/Input Load	**100 Nm**	**500 Nm**	**1000 Nm**	**2000 Nm**
Side gear washer left	27,15	27,15	27,13	27,12
Side gear washer right	23,32	23,33	23,32	23,34
Pinion gear washer top	18,50	18,50	18,50	18,44
Pinion gear washer bottom	18,50	18,50	18,40	18,47

It can be checked then that the equivalent radius keeps equally during all the wide range of torques. The four samples studied for 100, 500, 1000 and 2000 Nm are enough to claim that the deformation of the housing and gear set affects linearly the friction torque on the contact between gears and washers since the equivalent radius is

independent on the input load. Hence, the probable non-linear effects that could have been considered due to the results got from the rig (and due to the measurement method) and not due to the design of the differential. It may be claimed that the differential has a linear behaviour depending on the input torque, the slight non-linearity that was shown in the results from the rig might be due to several facts such as just the measurements mostly (for instance the misalignment of the rig may affect or the different gear mesh position every time or the wide spread got due to the measuring method), slight difference on the oil thickness in each washer (although the oil thickness can be neglected) and slight bending difference on the housing.

On the other hand, some other conclusions can be extracted from this deformation study of the differential.

First of all, the equivalent radius for the left washer is not the same as for the right one. Supposedly, the load should be symmetrically distributed so that the effects should be more or less equal. However, due to the asymmetrical gear mesh and maybe due to the asymmetrical torque application which is on the left and not on the centre (note that it will be studied in the Chapter 5.5) the behaviour of each washer is not the same. The total deformation of the gear set has different behaviours in both sides, so it will flex so that the left contact between washer and housing (and washer and gear) will be more towards the edge than the right one.

Whereas, it is not possible to see perfect the effect due to the gear mesh and it would be, perhaps, possible to vary gear mesh location to control how much it affects, but it is very difficult and time consuming.

Furthermore, the left part is bending more or less as it was expected (quite even), although it was thought to have even distribution through all the circumference, but as it is seen in the Figure 5.5 and Figure 5.6 the contact appears mostly in two regions diametrically opposite close to the contact mesh. As it has been explained before in the Chapter 5.2, this is because the washer is pushed with higher pressure close to the contact mesh, so the maximum contact is close to this region and due to the deformation the other zones, which are 90º respect the ones with contact, are lifted or without contact pressure.

Whereas, on the right side the pressure distribution changes through the entire surface, it becomes more even through the entire circumference (so it is more evenly pushed to the housing). Nevertheless, the section pressure is not even through the entire contact path in radial direction, depending on the section study, the distribution may change from having the maximum pressure close to the outer edge until having the maximum pressure close to the inner edge. That can be due to several facts, basically the hypothesis that could be said is that the non-symmetrical gear mesh may affect this distribution, the forces which push the gear towards the housing are different in both sides, in this case the forces through the left seem to be bigger (higher mean and peak pressure value) and they may affect the sitting of the washer between the housing and gears so that left and right are deformed differently.

If the force was just higher in left and smaller in right, it might be thought that the pressure distribution should be more or less the same with just lower nodal pressure values (one side respect the other side) and keeping the same equivalent radius in both sides. Though, in the plots below, it can be seen how the pressure distribution is different.

Finally, just to corroborate the previous study, the Table 5.3 shows the equivalent contact pressure and average for each part respectively, for the two of the input loads.

Table 5.3. Equivalent and average contact pressure for each part.

Contact pressure [N/m^2] / Input Load	**500Nm**		**1000 Nm**	
	$P_{equivalent}$	**$P_{average}$**	**$P_{equivalent}$**	**$P_{average}$**
Side gear washer left	$1{,}11 \cdot 10^9$	$1{,}08 \cdot 10^6$	$2{,}21 \cdot 10^9$	$2{,}16 \cdot 10^6$
Side gear washer right	$1{,}62 \cdot 10^9$	$1{,}58 \cdot 10^6$	$3{,}14 \cdot 10^9$	$3{,}07 \cdot 10^6$
Pinion gear washer top	$7.37 \cdot 10^8$	$2{,}75 \cdot 10^6$	$1.46 \cdot 10^9$	$5{,}47 \cdot 10^6$
Pinion gear washer bottom	$6.84 \cdot 10^8$	$2{,}55 \cdot 10^6$	$1{,}35 \cdot 10^9$	$5{,}03 \cdot 10^6$

In the table above is seen how the pressure values keep the same relation as the input load does, doubling the input load, the effective pressure is doubled as well as the average pressure.

Furthermore, the equivalent pressure is lower for the pinion gears that together with a smaller effective radius and surface contact area will yield to a lower friction torque in the contact between the pinion gear and its washer than between the side gear and its washer.

5.4 Pressure distribution

5.4.1 Analysis in the four washers

Moreover, in order to have a second proof that shows the linear effect of the deformation of the M66 differential, the pressure distributions (as a function of the input torque) for a section of each washer, where the maximum peak of the pressure is (note that just one section is taken as a overview of all in order to reduce the amount of samples), has been analysed.

The experiment has been done for 500Nm and 1000Nm and the sections, where the maximum peak of pressure is, are placed almost in the same geometrical coordinates since the results for both input loads are similar.

Then, to do such a study, a new coordinate system axis must be created. It is the same as the one which has been created for the deformation study but turning the x-axis some degrees until the plane x-y contains the geometrical section of the washer where the maximum value of the pressure is. By this way, the value of x will be directly the value of the radius and it will be able to calculate the value of the pressure against the respective radius.

First of all, for the side gear washer of the left side (closer to the ring where the torque in the housing is applied); it can be seen in the following Figure 5.9 the distribution that it has.

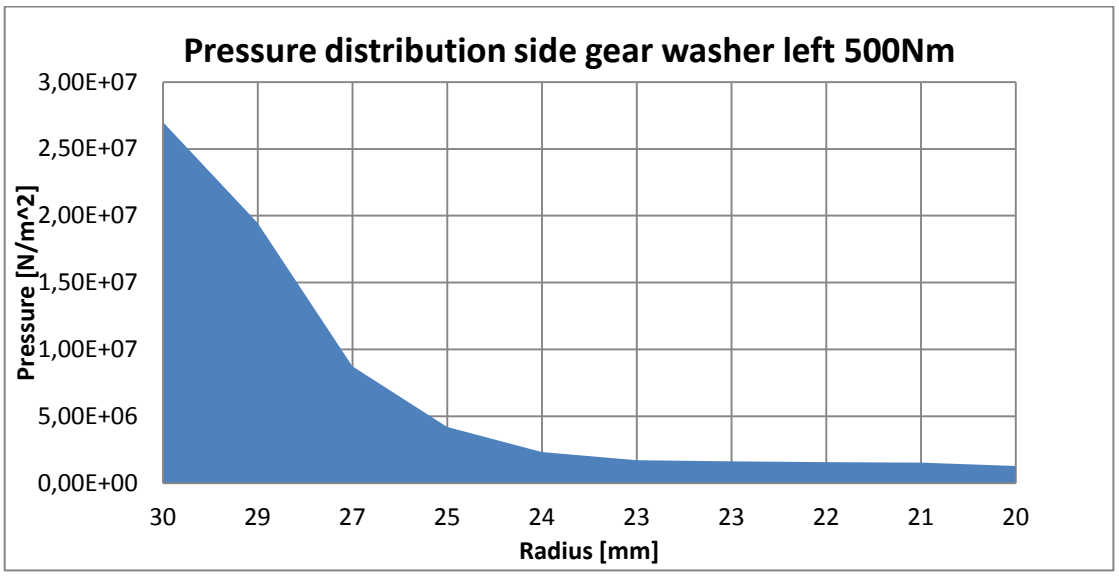

Figure 5.9. Pressure distribution of the side gear washer left for 500Nm.

As it has been mentioned before, this is just an overview of the distribution of the pressure for each section. In the Chapter 4.1 there are the figures where it has been explained how the pressure changes through the entire circumference. Thus, in the circumferential location of maximum contact pressure, the pressure distribution in radial direction is more or less similar, just the values change.

As an example, if for instance, the pressure distribution of the diametrically opposed section is taken (note that as it is not symmetrical, the peak of pressure is not in the exactly diametrically opposed section), there is contact as well but the value is lower. If the results are plotted overlapped with the figure above (not that as it is exactly the diametrically opposed section, the radius value should be negative):

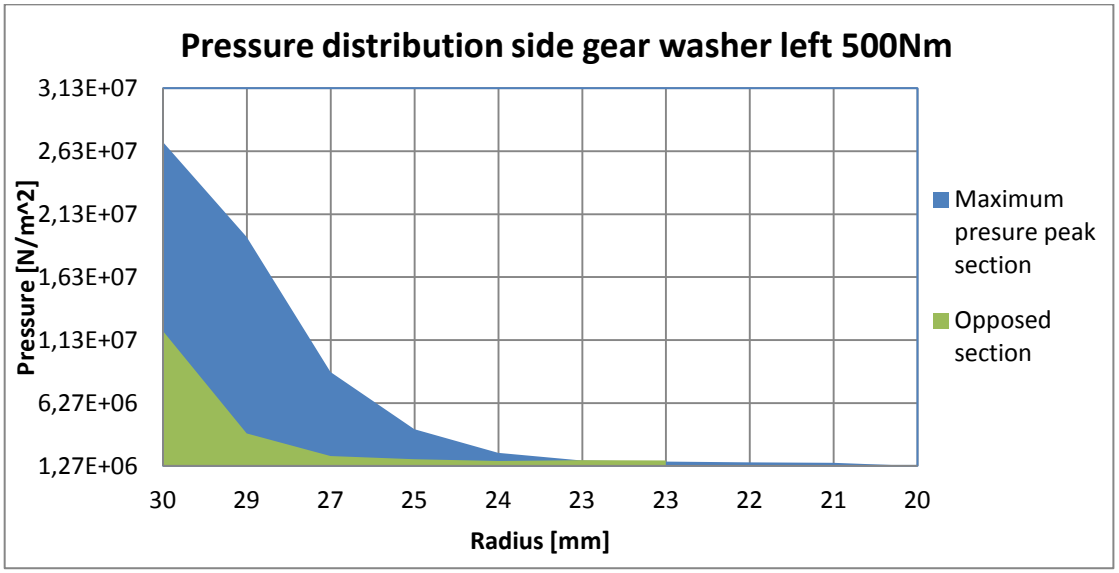

Figure 5.10. Comparison of pressure distribution between two different sections.

Clearly, the values of the pressure differ a lot depending on the section that is being studied, but the distribution itself is still the same.

Hence, this pressure distribution shows that the results got from the Chapter 5.3 are reliable and the equivalent radius of friction is more or less close to the outer edge. Besides, the pressure curve is not lineal from the inner until the outer edge. So, it means that the main contact is displaced to the outer edge (as it has been checked in the Chapter 5.2 and 5.3 where it has been seen where the contact is in the part and the final calculated equivalent radius of 27,15 mm for the overall pressure distribution). That makes false the initial hypothesis that it was done in the first rigid model in the Chapter 2.2 where it was considered that the equivalent friction radius was exactly in the midpoint between outer and inner edge.

In fact, this is the reason why the first test planning failed, since it was not possible to control the effect of the machined gears. First, the difference in results supposed to be smaller than the spread got due to the measurements and second, the effect that was thought was not the same as the real. Hence, it is shown that the contact does not move and the equivalent friction is taken from this equivalent radius from the revolution axis. Then, it was not true claiming that the contact was in the middle, and having machined the half lower part of the face will move the equivalent radius to the middle again and having machined the upper part of the face will move down the equivalent radius for the friction torque. Thus, that affirmation was wrong and this effect cannot be controlled in the rig.

Whereas, if the study is done for 1000 Nm. The results are plotted in the figures below (proceeding with the same way as it has been done for 500 Nm):

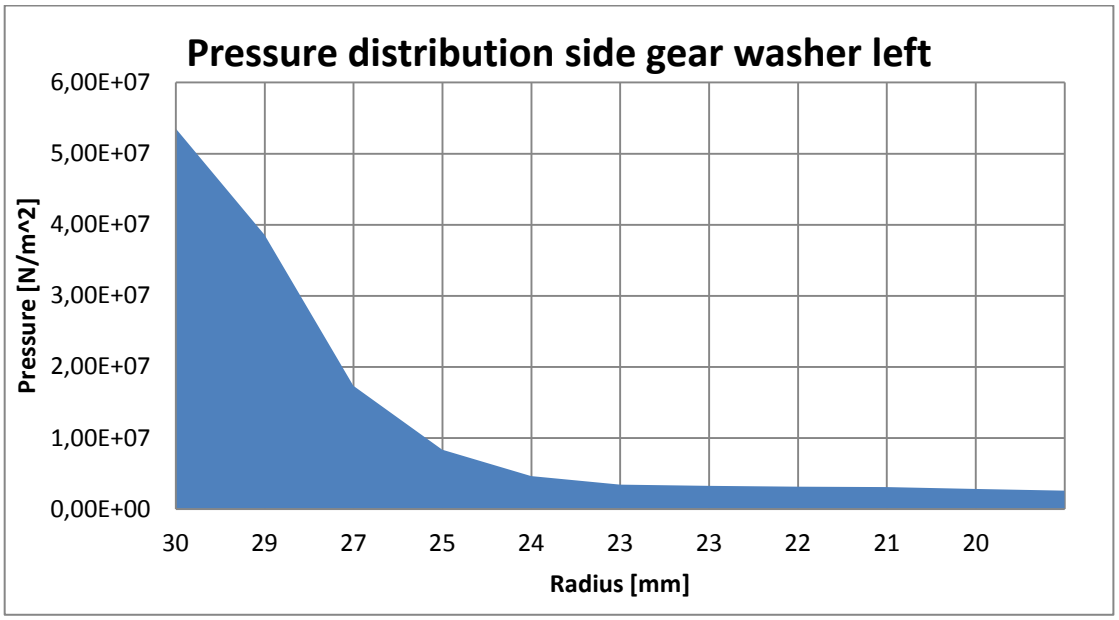

Figure 5.11. Pressure distribution of the side gear washer left for 1000Nm.

The opposed section could have been shown here as well, but it was just an example for 500 Nm not only to see that the peak was not in the exactly opposed diameter but also to check the difference of values depending on the section.

Now, if the comparison between both input loads is done, it will be seen how the distribution is mostly equal and since the load has been doubled, the pressure is roughly doubled as well.

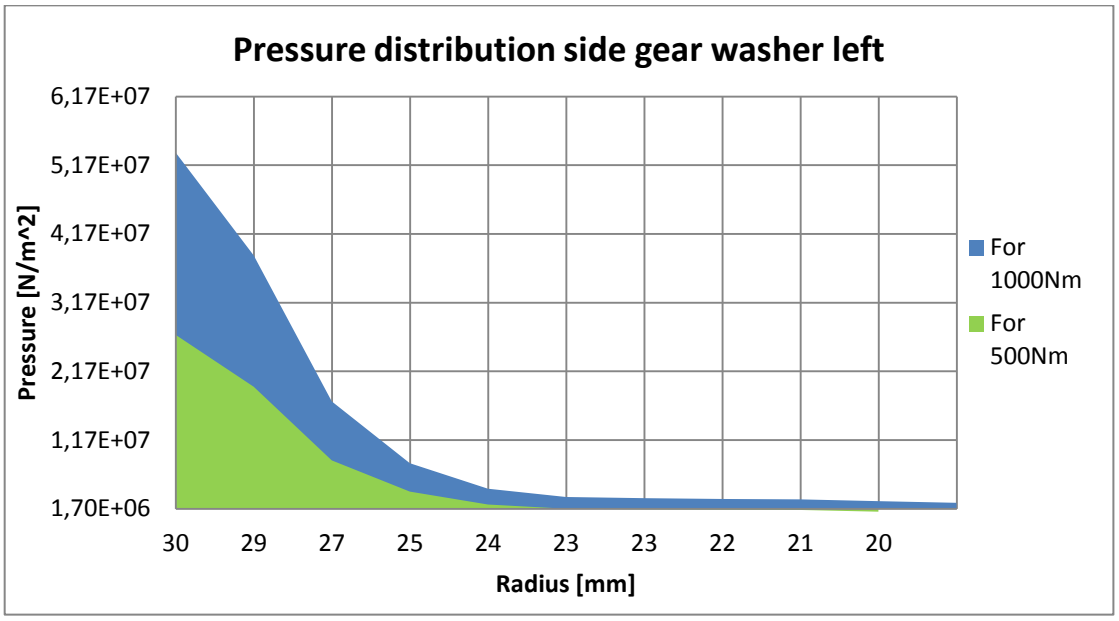

Figure 5.12. Comparison between both loads.

It is seen that there is slightly difference since the sections that are being compared are not exactly the same due to the asymmetrically gear mesh between top and bottom (the forces going through the teeth differ from the top gear mesh to the bottom one).

On the other hand, the same experiment can be done equally in the right washer. Now, it will be possible to check the difference between left and right as well as it has been already checked in the Chapter 5.2 and 5.3.

To make the study shorter, it was just studied the section which has the maximum peak.

In this case, as the radial pressure distribution changes for each section and the contact is more or less through the entire circumference, the curve of the pressure distribution might change quite much. However, the goal of this study is just to check if the effects are lineal in the pressure distribution as it has shown the Chapter 5.3.

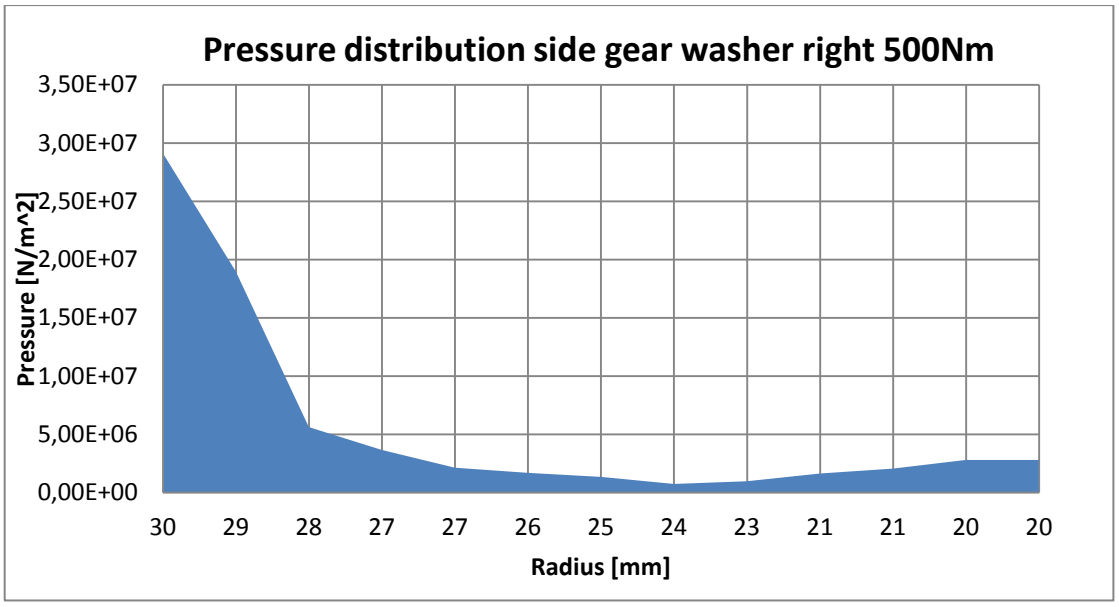

Figure 5.13. Pressure distribution side gear washer right for 500Nm.

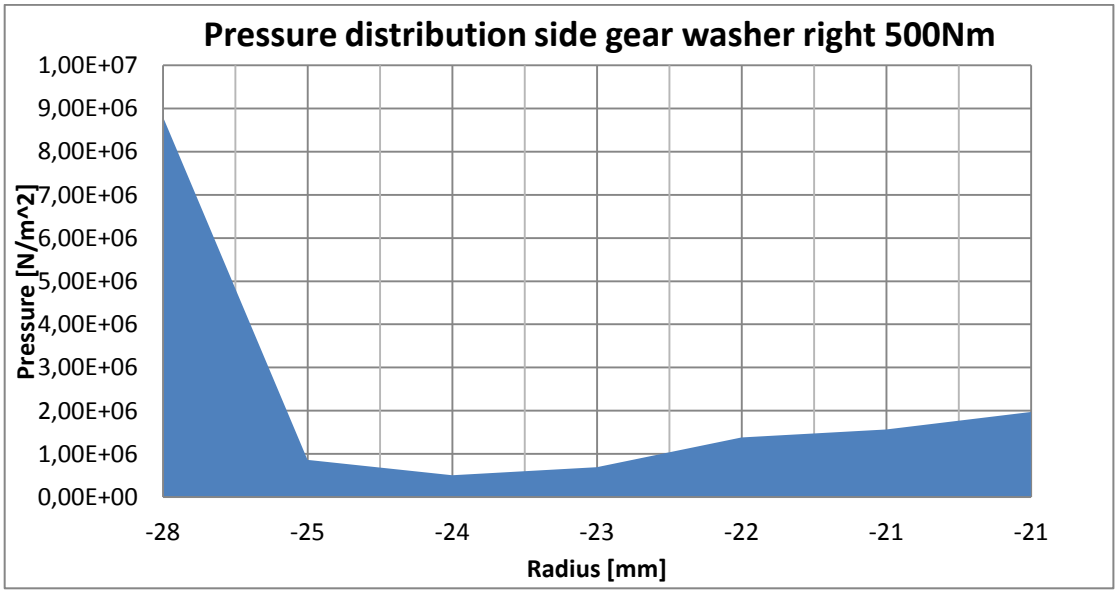

Figure 5.14. Pressure distribution side gear washer right opposed section for 500Nm.

It is clearly seen the results from the analysis of the Chapter 5.2, where it was shown that the contact appeared as well in the inner edge due to the asymmetric forces and deformation of the whole gear set in the right side due to the asymmetric gear mesh and that the radial distribution for each section may differ quite much.

The two opposite sections have roughly the same distribution of pressure through all the radius values. In fact, indeed that does not represent the distribution of the entire right washer, but with these values and the results got in the Chapter 5.2, it may be assumed how it behaves in the entire circumference.

On the other hand, for the input load of 1000 Nm:

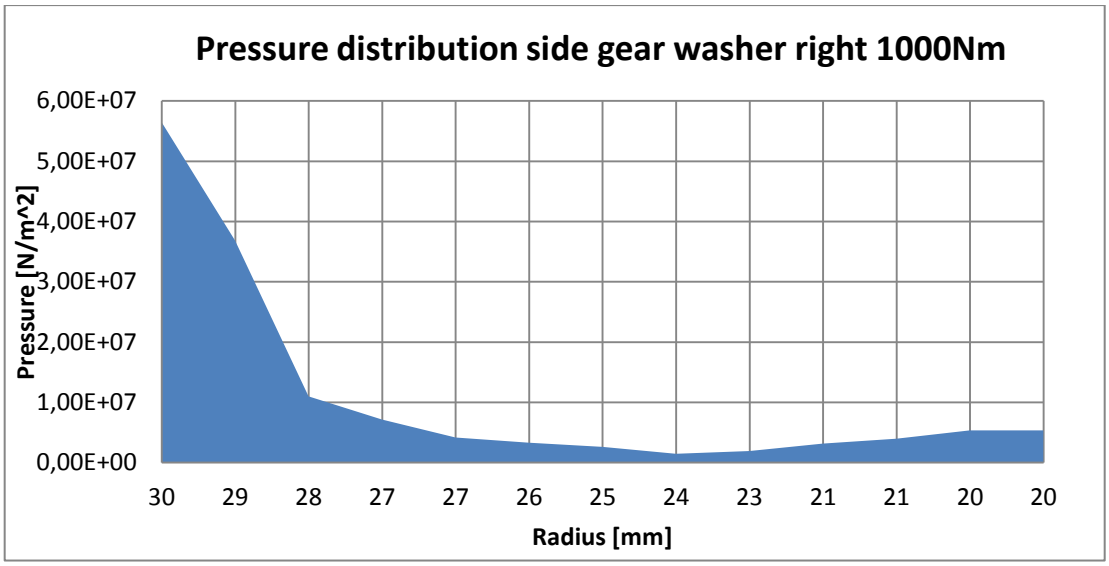

Figure 5.15. Pressure distribution side gear washer right for 1000Nm.

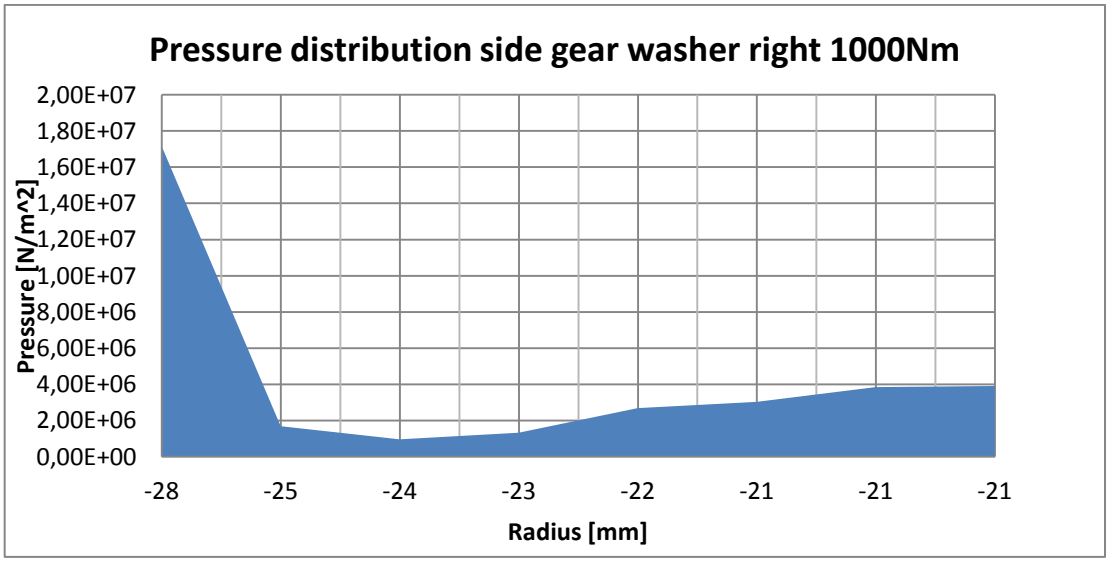

Figure 5.16. Pressure distribution side gear washer right opposed section for 1000Nm.

As well as it has been said before, here the effects are the same. The behaviour in the whole section may differ.

Although, here are the results of the pressure curves, it is not possible now to make any comparison with the results got in the Chapter 4.3, since the value 23.3mm of equivalent radius got does not fit this plot for instance. Whereas, if the results got in the Chapter 4.2 together with this pressure curve are used, it will be seen that the equivalent radius that was calculated can be trusted.

Now, if it is sum up it is seen here as well that the values of pressure are doubled and show how the pressure is totally lineally dependent on the input load:

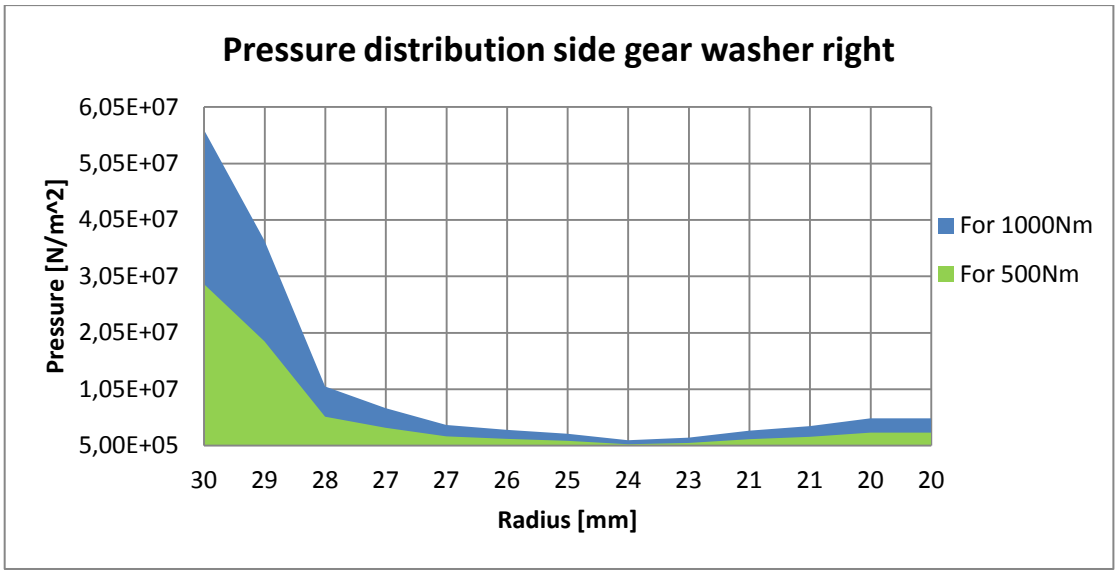

Figure 5.17. Comparison between both loads.

Hence, it is seen as the pressure is more or less doubled through all the radius once the input load is doubled as well.

Finally, if the same study is done with the pinion gear washers proceeding with the same way, the results are shown below.

In this case, the opposite section does not have to be studied because there is no contact so that the pressure value is neglected. As it can be observed in the Figure 5.5 and 5.6, the contact just appears in almost a half of the circumference due to the bending of the gear set and pinion with the "S" shape.

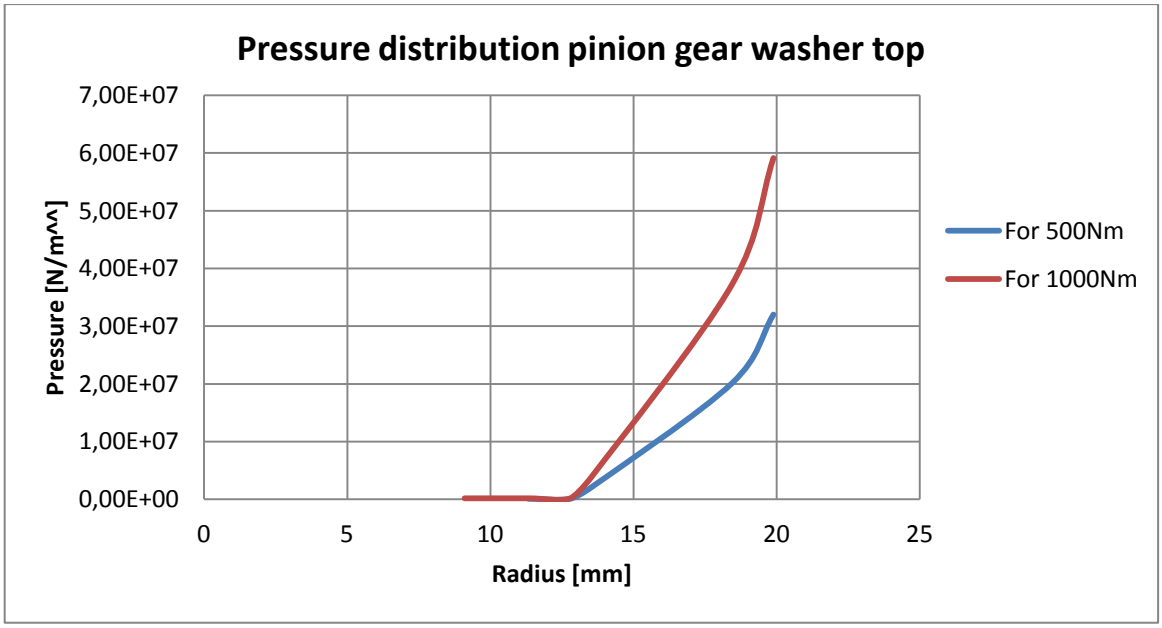

Figure 5.18. Comparison between both loads for the pinion gear washer top.

It can be checked the double amount of pressure for the same load and more or less the same pressure distribution for all the range.

In addition, it can be observed here that the equivalent radius got in the Chapter 5.3 of 18,15 mm suits the curve of the distribution of this contact pressure.

Furthermore, if the same is done for the bottom washer, the following plot is obtained:

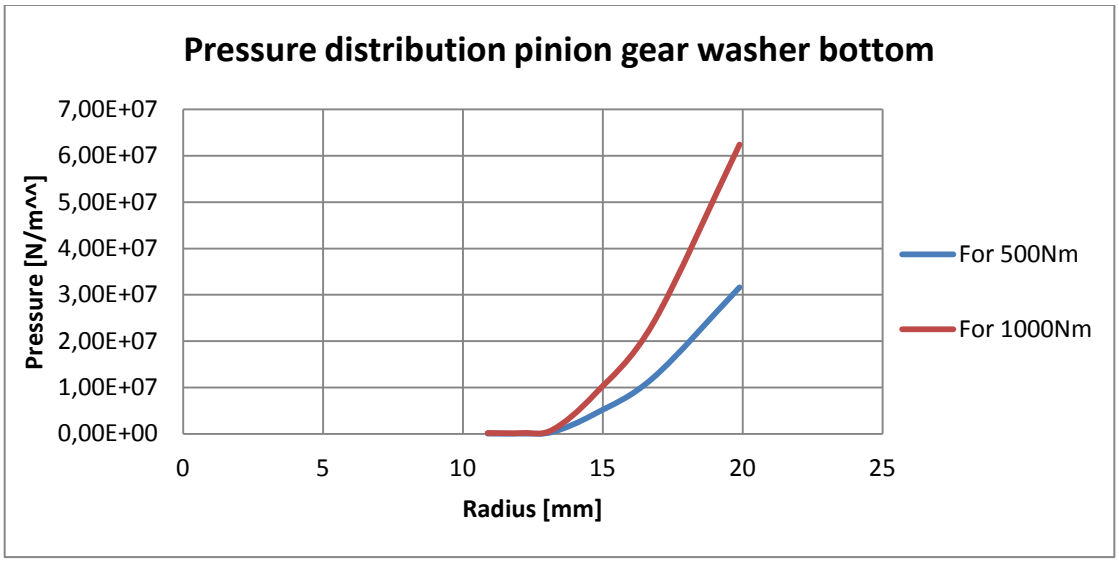

Figure 5.19. Comparison between both loads for the pinion gear washer bottom.

The conclusions are the same as the top washer. This is the reason why it can be claimed as well that due to the symmetrically conditions the behaviour of the pinion gear washers are quite similar whereas the effects of right and left washers differ due to the non-equal gear mesh in all the gear set.

5.4.2 Analysis in the pinion pin axle

Finally, if the pinion pin axle is analysed. The following plot shown in the Figure 5.21 can be obtained.

As well as it has been done with the washers in contact with the gears, in this case, it has been done the same analysis but with the pinion pin in contact with the pinion gears. It has taken just a section in the middle of the pin and it has been calculated the pressure distribution of this edge, both at the top (in contact with the top pinion gear) and at the bottom (in contact with the bottom pinion gear) and also studying both load cases 500 Nm and 1000 Nm to make the final check out.

Analogously as the pinion gear washers, the pin just has contact in a half of the circumference at the top and the opposite half at the bottom due to the bending in "s" shape of the whole gear set and the pinion pin itself. Thus, it has just been studied one section as a representative sample of the pressure distribution of these zones.

In the following sketch it is represented the coordinate "*Distance*" of the Figure 5.21 and the section where the pressure has been calculated. The maximum "*Distance*" value corresponds to the total surface contact between the pinion gear and pin

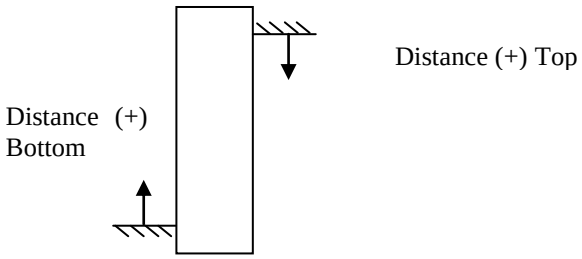

Figure 5.20. Sketch of the working section for the pressure distribution analysis.

The "Distance" value goes from zero (when the contact starts) until the maximum which is around 25mm when the contact disappears between the pinion pin and the pinion gear.

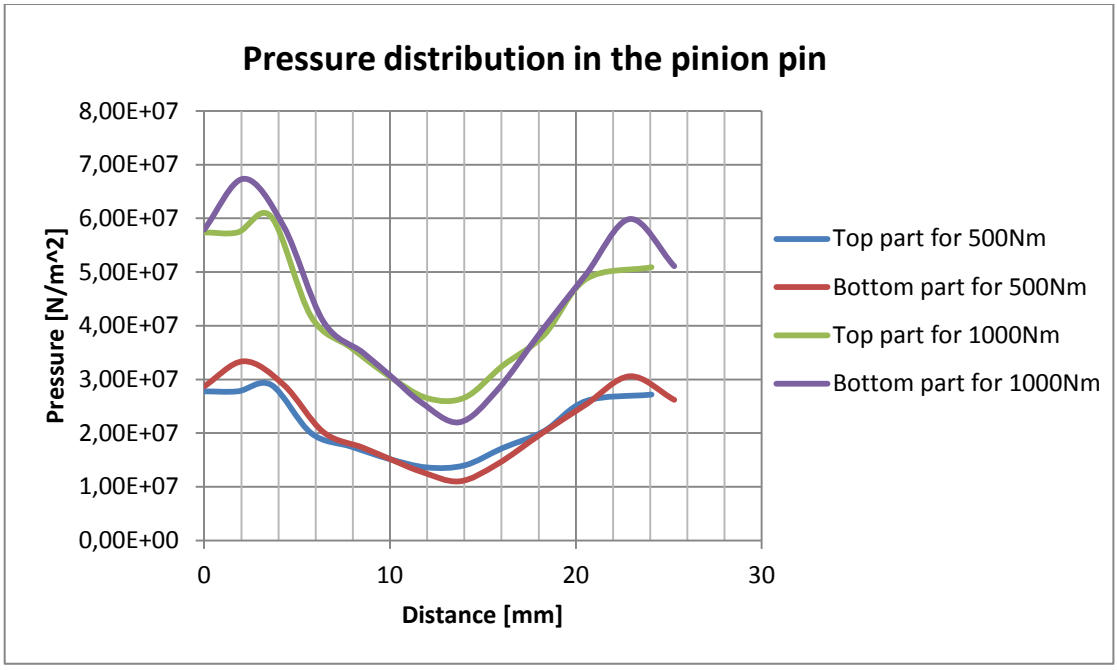

Figure 5.21. Pressure distribution in the pinion pin for both loads.

From the graphic above, it can be concluded saying that the pressure distribution still is similar from top to bottom so that it means that the forces from the housing to the pin are even to top and bottom part of the pin.

Moreover, according to VCC, the pinion pin is designed in such a way that the longitude where it is in contact with the pinion gear (*"Distance")* has a concave profile so that when it is bended, the surface is still in contact but still the contact pressure is higher for both *"Distance",* close to minimum and maximum.

It can also be said that due to the "S" shape that the gear set has when it is loaded, the pressure is higher in the edges of the contact than in the middle. It can be easily seen in the Figure 5.20 how much the pressure is reduced around the middle of the contact path compared to both extremes.

Actually, the bending shape can also explain that the effective *"Distance"* (where the equivalent pressure would be applied) value for all the loads remains when the

"Distance" takes the position of 10,5 mm, so closer to the outer edge than to the inner due to the way how the pinion pin is tilted.

Finally, it can be claimed again that the value of the pressure is related to the input load in a linear way, since the distribution is still the same for all the range of torques and there are the values of pressure that are increased according to how much the input load has increased.

5.5 Deformation contribution and stiffness analysis

In order to know the contribution of each part in the deformation, a study of the stiffness of the whole assembly and its parts is carried out.

First of all, to calculate the stiffness of the whole assembly (housing and gear assembly), it can be calculated the maximum angle that has been deformed. It is in the outer ring of the housing and the value depends (obviously) on the input load. So, for instance, in the case when the torque is 500 Nm, it yields with a deformation in the outer ring of 0,449 mm (the deformation value can be checked in the Figure 5.1).

This value is the total translational displacement (*dx*), but there is the need to calculate the rotational displacement. That can be approximated as:

$$\varphi = \frac{dx}{\pi d} 2\pi = \frac{0{,}449mm}{\pi \cdot 172mm} 2\pi = 0{,}0052\ rad \qquad (5.4)$$

Where πd is the circumference and 172mm is the outer diameter of the ring where the translational displacement has been 0,449mm.

In the following sketch it can be seen the theoretical torsional stiffness phenomena used to calculate the stiffness of the model.

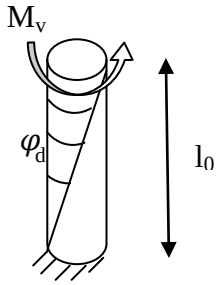

Angular displacement φ_d

Angular elongation $\theta_e = \varphi / l_0$

Figure 5.22. Sketch of theoretical torsional stiffness phenomena.

Then the torsional stiffness is defined using equations (5.5), (5.6) and it yields to (5.7):

$$\frac{M_v}{\theta_e} = GI_p \qquad (5.5)$$

$$\frac{M_v}{\varphi_d} = \frac{GI_p}{l_0} \qquad (5.6)$$

Where the term $\frac{GI_p}{l_0}$ is the rotational stiffness expressed in Nm/rad. Thus,

$$K_p = \frac{M_v}{\varphi_d} \qquad (5.7)$$

That yields to,

$$K_{assembly} = \frac{M_v}{\varphi_d} = \frac{500Nm}{0{,}0052\ rad} 10^{-3} = 96{,}153\ \frac{kNm}{rad} \quad (5.8)$$

Hence, in order to calculate the stiffness of the housing, there is the need to calculate the stiffness of the gear set according to the Equation (5.7):

$$\frac{1}{K_{assembly}} = \frac{1}{K_{housing}} + \frac{1}{K_{gear\ set}} \quad (5.9)$$

The gear set (gear assembly and pinion pin) stiffness can be calculated analogously as the whole assembly stiffness.

Thus, if the translational deformation of the gear set is checked, it is seen as for instance the deformation of the top of the pinion gear is 0,218mm and this deformation is in a outer diameter of 88mm. Then, it yields to:

$$\varphi = \frac{dx}{\pi d_g} 2\pi = \frac{0{,}218mm}{\pi \cdot 88mm} 2\pi = 0{,}005\ rad \quad (5.10)$$

$$K_{gear\ set} = \frac{M_v}{\varphi_d} = \frac{500Nm}{0{,}005\ rad} 10^{-3} = 100\ \frac{kNm}{rad} \quad (5.11)$$

So, finally the stiffness of the housing can be calculated removing it from the Equation (5.9):

$$K_{housing} = \frac{1}{\frac{1}{K_{assembly}} - \frac{1}{K_{gear\ set}}} = 2499 \frac{kNm}{rad} \quad (5.12)$$

Finally, it has been proved which parts contribute the most to the deformation and the contact.

The housing is stiffer than the gear set (around 25 times stiffer), so it means that the fact that the input torque is not applied in the centre of the housing should not affect the different deformation between left and right side in the inner part of the housing.

Furthermore, it can be said that since the housing is much stiffer than the gear set, the effects of the deformations come more or less from the gear set and not from the housing itself.

In fact, this result does not check the hypothesis that it was thought before doing this study. This hypothesis was that since the housing is casted, it would be the weakest part and the first part to be deformed. However, although it is casted, it has been proved that it is stiffer than the whole gear set, which was thought to be the strongest one).

Since there is no symmetrical gear mesh, it is not possible to split even more the stiffness of the gear set and be able to know the stiffness of the pinion pin for instance.

On the other hand, the results from the principal component of the tensor of strain can be used as well to corroborate the results from the stiffness test.

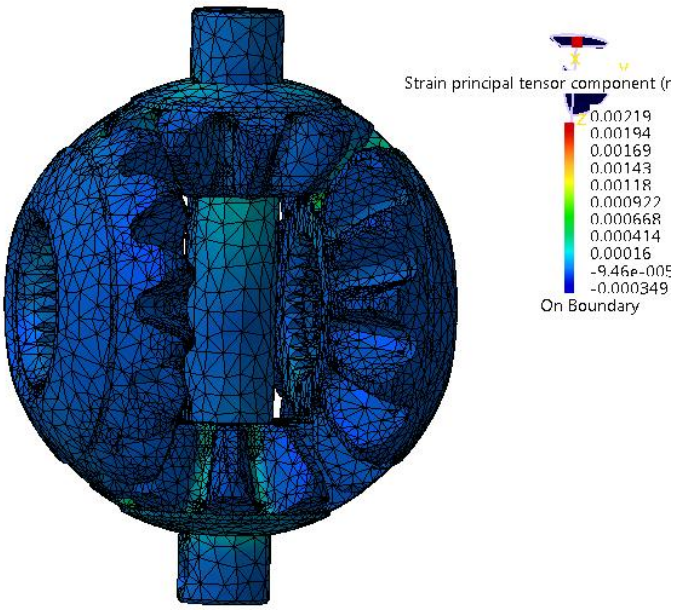

Figure 5.23. Principal strain component of the gear set.

Here, it is seen how the maximum strain deformation is in the pin and the gear mesh, so these parts might be the weakest once of this assembly.

Moreover, the Figure 5.24 is just done in order to get in more detail the strain distribution to the pin and gear mesh (in the *Appendix D*, more views of the strain of the other symmetric gears can be seen)

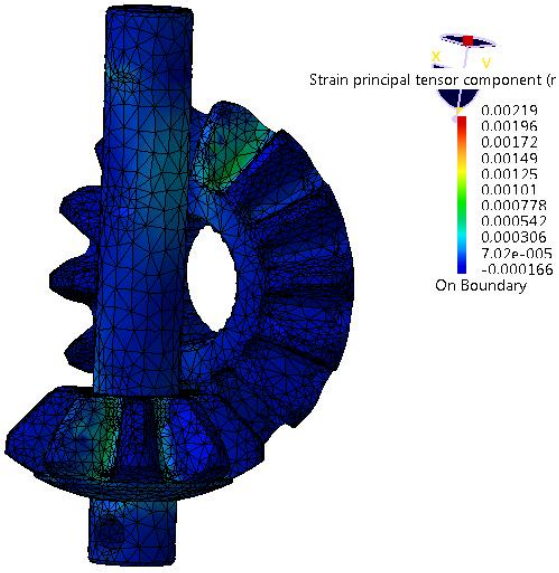

Figure 5.24. Principal strain component of the gear set (view 2).

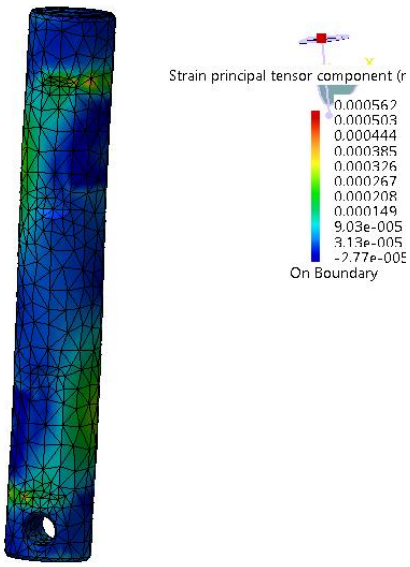

Figure 5.25. Principal strain component of the pinion pin.

It is observed how the maximum strain of the pin comes from the contact between the gear and also the contact between the housing.

On the other hand, if the principal component of the strain tensor is observed, the following Figure 5.26. In the *Appendix D* it is possible to check from different views, the maximum strains of the housing. Indeed, it is seen the lower strain in the housing compared to the gear set.

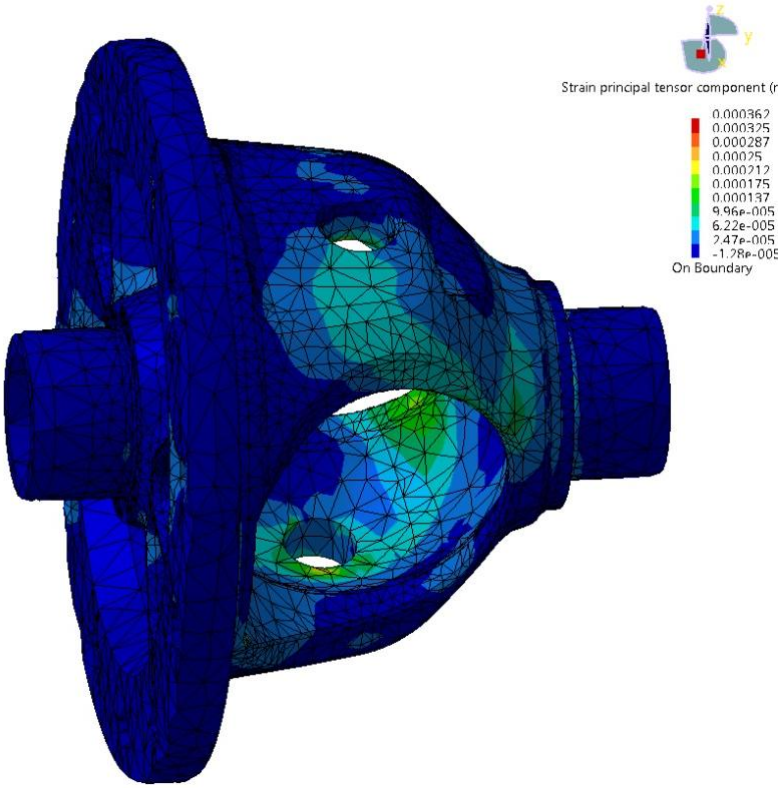

Figure 5.26. Principal strain component of the housing (view 1).

Basically all the strain contribution comes from the pressure that the gear set does to the housing, in all the internal housing. Whereas, the strain of the ring is almost neglected even though it has the biggest rotational displacement.

5.6 Comparison with the test results

After having done this FEM analysis, it may be claimed that the non-linear results from that were shown in the rig test are due to the measurement or misalignment in the rig. However, it is, perhaps, a too strong statement; it might be also possible that FE model lacks the capturing of some non-linear effects. But, providing that results from this model are used and without considering any other effect, the differential has a linear behaviour as far as the deformation and the contact pressures are concerned.

Basically, the approximation of all the measurements done in the rig should be using a linear curve instead of a second order polynomial, although it might minimize more the error, but it is not the real effect that the differential has.

5.7 Model conclusions

The FEM analysis can be concluded claiming that the differential M66 has a linear effect; all the deformations and contact pressures are depending on the input load. A re-distribution of contact pressure due to higher input torque does not seem to happen. So, the torque difference seen in measurements is not likely due to deformation of the housing, rather the asymmetry of the gear mesh or some other non-linear effect (for instance due to the measurement setup). However, the study has been done from 0Nm to 2000 Nm, but it might happen that the effect became non-linear for higher torques. It would be necessary then to make further studies for higher loads, but in this project, it was decided to study the effect of the differential during the wide range already analysed.

Hence, there is not any second order effect that causes an increase of difference torque between both shafts as soon as the input torque increases.

The equivalent radius of the friction torque between the four washers and the gears is not in the middle point between inner and outer radius as it was expected and supposed in the first simulation model studied in the Chapter 2. Then, it is checked how the design of the first test planning was wrong, since it was not possible to understand what was really happening after machining the gears in such a way. All the equivalent radius are constant during all the range of input load. The values got in this analysis will be used now for the simulation. However, there is this disturbance between left and right since the gear mesh was too difficult to be controlled and too much time consuming work in both the FEM analysis and the rig.

The results have shown different response between left and right and the choice of which equivalent radius should be used in the simulation becomes complex. The implication of having different radiuses due to an asymmetric gear mesh will have another output in the friction torque for each side. But, since when the diff is running assembled with the whole car, the gear mesh is changing all the time, using each equivalent radius in each side would not represent the other possible valuable combinations. Thus, it was decided to take the average between them in order to have the same effect in each side.

Finally, regarding the pressure distribution got in the pinion pin. It will not be able to be considered in the simulation since it will not affect the torque so much, the contact force that creates the friction torque between the pinion pin and the pinion gear will still have the same radius of the pin, so if the equivalent distance is not in the middle, it will not affect the results in the simulation.

The gear teeth contact mesh radius will still keep the same it was considered in the middle point of the contact of each tooth. It has been checked how the maximum pressure was just in the middle of the teeth, so the gear ratio was well supposed considering effective radius of the transmission torque in this point.

6 Final Rig Test Results

As soon as the FEM analysis is done, doing the test was easier since it was already known the behaviour and effects of the differential once it is loaded. In addition, having changed the test planning was a good point since in the beginning, using the old one, it was not possible to get reliable results from the machining of the gears since it is not known which were the effects after machining the gears in such a way, basically the assumption was wrong. The FEM results have shown that the equivalent radius of each contact surface becomes independent on the studied interval of input load.

6.1 Test 0

It has already shown in the Chapter 4, but it is plotted again in order to have the linear equation that minimize the error between the samples.

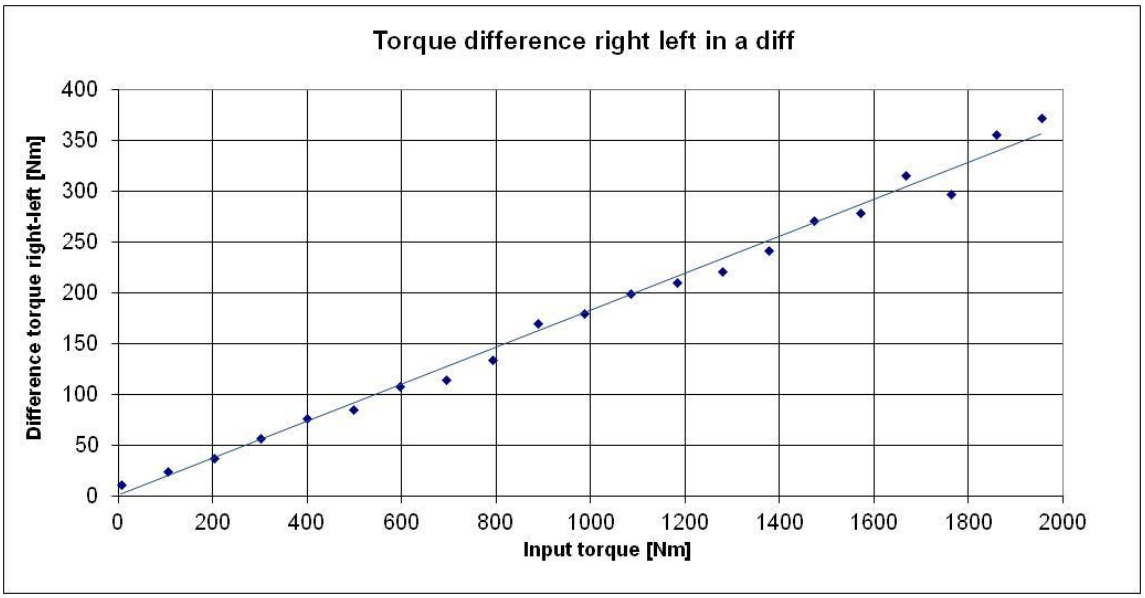

Figure 6.1. Results got for the original differential.

It is worth pointing out that the difference of torque between shafts becomes now the 18,18 % compared to the total input torque. If it is taken over the linear behaviour of the differential once the curve is adjusted to the Rig Test Results.

6.2 Test 1

These results should show the maximum difference, since all the washers were changed to Nedox coating.

In the following table the results can be observed:

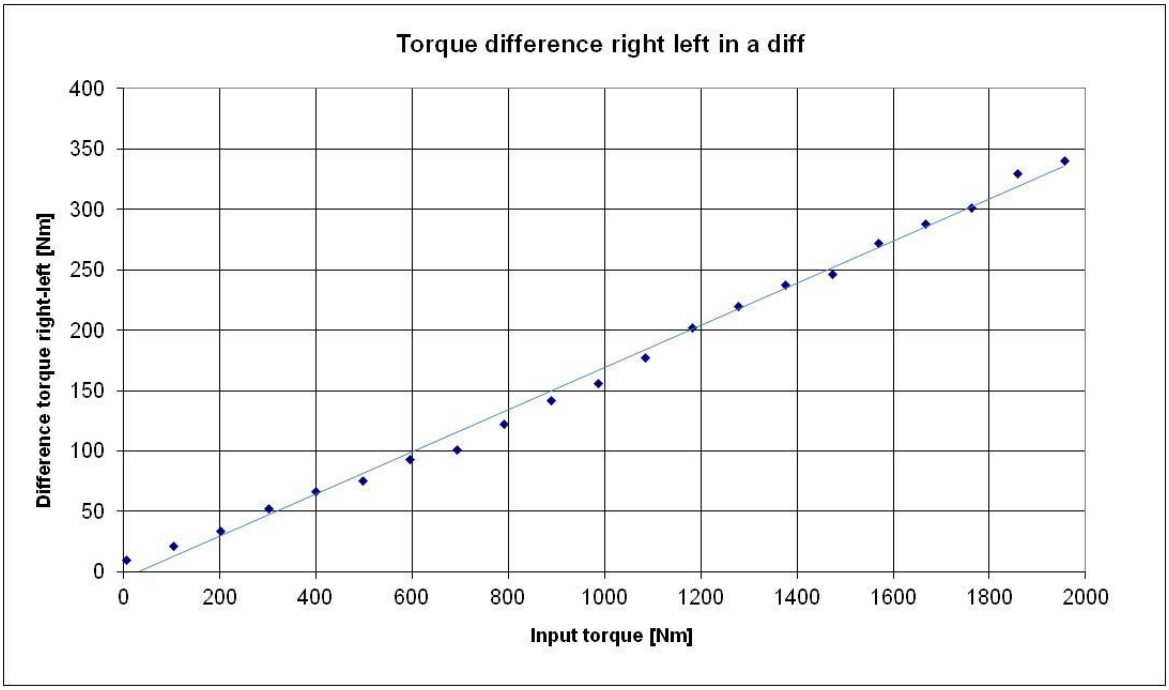

Figure 6.2. Results got for the first test.

The relation between the input torque and the difference between right and left is shown in the equation above. This is the equation that minimizes the square distance error from each point. But note that for 0 Nm of input torque the difference would be negative (it means that there would be gain instead of loss). So finally, this would be modified in order to begin at 0 Nm.

6.3 Test 2

In this case, when the Nedox is used just in the side gears washers the results are shown below:

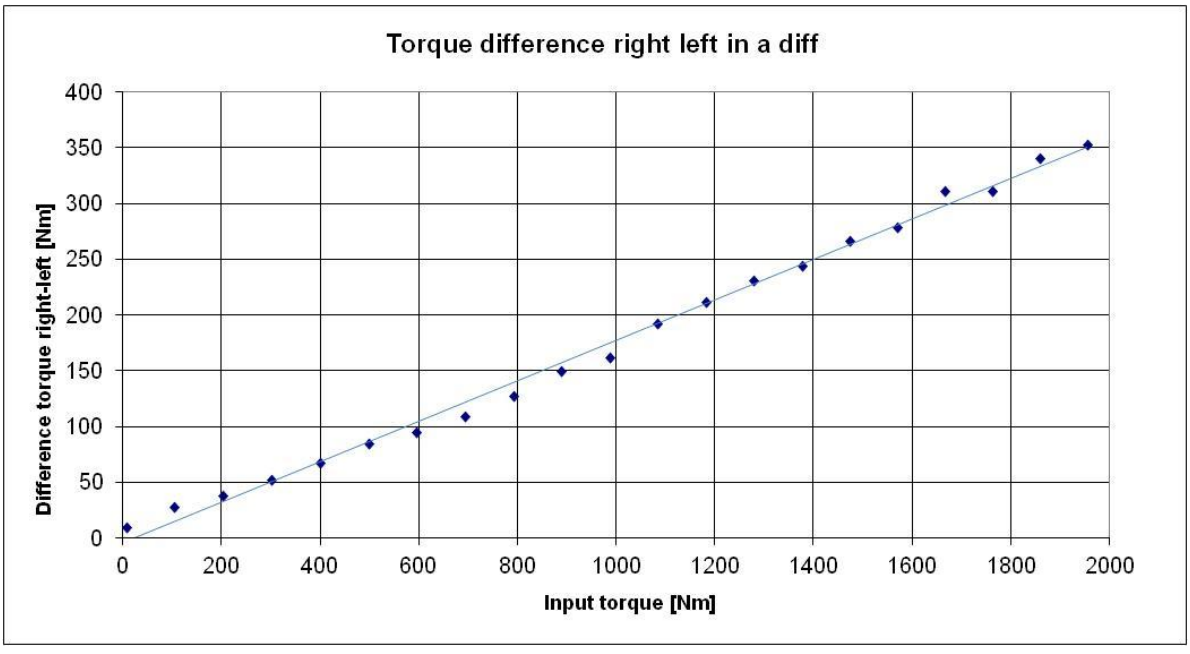

Figure 6.3. Results got for the second test.

It is seen how the losses are slightly lower than the original differential and higher than the first test, so that it is possible to trust the effects of the Nedox washers to reduce friction in these contact places.

6.4 Test 3

Finally, the third test using Nedox washers just in the pinion is done. The results are shown below:

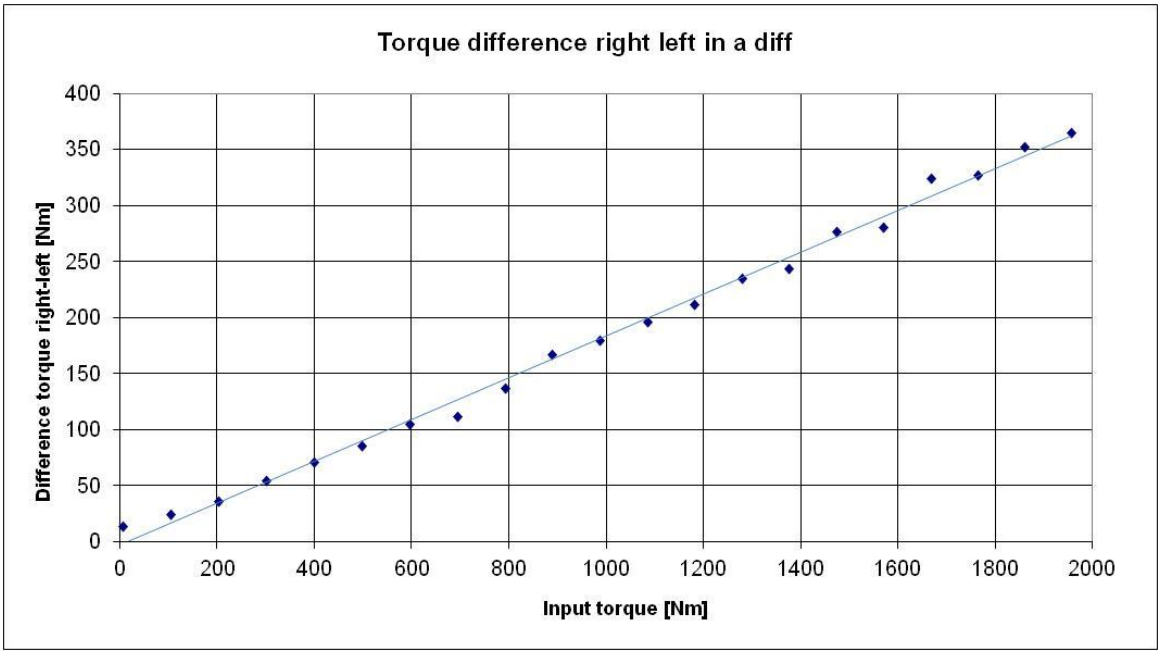

Figure 6.4. Results got for the third test.

It can be observed that the results are quite similar to the original differential, it means that the effect of the pinion gear would not be as strong as it would be in the side gear. This fits the results got in the Chapter 2, where it has been seen that the most contribution comes from the side gear friction in contact with the washer.

In this case, the results would be affected slightly by the measurement because the spread of the measurements could be bigger than the real difference comparing with the original differential.

To sum up, it might be claimed that maybe it is not possible to check the value of the change between Test 0 and Test 3, but it is enough to check the quality of the results, so that the effect pinion gear effect is weaker than the side gear.

6.5 Checking Rig Test with the Loss Model

Once the FEM analysis and the test planning has been done, the simulation can be adjusted in order to get the same values as the ones got in the rig and check how much the friction coefficient should be once the other parameters are changed to the values got in the FEM analysis.

The Figure 6.5 shows the results from the rig using the original differential (Test 0) and the simulation of the Loss Model.

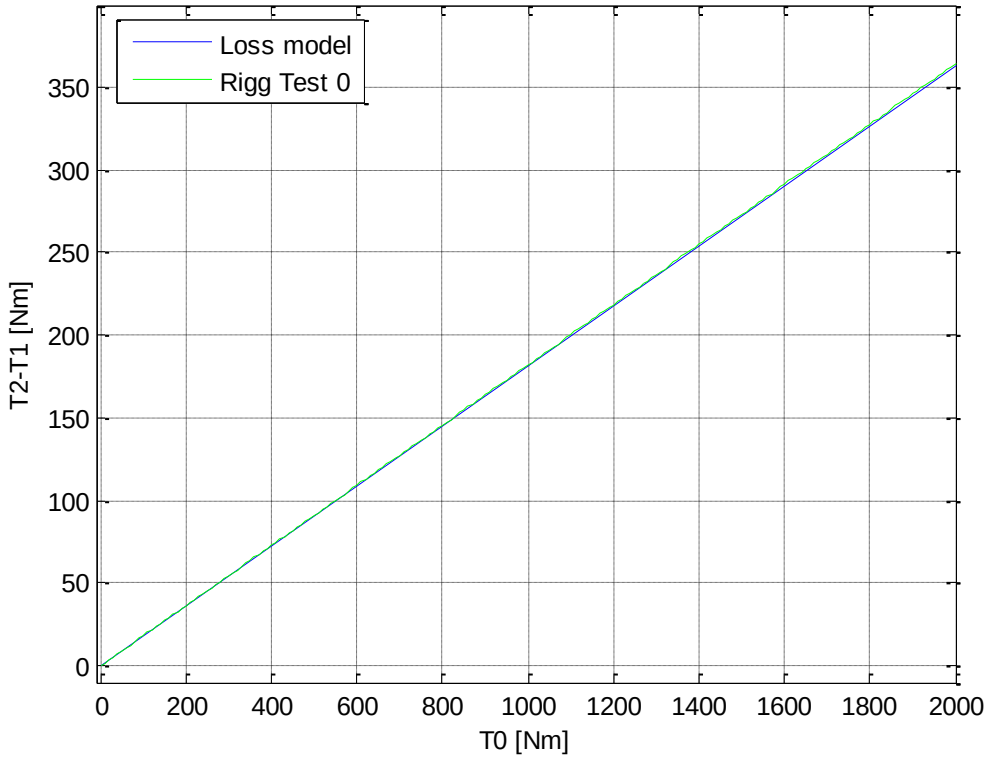

Figure 6.5. Fitting between simulation model and Original differential results.

In order to have both curve overlapped, the friction coefficient has to be 0,215, taking into account that the friction coefficient is equal for all the contact places. The torque difference between shafts still remains around 18% of the input torque as it was calculated before (equivalent to a torque ratio of 1,444).

Furthermore, this can be seen as the breakaway (static) friction that the differential has to overcome to allow the wheels spinning, relatively to the carrier, in opposite directions.

On the other hand, using the updated Loss Model, it is still around a 40% of the overall torque difference due to the side gear, a 34% due to the pinion pin in contact with the pinion gear and a 25% due to the pinion gear.

Now, if the friction coefficient between pinion gear and pin is kept the same (0,215) and the results from the Test 1 are tried to fit the Loss Model changing the friction coefficients of all the contacts gear-washer, then, the plot below is got:

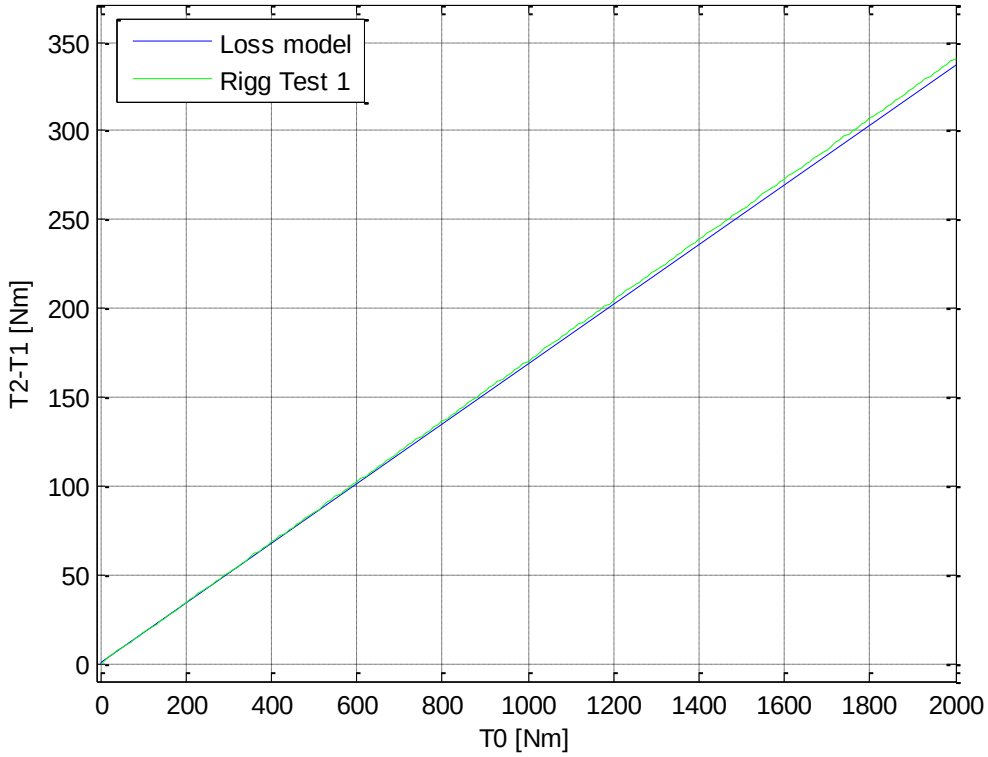

Figure 6.6. Fitting between simulation model and Test 1.

In this case, the friction coefficient of the contact gear-washer becomes 0.19 in order to fit both Loss Model and Rig Test, so that the friction coefficient is reduced by a 11,6%.

Actually, the total amount of losses yields to the 16,96% of the input torque (torque ratio of 1,406), for instance in the maximum input load of 2000Nm, the torque difference is 339,3 Nm. It means that compared to the Test 0 with the original diff, the amount of torque difference has been reduced by a 6,79%.

Note that to fit the simulation model, it has been taken into account the regression curve that approximated the results from the rig and it has been adjusted in order to start at 0Nm (see *Appendix A* to check the final values of the curves). Thus, it might be that the results are affected by the spread of the measurements (this is the reason why this post-process has been done).

On the other hand, in order to check the model, if the friction coefficients got during the checking with Test 0 and Test 1 are used, the Loss Model should fit more or less the Test 2 results got from the rig.

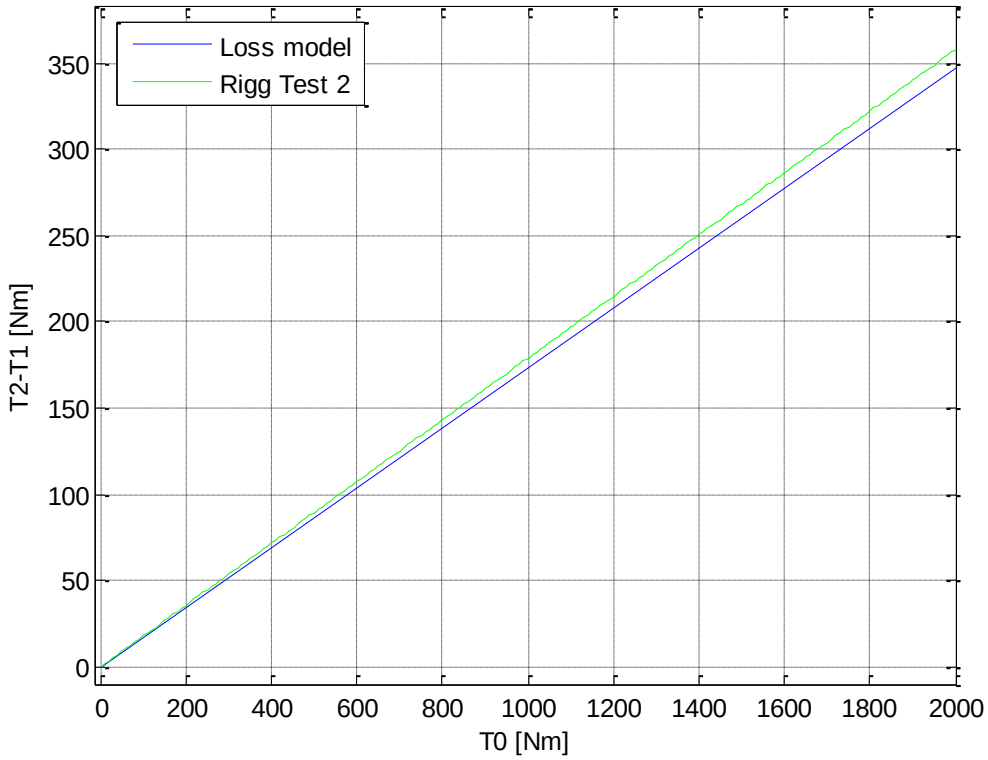

Figure 6.7. Fitting between simulation model and Test 2.

It is seen that there is a small difference. It is due to the spread, as lower are the changes done in the rig, more possible error they might have since they are closer to the spread range caused by the measurements.

Thus, since the measurement error should be lower when the difference was bigger (Test 1), the friction coefficients got from Test 1 will be used so as to check how much they have changed. Using the Loss Model with the Test 1, the error will be lower that if the Loss Model is used to fit both Test 2 and Test 3. The spread due to the measurement in the rig is relatively bigger in these last two tests.

On top of that, the losses due to the friction are, in this case, 17,38% of the input torque. They have been reduced by a 4,5% compared to the Test 0 output got.

Finally, if the Test 3 is studied, it yields to:

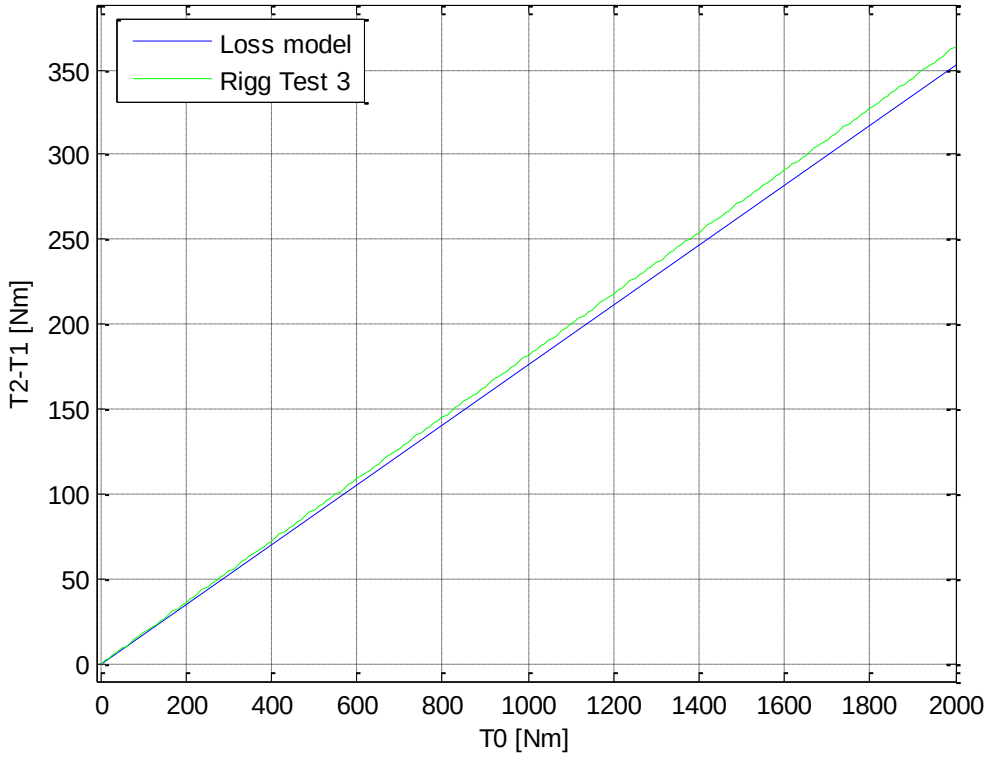

Figure 6.8. Fitting between simulation model and Test 3.

Proceeding analogously, the friction coefficient of the pinion gear in contact with the washer is set 0,19 and all the others are kept to 0,215.

By this way, the total percentage of difference between right and left compared to the input torque becomes 17,81%. It means that the losses have been reduced by a 2,14% compared with the Test 0.

Furthermore, it is seen that the effect of the pinion gears is lower than the side gear as it was already checked in the Chapter 2.

6.6 Testing conclusions

To sum up all the results got from the rig, the following table can be used.

Table 6.1. Summary of the results got in the test planning.

TEST	μ side gear	μ reduction [%]	μ pinion gear	μ reduction [%]	T2-T1 [%]	Reduction [%] (compared to Test 0)
0	0.215	-	0.215	-	18.20	-
1	0.19	11.6	0.19	11.6	16.96	6.79
2	0.19	11.6	0.215	0	17.38	4.5
3	0.215	0	0.19	11.6	17.81	2.14

Even though some disturbance in the final results might be occurred due to the error in the lecture of the results got from the rig not only due to the measurements, but also due to the change of results for different gear mesh. There is as well a difference compared to the differential running with the complete transmission where it is turning (inertia and centripetal acceleration must be considered) and where the oil film thickness is set to all the contact surfaces with the right optimum temperature.

The results shown in the Table 6.1 represent though quite much the effects of these changes and combinations between the different possible friction coefficients. Probably, the results got are the worst case scenario that can take place in the reality (with static or quasi-static friction model).

It has always been possible to check that the results from the FEM analysis are reliable since the effect of each combination yields the total effect. The percentage of reduction of the Test 2 plus the reduction of the Test 3 is equal to the total reduction of the Test 1 (with all the Nedox coating washers used) compared to the initial values using the original differential design.

Moreover, the results got in the Chapter 2 have been proved now with the Rig Test and FEM analysis and they have shown reliability, compromising the assumptions done. For instance, the effect on the contact surface between the side gear and its washer is much stronger than the friction between the pinion gear and its washer.

7 Comparison with Logged Data from Car Test

Some data was collected from tests done with a front wheel drive Volvo car on the testing tracks, using the same differential M66 which has been studied. The results have been collected from a wide range of data, in the *Appendix E*, the speed of each wheel, driveshafts torques and steering wheel angle can be seen. Whereas, the lateral acceleration has not been got, thus it is not possible to check the lateral acceleration to know the weight transfer, but all the results have tried to be got just when the vehicle started turning, as close as possible from the turning steady state (low speed).

Furthermore, as it is shown in the Table 7.1, six driving scenarios have been defined. The first three are for straight ahead conditions with the differential open, but as it is seen in the figures in the *Appendix E*, there is a slight relative speed between wheels, this is the reason why it has written between parenthesis right or left, in order to indicate if the slight difference was from left to right or viceversa. Whereas, the last three driving scenarios have been defined when the car was turning, it is indicated already in the table the turning side, but in the figures in the *Appendix E*, the exact relative speed can be checked.

Although the torque split results from the real car are not only due to the friction and the design of the differential but also due to the different drivehsafts stiffness, joints losses, slip on the wheels, weight transfer, suspension, etc, the results are still possible useable to check how much it differs from the difference torque got during the Rig Test which is around 18% difference between shafts. In fact, from all the logged data got, it was tried to see those instants where the car was going either straight ahead (when just the micro movement between gears occurs) or when it was just starting turning (when the relative speed starts showing up) in order to be as close as possible to the case scenario when the differential starts differentiating the wheel speed so that the weight transfer effect is as small as possible.

This was collected for different shaft torque levels in order to check how the difference is during the wide range of input torque in the differential.

The torque has been measured with a gages set on the driveshafts which have been calibrated in order to have as much accurate lecture as possible.

In the following Table 7.1 all the results got can be sum up.

Table 7.1. Log data from testing

Driving situation (approximately)	Left driveshaft torque [Nm]	Right driveshaft torque [Nm]	Absolute Difference [%]
1- Straight ahead (right)	121.15	138.54	4,28
2- Straight ahead (right)	272.63	335.27	10.30
3- Straight ahead (left)	849.01	952.06	5,72
4- Turning left	158.25	121.97	12,95
5- Turning right	407.57	521.09	12,22
6- Turning left	1173.57	932.43	11,45

First of all, if the straight ahead situations are studied, it is seen that there is a huge difference in the absolute difference torque between them. Theoretically, the car was driving roughly straight ahead, but as it is seen there was a slight difference between wheels that could be that it was not a perfect straight ahead driving, thus it might be that there is a friction over the differential, the micro relative speed might make the differential trying to overcome the breakaway ratio.

On the other hand, it might be that the shaft with higher torque was the "inner" one, but in the third driving situation, it is slightly turning left and the torque is still higher in the right driveshaft, it might have happened that the grip in the right was slightly higher than in the left when the car was driving in that instant. So, the right wheel had a much bigger friction coefficient on contact with the road compared to the right one. Actually, it might happen that one of the wheels has more pressure than the other, or that the weight distribution is not evenly delivered in both wheels.

In fact, this can yield that for straight ahead situations the torque in the right side is always higher, perhaps due to the stiffness of the driveshafts.

In these cases, the effect of the weight transfer between sides should not affect the difference of torque of both shafts. But, the slip angle, misalignment in gears and some effects of the differential might quantify this value. Actually it is not possible to extrapolate. It seems that the difference between axes can be higher or lower depending on which road conditions (that they are not known). The value should is around 5% of difference, but in the second driving situation rises up to 10%, it could be that the car hit a bump or the car had a much higher grip in right than in left for instance.

Anyway, what it is possible to claim is that in these first three driving situations the effect of the differential might affect the difference torque between driveshafts as much as it does when it is turning. But it is seen how many parameters might affect these results.

On the other hand, if the three last driving situations are analysed it is seen how the torque difference has increased due to the friction in the differential, but also the weight transfer might affect slightly the results even though the curves were not tight since the relative speed between wheels was quite small.

The values have tried to be obtained when the car was driving in a steady state (constant velocity and just when the differential starts working), but it was not totally possible to get these working points. So, the effect of the weight transfer or the dynamics friction (lower than static or quasi-static) might affect the results. However, the three instants of time for each driving scenario has been got when the friction is fully developed (the breakaway has been already overcome and it is working in sliding conditions) so that the differential allows the wheels turning in different rotational speeds (see Figure 7.1 and its description below and *Appendix E*) working as a semi locked (due to the dynamic friction) differential.

Finally, just to compare with the value of torque difference got in the Rig Test around a 18% (break away torque ratio of 1,444) of the input torque and the value in the reality around 12% (sliding torque ratio of 1,286), and indeed it becomes constant during all the time that might help claiming that the difference of torque between shafts depends on the input load linearly.

The Rig Test Results show the worst case scenario since it is working in the static or quasi-static conditions with higher friction, without the right temperature and oil film

thickness taken into account so that the efficiency is reduced, and in addition, the housing and all the system is standing still without having any motion and the torque is not applied as a pure torque on the rig. So, the sum of all these effects makes the difference much bigger than the real test. Whereas, in the results of the real test, there are some other effects, probably smaller than the differential friction effects, but they still help out increasing slightly the final value so that the differential effects should be slightly lower than this 12% of difference.

If the Loss Model is adjusted to have around 12% of split torque between left/right, the friction coefficient should be reduced by a 33% compared to the one found after having adjusted the model having done the Test 0 (with the original differential design). Then, it might be said that this reduction is mainly due to the dynamic friction (compared to the static-breakaway friction in the Rig Test) and the optimal working conditions with oil film thickness and temperature that makes the friction coefficient decreasing from 0.215 until 0.14.

To sum up, just to get an overview of the results got in the rig. The following Figure 7.1 in the driving scenario 4 can be checked. Where it is possible to see the difference of torque, wheel speed, slip angle and throttle position.

The figures for the other driving scenarios can be found in the *Appendix E*.

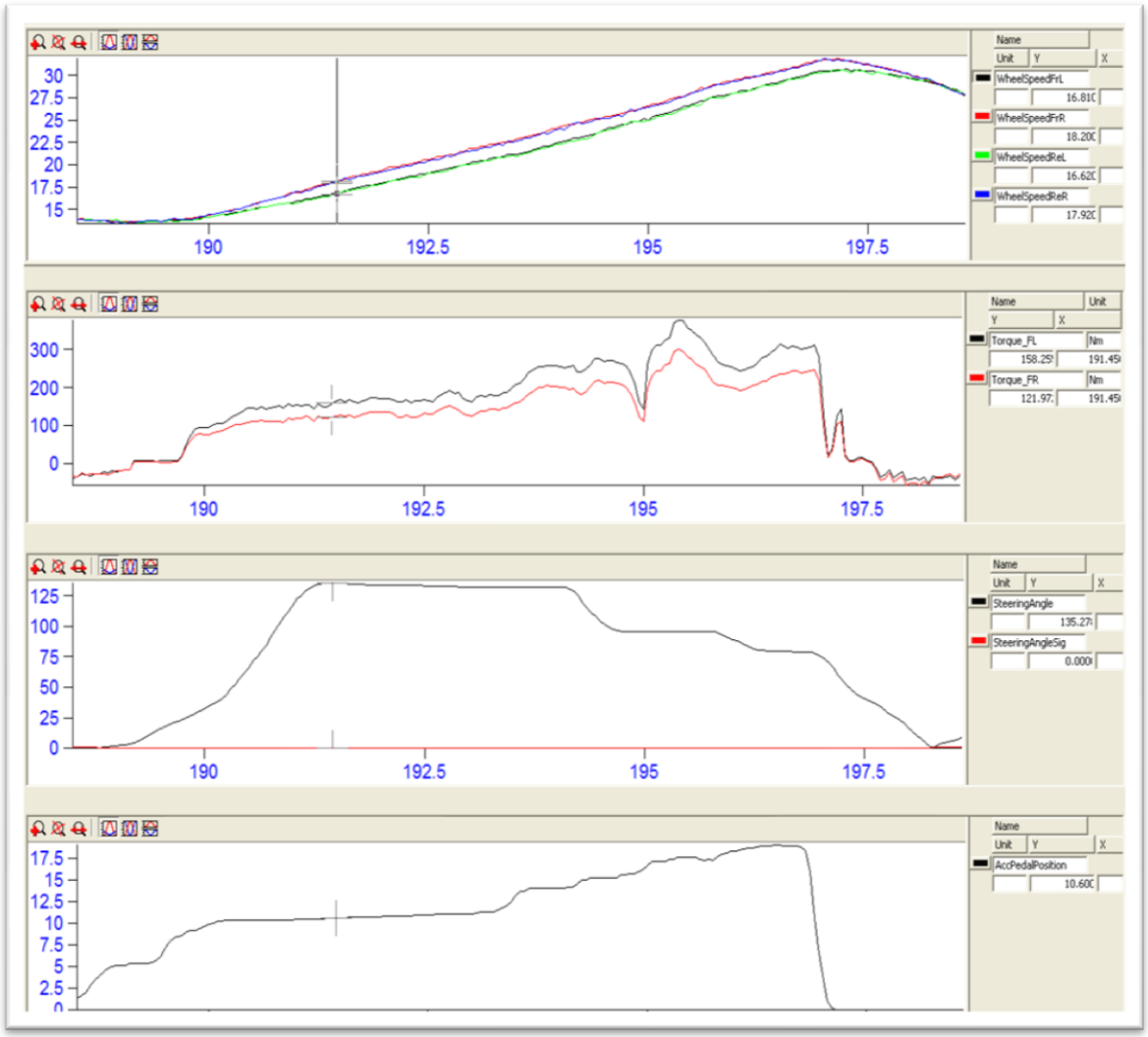

Figure 7.1. Vehicle log data driving scenario 4.

In this logged data from the diagram above, it can be seen, in the first plot, the difference speed of each wheel. In this case it is seen that the values on the right cells are got in the instant when it starts turning, around 1 second after having started turning. In the x-axis, the time in seconds is represented. Here it is seen the difference speed between the inner wheel (left) around 16,8 rad/s and the outer one of 18,2 rad/s. This corresponds to a carrier speed (the average of them) of 17,5 rad/s. Thus, the relative speed seen from the carrier is 0,7 rad/s on the outer and -0,7 rad/s on the inner. Thus, in this case the differential has overcome the breakaway ratio and it has started differentiating the rotational speed for both driveshafts, keeping the constant torque difference of 12,5% of the input torque during these sliding conditions.

The plot just below gives the understanding of the behaviour of the different torque between wheels. It is seen that as it is turning left, the inner shaft has always the higher torque, and the difference keeps more or less constant during the time it is turning.

Furthermore, the third plot shows the steering angle position, around 135º in each case and the signal 0 that gives information of the side that has been turned. The signal 0 means that the steering wheel is turned in the left, and 1 in the right.

Finally, the last plot is the throttle position in percentage of the total travel it has. In this case, the throttle is kept in the same position (around 10% of the maximum travel), so the speed of the car and the torque it has is not so big. It is actually a low torque case scenario.

8 Vehicle Dynamics Simulation

Two vehicle dynamics simulations will be carried out using the torque ratio found during the previous chapters in order to check the dynamics of the vehicle due to a not symmetric torque distribution on both driveshafts.

The first simulation consists on accelerating from standing still (or low speed) until around 20 m/s trying to keep the steering wheel released.

The Modelon Vehicle Dynamic Libraries (VDL) will be used in order to simulate the whole vehicle. The outcome of this simulation is checking the path that the vehicle follows due to the torque difference in driveshafts, instead of the straight ahead line that theoretically should follow and the torque steer effects.

On the other hand, the second simulation deals with a manoeuvre turning the steering wheel following a sinusoidal input signal with an amplitude of 80 degrees. This vehicle dynamics simulation will be done writing down all the equations considering the simple bicycle model and a linear slip model of the tires. The outcome is both getting a reliable model for this driving case scenario and checking the steering wheel torque jump effect.

8.1 Drift effects of a semi locked differential

The simulation is carried out considering the worst case scenario found during the Rig Test of the M66 differential of around 18% of difference when the relative speed in the differential occurs, which yields a torque ratio ($\frac{T_2}{T_1}$) of 1.444.

Moreover, the model has to be set using the VDL libraries and creating the FWD car suitable for the simulation. Then, the model for the differential is modified in order to have a difference torque distribution between shafts due to the losses over the differential. This equation can be easily written as:

$$\frac{T_2}{T_1} = 1 + \text{tanhyp}\ (k \cdot T_0\ (\omega_1 - \omega_2\ )) \cdot loss \qquad (8.1)$$

Thanks to this equation the torque in each shaft can be controlled in each instant of time having the right relative power sign depending on which wheel spins faster. The maximum torque ratio $\frac{T_2}{T_1}$ is then 1.444 that corresponds to a torque difference compared to the input torque around the 18% found during testing.

$T_0\ (\omega_1 - \omega_2\ )$ is an approximation of the realative power flow (power observed with the carrier as reference). The sign of this is a good indication of then power should be loosed from left to right or opposite.

The factor "*loss*" is 1-torque ratio, i.e loss is typically 0.444 considering the differential working in the worst case scenario (differentiating the wheel speed assuming breakaway friction)

The factor *k* should be infinite to model ideal stepping between the discrete states left to right and right to left. But then, the possibility to model the stick state in between is lost. Also, the numerical stiffness of dynamic model becomes not manageable with other solvers. Hence, different *k* has to be tested and an engineering judgement done

to interpret results. Another aspect is that difference static and dynamic friction cannot be modelled with *tanhyp* function. So, the way of modelling as continuous with *k* is not perfect, but pretty straight forward.

The hyperbolic tangent allows not having a perfect straight step that might cause an error to the solver, and then the step between a torque quotient of 1-1.444 and 1.444 is more controlled (Note that the interval should go from 1/1.444 until 1.444, thus this model function just will work for the positive wheel speed difference).

In fact, what was not possible to be considered in this model due to the complexity (see in Chapter 10 in the Future Recommendations) is having the locking mechanism in the beginning until the differential reaches the friction and starts differentiating and it switches to the sliding torque ratio. Using the hyperbolic tangent it was tried to model this behaviour, but the effect with this Equation (8.1) just models how the differential reaches the semi locked state, starting from fully lock (equal speeds in driveshafts) changing straight forward from this point, depending on how big the relative speed is, the torque ratio until the maximum value is got.

However, simulating the whole car might have some effects that might have been difficult to be predicted due to for instance the weight transfer, non symmetric tires, suspension linkages stiffness, etc.

Thus, the initial conditions and the constraints were set until it was managed to get the car straight ahead keeping the steering wheel released (as it is seen in the Figure F.1 in the *Appendix F*). The acceleration was decided to be reduced, with a constant throttle position of the 35% (equivalent acceleration around 2 m/s^2) and an initial speed of 5km/h (so as to avoid the initial numerical solver oscillations). See the Figure F.2 in the *Appendix F*. So, finally the simulation can be carried out considering equal stiffness between shafts (in order not to allow the different torsional stiffness affect the results). Actually, the tolerance of the Dassl computational solver had to be decreased until 10^{-8} in order to get the results clean of computational oscillations

Furthermore, in order to have a relative speed keeping the steering wheel released, some parameter had to be modified in order to make the car driving towards one side (so as to have a wheel speed difference), so that still keeping the VDL differential model (perfect 50% torque distribution to each driveshaft), it was decided to change the size of the right wheel in order to get a higher traction force in this wheel and force the car going towards the left since the car will be initially pulled.

However, this would cause a steering angle and after a transient period the car would go straight ahead again (albeit not along initial path) due to the alignment torque and weight transfer. Thus, as the whole vehicle model was being simulated, in order to see reliable results according to some Modelon expertises, it was decided to keep the steering wheel, to see the results as it was expected to do releasing the steering wheel.

Hence, to force the difference wheel speed, the steering wheel was kept at 5º. Then, as it was already known the path the car and so does the relative wheel speed, the Equation (8.1) in the model was changed to the following one:

$$\frac{T_1}{T_2} = 1.444 \qquad (8.2)$$

Using this equation, it was possible from the initial instant already allow the inner wheel (left wheel) having more torque than the outer, making in this case the car more understeered. In fact, this is an assumption, since the differential might remain lock the first instant of time, and then as the torque ratio has been considered in the worst

case scenario possible, the relative power flow might change from one side to the other, having them transient understeer and oversteer behaviours.

In the Figure 8.1 below it is seen the blue curve with the dynamics of the VDL model, and the red curved with the differential model modified to have the torque difference between driveshafts. Even though in both situations the steering wheel was kept at 5 degrees, the car did not follow the same path.

It should be point out that the car does not become understeered for all driving situations due to having a friction inside the differential. If the differential is totally locked there are rapid transitions between over/understeer depending on actual load case/driving scenario. However, with this case with small lateral and longitudinal acceleration, as well as a small steering wheel angle (big curve radius), the results are reliable. The differential becomes a semi-locked differential since the inner wheel releases more torque trying to get the car understeered.

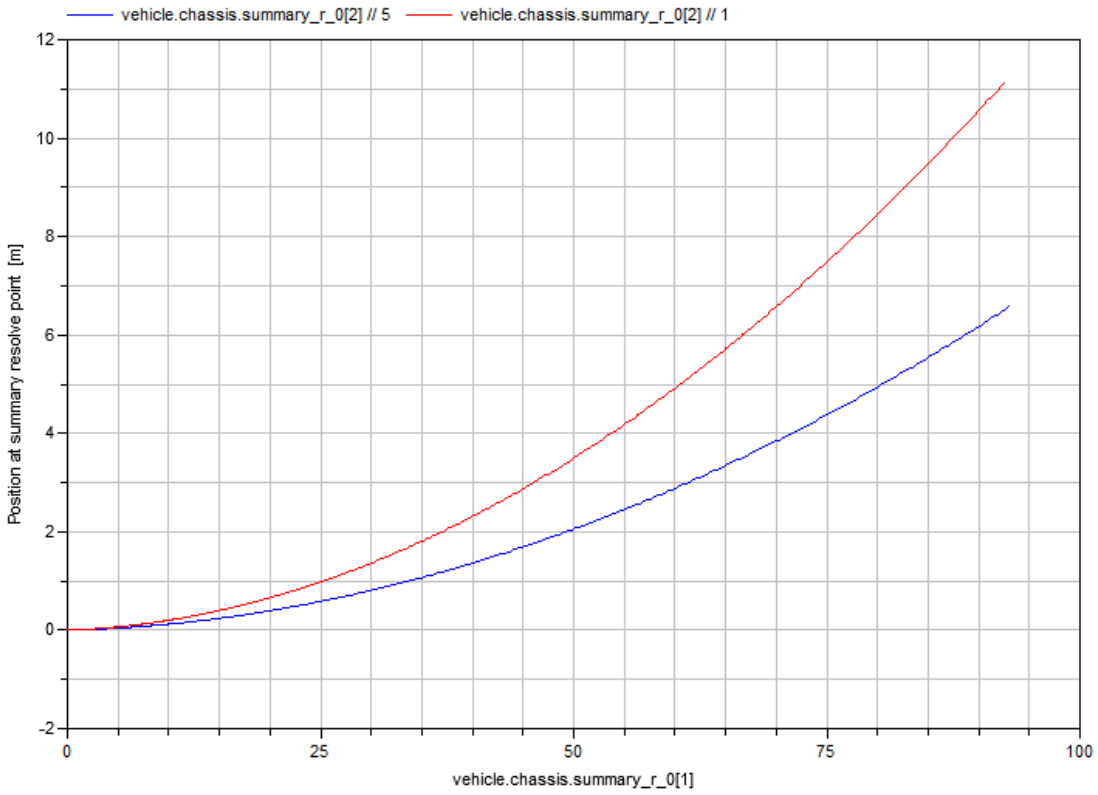

Figure 8.1. Lateral displacement vs. Longitudinal displacement [m].

Thus, if the yaw rate is plotted (Figure 8.2), the effect of the differential is seen to understeer the car since the model considering losses over the differential (blue curve) has a lower yaw rate, so for the same steering angle the yaw gain is lower (on top of that in the *Appendix F* the plots of the lateral slip of the car, the lateral speed and acceleration are shown).

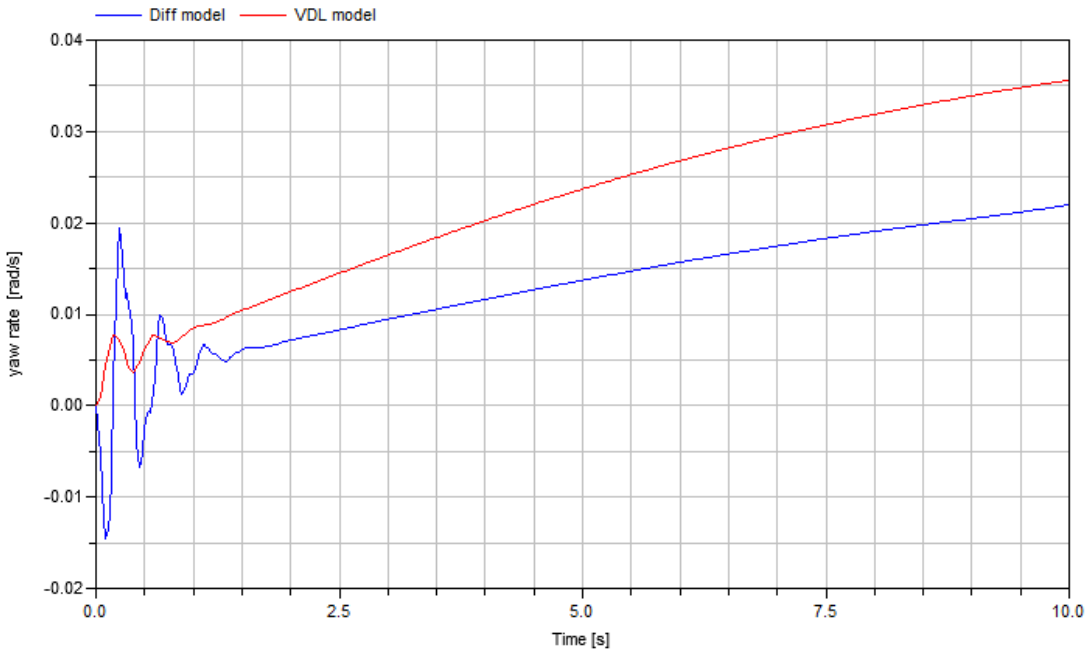

Figure 8.2. Yaw rate vs. Time.

As the steering wheel has been kept, once the differential is acting, the driver would notice a steering feeling due to this non-symmetric balance of the torque. The Figure 8.3 shows the results of the torque steer considering both models.

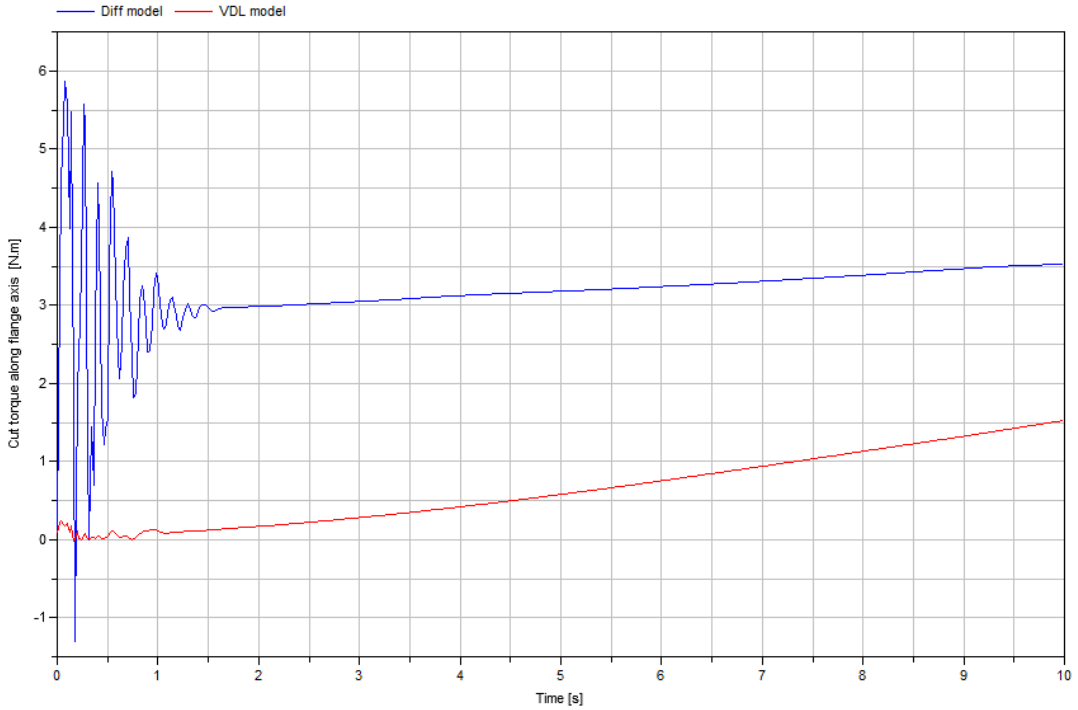

Figure 8.3. Torque steer vs. Time [in seconds].

In this case, the torque steer is around 3Nm which would mean that the driver should note a force of around 750 g in each hand when the steering wheel is kept. It is quite big due to the consideration of the worst case scenario the static breakaway torque

ratio during all the simulation. Whereas with the open differential the driver would not notice any steering feel. However, it is seen that the torque increases slightly even though the 50% distribution is done. This is due to the other asymmetries of the car, better said, the other causes of the steering feel, such as the kingpin, driveshafts constant velocity joints, weight transfer and slip of the tyres.

Actually, the slip is a factor to take into account as well when the differential is not distributing the torque equally between shafts. When the differential has theoretically perfect, the torque of the wheels is limited by the inner one (less traction) allowing having different slip in the wheels.

Whereas, when the differential is semi locked, it is forcing the wheels having a closer slip each other since there is a relative power flow towards the inner wheel (the worst case scenario is when a spool is used, where the slip of the wheels is really similar but, the traction force of each wheel is the maximum one allowed).

To sum up, if the wheel speed is compared for inner and outer for both models, for a small instant of time (see the behaviour of the wheel speed versus all the simulation time in the *Appendix F*), the plot below is got.

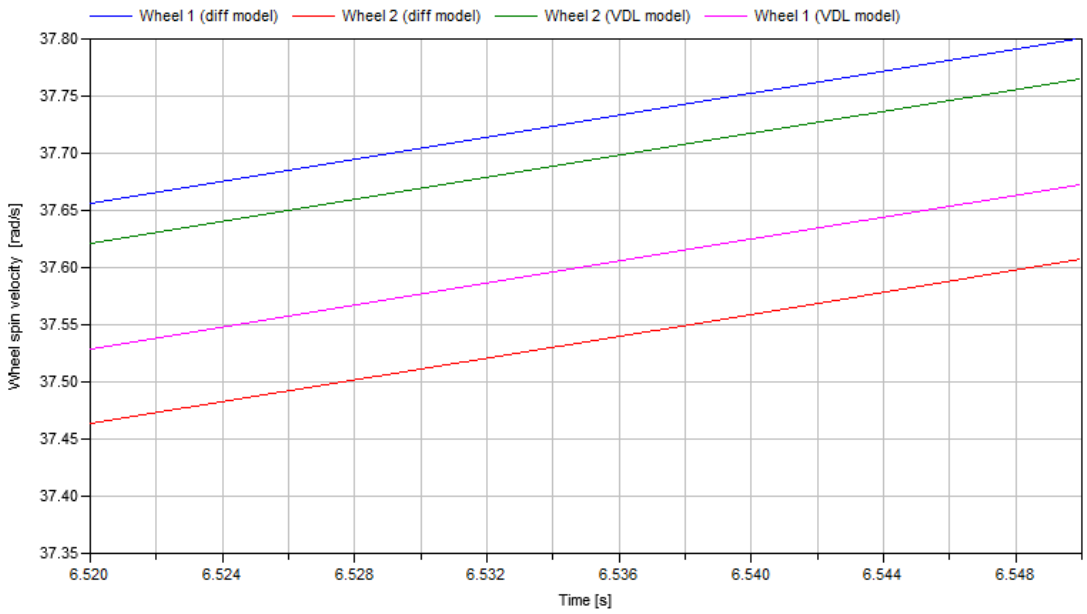

Figure 8.4. Wheel speed vs. Time [in seconds].

When the differential is fully open (VDL model), the inner wheel will always turn faster than the inner (speed wheel 1 slower than speed wheel 2). Actually a really small wheel speed difference (around 0.0718 rad/s) since the turning radius is considerably big.

But, when the differential has a relative power flow, it is seen how the inner wheel in this driving scenario has even higher speed than the outer. The cause might be that since the weight transfers is towards the right side, this wheel has a higher load force, when in the other side, the inner wheel has lost some normal force and also is getting a higher torque from the differential (actually in this case, relatively higher since the breakaway ratio is considered), it yields to some slip in this wheel. Thus, the wheel

speed difference has become higher (absolute value around 0.1936 rad/s). However, the results of the handling of the car can still be used to understand how the car would behave during this manoeuvre because the wheel speed difference is relatively low. Thus, even though the relative power should change the sign, it can be understood as an example of a permanent semi locked differential for a limited lateral acceleration and slip.

8.2 Sinusoidal steering wheel angle input

8.2.1 Model description

Analysing the effect in the torque steer due to the effect of a differential is the main goal of this second vehicle dynamic simulation.

Thus, in order to make the model working and trustable with a compromise with the difficulty and time consuming, it was decided to neglect the lateral slip (also, it was just needed the torque steer effect and the side slip would be just needed to determine path and cornering forces). The only reason to include the side slip would be if so much side slip was used that a combined slip tyre model was needed.

In the *Appendix F*, the Dymola model is shown with all the equations that have been set so as to analyse this driving scenario. However, this chapter covers the setting of all the equations and assumptions considered.

In order to start the model, the input in the steering wheel angle is set with the following equation:

$$SWA = SWA_{ampl}\frac{\pi}{180}\cos\left(2\pi f t + \frac{3\pi}{2}\right) \qquad (8.3)$$

Using this function the steering wheel input will be modelled as the following plot (considering a frequency of 1 Hz):

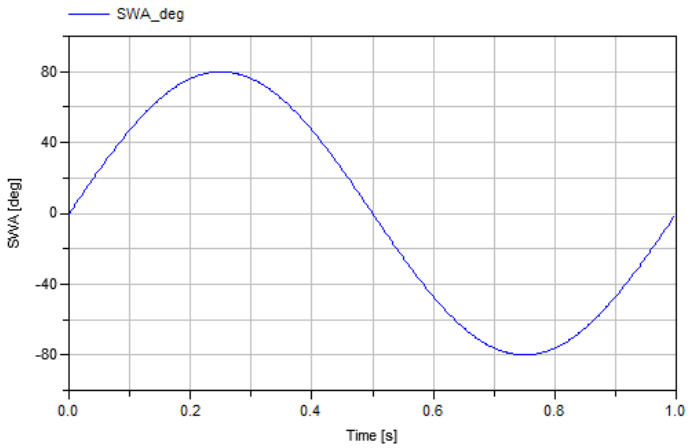

Figure 8.5. Steering wheel angle vs. Time [in seconds].

The other inputs in the system are:

- Output torque of the transmission set to 3600Nm (considering an engine torque of 300Nm and a 2nd gear ratio of 1:3 and a final drive of 1:4 given by VCC Chassis Department as the conditions where the steering feeling might be noticed).

- Longitudinal vehicle speed set to 10m/s.

- Static torque ratio of the differential (break away) $\frac{T_1}{T_2} = 1{,}444$

- Dynamic torque ratio of the differential (sliding) $\frac{T_1}{T_2} = 1{,}286$

Note that the first static torque ratio has been set from the results of the Rig Test, and the dynamic ratio has been got from the logged data of the Vehicle Test.

The model deals with a discrete dynamic model so that some different submodels will be needed as well as some boundary conditions in order to have the switch of equation one is needed.

Basically, the model has three positions (states) where it should be possible to switch the output.

1) When the differential is locked (when the relative speed between shafts is zero).In this case, the equations ser are:

$$\omega_0 = \frac{\omega_1 + \omega_2}{2} \quad (8.4)$$
$$\omega_1 = \omega_2 \quad (8.5)$$
$$T_0 = T_1 + T_2 \quad (8.6)$$

2) When the car goes towards the left side and differential is acting:

$$T_1 = loss_{fact1} \cdot T_2 \quad (8.7)$$

The other two equations are (8.4) and (8.6).

3) When the car goes towards the right side and differential is acting:

$$T_2 = loss_{fact1} \cdot T_1 \quad (8.8)$$

The other two equations are (8.4) and (8.6).

Finally, considering the linear slip model of the tire, the equations for slip, traction force and torque wheel are:

$$s_{x1} = \frac{(R_w\omega_1 - v_{1w})}{\frac{(R_w\omega_1 + v_{1w})}{2}} \quad (8.9)$$

$$s_{x2} = \frac{(R_w\omega_2 - v_{2w})}{\frac{(R_w\omega_2 + v_{2w})}{2}} \quad (8.10)$$

$$F_{x1} = C_w s_{x1} \quad (8.11)$$

$$F_{x2} = C_w s_{x2} \quad (8.12)$$

$$T_1 = F_{x1} R_w \tag{8.13}$$

$$T_2 = F_{x2} R_w \tag{8.14}$$

On the other hand, the kinematics equations of the vehicle, if the side slip is neglected and the bicycle model is used (see Figure 8.6 below and [36]) the equations yield to be:

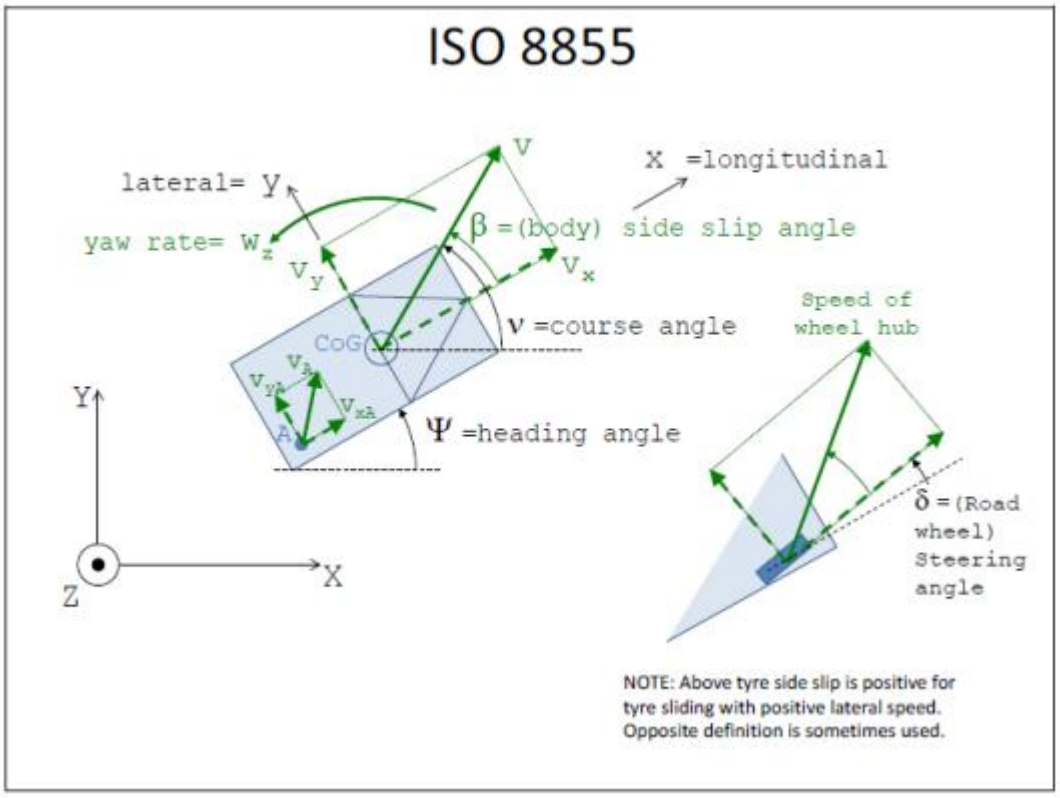

Figure 8.6. ISO coordinate system and motion in road plane, for body and wheel

- Road wheel steering angle

$$\delta_w = \frac{SWA}{S_{ratio}} \tag{8.15}$$

- Yaw rate (define positive when vehicle turns left)

$$\omega_z = \frac{v_x \tan(\delta)}{L} \tag{8.16}$$

- Longitudinal wheel speed (along x-axis)

$$v_{1v} = v_x - \omega_z \frac{tw}{2} \tag{8.17}$$

$$v_{2v} = v_x + \omega_z \frac{tw}{2} \tag{8.18}$$

- Longitudinal wheel speed

$$v_{1w} = \frac{v_{1v}}{\cos\delta} \tag{8.19}$$

$$v_{2w} = \frac{v_{2v}}{\cos\delta} \tag{8.20}$$

- Lateral wheel speed (in the middle between shafts)

$$v_y = \omega_z \frac{L}{2} \tag{8.21}$$

-Lateral wheel acceleration

$$a_y = \omega_z v_x \tag{8.22}$$

-Longitudinal acceleration (along *X-axis*)

$$\frac{dX}{dt} = v_x \cos\varphi_z - v_y \sin\varphi_z \tag{8.23}$$

- Lateral acceleration (along Y-axis)

$$\frac{dY}{dt} = v_y \cos\varphi_z + v_x \sin\varphi_z \tag{8.24}$$

-Yaw acceleration

$$\frac{d\varphi_z}{dt} = \omega_z \tag{8.25}$$

- Torque difference

$$SWT = T_1 - T_2 \tag{8.26}$$

-Torque ratio

$$T_{ratio} = \frac{T_1}{T_2} \tag{8.27}$$

- Relative power

$$P_{rel} = T_0(\omega_1 - \omega_2) \tag{8.28}$$

8.2.2 Simulation results

Hence, the discrete vehicle model is working in such a way that from the input from the driver and the gear box, the vehicle equations are calculated and to complete the kinematics and dynamics of the system, the model switches between 1), 2) or 3) depending on the conditions.

The Figure F.10 in the *Appendix F* shows the state of the vehicle during all the cycle, either if it is locked or if the differential is allowing the wheels turning freely.

From the first instant when the steering wheel is kept to 0º, the differential is working as if it was a spool. Suddenly, the driver starts turning it into the left, the first relative speed between wheels should appear, but the differential remains locked until the torque ratio reaches the break away, when just then the differential starts differentiating the speed between wheels at the same time as the torque ratio decreases to the dynamic condition. The model is working in this level (2) according to the positions described above) until the relative power flow changes sign as soon as the steering wheel angle is decreasing, when the differential becomes lock until the following break away ratio (when the car is turning right) is reached.

Once all the switches connections in the model are done, the results can be analysed. In plot below shows the trend of the torque ratio over the time:

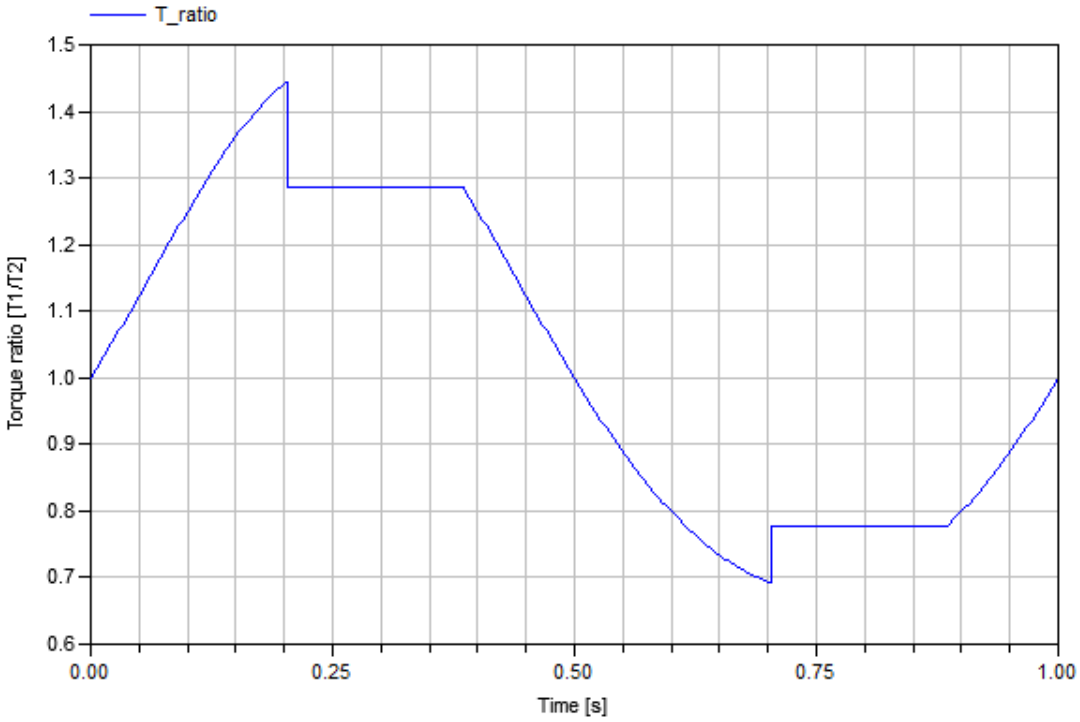

Figure 8.7. Torque ratio vs. Time [in seconds].

By means of this plot, the phenomena of the torque steer and particularly, the torque steer jump that occurs in driving conditions is figured out. This phenomena yields to jump effect in the steering feeling of the driver due to the friction in the differential. From the first instant the differential is acting as a lock differential for two reasons. The first, because the relative speed between wheels is zero and the second is because the torque ratio has not overcome the breakaway value needed to have the working point of the differential differentiating the speed towards the wheels, so until the torque ratio does not reach the breakaway value, the differential will not work as an open differential and will be still locked.

This is the reason why the driver may feel this torque steer jump as soon as decides to turn the steering wheels. Actually, during the first instants, the driver can already feel a torque steer in the steering wheel since the wheels should have different speed and due to the losses inside the differential is acting as a locked so that, instead of having a open differential without any torque steer (due to the differential effect), the driver feels already a torque in the steering wheel.

Furthermore, as soon as the driver keeps turning the differential will be under working conditions, differentiating the wheel speed and the inner wheel with a torque 1,286 times higher than the outer.

Once the steering wheel angle starts decreasing, the differential wheel still remain in these working conditions until the relative power flow changes the sign, when it goes towards the right wheel. This is the time when the differential will become locked again, until the torque ratio reaches the breakaway loss factor$\frac{T_1}{T_2} = \frac{1}{1{,}444}$.

If the relative power flow is plotted, it is seen how the instants that the power flow becomes zero, are the instants when the differential becomes locked again:

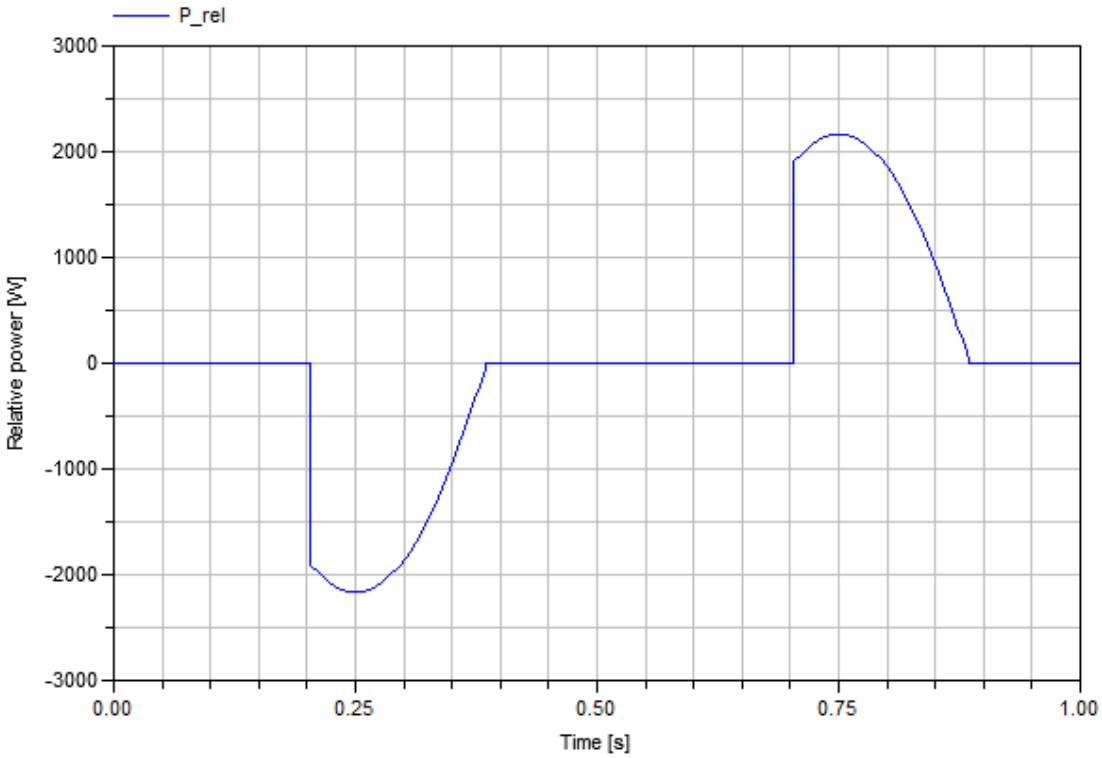

Figure 8.8. Relative power vs. Time.

Thus, the steering feeling that the driver will notice will be proportional (depending the kingpin, pneumatic trail and the driving conditions) to the torque difference between driveshafts. This torque distance is seen in the Figure 8.9 below:

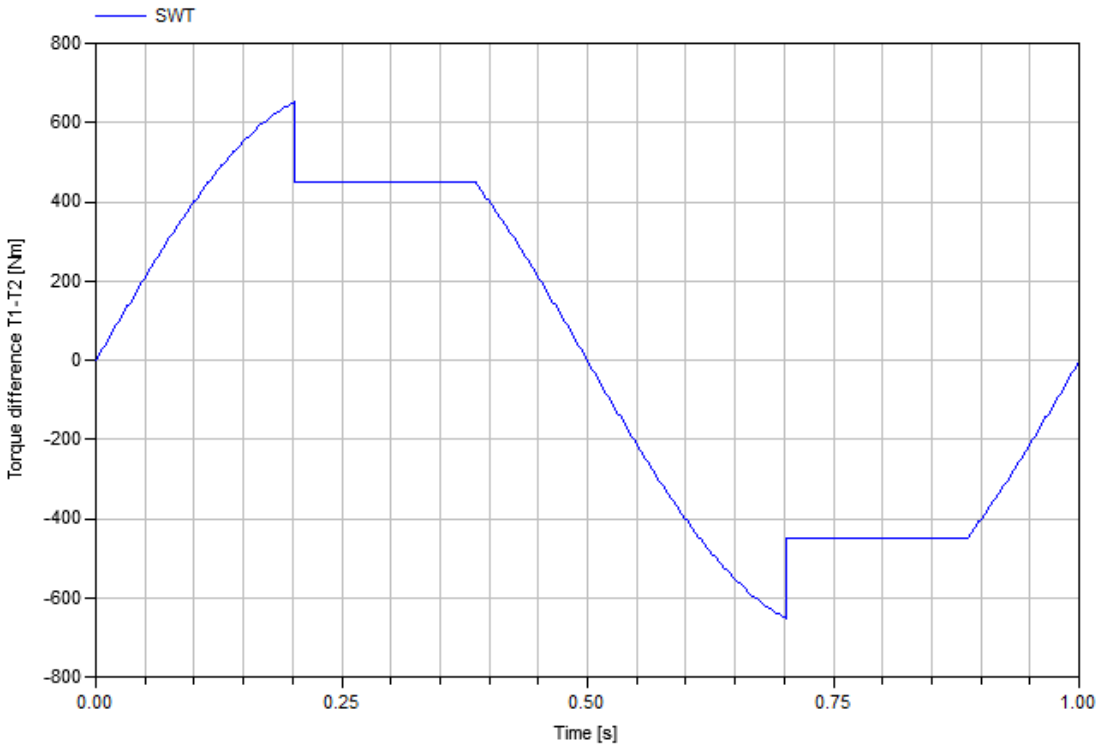

Figure 8.9. Toque difference vs. Time [in seconds].

Furthermore, the wheel speed difference shows that the model has some debatable simplifications. The wheel speed changes in steps, which is physically possible if the rotational inertia is neglected.

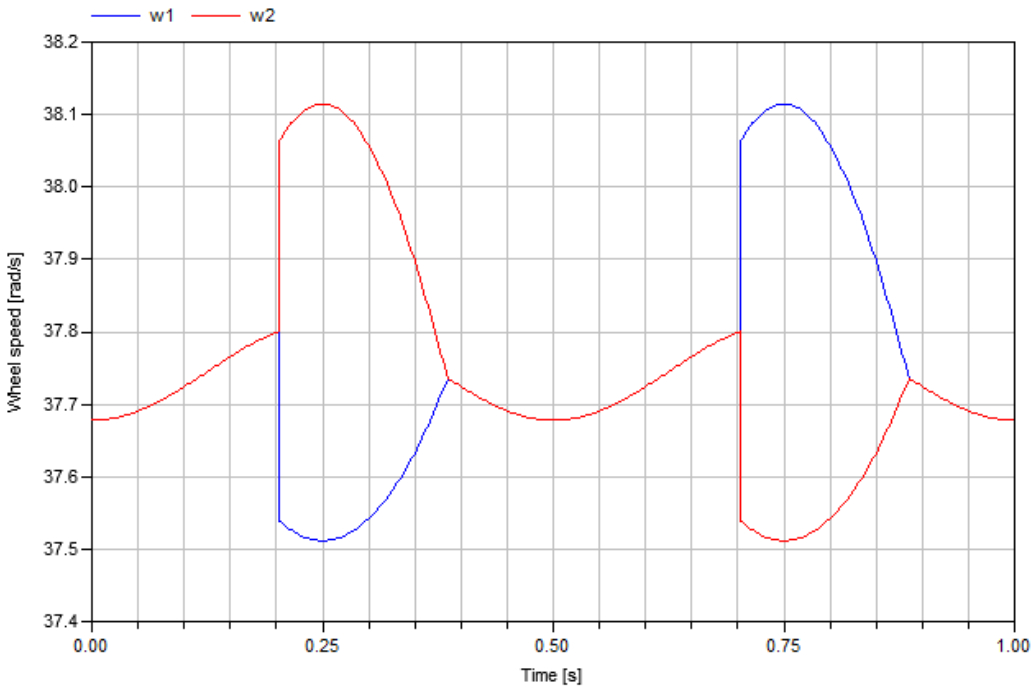

Figure 8.10. Wheel speed vs. Time.

Actually, if it is compared to the speed the wheels would have if the slip was neglected (infinite C_w), the plot would be as $\omega_{1Noslip}$ and $\omega_{2Noslip}$ in the following picture:

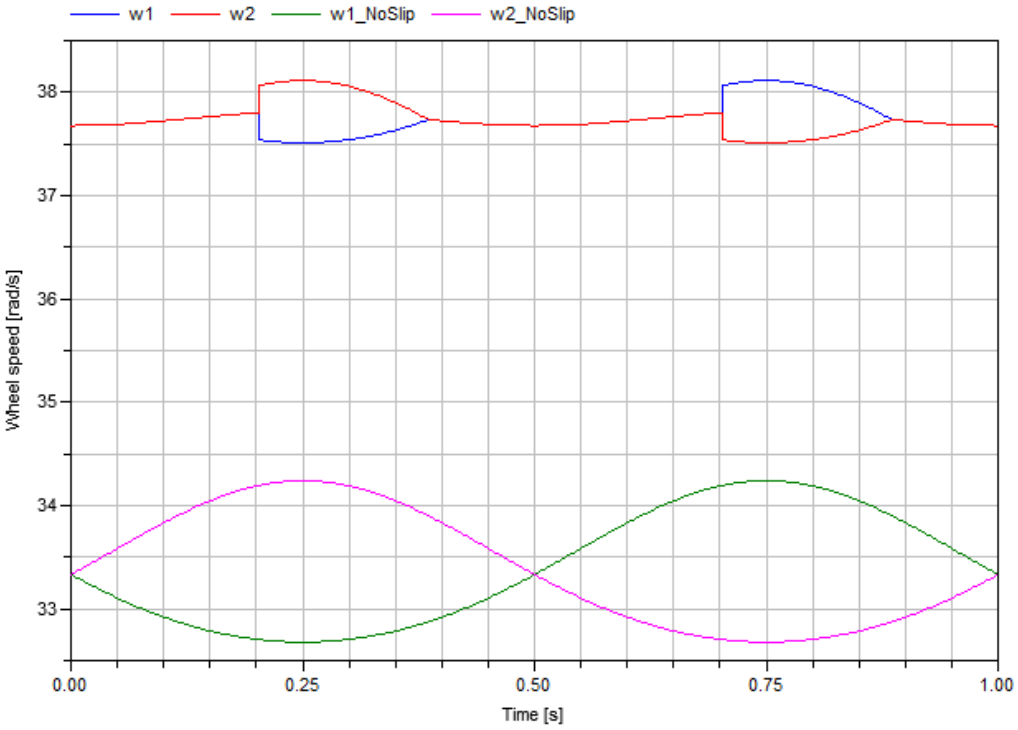

Figure 8.11. Wheel speed comparison vs. Time.

where the $\omega_{1Noslip}$ and $\omega_{2Noslip}$ are calculated with the kinematics equation of a perfect rolling (independently of the differential state) as it is seen below:

$$\omega_{1Noslip} = \frac{v_{1w}}{R_w} \tag{8.29}$$

$$\omega_{2Noslip} = \frac{v_{2w}}{R_w} \tag{8.30}$$

What happens is that the wheels are forced during the locking period and there is no relative speed. In addition, it is seen that the wheel speed in locking time is changing. For instance, in the beginning of the manoeuvre, the wheel speed increases. It is because it has assumed a constant longitudinal wheel speed along the vehicle axis, without assuming the conservation of the energy, then, as soon as the steering wheel angle increases the wheel speed increases as well due to the vehicle motion equations (in the *Appendix F* in the Figure F.12 there is plotted the rotational speed that the car would have if the differential was locked during all the manoeuvre).

Furthermore, as the relation between the rotational wheel speed and the lineal wheel speed has not been taken into account, then the model supposes a variable radius during the time due to the longitudinal slip.

Moreover, if the plot of lateral acceleration is shown, it is seen how the magnitude of the lateral acceleration is around 2,92 m/s^2, which is reasonable low and it seems then that the assumption taken into account that the lateral slip might be neglected seems alright. Assuming a large enough friction, the amount of grip is limited by the tire. If the amount of used lateral force is $m \cdot a_y$ and the maximum is $\mu \cdot mg$ (where mg is the vertical force) it is get that the car uses the tire contact around the 30% in lateral and around 14% in longitudinal (*x-axis*) direction (as it is seen in the Figure 8.14). This yields to a combined tire contact used around 33% ($\sqrt{14^2 + 30^2}$), which is below the 50% when the non-linear effects start appearing. So, if the combined slip was added, the results would not be affected strongly and the conclusions of the torque jump would still be analogously. Nevertheless, in the *Appendix F* it is checked the lateral force in each axle individually and that yaw dynamics do not require large lateral force on individual axles so as to be able to neglect the lateral effects.

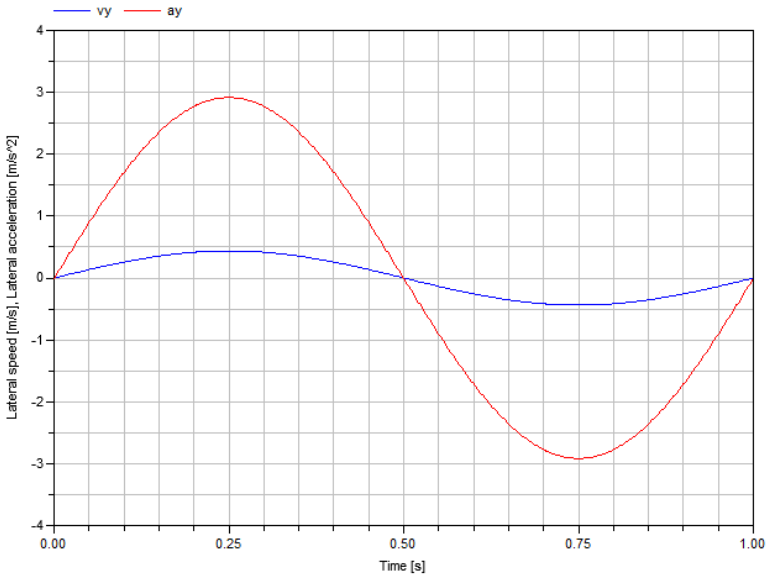

Figure 8.12. Lateral speed and acceleration vs. Time.

8.2.3 Influence of the stiffness

The stiffness of the tire will affect the dynamic behaviour of the vehicle. Thus, if a comparison between the stiffness of the wheels is carried out, for instance, doubling the tire stiffness from $4{,}9 \cdot 10^5$ N of the initial value until $9{,}8 \cdot 10^5$ N, it is seen in the Figure 8.13 how faster the response is once the tire used is stiffer.

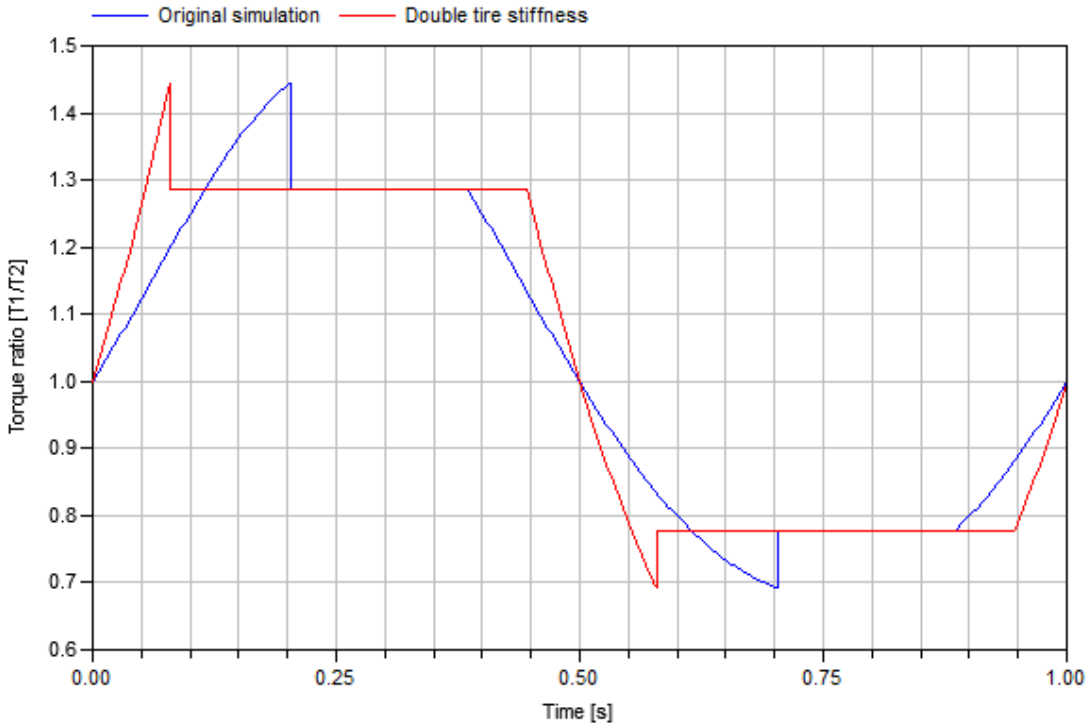

Figure 8.13. Comparison Torque ratio vs. Time.

The red curve represents the torque ratio over all the cycle with a double tire stiffness value. With a double tire stiffness value the jump appears earlier in each cycle. In addition, no change in level occurs during speed differentiating phase.

Whereas, the path that the car follows will be the same, since the path is constraint by the vehicle equations and does not depend on the stiffness of the tire, since we have not taken into account lateral accelerations.

8.2.4 Comparison traction force and wheel slip for different torque

In order to compare the behaviour of the traction force and the wheel slip. The parameters are plot through the cycle and are compared within two different input loads, one for the current torque of 3600 Nm and the other for 1800 Nm.

The results are shown below, it is seen that as the traction forces is lineally dependent on the slip, the curve of the traction force will remain the same as the slip just multiplied per the tire stiffness. It is seen as well, that doubling the input torque, the traction force is doubled. In addition, the breakaway occurs faster (this will be studied in more detail in the following subchapter).

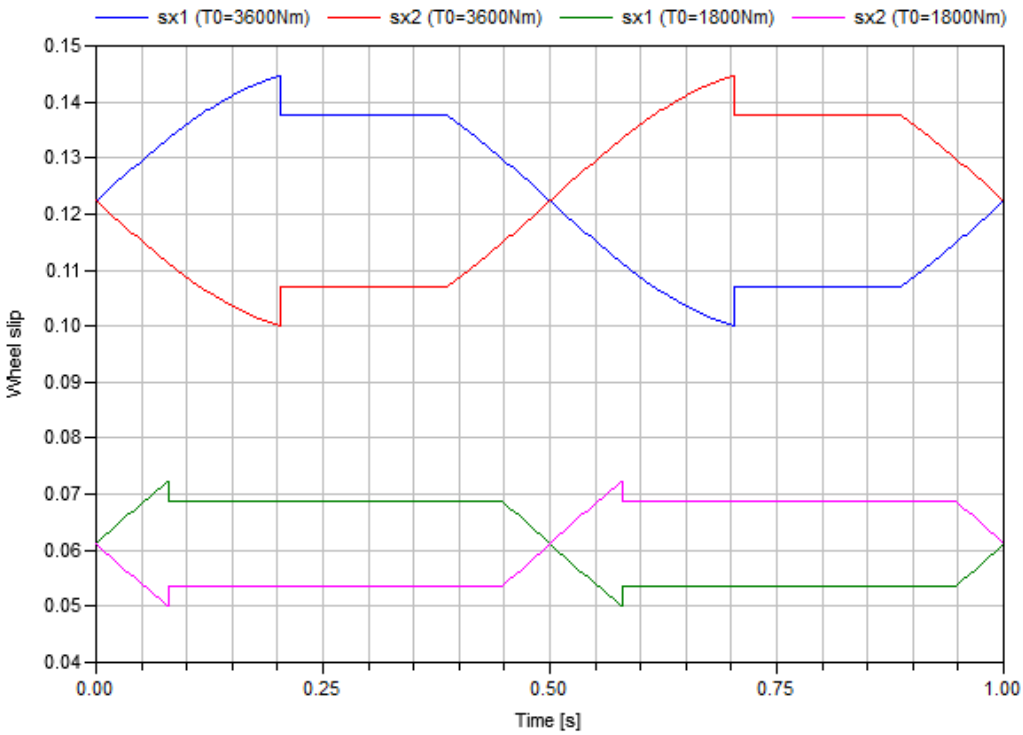

Figure 8.14. Wheel slip vs. Time.

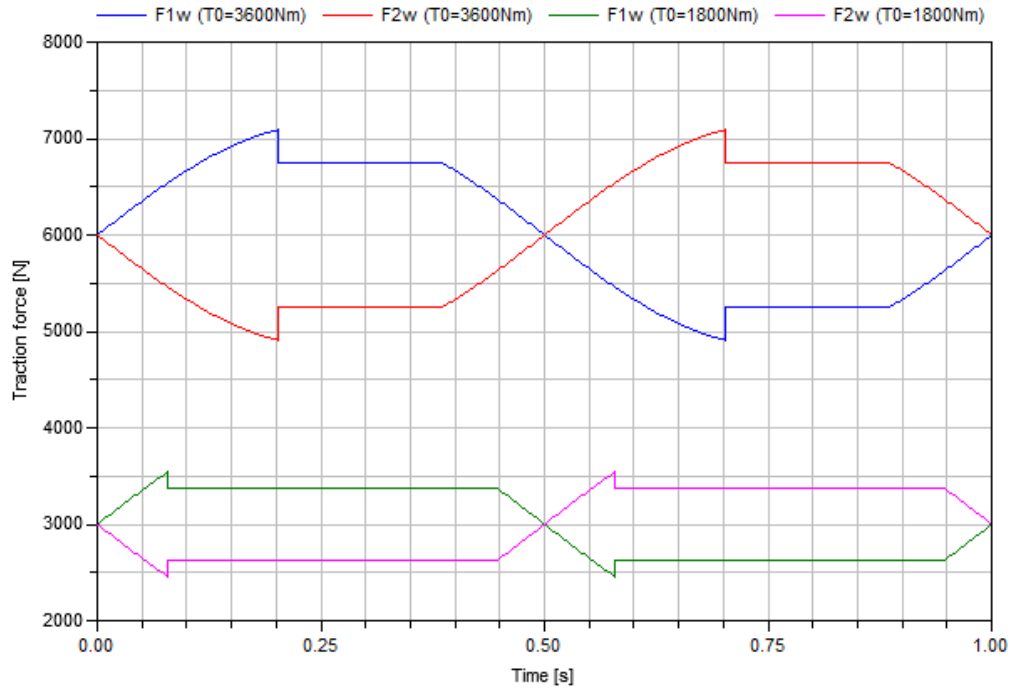

Figure 8.15. Traction longitudinal force vs. Time.

8.2.5 Variation in total traction force

If the traction torque is increased from 3600 Nm to 4000 Nm, the character of the solution swops dramatically for this driving scenario.

This can be understood by studying how the tire slip characteristics influence shaft torques. At the higher traction, the shaft rotational speed is higher so that with linear (not saturated) tire models and a traction independent from a vehicle speed, which means that $T_1/T_2 \propto s_{x1}/s_{x2}$ goes towards a unitary torque ratio since the slips increases unlimited. If the torque ratio is higher than 1,444 at lower traction, then for higher traction it should not reach the breakaway value. The value from when the vehicle does not reach this torque ratio is around 3665 Nm, for this boundary conditions and driving scenario.

Below, it can be seen how the torque ratio does not reach the characteristic value of the differential.

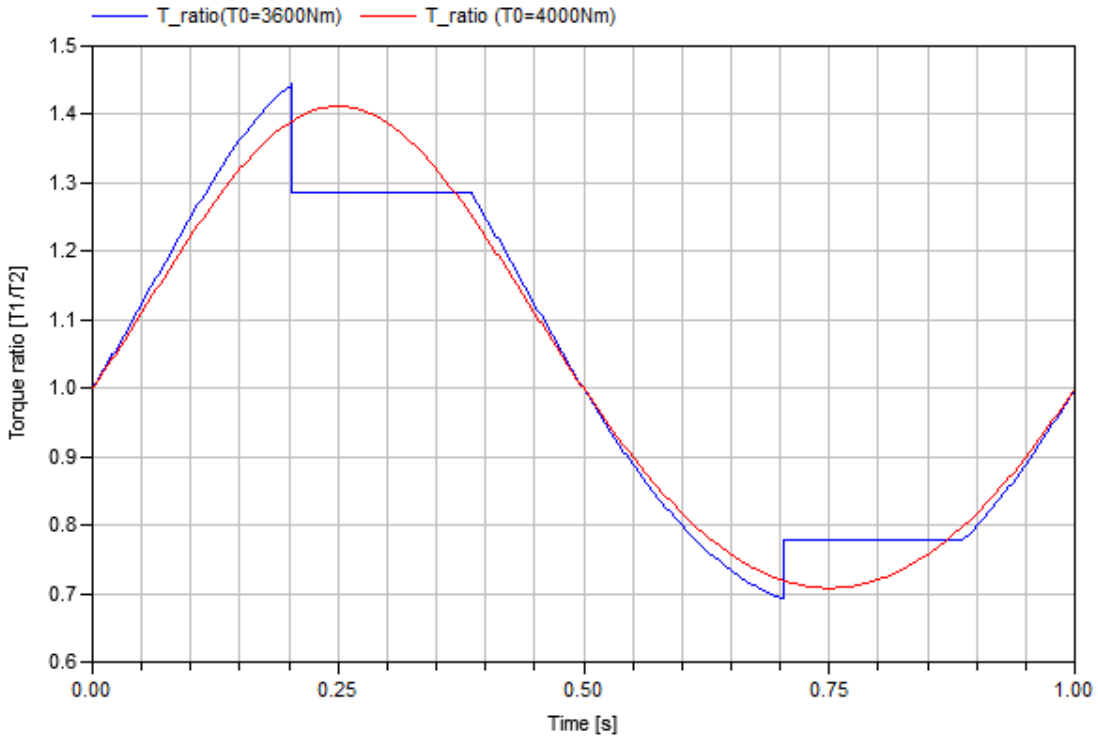

Figure 8.16. Comparison Torque ratio vs. Longitudinal displacement.

So, just increasing in this case the input torque to 500Nm, the vehicle will not achieve to overcome the value needed for the differential so that the differential will remain lock during the whole range of the cycle.

The wheel speed difference will be zero for this higher input torque. In the Figure 8.17 below it can be seen.

In the *Appendix F*, the plots of the wheel speed for each load case can be found independently.

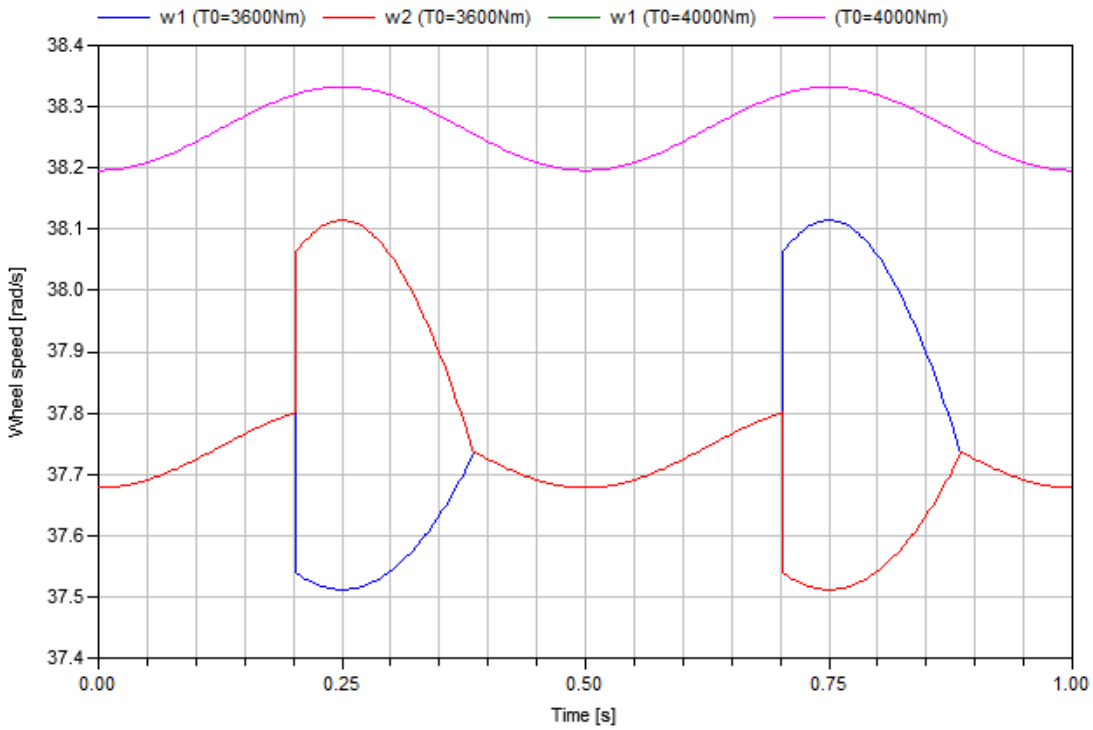

Figure 8.17. Comparison Wheel speed vs. Longitudinal displacement.

Below a longer simulation where the traction is increased linearly in the time is shown. The sliding state duration becomes smaller and smaller until when eventually vanishes. One can probably find certain areas in a longitudinal speed – acceleration diagram where the jumping phenomena can occur (or will occur if suitable steering amplitude is used).

For this slope of input torque over the time, the results are seen in the figures below:

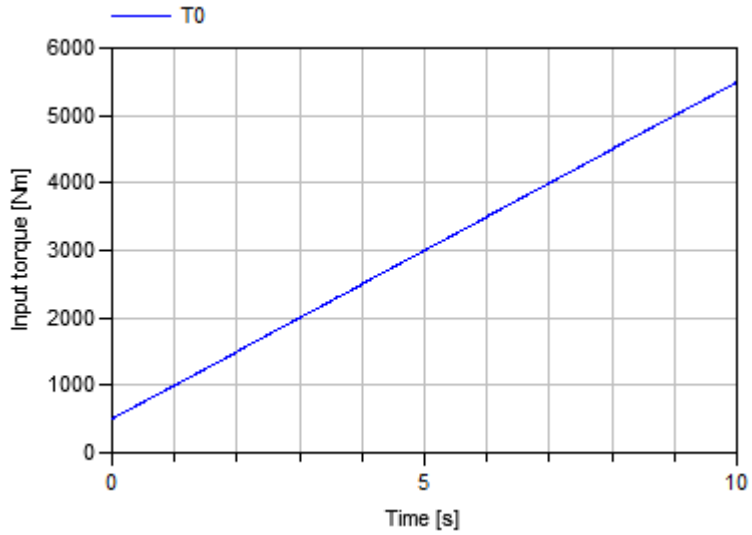

Figure 8.18. Linear input torque vs. Time.

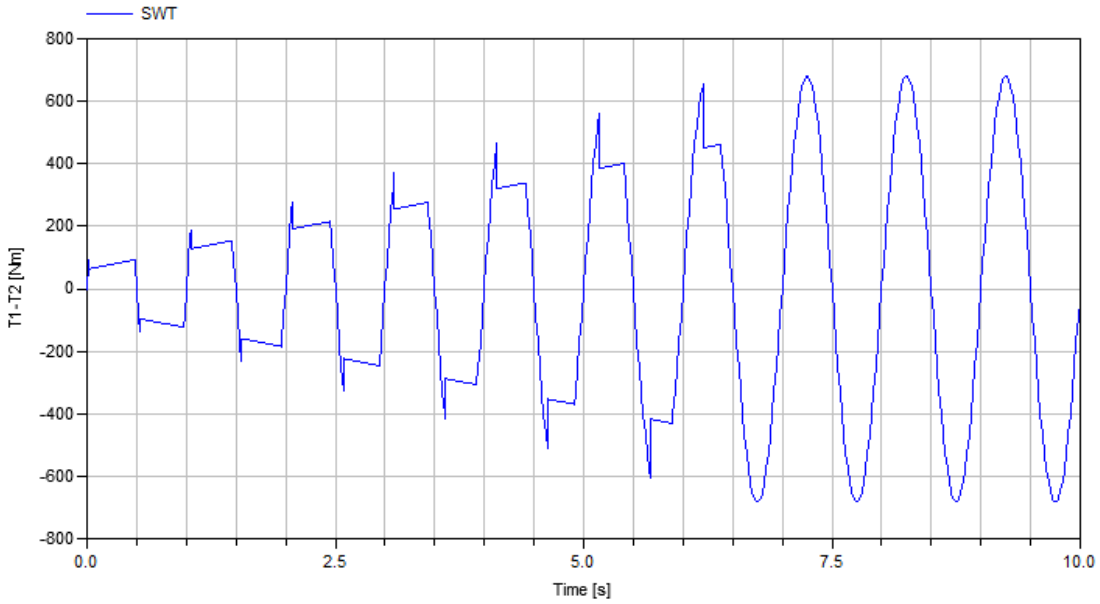

Figure 8.19. Torque difference vs. Time.

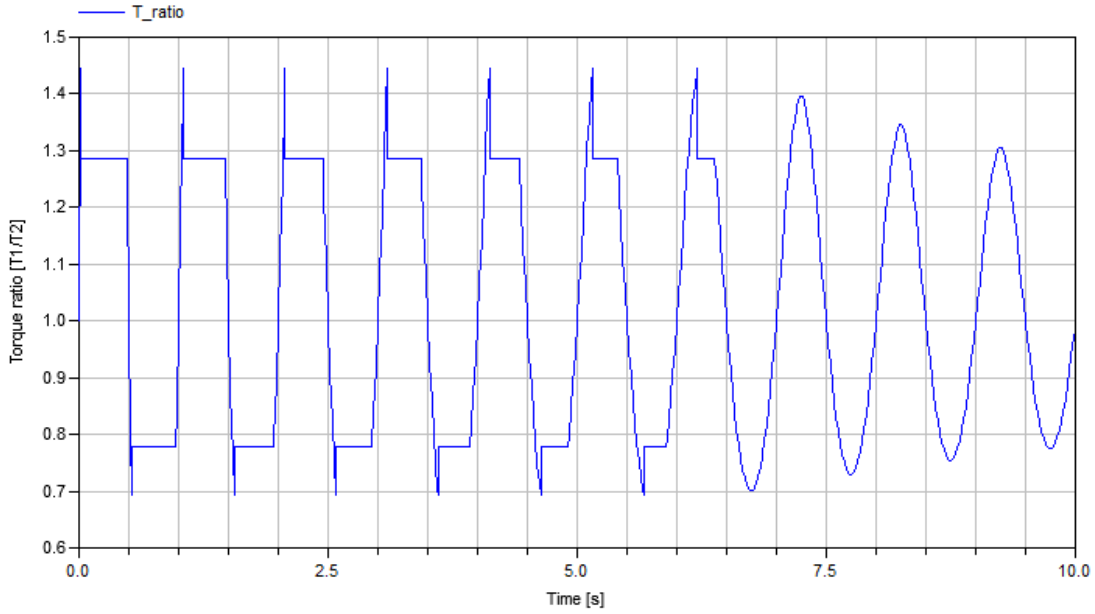

Figure 8.20. Torque ratio vs. Time.

If the input torque linear variation is done in two steps, starting from 3000 Nm and increasing lineally 650 Nm with the time, the evolution of the torque difference and the torque ratio can be seen in more detail.

As the torque is increasing during all the cycle, it is seen that even during the time when the differential is working, the torque difference is still increasing instead of remaining constant.

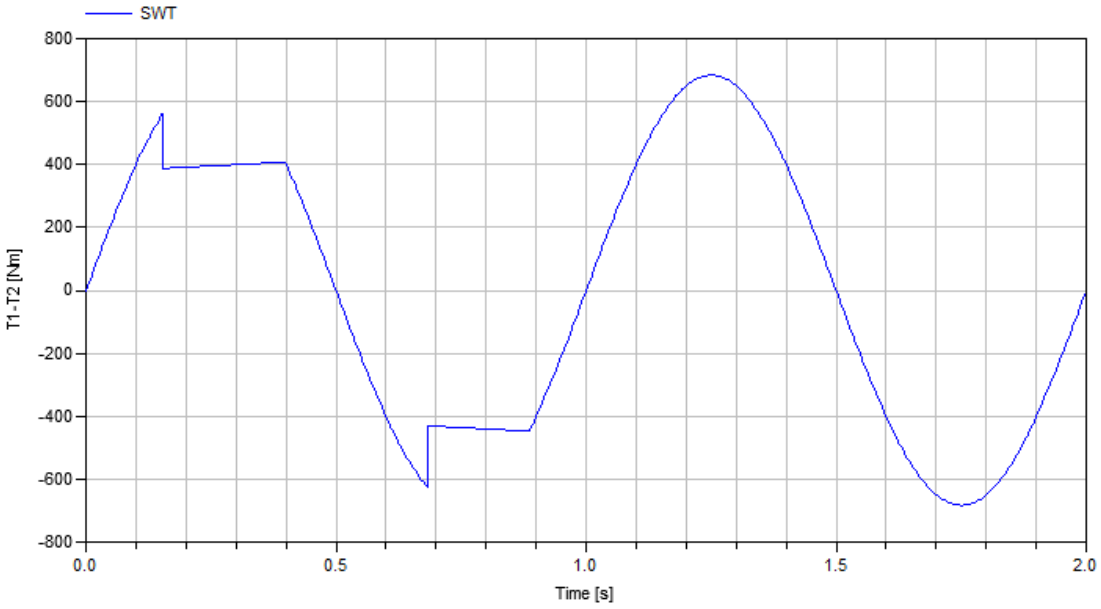

Figure 8.21. Torque difference vs. Time.

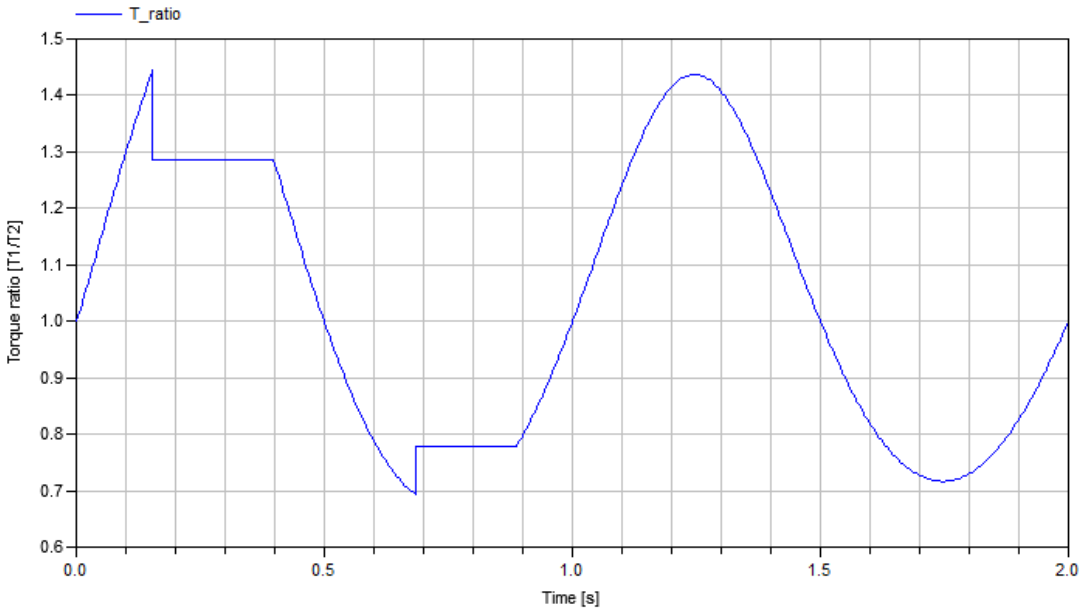

Figure 8.22. Torque ratio vs. Time.

Below, the effect of the slip during the time can be seen. From the instant where the slip is restricted by the differential locked or semi locked position, until when the differential remains lock during the rest of the cycle.

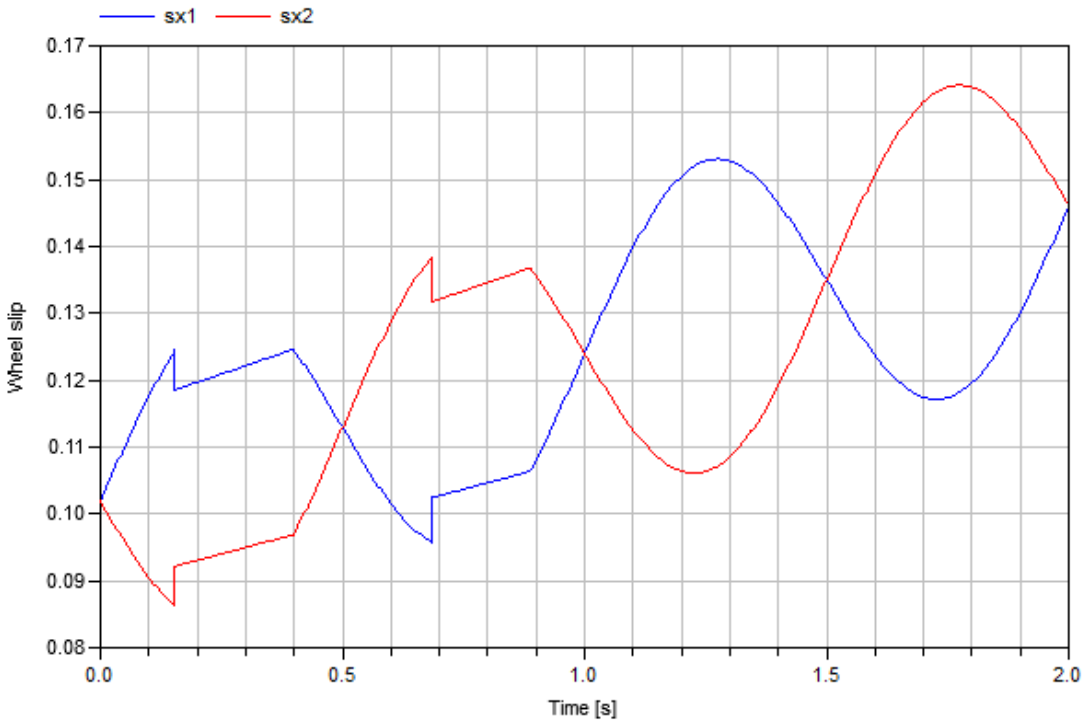

Figure 8.23. Wheel slip vs. Time.

The plot where the traction force is represented corresponding to this load case can be found in the *Appendix F* (it is the same plot times the tire stiffness).

9 Conclusions

This analysis has given an understanding of which are the causes of the torque steer effects due to the differential in those driving situations when it affects the torque distribution. From this study, some design modifications can be done so as to minimize the contribution of the differential in the steering feeling (such as using a flat surface in side gear or switching the washer material). Not only, modify the design, but also change the concept of the differential since for example a spur planetary differential, where the contacts in the housing do not exist, or having a flat surface in contact between the side gear and the housing, if the goal in VCC is reducing the friction over the differential.

Furthermore, it has been checked that the parameter that contributes the most is the contact between the housing (washer in this case, since it has been proved the sliding appears between the washer and the gear) and the side gears around a 40% of the overall torque difference. Then, the second most relevant is the friction torque that appears between the pinion gear and the pin, around a 34% of the overall. Finally, the least is the friction torque between the pinion gear and its washer. In this first analysis, the torque difference seems to have a linear behaviour depending on the input torque.

Thanks to the design of a rig, where the differential assembly was clamped on the bench and the driveshafts were used to load the differential, not only the test of the original design of the differential could be checked, but also a test planning could be set in order to check the influence of some parameters to the output.

During the first experiment planning, is shown as well that the parameters set according to the assumption done *a priori* was not true and after the statistical analysis it is possible to claim that no correlation between tests exists. Thus, it contributes to the statement that the equivalent radius is not moving due to the load and it is not situated in the centre of the contact surface.

After having carried out the FEM analysis of the complete system (differential assembly), it has been checked how the contact points in each parts where the contact exists behave. The equivalent radius in the side and pinion gears with the washers is independent on all the wide range of input torque from 0 Nm to 2000 Nm. These equivalent friction radiuses are not in the mid radial point of the washer surface, which makes the first statement for the first test planning wrong. Besides, the contact between the pinion gear and the pin has a normal contact pressure linearly with the input torque keeping the equivalent radius constant in the midpoint of the contact pattern.

The housing is the stiffest part of the system, around 25 stiffer compared to the gear set (gears plus pinion pin). Thus, once the differential is loaded, the pinion pin is tilted in a "S" shape that effects the contact between the pinion gear and pin and the pinion pin and the washer (where there is no normal pressure in half of the washer since due to this bending, it is lifted and the contact is concentrated in half of the washer).

Hence, it can be claimed, that the differential has a linear behaviour with the input torque. Perhaps, the solver has missed some non-linear effects that might become the differential non-linear. But, as far as it has been checked, the differential does not seem to have any of these effects. The overall torque difference is linearly and

represents a 18% of the input torque (breakaway torque ratio of 1,444), yielding to a static friction coefficient of 0,215 in all the contact surfaces.

Moreover, once the test planning is reset and done again using the only parameter possible to be controlled (the material of the washers, either the original hard steel or the coating by Nedox), it is not only seen how much the effects of the Nedox washers is, but also to corroborate how much it affects if it is changed in all the places (side gears and pinion gears) or if it is just applied in side gear or pinion gear independently.

Thus, it has been proved that the difference torque between both driveshafts is reduced by an around 7% when the Nedox washers are used in all the gears compared to the original design. This is due to the friction of the washers after coating them, which is reduced by an around 12%, to a value of 0,19. However, since the rig does not work in the same conditions as the car, it does not have the right working temperature, the oil film thickness is not set, for instance, the quantity of the results is not hundred percent reliable since it is the "worst case scenario" that the differential will always be. So, comparing the percentage of reduction is more reliable to have an overview of how strong the effects are rather than using the static friction coefficient value.

On top of that, if the simulation model is adjusted to fit the test results, it is seen how the final torque difference between driveshafts yields to a value of around 18,2% of the input torque (with a torque ratio of 1,444) using the original differential (with a linear behaviour during the wide range of input torque). Besides, when the all Nedox are applied, the difference becomes 16.9% (with a torque ratio of 1,406).

Moreover, it is possible to see as well that when the Nedox are applied in the side gear washers, the difference of torque is reduced by a higher percentage than when the Nedox washers are applied just in the pinion gear washers. In addition, the overlapping of these two individual effects sums the same as the total effect when the washers are changed all in the same time. Hence, it corroborates the results got before, that the side gear friction torque in the side gear contributes the most in the total difference of torque between shafts than the pinion gear friction, the differential has a linear behaviour since the overlapping of combinations has the same effect as when all the washers used are with the Nedox coating, and finally, that the rig gives reliable results, since the correlations of the parameters are coherent with also a linear behaviour of the output.

As far as the comparison between the test and model results against the logged data from a real car is concerned, it has checked that the torque difference between driveshafts in the real car when it starts turning is quite constant during the wide range of input torques, although in the real test with the running car, there are some other contributions such as the slip angle, weight transfer and suspension. This difference is around a 12% of the input torque (with a sliding torque ratio of 1,286), which if it is compared to the one got in the Rig Test and the Loss Model around 18% it can be checked how much more friction the rig has compared to the vehicle, likely due to all the working conditions which represent the worst case scenario in the rig. Actually the Rig Test value could be used as the breakaway torque ratio and the value got from the Car Test is the sliding torque ratio, so that, the differential works in normal conditions differentiating the speed with this dynamic torque ratio (with an sliding friction coefficient of 0,14), but to reach it, first it has to overcome the static friction.

Finally, once the Dymola simulation of the vehicle dynamics of a front wheel drive car, it can be claimed that having a non perfect distribution of torque 50% in each driveshafts makes the car understeered for a certain driving situation where the acceleration is controllable (not so high) and the weight transfer is low (big cornering radius). When the differential starts to differentiate the rotational speed of the wheels, there is a relative power flow to the outer side so that the torque of the inner wheel is increased making the inner wheel not having the slip wished and getting the car understeered (drifting), if no other parameters of the car are considered (such as weight transfer, suspension and linkage stiffness, driveshafts stiffness, etc).

Furternmore, the driver can feel a torque steer in the steering wheel as long as the differential works. Compared to the theoretically perfect differential without internal friction where the torque steer regarding it should be close to zero.

On the other hand, after having simulated a driving scenario where the steering wheel angle is sinusoidal over the time, the explanation of the steering feeling of the torque jump may be basically explained. Due to the breakaway torque ratio, in the first instants of a theoretically relative speed, the differential remains lock until it reaches the breakaway torque ratio. This is the moment when the differential starts allowing the shafts turning in different speeds and the torque ratio is reduced until the dynamical working conditions. Thus, this is the reason why the driver feels a "jump" in the steering wheel when starts turning towards one side. This is the jump between having a locked differential until the differential works, which the ratio between torques (the semilocked state) changes in two, having the inner wheel first during the break away slightly higher torque than in dynamical conditions.

In addition, it should be pointed out that depending on the driving conditions (steering wheel angle amplitude and lateral acceleration), the phenomena can be modified depending on the input torque. For instance, in this studied case, there is a boundary torque where the car will not achieve the breakaway torque ratio needed in order to allow the differential working in semi locked conditions since the linear (not saturated) tire model has been used.

10 Future Recommendations

Due to the limitation of the rig where the housing (carrier) is totally fixed, the inertia and centripetal acceleration are neglected. But also, the working parameters differ from the real car, the oil film thickness is not set, the temperature is not the optimal, and the friction is higher since it is done a static (or quasi-static) study of the friction of the differential (as it is seen in Chapter 1.3). Hence, a recommendation would be running the whole transmission with such a rig which allowed the driveshaft turning in different speed so as to check the behaviour of the differential when it started turning. Actually, it may be also possible testing without turning the whole transmission, the housing could be still fixed on the bench, and instead of using the loaded arm, a chain or belt should be used to load the driveshafts through a parallel shaft preloaded by means of a clutch. Then, using an electrical motor, for instance, the system can be loaded and the dynamic friction can be tested.

On the other hand, the differential might be tested with the whole car analysing, then, all the parameters that may affect the torque split left/right over the driveline. However, this would be a thesis work for several students focusing each of them on one of the possible causes (differential, driveshafts, constant velocity joints, weight transfer and so on) so as to qualify and quantify them.

Moreover, there is the limitation of the gear mesh, since it is a static test, depending on the gear mesh which is used the results may differ. Thus, in case it is running in the whole transmission the results will be already got within the band where all the different values of force due to the sinusoidal shape that the force distribution towards the time has. However, it also affects the FEM analysis, since the gear mesh study could be a thesis itself. So, if these effects have to be quantified, a recommendation would be just studying the effect of the possible different contact tooth mesh and the different effect in the deformation and pressure distribution of the differential parts. On the other hand, it would be useful to analyse the deformation of the gear mesh in order to check if the equivalent radius of the gear mesh becomes independent on the load or depends on the load either linearly or non-linearly, to check out if the gear ratio is independent or dependent on the input torque.

Hence, it could be done the same study in more detail but switching from CATIA to Abaqus in order to capture if there is some non-linear effect for high torques.

As far as the tests are concerned, some other tests could be done in the rig using the old VCC differential with flat surfaces on the side gears. The comparison of the results between this other differential design and the M66 studied would give useful information, as well as testing a planetary spur gear differential.

On the other hand, just keeping the current design , the differential could be just slightly changed and using the same differential with a flat surface between the side gears and the housing, rather than spherical, in order to reduce the thrust force which provides the friction torque in these contacts.

Finally, in case VCC decides to incorporate the Nedox coating washers to the differential, they should be redesigned since once the coating is done, each washer increases the thickness until around two hundreds of millimetre. It means that it is not possible to assemble the side gears in the housing because the original design assembly is already tight to avoid having some free play and misalignment between gears and washers. In this work, as the coating was done from the original washer design, the washers became thicker after the heat treatment. Thus, the outer surface of

the washers was machined on the lathe. On top of that, to avoid this, the design of these new washers should be done taking care the future coating.

Furthermore, these Nedox coating does not seem to reduce the breakaway friction so much. Hence, it would be really useful to quantify the effects of the sliding friction of the washers, testing them, for instance, in a running rig or the whole vehicle as it has been said above. Perhaps, the dynamic friction coefficient of the Nedox will be reduced more than the static compared to the original material.

Regarding the vehicle dynamics simulations, the first recommendation would be trying to study in more detail the effect in the dynamic of the whole car of the differential more carefully, taking into account more driving scenarios (different paths, lateral accelerations, longitudinal accelerations, etc) in order to study in more detail the effect of the differential in the torque steer and the path that the car would like to follow. In addition, try to edit, if it is necessary, the differential model in order to get a reliable model valid for different driving scenarios in order to study the transient relative power and the handling of the car due to that (oversteering/understeering). The model would need to take into account, perhaps, the first initial locking of the differential (when the torque ratio does not achieve the breakaway) and splitting the torque ratio between static and dynamic state.
Furthermore, in order to continue studying the jump steering feeling. Some experiments in the real vehicle should be done in order to see if the model that has been got so far can predict this effect or more parameters should be included, such as lateral slip (combined slip model taking into account the lateral forces), inertia or non-constant tire stiffness model (also depending on the driving scenario studied), or if the model has to be defined in a more specific way modelling the whole car rather than assuming the bicycle model. Once this is done, it can judge if the model has to be redefined or it already explains the jump steering feeling effect. Basically, the assumptions done in this model make a physically impossible wheel speed jump, but ideally physically possible in the model since the inertia and lateral acceleration where neglected according to the initial driving scenario.

11 References

[1] Heinz Heisler (1999): *Vehicle and engine technology.* Ed Arnold, second edition, London.

[2] Heinz Heisler (2002): *Advanced vehicle technology*. Ed Arnold, second edition, London.

[3] Mart Mägi och Kjell Melkersson (2011): *Lärobok I Maskinelement.* EcoDev International AB, Kompendiet.

[4] http://www.freepatentsonline.com/8079929.pdf 2012/01/25

[5] http://www.mathworks.se/help/toolbox/physmod/sdl/ref/differential.html 2012/01/25

[6] http://www.patentgenius.com/patent/6083133.html 2012/01/25

[7] http://www.scribd.com/doc/51421398/227/Differential-Gears-and LockingDifferentials 2012/01/26

[8] http://www.docstoc.com/docs/46632660/Bevel-Gear-Differential-With-Asymmetrically-Distributed-Pinions---Patent-6083133 2012/01/27

[9] http://www.machinerylubrication.com/Read/167/synthetic-gear-oil 2012/01/27

[10] http://www.miata.net/garage/diffguide/index.html 2012/01/27

[11]http://scitation.aip.org/getabs/servlet/GetabsServlet?prog=normal&id=JDSMAA0132000006061501000001&idtype=cvips&gifs=yes&ref=no 2012/01/27

[12] V.B.Bhandari (2008): *Design of Machine Elements*. Tata McGraw-Hill, second edition, New Delhi.

[13] http://auto.howstuffworks.com/differential1.htm 2012/02/01

[14] http://www.cdxetextbook.com/trans/finalDrives/frontWheel/fwdfinaldrive.html 2012/02/01

[15] Allen S. Hall, Alfred R. Holowenko and Herman G. Laughlin (2005): *Machine Design.* Tata McGraw-Hill, New York.

[16] http://www.enotes.com/topic/Differential_(mechanical_device) 2012/02/01

[17] http://www.romaxtech.com/write/documents/Perpendicular%20Modeller%20Apr11%20low%20res.pdf 2012/02/05

[18]http://web.mit.edu/2.75/resources/FUNdaMENTALs%20Book%20pdf/FUNdaMENTALs%20Topic%206.PDF 2012/02/05

[19] http://www.freestudy.co.uk/nc%20mech%20princ/outcome4%20t1.pdf 2012/02/05

[20] http://agma.server294.com/images/uploads/OSU_phase1.pdf 2012/02/07

[21] Naunheimer, H., Bertsche, B., Ryborz, J., Novak, W (2011): *Automotive transmission. Fundementals, Selection, Design and Application.* 2nd edition, Berlin.

[22] Prof. Dr. –Ing. Habil. Walter Sextro (2002): *Dynamical contact problems with friction.* Ed. Springer, second edition, Graz.

[23] Jens Dornhege (2011): Torque *Steer influences on McPherson Front Axles*. Ford Werke AG.

[24] Pierre E. Dupont (2006): *Friction Modeling in Dynamic Robot Simulation*. Robotics Laboratory. Harvard University, Cambridge, MA 02138.

[25] Differential Behaviour. Optimum vehicle dynamics simulations.

[26] Richland (2005): Metric Mechanic's Differentials. Metric Mechanic Inc^{TM} 505 East Main M0 65556, Stuttgart

[27] Allan Freer Potter. B. Sc (1958): *A Study of a Friction Induced Vibration*. University of Manitoba, USA.

[28] http://ptumech.loremate.com/md2/node/5 2012/02/10

[29] http://www.roymech.co.uk/Useful_Tables/Tribology/co_of_frict.htm 2012/02/10

[30] V.B.Bhandari (2010): *Design of Machine Elements*. Ed. Tata McGraw-Hill, third edition, New Delhi.

[31] http://ieeexplore.ieee.org/xpls/abs_all.jsp?arnumber=126193&tag=1 2012/02/11

[32] Volvo Car Corporation's private information.

[33] B.N.J. Persspm (2000): *Sliding Friction (Physical principles and applications).* Second edition. Ed. Springer, Jülich.

[34] Lina Björnheden (2004*): Verification of friction calculations (A parameters study of friction torque in bearings).* Chalmers University of Technology, Göteborg.

[35] Milliken & Milliken (1995): *Race car vehicle dynamics.* W.F Milliken & D.L Milliken. Society of Automotive Engineers, Warrendale, PA (U.S.A).

[36] Bengt Jacobson (2011): *Lecture Notes for course MMF062 Vehicle Dynamics.* Division of Vehicle and Autonomous Systems, Department of Applied Mechanics, Chalmers University of Technology, Göteborg, (Sweden).

[37] André Chevalier (2004): *Guide du dessinateur industriel*. Ed. Hachette Tecnique, Paris (France).

[38] Daniel Clos (2011): *Disseny de Màquines I, Quadern D3 Preprojectes*. Escola Tècnica Superior d'Enginyeria Industrial de Barcelona – UPC, Barcelona (Catalonia).

[39] Fenollosa, Martínez i Veciana (2010): *Càlcul de Màquines, Quadern CM2 Rodaments.* Escola Tècnica Superior d'Enginyeria Industrial de Barcelona - UPC, Barcelona (Catalonia).

[40] Josep Fenollosa Coral (2009): *Unions Cargolades.* Edicions UPC. Departament d'Enginyeria Mecànica, Escola Tècnica Superior d'Enginyeria Industrial de Barcelona – UPC, Barcelona (Catalonia).

Appendix A. Differential Loss Model: Matlab code

Below is it attached the Matlab code for the different analysis during the Chapter 2, Chapter 3 , Chapter 4 and Chapter 5. However, before that there is the analysis carried out in order to show the numerical problem occurred in the modelling seen in the Loss Differential model chapter.

In the Chapter 2, it has been seen how, in the Table 2.3, the total sum of each parameter individually does not sum 100%.
In the Figure 2.5 it is possible to see the contribution of each parameter summed consecutively, starting from one parameter until all are kept in the same model. Whereas, if instead of studying the sum of the consecutively losses, the individual study is one so as to know how much every parameter contributes to the final torque difference the Figure 2.6 is got.
Nevertheless, the results are not exactly the same. Each parameter does not seem to contribute the same when it is studied alone without any other contribution than if it is studied together with all the system. Thus, the reason why this happens will be figured out. In the following tables, it can be observed the difference between outputs if each parameter is considered alone or mixed with some other.

Table A.1. Quotient between right and left torque for each parameter.

Parameter (*i*)	$\boldsymbol{\frac{T_2}{T_1}\vert_i}$
Due to contact in the sun gear	1.149
Due to the contact in planetary gear	1.083
Due to the contact in pinion pin	1.124
Due to the gear mesh	1.021
TOTAL (product)	1.428

Table A.2. Quotient between right and left torque overlapping parameters.

Parameter (*i*)	$\boldsymbol{\frac{T_2}{T_1}\vert_i}$
Due to the gear mesh	1.021
Due to the gear mesh + Contact in sun gear	1.157
Due to the gear mesh + Contact in sun gear + Contact in planetary	1.271
Due to the gear mesh + Contact in sun gear + planetary + pinion pin	1.409

The total result is equal for both (of course since the equations are the same when all the system is studied) and as the model is lineal the Equation (A.1) should be true since the effect of each one studied alone should sum the same as if all the parameter are put together in the model to get the total output:

$$\prod \frac{T_2}{T_1}\vert_i = \frac{T_2}{T_1}\vert_{Total} \qquad \text{(A.1)}$$

That yields to:

$$\frac{T_2}{T_1}|_{Gear\ mesh}\ x\ \frac{T_2}{T_1}|_{Pinion\ pin}\ x\ \frac{T_2}{T_1}|_{Sun\ gear}\ x\ \frac{T_2}{T_1}|_{Pinion\ gear}\ = \frac{T_2}{T_1}|_{Total} \quad (A.2)$$

$$1.021\ x\ 1.124\ x\ 1.083\ x\ 1.149 = 1.428\ \neq \frac{T_2}{T_1}|_{Total} = 1.409 \quad (A.3)$$

Either there is an internal computation solver problem due to the approximation done or the contribution of one or some of the parameters should not be possible to be studied alone. Thus, if is checked step by step:

$$\frac{T_2}{T_1}|_{Gear\ mesh}\ x\ \frac{T_2}{T_1}|_{Sun}\ = 1.021\ x\ 1.149 = 1.173\ \neq \frac{T_2}{T_1}|_{Gearmesh+sun} \quad (A.4)$$

$$\frac{T_2}{T_1}|_{Gear\ mesh}\ x\ \frac{T_2}{T_1}|_{Sun\ gear}\ x\ \frac{T_2}{T_1}|_{Planetary\ gear} = 1.270\ \neq \frac{T_2}{T_1}|_{Gearmesh+sun+planetary} = 1.271 \quad (A.5)$$

$$\frac{T_2}{T_1}|_{Gear\ mesh}\ x\ \frac{T_2}{T_1}|_{Sun\ gear}\ x\ \frac{T_2}{T_1}|_{Planetary\ gear}\ x\ \frac{T_2}{T_1}|_{Pinion\ pin} = 1.428\ \neq \frac{T_2}{T_1}|_{Gearmesh+sun+planetary+pinion\ pin} = 1.409 \quad (A.6)$$

Actually, the solver takes 14 significant figures in order to proceed with the calculations, but just uses 2 significant figures in the plot results. If the same calculation is done taking all the decimals, the final difference between the relations of torques being calculated as a product or as a system together becomes 1, 39%, as it is checked in the equation below:

$$\frac{1{,}42896363388299 - 1{,}40933754270665}{1{,}40933754270665} x100 = 1{,}39\% \quad (A.7)$$

Thus, it might be claimed that this differences that have been seen are due to the internal solver and not to any parameter that affects the outcome relationship.

Matlab code

Reference model

Differential data

```
%Differential data
f=0.15; %Gear mesh losses (equivalent of a gear mesh efficiency of
99%)
Rh=89/2/1000; %Housing radius
rsi=26/2/1000; %Drive shaft radius
fi=54.28*pi/180; %Angle bevel teeth
alpha=20*pi/180; %Angle contact point (forces angle)

r01=26/1000;  %Radius tooth contact force Sun 1 (without contact mesh
losses)
r02=26/1000;  %Radius tooth contact force Sun 2 (without contact mesh
losses)
rp01=17/1000; %Radius tooth contact force Planetary 1 (without
contact mesh losses)
rp02=17/1000;  %Radius tooth contact force Planetary 2 (without
contact mesh losses)
```

```
rpin=8.736/2/1000; %Radius pin

rfl=25/1000; %Radius friction left (housing-sun)
rfr=25/1000; %Radius friction right (housing-sun)

rpf1=15/1000; %Radius friction planetary top (housing-planetary)

bw=0.78/1000; %bushing width(in radial direction)

c_beta=cos(asin(rfr/(Rh-bw))); %Cosinus of Normal force angle on the
sun
c_theta=cos(asin(rpf1/(Rh-bw))); %Cosinus of Normal force angle on
the planetary

mu=0.2;  %Friction coefficient

T0_vec=[0,1,2000];  %Engine torque (input)

r1=r01-f*cos(fi)/1000; %Radius tooth contact force Sun 1 (with
contact mesh losses)
r2=r01+f*cos(fi)/1000; %Radius tooth contact force Sun 2 (with
contact mesh losses)
rp1=rp01+f*sin(fi)/1000; %Radius tooth contact force Planetary 1
(with contact mesh losses)
rp2=rp02-f*sin(fi)/1000; %Radius tooth contact force Planetary 2
(with contact mesh losses)
```

Basic Loss Model

```
%ALL LOSSES
syms T1 T2 Ft1 Ft2 R1 T2mT1 Fn1 Fn2 Nfl Nfr Npf1 Ffl Ffr Fpf1 Fp1

%Sun left
Eq1='T1=Ft1*r1 -Ffl*rfl';
Eq2='Nfl*c_beta=Fn1*sin(fi)';

%Planetary top
Eq3='Ft1+Ft2=R1';
Eq4='Ft1*rp1+Fpf1*rpf1+Fp1*rpin=Ft2*rp2';
Eq5='Npf1*c_theta=Fn1*cos(fi)+Fn2*cos(fi)';

%Sun right
Eq6='T2=Ft2*r2 +Ffr*rfr';
Eq7='Nfr*c_beta=Fn2**sin(fi)';

%Differential balance
Eq8='T1+T2=T0';

%Torque differences
Eq9='T2mT1=T2-T1';

%Forces teeth left
Eq10='Fn1/Ft1=tan(alpha)';
Eq11='Fn2/Ft2=tan(alpha)';

%Friction forces
Eq12='Ffl=mu*Nfl';
```

```
Eq13='Ffr=mu*Nfr';
Eq14='Fpf1=mu*Npf1';
Eq15='Fp1=mu*R1';

sol=solve(Eq1, Eq2, Eq3, Eq4, Eq5, Eq6, Eq7, Eq8, Eq9, Eq10, Eq11,
Eq12, Eq13, Eq14, Eq15, T1, T2, Ft1, Ft2, R1, T2mT1, Fn1, Fn2, Nfl,
Nfr, Npf1, Ffl, Ffr, Fpf1, Fp1);
disp('T2-T1='), disp(sol.T2mT1)
```

Parameter contribution

Individual parameter study

```
%SUN GEAR MESH RADIUS EFFECT
%Variables definition
T0=1500;
T2mT1_vec=[];
for i=1:length(r1_vec)
    r1=r1_vec(i);
    T2mT1_vec(i)=eval(sol.T2mT1);

end

figure(1);
plot(r1_vec, (T2mT1_vec/T0)*100,'r'),hold on
xlabel('Radius [mm]'), ylabel('T2-T1 [Nm]')
axis([0 100 0 200])

%PLANETARY GEAR MESH RADIUS EFFECT
%Variables definition
rp1_vec=[5:1:50];

T0=1500;
T2mT1_vec=[];
for i=1:length(rp1_vec)
    rp1=rp1_vec(i);
    T2mT1_vec(i)=eval(sol.T2mT1);
end

plot(rp1_vec, (T2mT1_vec/T0)*100,'r--'),hold on

%SUN FRICTION RADIUS
%Variables definition
rfl_vec=[5:1:50];

T0=1500;
T2mT1_vec=[];
for i=1:length(rfl_vec)
    rfl=rfl_vec(i);
    T2mT1_vec(i)=eval(sol.T2mT1);
end

plot(rfl_vec, (T2mT1_vec/T0)*100,'g'),hold on

%PLANETARY FRICTION RADIUS
%Variables definition
rpf1_vec=[5:1:50];
```

```
T0=1500;
T2mT1_vec=[];
for i=1:length(rpf1_vec)
    rpf1=rpf1_vec(i);
    T2mT1_vec(i)=eval(sol.T2mT1);
end

plot(rpf1_vec, (T2mT1_vec/T0)*100,'g--'),hold on

%PIN TORQUE RADIUS EFFECT
%Variables definition
rp_vec=[10:1:100];

T0=1500;
T2mT1_vec=[];
for i=1:length(rp_vec)
    rp=rp_vec(i);
    T2mT1_vec(i)=eval(sol.T2mT1);
end

plot(rp_vec, (T2mT1_vec/T0)*100,'b'),hold on

%PIN RADIUS
%Variables definition
rpin_vec=[1:1:10];

T0=1500;
T2mT1_vec=[];
for i=1:length(rpin_vec)
    rpin=rpin_vec(i);
    T2mT1_vec(i)=eval(sol.T2mT1);
end

plot(rpin_vec, (T2mT1_vec/T0)*100,'b--'),hold on
```

Manufacturing parameter study

```
%HOUSING MODEL
%ALL LOSSES
syms T1 T2 T2mT1 F1 F2 Ft1 Ft2 Fn1 Fn2 Nfl Nfr Ffl Ffr Fpf1 Npf1 Fp1
R1 r01 r02 rp01 rp02 r1 r2 rp1 rp2 rp

%Sun left
Eq1='T1=Ft1*r1-Ffl*rfl';
Eq2='Nfl=Fn1*sin(fi)';

%Planetary top
Eq3='Fn1=Fn2';
Eq4='Ft1+Ft2=R1';
Eq5='Ft1*rp1+Fpf1*rpf1+Fp1*rpin-Ft2*rp2=0';
Eq6='Npf1=Fn1*cos(fi)+Fn2*cos(fi)';

%Sun right
Eq7='T2=Ft2*r2+Ffr*rfl';
Eq8='Nfr=Fn2*sin(fi)';

%Pinion pin
```

```
Eq9='R1=2*T0/(2*rp)';

%Torque differences
Eq10='T2mT1=T2-T1';

%Forces teeth left
Eq11='Ft1=F1*cos(alpha)';
Eq12='Fn1=F1*sin(alpha)';

%Forces teeth right
Eq13='Fn2=F2*sin(alpha)';

%Friction forces
Eq14='Ffl=mu*Nfl';
Eq15='Ffr=mu*Nfr';
Eq16='Fpf1=mu*Npf1';
Eq17='Fp1=mu*R1';

%Radius variations
Eq18='r01=(Rh-bw-gap-B/2)*sin(fi)';  %Radius tooth contact force Sun
1 (without contact mesh losses)
Eq19='r02=(Rh-bw-gap-B/2)*sin(fi)';  %Radius tooth contact force Sun
2 (without contact mesh losses)
Eq20='rp01=(Rh-bw-gap-B/2)*cos(fi)'; %Radius tooth contact force
Planetary 1 (without contact mesh losses)
Eq21='rp02=(Rh-bw-gap-B/2)*cos(fi)';  %Radius tooth contact force
Planetary 2 (without contact mesh losses)
Eq22='r1=r01-f*cos(fi)/1000'; %Radius tooth contact force Sun 1 (with
contact mesh losses)
Eq23='r2=r01+f*cos(fi)/1000'; %Radius tooth contact force Sun 2 (with
contact mesh losses)
Eq24='rp1=rp01+f*sin(fi)/1000'; %Radius tooth contact force Planetary
1 (with contact mesh losses)
Eq25='rp2=rp02-f*sin(fi)/1000'; %Radius tooth contact force Planetary
2 (with contact mesh losses)
Eq26='rp=Rh-Bp/2-bw'; %Radius reaction pin (torque transmission)

sol=solve(Eq1, Eq2, Eq3, Eq4, Eq5, Eq6, Eq7, Eq8, Eq9, Eq10, Eq11,
Eq12, Eq13, Eq14, Eq15, Eq16, Eq17, Eq18, Eq19, Eq20, Eq21, Eq22,
Eq23, Eq24, Eq25, Eq26, T1, T2, T2mT1, F1, F2, Ft1, Ft2, Fn1, Fn2,
Nfl, Nfr, Ffl, Ffr, Fpf1, Npf1, Fp1, R1, r01, r02, rp01, rp02, r1,
r2, rp1, rp2, rp);
disp('T2-T1='), disp(sol.T2mT1)

%Parameters definition
Rh_vec=([60:1:100]/1000)/2; %Sphere housing's diameter

%PIN MODEL
%ALL LOSSES
syms T1 T2 T2mT1 F1 F2 Ft1 Ft2 Fn1 Fn2 Nfl Nfr Ffl Ffr Fpf1 Npf1 Fp1
R1

sol=solve(Eq1, Eq2, Eq3, Eq4, Eq5, Eq6, Eq7, Eq8, Eq9, Eq10, Eq11,
Eq12, Eq13, Eq14, Eq15, Eq16, Eq17, T1, T2, T2mT1, F1, F2, Ft1, Ft2,
Fn1, Fn2, Nfl, Nfr, Ffl, Ffr, Fpf1, Npf1, Fp1, R1);
disp('T2-T1='), disp(sol.T2mT1)

%Parameters definition
rpin_vec=[2:1:15]/1000; %Radius pin
```

```
%SUN WIDTH
syms T1 T2 T2mT1 F1 F2 Ft1 Ft2 Fn1 Fn2 Nfl Nfr Ffl Ffr Fpf1 Npf1 Fp1
R1 rfl

%Width surface parameters
Eq29='rfl=rsi+chs+ws/2'; %Radius friction left (housing-sun)

sol=solve(Eq1, Eq2, Eq3, Eq4, Eq5, Eq6, Eq7, Eq8, Eq9, Eq10, Eq11,
Eq12, Eq13, Eq14, Eq15, Eq16, Eq17, Eq29, T1, T2, T2mT1, F1, F2, Ft1,
Ft2, Fn1, Fn2, Nfl, Nfr, Ffl, Ffr, Fpf1, Npf1, Fp1, R1, rfl);
disp('T2-T1='), disp(sol.T2mT1)

%Parameters definition
ws_vec=[5:1:30]/1000; %Width surface in contact between sun and
housing

%PLANETARY WIDTH
syms T1 T2 T2mT1 F1 F2 Ft1 Ft2 Fn1 Fn2 Nfl Nfr Ffl Ffr Fpf1 Npf1 Fp1
R1 rpf1

%Width surface parameters
Eq30='rpf1=rpin+chp+wp/2'; %Radius friction left (housing-sun)

sol=solve(Eq1, Eq2, Eq3, Eq4, Eq5, Eq6, Eq7, Eq8, Eq9, Eq10, Eq11,
Eq12, Eq13, Eq14, Eq15, Eq16, Eq17, Eq30, T1, T2, T2mT1, F1, F2, Ft1,
Ft2, Fn1, Fn2, Nfl, Nfr, Ffl, Ffr, Fpf1, Npf1, Fp1, R1, rpf1);
disp('T2-T1='), disp(sol.T2mT1)

%Parameters definition
wp_vec=[5:1:30]/1000; %Width surface in contact between sun and
housing in radial direction
```

Friction coefficient dependence

```
%Parameters definition
mu_vec=[0.05:0.01:0.35]

T2mT1_vec=[];
for i=1:length(mu_vec)
    mu=mu_vec(i);
    T2mT1_vec(i)=eval(sol.T2mT1);

end

figure(1);

%INDEPENDENTLY ANALYSIS
%JUST IN SIDE GEAR
%Parameters definition
mu_s_vec=[0.05:0.01:0.35]
mu_p=0.2;
mu_pin=0.2;

%JUST IN PINION GEAR
%Parameters definition
mu_p_vec=[0.05:0.01:0.35]
mu_s=0.2;
```

```
mu_pin=0.2;

%JUST IN CONTACT PINION GEAR AND PIN
%Parameters definition
mu_pin_vec=[0.05:0.01:0.35]
mu_s=0.2;
mu_p=0.2;
```

Comparison with the rig test results

Considering rig losses

```
%Differential data
f=0.15; %Gear mesh losses (equivalent of a gear mesh efficiency of
99%)
Rh=89/2/1000; %Housing radius
rsi=26/2/1000; %Drive shaft radius
fi=54.28*pi/180; %Angle bevel teeth
alpha=20*pi/180; %Angle contact point (forces angle)

r01=26/1000;  %Radius tooth contact force Sun 1 (without contact mesh
losses)
r02=26/1000;  %Radius tooth contact force Sun 2 (without contact mesh
losses)
rp01=17/1000; %Radius tooth contact force Planetary 1 (without
contact mesh losses)
rp02=17/1000;  %Radius tooth contact force Planetary 2 (without
contact mesh losses)

rpin=8.736/2/1000; %Radius pin

rfl=25/1000; %Radius friction left (housing-sun)
rfr=25/1000; %Radius friction right (housing-sun)

rpf1=15/1000; %Radius friction planetary top (housing-planetary)

bw=0.78/1000; %bushing width(in radial direction)

c_beta=cos(asin(rfr/(Rh-bw))); %Cosinus of Normal force angle on the
sun
c_theta=cos(asin(rpf1/(Rh-bw))); %Cosinus of Normal force angle on
the planetary

mu=0.17;  %Friction coefficient

T0_vec=[0,1,2000];  %Engine torque (input)

r1=r01-f*cos(fi)/1000; %Radius tooth contact force Sun 1 (with
contact mesh losses)
r2=r01+f*cos(fi)/1000; %Radius tooth contact force Sun 2 (with
contact mesh losses)
rp1=rp01+f*sin(fi)/1000; %Radius tooth contact force Planetary 1
(with contact mesh losses)
rp2=rp02-f*sin(fi)/1000; %Radius tooth contact force Planetary 2
(with contact mesh losses)

Static_loss=12.5;
```

```
L1=(436+12.5+33/2+23+16.2+12.5)/1000;  %Distance between welding
support and housing support
L2=(23+16.2+12.5)/1000;   %Distance between bearing and welding
support
%Without considering losses in shafts
%ALL LOSSES
syms T1 T2 Ft1 Ft2 R1 T2mT1 Fn1 Fn2 Nfl Nfr Npf1 Ffl Ffr Fpf1 Fp1

%Sun left
Eq1='T1=Ft1*r1-Ffl*rfl';
Eq2='Nfl*c_beta=Fn1*sin(fi)';

%Planetary top
Eq3='Ft1+Ft2=R1';
Eq4='Ft1*rp1+Fpf1*rpf1+Fp1*rpin=Ft2*rp2';
Eq5='Npf1*c_theta=Fn1*cos(fi)+Fn2*cos(fi)';

%Sun right
Eq6='T2=Ft2*r2+Ffr*rfr';
Eq7='Nfr*c_beta=Fn2*sin(fi)';

%Differential balance
Eq8='T1+T2=T0';

%Torque differences
Eq9='T2mT1=T2-T1';

%Forces teeth left
Eq10='Fn1/Ft1=tan(alpha)';
Eq11='Fn2/Ft2=tan(alpha)';

%Friction forces
Eq12='Ffl=mu*Nfl';
Eq13='Ffr=mu*Nfr';
Eq14='Fpf1=mu*Npf1';
Eq15='Fp1=mu*R1';

sol=solve(Eq1, Eq2, Eq3, Eq4, Eq5, Eq6, Eq7, Eq8, Eq9, Eq10, Eq11,
Eq12, Eq13, Eq14, Eq15, T1, T2, Ft1, Ft2, R1, T2mT1, Fn1, Fn2, Nfl,
Nfr, Npf1, Ffl, Ffr, Fpf1, Fp1);
disp('T2-T1='), disp(sol.T2mT1)

%Modelling considering shaft losses
%ALL LOSSES
syms T01 T02 T1 T2 Ft1 Ft2 R1 T2mT1 Fn1 Fn2 Nfl Nfr Npf1 Ffl Ffr Fpf1
Fp1
%Sun left
Eq1='T01=Ft1*r1-Ffl*rfl';
Eq2='Nfl*c_beta=Fn1*sin(fi)';

%Planetary top
Eq3='Ft1+Ft2=R1';
Eq4='Ft1*rp1+Fpf1*rpf1+Fp1*rpin=Ft2*rp2';
Eq5='Npf1*c_theta=Fn1*cos(fi)+Fn2*cos(fi)';

%Sun right
Eq6='T02=Ft2*r2+Ffr*rfr';
Eq7='Nfr*c_beta=Fn2*sin(fi)';
```

```
%Differential balance
Eq8='T01+T02=T0';

%Torque differences
Eq9='T2mT1=T2-T1';

%Forces teeth left
Eq10='Fn1/Ft1=tan(alpha)';
Eq11='Fn2/Ft2=tan(alpha)';

%Friction forces
Eq12='Ffl=mu*Nfl';
Eq13='Ffr=mu*Nfr';
Eq14='Fpf1=mu*Npf1';
Eq15='Fp1=mu*R1';

%Shaft losses
Eq16='T1=T01-T0*(L2/(L1-L2))*mu*rsi';
Eq17='T2=T02+T0*(L2/(L1-L2))*mu*rsi';

sol=solve(Eq1, Eq2, Eq3, Eq4, Eq5, Eq6, Eq7, Eq8, Eq9, Eq10, Eq11,
Eq12, Eq13, Eq14, Eq15, Eq16, Eq17, T01, T02, T1, T2, Ft1, Ft2, R1,
T2mT1, Fn1, Fn2, Nfl, Nfr, Npf1, Ffl, Ffr, Fpf1, Fp1);
disp('T2-T1='), disp(sol.T2mT1)
```

Final adjusted curves of the rig test results

Note that here, the program is the same for each test, just the parameters *mu_s, mu_p* and *mu_pin* are changed depending on the place where the Nedox washer has been installed. Thus, just one code of the program is shown.

```
%Differential data
f=0.15; %Gear mesh losses (equivalent of a gear mesh efficiency of
99%)
Rh=89/2/1000; %Housing radius
B=17/1000; %Tooth length (contact mesh) of both gears
Bp=21/1000; %Planetary total width (from bottom to top). It is the
length of the contact surface between this gear and the pinion gear
ws=12.5/1000; %Sun contact friction surface width (in vertical
direction)
rsi=26/2/1000; %Drive shaft radius
chs=6.5/1000; %Chamfer in the sun gear
wp=10.5/1000; %Planetary contact friction surface width
bw=0.78/1000; %bushing width(in radial direction)
fi=54.28*pi/180; %Angle bevel teeth
alpha=20*pi/180; %Angle contact point (forces angle)
gap=1.5/1000; %Gap between the final of the gear tooth and the
housing in the bevel angle direction

r01=26/1000;  %Radius tooth contact force Sun 1 (without contact mesh
losses)
r02=26/1000;  %Radius tooth contact force Sun 2 (without contact mesh
losses)
rp01=17/1000; %Radius tooth contact force Planetary 1 (without
contact mesh losses)
rp02=17/1000;  %Radius tooth contact force Planetary 2 (without
contact mesh losses)
```

```
rpin=8.736/2/1000; %Radius pin
chp=1.27/1000; %Chamfer of the pinion gear

rfl=25.24/1000; %Radius friction left (housing-sun)
rfr=25.24/1000; %Radius friction right (housing-sun)

rpf1=18.5/1000; %Radius friction planetary top (housing-planetary).
The geometrical equation is rpf1=rpin+chp+wp/2 considering the
equivalent radius applied in the middle point between both edges

c_beta=cos(asin(rfr/(Rh-bw))); %Cosinus of Normal force angle on the
sun
c_theta=cos(asin(rpf1/(Rh-bw))); %Cosinus of Normal force angle on
the planetary

mu_s=0.19;  %Friction coefficient in sun gear
mu_p=0.19;  %Friction coefficient in pinion gear
mu_pin=0.215; %Friction coefficient in pinion pin and gear

T0_vec=[0,1,2000];  %Output torque from transmission (input for diff)

r1=r01-f*cos(fi)/1000; %Radius tooth contact force Sun 1 (with
contact mesh losses)
r2=r01+f*cos(fi)/1000; %Radius tooth contact force Sun 2 (with
contact mesh losses)
rp1=rp01+f*sin(fi)/1000; %Radius tooth contact force Planetary 1
(with contact mesh losses)
rp2=rp02-f*sin(fi)/1000; %Radius tooth contact force Planetary 2
(with contact mesh losses)
Static_loss=0; %Static loss for 0Nm input

%ALL LOSSES
syms T1 T2 T2mT1 F1 F2 Ft1 Ft2 Fn1 Fn2 Nfl Nfr Ffl Ffr Fpf1 Npf1 Fp1
R1

%Sun left
Eq1='T1=Ft1*r1-Ffl*rfl';
Eq2='Nfl*c_beta=Fn1*sin(fi)';

%Planetary top
Eq3='Fn1=Fn2';
Eq4='Ft1+Ft2=R1';
Eq5='Ft1*rp1+Fpf1*rpf1+Fp1*rpin-Ft2*rp2=0';
Eq6='Npf1*c_theta=Fn1*cos(fi)+Fn2*cos(fi)';

%Sun right
Eq7='T2=Ft2*r2+Ffr*rfr';
Eq8='Nfr*c_beta=Fn2*sin(fi)';

%Whole diff
Eq9='T0=T1+T2';

%Torque differences
Eq10='T2mT1=T2-T1';

%Forces teeth left
Eq11='Ft1=F1*cos(alpha)';
Eq12='Fn1=F1*sin(alpha)';
```

```
%Forces teeth right
Eq13='Fn2=F2*sin(alpha)';

%Friction forces
Eq14='Ffl=mu_s*Nfl';
Eq15='Ffr=mu_s*Nfr';
Eq16='Fpf1=mu_p*Npf1';
Eq17='Fp1=mu_pin*R1';
```

Adjusting model with rig results

```
%TEST RESULTS (all starting in (0,0))
%Original diff
T0=[0:10:2000];
for i=1:length(T0)
    T2mT1(i)=0.1820*T0(i);
end
figure(1);
%All Nedox
for i=1:length(T0)
    T2mT1(i)=0.1705*T0(i);
end
%Nexdox in side gear washer
for i=1:length(T0)
    T2mT1(i)=0.1790*T0(i);
end
%Nedox in pinion gear washer
for i=1:length(T0)
    T2mT1(i)=0.1818*T0(i);
end
```

It yields to the following plot:

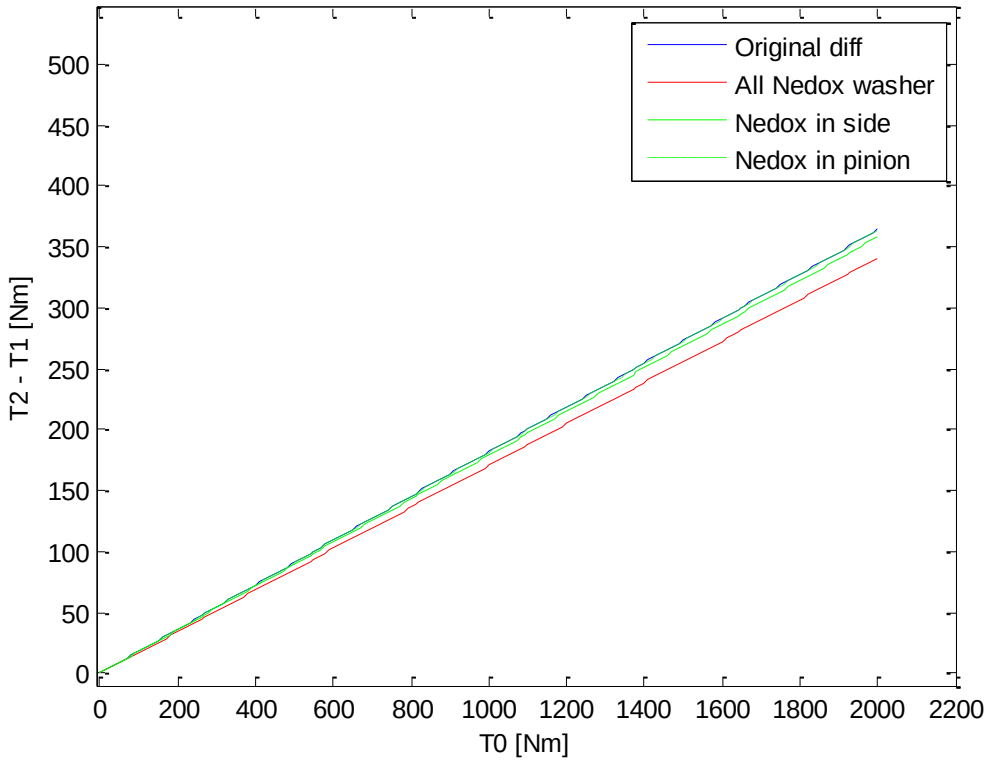

Figure A.1. Results from the final test planning

Appendix B. Rig Test Data

Test data (comparison between new and old differential)

New and old differential results

Table B.1. Input data valid for all the experiments.

INPUT DATA FOR ALL EXPERIMENTS				
Weight each side [kg]	**Maximum deflection arm right [m]**	**Slope at free end [rad]**	**Longitude due to the deflection for each load [m]**	**Total input torque [Nm]**
0	0,001	0,001	1,000	5,512
5	0,005	0,007	1,000	103,709
10	0,009	0,013	1,000	201,895
15	0,013	0,019	1,000	300,057
20	0,017	0,025	1,000	398,185
25	0,021	0,032	1,000	496,267
30	0,025	0,038	0,999	594,294
35	0,029	0,044	0,999	692,253
40	0,033	0,050	0,999	790,135
45	0,037	0,056	0,998	887,927
50	0,041	0,062	0,998	985,619
55	0,045	0,068	0,998	1083,199
60	0,049	0,074	0,997	1180,658
63	0,052	0,078	0,997	1239,069
65	0,054	0,080	0,997	1277,983
66	0,054	0,082	0,997	1297,431
70	0,058	0,086	0,996	1375,163
73	0,060	0,090	0,996	1433,397
75	0,062	0,093	0,996	1472,188
76	0,062	0,094	0,996	1491,573
80	0,066	0,099	0,995	1569,046
85	0,070	0,105	0,995	1665,725
90	0,074	0,111	0,994	1762,216
95	0,078	0,117	0,993	1858,505
100	0,082	0,123	0,992	1954,583

To weight has been considered to be not only the load applied every time, but also the permanent weight of the hook, the rope and washers where the weights are held and also the weight of the bar itself. These weights are:

$m_{hooke+rope+wahsers} = 0.832kg$

$m_{bar} = 3.848kg$

Although the mass of the bar has not been taken into account for the deflections and to calculate the effective longitude length, it has been considered for the input torque with the force applied in the middle of the road as if it was not deformed.

The effective longitude due to the deflection, the maximum deflection and the slope at free end have been calculated how is explained in the *Appendix C*.

Table B.2. Rigg results for the experiment 1 (New differential).

NEW DIFFERENTIAL RESULTS EXPERIMENT 1				
Extra load [Kg]	**Maximum deflection extra loaded arm [m]**	**Slope at free end [rad]**	**Longitude due to the deflection in extra loaded arm [m]**	**Difference torque left and right [Nm]**
2	0,002	0,003	1,000	19,640
3	0,007	0,011	1,000	29,458
4,5	0,012	0,019	1,000	44,182
6	0,018	0,027	1,000	58,899
8,5	0,024	0,036	0,999	83,417
10,5	0,030	0,044	0,999	103,009
12,5	0,035	0,053	0,999	122,578
14,5	0,041	0,061	0,998	142,121
17	0,047	0,071	0,998	166,524
17	0,051	0,077	0,997	166,449
19	0,057	0,085	0,996	185,902
25,5	0,066	0,099	0,995	249,174
28,5	0,073	0,109	0,994	278,203
31	0,079	0,118	0,993	302,288
31	0,083	0,124	0,992	302,062
30	0,086	0,129	0,992	292,134
35,5	0,095	0,142	0,990	345,081
35	0,098	0,147	0,989	339,945
43	0,109	0,163	0,987	416,594
45	0,115	0,172	0,985	435,329
44	0,118	0,177	0,984	425,282

Table B.3. Rig results for the experiment 2 (New differential).

USED DIFFERENTIAL RESULTS EXPERIMENT 1				
Extra load [Kg]	**Maximum deflection extra loaded arm [m]**	**Slope at free end [rad]**	**Longitude due to the deflection in extra loaded arm [m]**	**Difference torque left and right [Nm]**
1,5	0,002	0,003	1,000	14,730
3,5	0,008	0,011	1,000	34,368
5,5	0,013	0,020	1,000	53,999
6,5	0,018	0,027	1,000	63,806
7,5	0,023	0,035	0,999	73,606
10	0,029	0,044	0,999	98,106
14,5	0,037	0,055	0,998	142,172
16	0,042	0,063	0,998	156,806
18	0,048	0,072	0,997	176,304
21	0,054	0,082	0,997	205,533
24	0,061	0,091	0,996	234,696
26,5	0,067	0,100	0,995	258,914
31	0,075	0,112	0,994	302,504
27	0,074	0,111	0,994	263,507
39	0,085	0,128	0,992	379,835
29	0,078	0,117	0,993	282,827
39	0,089	0,134	0,991	379,526
37	0,090	0,135	0,991	360,003

42	0,096	0,144	0,990	408,156
41	0,096	0,144	0,990	398,438
41	0,099	0,149	0,989	398,148
46,5	0,108	0,161	0,987	450,640
51	0,115	0,173	0,985	493,266
56	0,123	0,185	0,983	540,404
61	0,132	0,197	0,980	587,229

Table B.4. Rig results for the experiment 3 (New differential).

NEW DIFFERENTIAL RESULTS EXPERIMENT 2				
Extra load [Kg]	**Maximum deflection extra loaded arm [m]**	**Slope at free end [rad]**	**Longitude due to the deflection in extra loaded arm [m]**	**Difference torque left and right [Nm]**
1,5	0,002	0,003	1,000	14,730
3,5	0,008	0,011	1,000	34,368
4,5	0,012	0,019	1,000	44,182
7	0,019	0,028	1,000	68,713
9	0,024	0,036	0,999	88,321
11	0,030	0,045	0,999	107,911
13	0,036	0,053	0,999	127,477
15	0,041	0,062	0,998	147,016
16,5	0,047	0,070	0,998	161,633
20	0,054	0,080	0,997	195,766
21	0,058	0,088	0,996	205,427
23,5	0,065	0,097	0,995	229,687
27,5	0,072	0,108	0,994	268,477
30,5	0,078	0,118	0,993	297,434
31	0,083	0,124	0,992	302,062
32	0,088	0,132	0,991	311,509
37,5	0,096	0,144	0,990	364,393
35	0,098	0,147	0,989	339,945
38	0,105	0,157	0,988	368,522
45	0,115	0,172	0,985	435,329
46	0,119	0,179	0,984	444,413

Table B.5. Rigg results for the experiment 1 (Used differential).

USED DIFFERENTIAL RESULTS EXPERIMENT 2				
Extra load [Kg]	**Maximum deflection extra loaded arm [m]**	**Slope at free end [rad]**	**Longitude due to the deflection in extra loaded arm [m]**	**Difference torque left and right [Nm]**
2	0,002	0,003	1,000	19,640
7,5	0,011	0,016	1,000	73,640
5,5	0,013	0,020	1,000	53,999
8	0,019	0,029	1,000	78,527
12	0,027	0,040	0,999	117,745
13,5	0,032	0,048	0,999	132,417
15,5	0,038	0,057	0,998	151,967
17	0,043	0,064	0,998	166,593
22	0,051	0,077	0,997	215,404
24	0,057	0,085	0,996	234,823

25	0,062	0,093	0,996	244,447
28,5	0,069	0,103	0,995	278,385
30	0,074	0,111	0,994	292,786
31	0,077	0,116	0,993	302,376
35	0,082	0,123	0,992	341,090
31	0,080	0,119	0,993	302,244
36	0,087	0,130	0,991	350,505
37,5	0,091	0,136	0,991	364,837
36	0,091	0,136	0,991	350,214
42	0,097	0,145	0,989	408,083
41,5	0,099	0,149	0,989	402,966
42	0,104	0,156	0,988	407,394
50	0,115	0,172	0,985	483,699
51	0,119	0,179	0,984	492,719
63	0,133	0,200	0,980	606,177

Table B.6. Rig results for the experiment 2 (Used differential).

NEW DIFFERENTIAL RESULTS EXPERIMENT 3				
Extra load [Kg]	**Maximum deflection extra loaded arm [m]**	**Slope at free end [rad]**	**Longitude due to the deflection in extra loaded arm [m]**	**Difference torque left and right [Nm]**
2	0,002	0,003	1,000	19,640
3,5	0,008	0,011	1,000	34,368
6,5	0,014	0,021	1,000	63,816
8	0,019	0,029	1,000	78,527
10	0,025	0,038	0,999	98,131
11	0,030	0,045	0,999	107,911
13	0,036	0,053	0,999	127,477
15,5	0,042	0,063	0,998	151,911
15	0,045	0,068	0,998	146,958
17	0,051	0,077	0,997	166,449
21	0,058	0,088	0,996	205,427
23,5	0,065	0,097	0,995	229,687
25	0,070	0,105	0,995	244,150
29	0,077	0,116	0,993	282,868
33	0,084	0,127	0,992	321,450
31	0,087	0,130	0,991	301,823
33	0,093	0,139	0,990	320,920
37	0,100	0,150	0,989	359,237
41	0,107	0,161	0,987	397,379
48	0,117	0,175	0,984	464,047
51	0,123	0,185	0,983	492,153

Table B.7. Rig results for the experiment 3 (Used differential).

USED DIFFERENTIAL RESULTS EXPERIMENT 3				
Extra load [Kg]	**Maximum deflection extra loaded arm [m]**	**Slope at free end [rad]**	**Longitude due to the deflection in extra loaded arm [m]**	**Difference torque left and right [Nm]**
2	0,002	0,003	1,000	19,640
4	0,008	0,012	1,000	39,277

6,5	0,014	0,021	1,000	63,816
8,5	0,020	0,030	1,000	83,433
12	0,027	0,040	0,999	117,745
15,5	0,034	0,050	0,999	152,016
16,5	0,038	0,058	0,998	161,760
17,5	0,043	0,065	0,998	171,486
22	0,051	0,077	0,997	215,404
23	0,056	0,084	0,996	225,062
26	0,062	0,094	0,996	254,196
28,5	0,069	0,103	0,995	278,385
29	0,073	0,110	0,994	283,065
30	0,076	0,114	0,993	292,663
37,5	0,084	0,126	0,992	365,312
31	0,080	0,119	0,993	302,244
36,5	0,087	0,131	0,991	355,344
38,5	0,091	0,137	0,991	374,503
37	0,092	0,138	0,990	359,881
43	0,097	0,146	0,989	417,723
41	0,099	0,149	0,989	398,148
41	0,103	0,155	0,988	397,771
54	0,118	0,177	0,984	521,937
54	0,122	0,183	0,983	521,346
63	0,133	0,200	0,980	606,177

Table B.8. Average Test 1(New differential).

AVERAGE NEW DIFFERENTIAL TEST 1	
Total input [Nm]	**Difference torque left and right [Nm]**
5,512	18,003
103,709	32,731
201,895	50,727
300,057	68,713
398,185	89,956
496,267	106,277
594,294	125,844
692,253	147,016
790,135	158,372
887,927	188,900
985,619	198,918
1083,199	236,183
1180,658	260,095
1277,983	294,197
1375,163	290,130
1472,188	301,822
1569,046	335,795
1665,725	346,376
1762,216	386,050
1858,505	444,901
1954,583	493,220

Table B.9. Average Test 1(Used differential).

AVERAGE USED DIFFERENTIAL TEST 1	
Total input [Nm]	**Difference torque left and right [Nm]**
5,512	18,003
103,709	49,095
201,895	57,271
300,057	75,255
398,185	103,032
496,267	127,513
594,294	151,966
692,253	164,961
790,135	202,371
887,927	221,806
985,619	244,446
1083,199	271,895
1180,658	292,785
1239,069	286,182
1277,983	362,079
1297,431	295,772
1375,163	332,265
1433,397	366,448
1472,188	372,751
1491,573	408,081
1569,046	399,754
1665,725	418,602
1762,216	499,634
1858,505	518,156
1954,583	599,861

Test data (first rig test result with original design)

In the tables below, the results of the three experiments for the first test using the new differential, but with different setting can be seen.

Table B.10. Rig results for the experiment 1 (new differential with different setting).

NEW DIFFERENTIAL (final setting) EXPERIMENT 1			
Extra load [Kg]	**Slope at free end [rad]**	**Longitude due to the deflection in extra loaded arm [m]**	**Difference torque left and right [Nm]**
1,5	0,005	1,000	14,730
3,5	0,009	1,000	34,369
4,5	0,012	1,000	44,187
7	0,017	1,000	68,730
9	0,023	1,000	88,357
12	0,029	1,000	117,792
15	0,035	0,999	147,211
18	0,041	0,999	176,612
20	0,046	0,999	196,189
22	0,049	0,999	215,783
24	0,054	0,999	235,340
26	0,064	0,998	254,796
30	0,073	0,997	293,823
30	0,076	0,997	293,756

38	0,085	0,996	371,797
39	0,085	0,996	381,581
42,5	0,096	0,995	415,407
44	0,098	0,995	430,017
46	0,110	0,994	448,989
47	0,113	0,994	458,560
50	0,116	0,993	487,692

Table B.11. Rig results for the experiment 2 (new differential with different setting).

NEW DIFFERENTIAL (final setting) EXPERIMENT 2			
Extra load [Kg]	**Slope at free end [rad]**	**Longitude due to the deflection in extra loaded arm [m]**	**Difference torque left and right [Nm]**
1,5	0,022	1,000	14,727
3,5	0,050	0,999	34,326
4,5	0,065	0,998	44,097
6	0,100	0,995	58,626
9	0,130	0,992	87,633
12	0,172	0,985	116,089
13	0,211	0,977	124,777
18	0,256	0,967	170,883
17	0,280	0,960	160,252
20	0,312	0,950	186,593
24	0,342	0,940	221,468
30	0,376	0,927	272,968
29	0,427	0,904	257,461
33	0,436	0,900	291,661
36	0,535	0,845	298,600
39	0,552	0,834	319,310
39,5	0,601	0,799	310,100
41,5	0,618	0,786	320,410
40,8	0,644	0,765	306,548
44,5	0,669	0,744	324,947
49	0,711	0,703	338,424

Table B.12. Rig results for the experiment 3 (new differential with different setting).

NEW DIFFERENTIAL (final setting) EXPERIMENT 3			
Extra load [Kg]	**Slope at free end [rad]**	**Longitude due to the deflection in extra loaded arm [m]**	**Difference torque left and right [Nm]**
2	0,006	1,000	19,640
3,5	0,009	1,000	34,369
4	0,012	1,000	39,277
7,5	0,018	1,000	73,638
10	0,024	1,000	98,172
12,5	0,029	1,000	122,697
15,5	0,035	0,999	152,115
18	0,041	0,999	176,612
19	0,045	0,999	186,390
21	0,048	0,999	205,986
23	0,052	0,999	225,549
27	0,065	0,998	264,575

30	0,073	0,997	293,823
32	0,078	0,997	313,281
36	0,083	0,997	352,302
38	0,084	0,996	371,836
39,5	0,093	0,996	386,219
43	0,096	0,995	420,295
44	0,107	0,994	429,583
43	0,109	0,994	419,764
47	0,112	0,994	458,624

Now, in the following plot, the average of these three experiments is shown:

Table B.13. Average for Test 1 (new differential with different setting).

AVERAGE NEW DIFFERENTIAL TEST 1 (final setting)	
Total input [Nm]	**Difference torque left and right [Nm]**
5,512	16,365
103,709	34,354
201,895	42,520
300,057	66,998
398,185	91,388
496,267	118,859
594,294	141,368
692,253	174,702
790,135	180,944
887,927	202,787
985,619	227,452
1083,199	264,113
1180,658	281,702
1277,983	299,566
1375,163	340,899
1472,188	357,576
1569,046	370,576
1665,725	390,241
1762,216	395,040
1858,505	401,090
1954,583	428,247

Finally, the total average of the first test is plot below, taking into account the average of all six experiments with both settings.

Table B.14. Definitive results Test 1.

AVERAGE NEW DIFFERENTIAL TEST 1	
Total input [Nm]	**Difference torque left and right [Nm]**
5,512	17,184
103,709	33,543
201,895	46,624
300,057	67,856
398,185	90,672
496,267	112,568

594,294	133,606
692,253	160,859
790,135	169,658
887,927	195,844
985,619	213,185
1083,199	250,148
1180,658	270,899
1277,983	296,881
1375,163	315,515
1472,188	329,699
1569,046	353,185
1665,725	368,308
1762,216	390,545
1858,505	422,996
1954,583	460,733

Test data (First test planning)

Here, the results of the first test planning can be seen. There are the results corresponding to the Chapter 4, when the results of the rig test did not have correlation.

First test (Original)

The results using the original differential design changed again due to the final checking of misalignment and error in the rig, they differ from the once defined before in Test Data (First test result with original differential).

So, these are the final results that can be extracted from the rig regarding this first test keeping the original design.

Table B.15. Rig results for the experiment 1.

ORIGINAL DIFFERENTIAL DESIGN (EXPERIMENT 1)			
Extra load [Kg]	**Slope at free end [rad]**	**Longitude due to the deflection in extra loaded arm [m]**	**Difference torque left and right [Nm]**
1,5	0,003	1,000	14,730
2,5	0,010	1,000	24,549
4	0,018	1,000	39,274
6,5	0,027	1,000	63,806
7	0,034	0,999	68,700
8,5	0,042	0,999	83,397
10	0,050	0,999	98,078
12	0,058	0,998	117,639
13	0,066	0,998	127,384
17	0,077	0,997	166,449
18,5	0,085	0,996	181,019
19	0,091	0,996	185,801
21,5	0,100	0,995	210,062
21	0,106	0,994	205,060
25,5	0,118	0,993	248,675
27,5	0,126	0,992	267,896
28	0,133	0,991	272,526
30	0,141	0,990	291,644

32	0,150	0,989	310,692
38	0,163	0,987	368,153
39	0,171	0,985	377,366

Table B.16. Rig results for the experiment 2.

ORIGINAL DIFFERENTIAL DESIGN (EXPERIMENT 2)			
Extra load [Kg]	**Slope at free end [rad]**	**Longitude due to the deflection in extra loaded arm [m]**	**Difference torque left and right [Nm]**
1	0,002	1,000	9,820
2,5	0,010	1,000	24,549
3,5	0,017	1,000	34,365
5	0,025	1,000	49,084
8	0,035	0,999	78,511
9,5	0,043	0,999	93,203
11,5	0,052	0,999	112,779
11	0,057	0,998	107,844
13	0,066	0,998	127,384
17	0,077	0,997	166,449
18	0,084	0,996	176,136
21	0,094	0,996	205,312
21	0,100	0,995	205,190
25	0,111	0,994	243,988
23	0,114	0,993	224,375
27	0,125	0,992	263,045
30	0,135	0,991	291,895
34	0,146	0,989	330,293
30	0,147	0,989	291,382
38	0,163	0,987	368,153
37,5	0,169	0,986	362,968

Table B.17. Rig results for the experiment 3.

ORIGINAL DIFFERENTIAL DESIGN (EXPERIMENT 3)			
Extra load [Kg]	Slope at free end [rad]	Longitude due to the deflection in extra loaded arm [m]	Difference torque left and right [Nm]
1	0,002	1,000	9,820
2,5	0,010	1,000	24,549
4	0,018	1,000	39,274
6	0,027	1,000	58,899
8,5	0,036	0,999	83,417
8	0,041	0,999	78,493
11,5	0,052	0,999	112,779
12	0,058	0,998	117,639
15	0,068	0,998	146,958
18	0,078	0,997	176,223
18,5	0,085	0,996	181,019
21	0,094	0,996	205,312
22	0,101	0,995	214,934
22	0,107	0,994	214,796
26	0,118	0,993	253,532
29	0,128	0,992	282,441
28	0,133	0,991	272,526

33,5	0,146	0,989	325,465
29,75	0,147	0,989	288,967
34	0,158	0,987	329,665
39	0,171	0,985	377,366

Table B.18. Average results for the first test.

Total input [Nm]	Difference torque left and right [Nm]
5,512	11,457
103,709	24,549
201,895	37,637
300,057	57,263
398,185	76,876
496,267	85,031
594,294	107,879
692,253	114,374
790,135	133,909
887,927	169,707
985,619	179,391
1083,199	198,808
1180,658	210,062
1277,983	221,281
1375,163	242,194
1472,188	271,127
1569,046	278,982
1665,725	315,801
1762,216	297,013
1858,505	355,323
1954,583	372,567

Second test (minimum side gear and maximum in pinion gear)

Table B.19. Rig results for the experiment 1.

SIDE MIN, PINION MAX (EXPERIMENT 1)			
Extra load [Kg]	Slope at free end [rad]	Longitude due to the deflection in extra loaded arm [m]	Difference torque left and right [Nm]
1	0,002	1,000	9,820
3	0,010	1,000	24,549
4	0,018	1,000	39,274
5	0,025	1,000	49,084
6	0,033	0,999	58,888
8	0,041	0,999	78,493
9	0,049	0,999	88,276
12	0,058	0,998	112,742
14	0,066	0,998	132,278
16	0,075	0,997	156,672
19	0,085	0,996	185,902
21	0,094	0,996	205,312
22	0,101	0,995	214,934
24	0,109	0,994	229,395
26	0,118	0,993	253,532

28	0,127	0,992	272,745
29	0,134	0,991	282,212
31	0,143	0,990	301,312
34	0,152	0,988	329,985
33	0,157	0,988	320,032
32	0,162	0,987	310,086

Table B.20. Rig results for the experiment 2.

SIDE MIN, PINION MAX (EXPERIMENT 2)			
Extra load [Kg]	**Slope at free end [rad]**	**Longitude due to the deflection in extra loaded arm [m]**	**Difference torque left and right [Nm]**
2	0,003	1,000	19,640
2,5	0,010	1,000	24,549
3,5	0,017	1,000	34,365
5	0,025	1,000	49,084
7,5	0,035	0,999	73,606
9	0,042	0,999	88,300
9,5	0,049	0,999	93,177
12	0,058	0,998	117,639
15,5	0,069	0,998	151,850
17,5	0,077	0,997	171,336
18,5	0,085	0,996	181,019
20	0,093	0,996	195,558
22	0,101	0,995	214,934
22,5	0,108	0,994	219,663
26	0,118	0,993	253,532
27,5	0,126	0,992	267,896
28,5	0,133	0,991	277,369
28	0,139	0,990	272,296
31	0,149	0,989	301,039
31,5	0,155	0,988	305,575
31	0,161	0,987	300,457

Table B.21. Rig results for the experiment 3.

SIDE MIN, PINION MAX (EXPERIMENT 3)			
Extra load [Kg]	**Slope at free end [rad]**	**Longitude due to the deflection in extra loaded arm [m]**	**Difference torque left and right [Nm]**
1	0,002	1,000	9,820
2,5	0,010	1,000	24,549
4,5	0,019	1,000	44,182
6	0,027	1,000	58,899
7	0,034	0,999	68,700
9,5	0,043	0,999	93,203
10,5	0,050	0,999	102,979
13	0,060	0,998	127,433
15,5	0,069	0,998	151,850
18	0,078	0,997	176,223
19	0,085	0,996	185,902
21	0,094	0,996	205,312
22,5	0,102	0,995	219,805

24	0,110	0,994	234,260
26	0,118	0,993	253,532
28	0,127	0,992	272,745
28,5	0,133	0,991	277,369
29	0,140	0,990	281,972
30	0,147	0,989	291,382
31,5	0,155	0,988	305,575
32	0,162	0,987	310,086

Table B.22. Average for Second Test.

Total input [Nm]	Difference torque left and right [Nm]
5,512	13,093
103,709	24,549
201,895	39,274
300,057	52,356
398,185	67,065
496,267	86,666
594,294	94,810
692,253	119,271
790,135	145,326
887,927	168,077
985,619	184,274
1083,199	202,061
1180,658	216,558
1277,983	227,773
1375,163	253,532
1472,188	271,129
1569,046	278,983
1665,725	285,193
1762,216	307,469
1858,505	310,394
1954,583	306,877

Third test (maximum in side gear and minimum in pinion gear)

Table B.23. Rig results for the experiment 1.

SIDE MAX, PINION MIN (EXPERIMENT 1)			
Extra load [Kg]	**Slope at free end [rad]**	**Longitude due to the deflection in extra loaded arm [m]**	**Difference torque left and right [Nm]**
1,500	0,003	1,000	14,730
3,000	0,011	1,000	29,458
4,000	0,018	1,000	39,274
6,000	0,027	1,000	58,899
7,500	0,035	0,999	73,606
9,000	0,042	0,999	88,300
12,000	0,052	0,999	117,679
15,500	0,063	0,998	151,911
17,000	0,071	0,998	166,524
18,000	0,078	0,997	176,223
20,000	0,086	0,996	195,665

22,000	0,095	0,995	215,064
23,000	0,102	0,995	224,676
25,000	0,111	0,994	243,988
28,000	0,121	0,993	272,954
31,000	0,130	0,991	301,823
33,5	0,139	0,990	325,754
31,5	0,143	0,990	306,145
30,5	0,148	0,989	296,211
35	0,160	0,987	339,294
32,5	0,163	0,987	314,899

Table B.24. Rig results for the experiment 2.

SIDE MIN, PINION MAX (EXPERIMENT 2)			
Extra load [Kg]	**Slope at free end [rad]**	**Longitude due to the deflection in extra loaded arm [m]**	**Difference torque left and right [Nm]**
1,5	0,003	1,000	14,730
3,5	0,011	1,000	34,368
5	0,019	1,000	49,091
6	0,027	1,000	58,899
9,5	0,037	0,999	93,226
10	0,044	0,999	98,106
14	0,055	0,999	137,274
15	0,062	0,998	147,016
16	0,069	0,998	156,742
18	0,078	0,997	176,223
20	0,086	0,996	195,665
22	0,095	0,995	215,064
24	0,103	0,995	234,414
25	0,111	0,994	243,988
26	0,118	0,993	253,532
28	0,127	0,992	272,745
31,5	0,137	0,991	306,412
34	0,146	0,989	330,293
35	0,154	0,988	339,626
36	0,161	0,987	348,918
37	0,168	0,986	358,166

Table B.25. Rig results for the experiment 3.

SIDE MAX, PINION MIN (EXPERIMENT 3)			
Extra load [Kg]	**Slope at free end [rad]**	**Longitude due to the deflection in extra loaded arm [m]**	**Difference torque left and right [Nm]**
2	0,003	1,000	19,640
3,5	0,011	1,000	34,368
5,5	0,020	1,000	53,999
7,25	0,028	1,000	71,167
9,5	0,037	0,999	93,226
11	0,045	0,999	107,911
13,5	0,054	0,999	132,376
15,5	0,063	0,998	151,911
16,5	0,070	0,998	161,633

18,5	0,078	0,997	181,110
20	0,086	0,996	195,665
22	0,095	0,995	215,064
24,25	0,104	0,995	236,849
25,5	0,111	0,994	248,851
27,25	0,120	0,993	265,672
29,3	0,128	0,992	285,350
31,8	0,137	0,991	309,314
34	0,146	0,989	330,293
34	0,152	0,988	329,985
34,5	0,159	0,987	334,480
39	0,171	0,985	377,366

Table B.26. Rig results for the average of third test.

Total input [Nm]	Difference torque left and right [Nm]
5,512	16,367
103,709	32,731
201,895	47,455
300,057	62,988
398,185	86,686
496,267	98,106
594,294	129,110
692,253	150,280
790,135	161,633
887,927	177,852
985,619	195,665
1083,199	215,064
1180,658	231,980
1277,983	245,609
1375,163	264,053
1472,188	286,639
1569,046	313,827
1665,725	322,243
1762,216	321,941
1858,505	340,897
1954,583	350,144

Extra test (original side gear and maximum pinion gear)

Table B.27. Rig results for the experiment 1.

SIDE ORIGINAL, PINION MAX (EXPERIMENT 1)			
Extra load [Kg]	Slope at free end [rad]	Longitude due to the deflection in extra loaded arm [m]	Difference torque left and right [Nm]
1,5	0,003	1,000	14,730
2,5	0,010	1,000	24,549
4	0,018	1,000	39,274
6	0,027	1,000	58,899
10,5	0,038	0,999	103,035
12,5	0,047	0,999	122,616
15,5	0,057	0,998	151,967

12	0,058	0,998	117,639
14	0,067	0,998	137,172
19	0,079	0,997	185,995
18	0,084	0,996	176,136
18	0,090	0,996	176,041
19	0,097	0,995	185,693
21	0,106	0,994	205,060
23	0,114	0,993	224,375
24	0,122	0,993	233,925
25	0,129	0,992	243,445
27	0,138	0,990	262,616
29	0,146	0,989	281,720
31	0,155	0,988	300,754
33	0,163	0,987	319,711

Table B.28. Rig results for the experiment 2.

SIDE ORIGINAL, PINION MAX (EXPERIMENT 2)			
Extra load [Kg]	**Slope at free end [rad]**	**Longitude due to the deflection in extra loaded arm [m]**	**Difference torque left and right [Nm]**
1,5	0,003	1,000	14,730
3	0,011	1,000	29,458
4,5	0,019	1,000	44,182
5,5	0,026	1,000	53,992
8	0,035	0,999	78,511
9,5	0,043	0,999	93,203
11	0,051	0,999	107,879
12	0,058	0,998	117,639
14	0,067	0,998	137,172
16	0,075	0,997	156,672
17	0,083	0,997	166,367
17	0,089	0,996	166,280
20	0,099	0,995	195,443
22	0,107	0,994	214,796
23	0,114	0,993	224,375
23,5	0,121	0,993	229,069
25,5	0,130	0,992	248,294
27	0,138	0,990	262,616
29,5	0,147	0,989	286,551
31	0,155	0,988	300,754
33,5	0,164	0,986	324,522

Table B.29. Rig results for the experiment 3.

SIDE ORIGINAL, PINION MAX (EXPERIMENT 3)			
Extra load [Kg]	**Slope at free end [rad]**	**Longitude due to the deflection in extra loaded arm [m]**	**Difference torque left and right [Nm]**
1,5	0,003	1,000	14,730
2,5	0,010	1,000	24,549
4,5	0,019	1,000	44,182
5,5	0,026	1,000	53,992
8	0,035	0,999	78,511

9,5	0,043	0,999	93,203
11	0,051	0,999	107,879
11,5	0,058	0,998	112,742
14	0,067	0,998	137,172
16	0,075	0,997	156,672
16,5	0,082	0,997	161,482
17,5	0,089	0,996	171,161
20	0,099	0,995	195,443
22	0,107	0,994	214,796
23,5	0,115	0,993	229,237
24,5	0,122	0,992	238,781
25	0,129	0,992	243,445
27	0,138	0,990	262,616
30	0,147	0,989	291,382
31	0,155	0,988	300,754
32	0,162	0,987	310,086

Table B.30. Rig results for the average of extra test.

Total input [Nm]	Difference torque left and right [Nm]
5,512	14,730
103,709	26,185
201,895	42,546
300,057	55,628
398,185	86,686
496,267	103,007
594,294	122,575
692,253	116,007
790,135	137,172
887,927	166,447
985,619	167,995
1083,199	171,161
1180,658	192,193
1277,983	211,551
1375,163	225,996
1472,188	233,925
1569,046	245,061
1665,725	262,616
1762,216	286,551
1858,505	300,754
1954,583	318,107

Test Data (Final test planning)

Now, it can be see the results corresponding to the last test planning where the only parameter has been the material of the washer, either keeping the original material or treat it in order to get the Nedox coating. The tables correspond to the plot results in the Chapter 6.

Test 0

The results of the test for the original differential design are still the same as have been shown before in the Test Data (First test planning results).

Test 1 (all Nedox washers)

Table 12.31. Rig results for the experiment 1.

TEST 1 (EXPERIMENT 1)			
Extra load [Kg]	**Slope at free end [rad]**	**Longitude due to the deflection in extra loaded arm [m]**	**Difference torque left and right [Nm]**
1	0,002	1,000	9,820
2	0,010	1,000	19,639
3,5	0,017	1,000	34,365
5,5	0,026	1,000	53,992
7	0,034	0,999	68,700
8	0,041	0,999	78,493
9	0,049	0,999	88,276
10	0,056	0,998	98,046
12	0,064	0,998	117,595
14	0,073	0,997	137,113
17	0,083	0,997	166,367
19	0,091	0,996	185,801
22	0,101	0,995	214,934
23	0,108	0,994	224,530
23	0,114	0,993	224,375
24	0,122	0,993	233,925
26	0,130	0,991	253,142
27	0,138	0,990	262,616
29	0,146	0,989	281,720
32	0,156	0,988	310,395
35	0,166	0,986	338,948

Table 12.32. Rig results for the experiment 2.

TEST 1 (EXPERIMENT 2)			
Extra load [Kg]	**Slope at free end [rad]**	**Longitude due to the deflection in extra loaded arm [m]**	**Difference torque left and right [Nm]**
1	0,002	1,000	9,820
2,5	0,010	1,000	24,549
3	0,017	1,000	29,456
4,5	0,025	1,000	44,176
6	0,033	0,999	58,888
7	0,040	0,999	68,685
9	0,049	0,999	88,276
10	0,056	0,998	98,046
12,5	0,065	0,998	122,490
14,5	0,074	0,997	142,004
15	0,080	0,997	146,824
17,5	0,089	0,996	171,161
20	0,099	0,995	195,443
22	0,107	0,994	214,796
25	0,117	0,993	243,816

25	0,123	0,992	243,635
28	0,133	0,991	272,526
30	0,141	0,990	291,644
31	0,149	0,989	301,039
35	0,160	0,987	339,294
34	0,164	0,986	329,332

Table 12.33. Rig results for the experiment 3.

TEST 1 (EXPERIMENT 3)			
Extra load [Kg]	**Slope at free end [rad]**	**Longitude due to the deflection in extra loaded arm [m]**	**Difference torque left and right [Nm]**
1	0,002	1,000	9,820
2	0,010	1,000	19,639
4	0,018	1,000	39,274
6	0,027	1,000	58,899
7,5	0,035	0,999	73,606
8	0,041	0,999	78,493
10,5	0,050	0,999	102,979
11	0,057	0,998	107,844
13	0,066	0,998	127,384
15	0,074	0,997	146,894
16	0,082	0,997	156,597
18	0,090	0,996	176,041
20	0,099	0,995	195,443
22,5	0,108	0,994	219,663
25	0,117	0,993	243,816
27	0,125	0,992	263,045
30	0,135	0,991	291,895
32	0,144	0,990	310,976
33	0,151	0,989	320,341
35	0,160	0,987	339,294
36,5	0,168	0,986	353,364

Table 12.34. Final results (average of the three experiments).

Total input [Nm]	**Difference torque left and right [Nm]**
5,512	9,820
103,709	21,276
201,895	34,365
300,057	52,356
398,185	67,065
496,267	75,224
594,294	93,177
692,253	101,312
790,135	122,490
887,927	142,004
985,619	156,596
1083,199	177,668
1180,658	201,940
1277,983	219,663
1375,163	237,336

1472,188	246,869
1569,046	272,521
1665,725	288,412
1762,216	301,033
1858,505	329,661
1954,583	340,548

Test 2 (Nedox just in side gears)

Table 12.35. Rig results for the experiment 1.

TEST 2 (EXPERIMENT 1)			
Extra load [Kg]	**Slope at free end [rad]**	**Longitude due to the deflection in extra loaded arm [m]**	**Difference torque left and right [Nm]**
1,0	0,002	1,000	9,820
2,5	0,010	1,000	24,549
4,0	0,018	1,000	39,274
6,0	0,027	1,000	58,899
6,0	0,033	0,999	58,888
9,5	0,043	0,999	93,203
10,5	0,050	0,999	102,979
11,0	0,057	0,998	107,844
12,0	0,064	0,998	117,595
15,0	0,074	0,997	146,894
17,0	0,083	0,997	166,367
19,0	0,091	0,996	185,801
22,0	0,101	0,995	214,934
24,0	0,110	0,994	234,260
23,0	0,114	0,993	224,375
28,0	0,127	0,992	272,745
29,0	0,134	0,991	282,212
32,0	0,144	0,990	310,976
30,0	0,147	0,989	291,382
34,0	0,158	0,987	329,665
37,0	0,168	0,986	358,166

Table 12.36. Rig results for the experiment 2.

TEST 2 (EXPERIMENT 2)			
Extra load [Kg]	**Slope at free end [rad]**	**Longitude due to the deflection in extra loaded arm [m]**	**Difference torque left and right [Nm]**
1,0	0,002	1,000	9,820
3,0	0,011	1,000	29,458
3,5	0,017	1,000	34,365
5,0	0,025	1,000	49,084
7,0	0,034	0,999	68,700
8,0	0,041	0,999	78,493
9,0	0,049	0,999	88,276
11,0	0,057	0,998	107,844
14,0	0,067	0,998	137,172
16,0	0,075	0,997	156,672
16,5	0,082	0,997	161,482

20,0	0,093	0,996	195,558
21,0	0,100	0,995	205,190
24,0	0,110	0,994	234,260
26,0	0,118	0,993	253,532
27,0	0,125	0,992	263,045
28,0	0,133	0,991	272,526
32,0	0,144	0,990	310,976
33,0	0,151	0,989	320,341
35,0	0,160	0,987	339,294
35,3	0,166	0,986	341,351

Table 12.37. Rig results for the experiment 3.

TEST 2 (EXPERIMENT 3)			
Extra load [Kg]	**Slope at free end [rad]**	**Longitude due to the deflection in extra loaded arm [m]**	**Difference torque left and right [Nm]**
1,0	0,002	1,000	9,820
3,0	0,011	1,000	29,458
4,0	0,018	1,000	39,274
5,0	0,025	1,000	49,084
7,5	0,035	0,999	73,606
8,5	0,042	0,999	83,397
9,5	0,049	0,999	93,177
11,5	0,058	0,998	112,742
13,0	0,066	0,998	127,384
15,0	0,074	0,997	146,894
16,0	0,082	0,997	156,597
20,0	0,093	0,996	195,558
22,0	0,101	0,995	214,934
23,0	0,108	0,994	224,530
26,0	0,118	0,993	253,532
27,0	0,125	0,992	263,045
29,0	0,134	0,991	282,212
32,0	0,144	0,990	310,976
33,0	0,151	0,989	320,341
36,5	0,161	0,987	353,728
37,0	0,168	0,986	358,166

Table 12.38. Final results (average of the three experiments).

Total input [Nm]	**Difference torque left and right [Nm]**
5,512	9,820
103,709	27,822
201,895	37,637
300,057	52,356
398,185	67,065
496,267	85,031
594,294	94,810
692,253	109,476
790,135	127,384

887,927	150,153
985,619	161,482
1083,199	192,305
1180,658	211,686
1277,983	231,017
1375,163	243,813
1472,188	266,279
1569,046	278,983
1665,725	310,976
1762,216	310,688
1858,505	340,896
1954,583	352,561

Test 3 (Nedox just in pinion gears)

Table 12.39. Rig results for the experiment 1.

TEST 3 (EXPERIMENT 1)			
Extra load [Kg]	**Slope at free end [rad]**	**Longitude due to the deflection in extra loaded arm [m]**	**Difference torque left and right [Nm]**
1,5	0,003	1,000	14,730
2,5	0,010	1,000	24,549
3,5	0,017	1,000	34,365
5,0	0,025	1,000	49,084
7,0	0,034	0,999	68,700
9,0	0,042	0,999	88,300
10,0	0,050	0,999	98,078
12,0	0,058	0,998	117,639
13,0	0,066	0,998	127,384
17,5	0,077	0,997	171,336
18,0	0,084	0,996	176,136
20,0	0,093	0,996	195,558
22,0	0,101	0,995	214,934
24,0	0,110	0,994	234,260
26,0	0,118	0,993	253,532
28,0	0,127	0,992	272,745
28,0	0,133	0,991	272,526
33,0	0,145	0,989	320,637
33,0	0,151	0,989	320,341
36,0	0,161	0,987	348,918
38,0	0,169	0,986	367,769

Table 12.40. Rig results for the experiment 2.

TEST 3 (EXPERIMENT 2)			
Extra load [Kg]	**Slope at free end [rad]**	**Longitude due to the deflection in extra loaded arm [m]**	**Difference torque left and right [Nm]**
1,5	0,003	1,000	14,730
3,0	0,011	1,000	29,458
4,0	0,018	1,000	39,274
6,0	0,027	1,000	58,899
7,5	0,035	0,999	73,606

9,0	0,042	0,999	88,300
11,0	0,051	0,999	107,879
11,5	0,058	0,998	112,742
13,5	0,066	0,998	132,278
17,0	0,077	0,997	166,449
18,5	0,085	0,996	181,019
19,0	0,091	0,996	185,801
21,0	0,100	0,995	205,190
23,0	0,108	0,994	224,530
25,0	0,117	0,993	243,816
28,0	0,127	0,992	272,745
29,0	0,134	0,991	282,212
33,0	0,145	0,989	320,637
34,0	0,152	0,988	329,985
36,0	0,161	0,987	348,918
39,0	0,171	0,985	377,366

Table 12.41. Rig results for the experiment 3.

TEST 3 (EXPERIMENT 3)			
Extra load [Kg]	**Slope at free end [rad]**	**Longitude due to the deflection in extra loaded arm [m]**	**Difference torque left and right [Nm]**
1,0	0,002	1,000	9,820
2,0	0,010	1,000	19,639
3,5	0,017	1,000	34,365
5,5	0,026	1,000	53,992
7,0	0,034	0,999	68,700
8,0	0,041	0,999	78,493
11,0	0,051	0,999	107,879
10,5	0,057	0,998	102,945
15,5	0,069	0,998	151,850
16,5	0,076	0,997	161,561
18,5	0,085	0,996	181,019
21,0	0,094	0,996	205,312
22,0	0,101	0,995	214,934
25,0	0,111	0,994	243,988
24,0	0,116	0,993	234,097
29,0	0,128	0,992	282,441
29,5	0,135	0,991	287,054
34,0	0,146	0,989	330,293
34,0	0,152	0,988	329,985
37,0	0,162	0,987	358,537
36,0	0,167	0,986	348,560

Table 12.42. Final results (average of the three experiments).

Total input [Nm]	**Difference torque left and right [Nm]**
5,512	13,093
103,709	24,549
201,895	36,001
300,057	53,992
398,185	70,336

496,267	85,031
594,294	104,612
692,253	111,109
790,135	137,171
887,927	166,449
985,619	179,391
1083,199	195,557
1180,658	211,686
1277,983	234,259
1375,163	243,815
1472,188	275,977
1569,046	280,597
1665,725	323,855
1762,216	326,771
1858,505	352,124
1954,583	364,565

Appendix C. Rig Test Design

Rig design

Testing means also an extra design to be done. Thus, parallel to the model building stage, the design of the complete rig is done. Then, in order to deal with the Chapter 3 further, the information is sum up below.

The goal is getting a reliable and adjustable design that allows testing and changing the parameters easily and quickly. Hence, the design is done using CATIA V5 R19.

In addition, the design does not add any simulation since they are not needed, just some calculations (see below in this *Appendix C*) are done to know the dimensions of some of the parts. But as it has been said before, the objectives are reliability and adjustability, by this way just some mechanical design is done in the best way possible in order to be optimum from the engineering point of view.

There are some limitations to do this kind of test. One of them is the impossibility to fix the differential using the bearings and simulate the engine torque using the ring gear attached to the housing. In addition, there was no possibility to use the whole drive shafts since the effects of the constant velocity housing would have affected the results. Then, the differential housing (or carrier) has been fixed on the bench using two supports (one in each side of the differential where the bearings are) clamped on the bench. By this way the differential is totally fixed. Furthermore, in both sides of the differential, the right driveshaft of the XC30 Volvo car is used. The right driveshaft is longer compared to the left, so it is not as stiff as the left but the misalignment might be lower. This is the reason why the right shaft is used in both sides.

The whole driveshaft assembly was got from the supplier (GFT) and then it was cut in order to remove all the constant velocity housings. Furthermore, the driveshaft was machined in the opposite side from the splines to be able to assemble a support.

Once all the parts are machines, the rig can be assembled. As it has been said before, the differential is totally attached on its supports and then the driveshafts are attach on the splines (contact with the side gear) and with the bearing support (clamped on the bench).

Finally, to be able to explain how the rig works, the drawings and the CAD isometric view may help (see below in this *Appendix C*). Two arms are attached, by means of a support, on the shaft. These arms are being used to hold the weights at 1m of distance *d* (when no deflection occurs) from the axis of the shaft. By this way some weights will be attach and the torque in the shaft will be mainly the load multiplied for the effective distance ($T = F \cdot d$). But also, some other torque contribution exists and it will be taken into account, although it is lower compared to the load itself, more accuracy will be got. These extra loads are the weight of the platform, the hook and the rope applied at the same distance as the load, and the weight of the rod itself.

The arms are being loaded equally, then the differential will become preloaded with a torque of double time the input.

Next step is just adding the amount of weight enough in one of the sides until the arms start turning in different directions. This moment is when the weight added will be the "torque losses" for the input torque.

Basically, all what has been explained so far is the main idea to make the rig working and be able to get right results. For each test, different measurements will be done for each load case, from 0Nm until 2000Nm of input torque (1000Nm in each side roughly).

Loads on the shafts

The resistances reaction loads that the system does are due to the input load. This load is transmitted first from the end of the rod to the welding support.

It can be represented like the following Figure C.1:

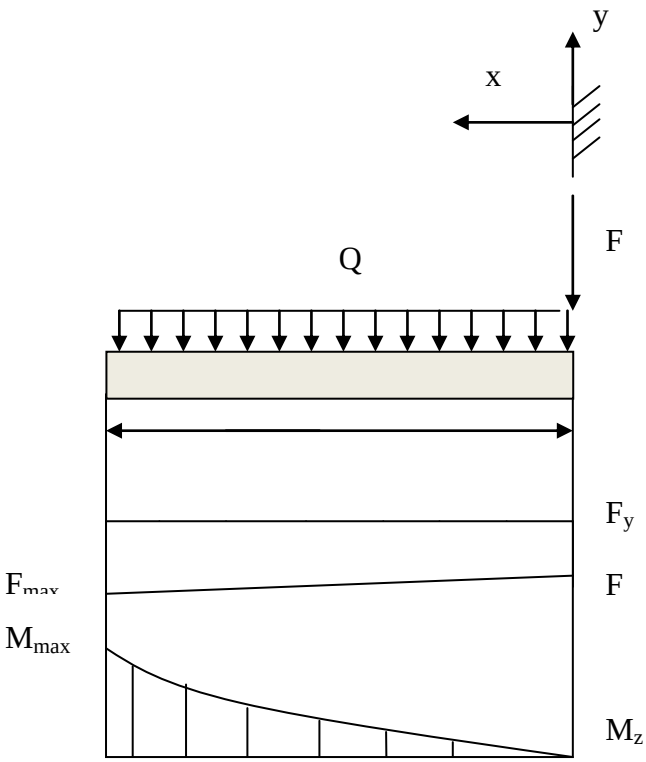

Figure C.1. Shear forces and flection moments diagram.

where the maximum shear forces F_{max} and the maximum flection moment are:

$$F_{max} = F + Ql \quad \text{(C.1)}$$

$$M_{max} = Fl + \frac{QL^2}{2} \quad \text{(C.2)}$$

Now, if the reactions are set on the shaft the following free body diagram (plane y-z) in the Figure C.2 is got:

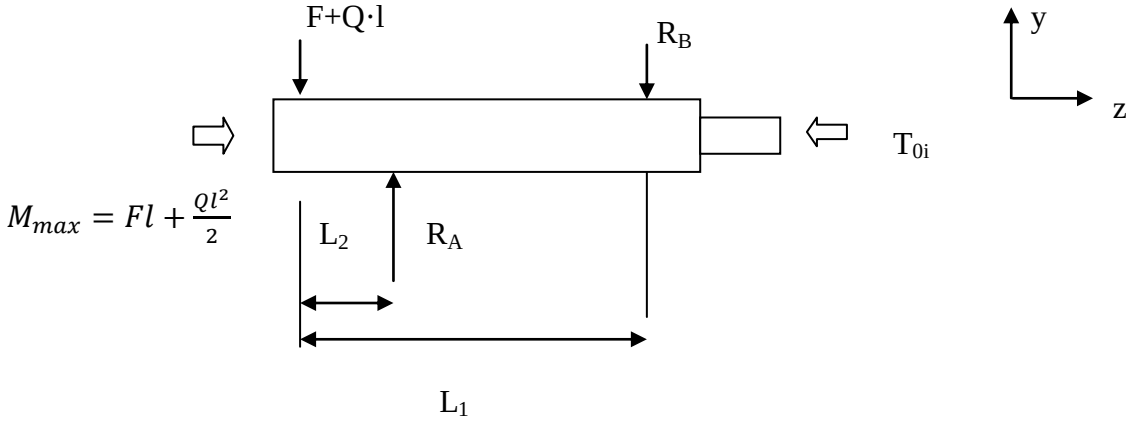

Figure C.2. Free body diagram sketch of the driveshaft.

- $\sum F_y = 0$:

$$R_A - R_B = F + Ql \quad \text{(C.3)}$$

-$\sum M_z = 0$:

$$M_{max} = Fl + \frac{Ql^2}{2} \quad \text{(C.4)}$$

- $\sum M_x = 0$:

$$(F + Ql)L_2 = R_B(L_1 - L_2) \quad \text{(C.5)}$$

Hence, the reaction in the bearing (A) and the reaction in the housing (B) are:

$$R_A = (F + Ql)(1 + \frac{L_1}{L_1 - L_2}) \quad \text{(C.6)}$$

$$R_B = (F + Ql)\frac{L_2}{L_1 - L_2} \quad \text{(C.7)}$$

Rod dimensions

According to the results showed in subchapter above, the dimensions of the rods can be calculated regarding the traction strength maximum admissible.

Taking into account that the maximum load that it will be set on the arm is approximated 1500Nm, the traction strength can be calculated as:

$$\sigma = \frac{M_x}{I_{zz}} y = \frac{1500000\frac{D}{2}}{\frac{\pi D^4}{64}} \leq \sigma_{adm} \quad \text{(C.8)}$$

If it is assumed that the plastic deformation can happen in order not to have a huge rod, then the maximum tensile of the steel used is around 650Mpa.

Then, it yields that the diameter of the rod should be around 27 mm at least.

However, the rod is not just clamped in the end, regarding the rig design, it was decided to clamp it on a support, which is welded on the driveshaft in order to transmit the torque to the driveshaft, to weld the rod inside and by this way have some extra shoulder to give a little more stiffness. Then, it was decided to use a rod of

25mm diameter with having a compromise between reliability and optimization of the material, as well as a light weight in order to gain adjustability every time the differential has to be removed. By this way a standard and relative light bar could be used.

In fact, the maximum torque allowed to study in this rig is 1000Nm to each drive shaft. So, there is a safety factor applied. Whereas, when the maximum load is tested, one of the roads might be loaded up to 1500Nm just for a short time, but it should not be a problem regarding these calculations.

Bearings choice and fatigue life

The idea was using a simple, reliable and low cost bearing on the driveshafts so as to optimize the bearings for their use.

That was because the number of turns or hours that the bearing had to run were really small compared to the dynamic capacity of the bearing. So, just using a bearing with the dimensions needed and the static and dynamic capacity big enough would have already fit the requisites.

Thus, the first thought was using a light needle bearing (since there is no axial load) or a groove ball bearing in each driveshaft, fixing the inner and outer ring with the shaft itself and using some circlip for instance (always trying to make it as simple as possible because as there are no axial forces the fixation of the rings are just to secure the assembly).

However, the driveshafts had to be ordered as spare parts from the supplier GFT (as it has been said above). This means that the received driveshaft was the assembly, including the constant velocities housings, bearings, bearings fixations and the whole shafts. Thus, the bearing concept choice was already set, just the outer rings were fixed by interference with the support.

Finally, just to keep safety the bearing life was calculated in order to check how over dimensioned was (*following* [39]).

The bearing had a dynamic capacity of 22,1 kN and a static capacity of 14,6 kN.

Hence, the durability in turns is (considering the safety margin of having applied during 100% of the maximum load of 2000N).

$$L_t = \frac{C^p 10^6}{P^p} = 1349232625\ turns \qquad \text{(C.9)}$$

which is clearly above 10^6 turns, so that no problem should appear during testing as far as the bearings are concerned since the bearing life is endless.

Rod deflection (effective length)

Due to the load that the rod is holding, the effective length is reduced. The weights are always perpendicular to the ground plane, not to the rod. By this way the effective load that creates the momentum is also reduced.

In the following Figure C.3 this phenomenon can be observed if the rod is simulated by a Cantilever beam with the concentrated load in the end of the rod.

Considering this option, the deflection due to the uniformly distributed load of the weight can be neglected.

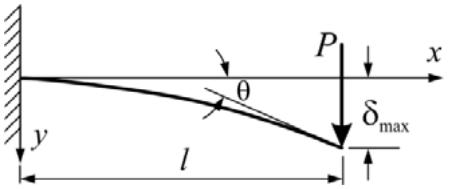

Figure C.3. Cantilever beam with concentrated load P at the free end.

The maximum deflection of the bar can be approximated with the following expression:

$$\delta_{max} = \frac{Pl^3}{3EI} \quad \text{(C.10)}$$

where l=1m, E=210 GPa (Steel Young module) and I is the inertia of the bar in the z-axis which can be written as:

$$I = \frac{\pi D^4}{64} \quad \text{(C.11)}$$

Thus, if the hypotenuse of the triangle is approximated with the initial length of the bar without taking the curvature, the effective length could be written as:

$$L' = l\cos\left(\frac{\delta}{L_0}\right) \quad \text{(C.12)}$$

where L_0=1m is the initial longitudinal dimension of the bar.

Whereas, if the angle considered (θ) is the tangency in the point where the maximum deflection, then the effective length can be written as:

$$L' = l\cos\left(\theta'\right) \quad \text{(C.13)}$$

$$\theta' = \frac{Pl^2}{2EI} \quad \text{(C.14)}$$

In the *Appendix B* above, all the tables of deflections and effective lengths calculations for each load which have been considered in order to get as more accuracy regarding the torque as possible (so as not to neglect the deformation and claim that the length of the bar reminds constant during all the experiment).

Number of bolts needed

In order not to use the 12 bolts M10 10.9 that are used for attaching the housing to the ring, some calculations are done (*see* [40]) in order to know how much bolts are needed to clamp and fix the housing to the support.

Setting the maximum torque of the housing to 2500Nm, the normal contact force is then:

$$F_t = \frac{T}{r} = 2500\frac{1000}{75} = \mu N \quad \text{(C.15)}$$

where μ_H=0.4 between cast iron and steel and the radius of the bolt pattern is 75mm.

That yields to a value of the normal force of:

N=83500N

Furthermore, according to the material of the bolt, the global friction coefficient for this dry condition of use is:

$\mu_G = 0.14$

In addition, the limit mounting force for a 10.9 class is $F_{MLim} = 36900\ N$

The sitting deformation is

δ_{xj} = 2 x 4 μm (for both junctures)

δ_{xr} = 5 μm (for the fillet)

Totally $\delta_{total} = \delta_{xj} + \delta_{xr} = 13$ μm

So, it yields to:

$$\Delta F_M = \frac{13\ 10^{-3}}{\frac{1}{K_c}+\frac{1}{K_p}} = 3700N \quad \text{(C.16)}$$

The limit mounting force of the bolt is reduced to a third due to the use of a handling tool:

$$F_{Mmin} = \frac{F_{Mmax}}{3} = 12300\ N \quad \text{(C.17)}$$

So, the force discounting the sitting force is reduced to:

$$F'_{Mmin} = F_{Mmin} - \Delta F_M = 8594\ N \quad \text{(C.18)}$$

Taking into account the c factor, the compressor/traction factor i=0.5, the expression of the clamping force is:

$$F'_p = F'_{Mmin} - (1 - c')F_s = 8954N > 0 \quad \text{(C.19)}$$

where $c = \frac{K_c}{K_c+K_p}$ depends on the stiffness coefficients of the bolt and the part. It is usually a value around 0.1-0.3, and $c' = c\ i$.

Fs is neglected since there is no splitting force in the system.

Thus, the K_p and K_c have set to be according to the bolts used:

K_p=3200·10^3 N/mm and K_c=315·10^3 N/mm

As there is no big separation force to include in the system, it is possible to claim that the pressure force will always be higher than zero, and thus, there will be contact force, but it is not high enough to keep the normal force needed. To know the number of bolts needed, it can be proceeded dividing the clamping force needed for the limited force of the bolt:

$$n = \frac{N}{F'_P} = 9.7\ bolts \quad \text{(C.20)}$$

So, 10 bolts will be used in the rig in order to be sure and not have any problem during the whole test, tightening them by hand tool.

Rig outcome

Rig measurement limitation

Due to the use of the rig instead of the integer vehicle, two main limitations appear. The first one is the fact that the study is static or quasi-static and it will not be possible

to do the dynamic one when the differential is in motion. The static case is the worst scenario that may happen, so there will be a safety margin. Actually, the function of the differential is mainly quasi-static since the relative speed is really small. There are just a few numbers of operations that the differential cannot be considered static, such as when the car is turning towards tight corners with a big steering angle and low speed (for instance, a city driving situation). Nevertheless, the most important outcome for this study is the torque steer for small steering angles (highway driving for example), by this way, the static/quasi-static study is a good approximation.

On the other hand, the second limitation is the gear mesh. It is extremely difficult to control and it might affect the results slightly. It was tried to keep the same gear mesh as exact as possible every time in order not to have this disturbance. That will be explained further in the following subchapter.

Moreover, there is a permanent variation of the measurement every time the differential is disassembled and assembled again, since it will never be in the exact same position as it used to be before (see following subchapter).

In addition, at the beginning of the measurements, there was a misalignment between the driveshaft and the differential housing that affected really strongly the output response of the system since both the shaft and the housing had some wear due to this misalignment. This friction that was supposed to be neglected was the one which affected the most the response for low-mid torques when there was still some misalignment. But, although the misalignment was solved, this friction torque on these surfaces might affect the real values that are in the running vehicle (see below in this *Appendix C*).

On top of that, the measurements for high torque (above 2.000 Nm) were not possible due to physical limitation of the rig, huge bending of the differential supports and the housing. So, the test had to be kept below 2.000 Nm, although it was aimed to study until 3000Nm.

Test measurements

Before beginning to proceed with the test planning, some experiments using the current new (with no wear) differential M66 without any change are done. By this way, it can be known how many experiments are needed for each test in order to get right results. Moreover, the first test was used also to check and improve the rig in order to have a clear understanding of its behaviour and what might or might not affect the results.

Thus, some experiments were done as soon as it was managed the rig to work properly.

The same test was done three times (as soon as it was managed to make the rig working), from no applied load until the maximum load with steps of 50Nm for small loads (5 Kg each time). These were tried to be done keeping the same gear since it may affect strongly the results.

However, keeping always the same gear mesh is extremely difficult to achieve, better said, even it is tried to keep it every time, it is not possible to claim that the gear mesh is exactly the same for either one test or every time that the differential is disassembled and assembled again when some changes are done. In order to minimize the effects of this parameter, some marks were done on the gear and on the

differential. If the differential was turning attached to the transmission in another rig (dynamic conditions), it would be seen that the gear mesh effects make the shape slightly sinusoidal, so the results are always between a wide band.

Nevertheless, the rig that is used will not explain this effect, so all the results are going to be between this band. However, there was the possibility to keep the gear mesh as a parameter so as to check this effect but, no mechanism to control was available, just as it has been said above, some marks were done so as to keep the mark on the gear aligned with the mark on the housing. Although, it is not possible to claim that the contact teeth are standing still during all the measurements, but at least the spread between different measurements will be narrower.

On top of that some other two measurements were done changing the gear mesh (just turning slightly one arm up and the other down) to check how big this effect might be and how much variation with the results had. In fact, it was seen how big this impact could be and how much it would affect the results.

As the data is got from the rig, it may happen that there was some error due to the measurement. This is the reason why statistic study gage R&R, which uses analysis of variance (ANOVA) random effects model to assess a measurement system, is carried out.

In the tables below it can be seen the results of this statistical method. It says the quantity of result which is due to the input and due to the measurement.

It has split up in three different steps. First of all, all the different measurements were done when it was tried to keep the same contact teeth. Then , it is seen that there is a huge difference for the measurements below 1000Nm and above this value. So, it has been split up in these two cases, below and above this value. Then the variation shows that when the test is done below 1000Nm the disturbance due to the measurement is 4% (good from a statistical point of view) and when it is done above the disturbance due to the measurement is around 25%. This means that more than one experiment would be needed for each test.

The amount of experiments for each test is set then to three, in order to make it efficient (minimum amount of experiments for each test) and reliable.

Actually, in the column 2 of the Table 4.1 in the Chapter 4.2, it can be seen the comparison between the standard deviation and the average of the three measurements for each input load using the original differential. Thus, it is checked how the average value is 0.069, which is really low. So, it means that the number of experiments is already good. The deviation and the average value do not differ so much for each experiment. Thus, three experiments were set as a suitable number of experiments enough to get reliable values according to the spread show in these measurements. However, more experiments could have been done, but so as to minimize the time consuming factor, three was a minimum and enough value to compromise both the reliability and time consuming.

Note that, the reference to the Table 4.1 (future Chapter 4.2) is done which the final results using the original design of the differential are, but the goal of setting the minimum amount of experiments was defined before starting the test planning, using some other values got after testing the original design differential. Besides, in order to show the final values, the reference is done in this future chapter.

In addition, the study for the two other experiments where the contact teeth was tried to be changed and the results were quite similar to the ones got before although the standard deviation was higher and the relation between the other experiments was higher. But as it has been said before, it was decided not to take into account the influence of the gear mesh changes as long as the results are always between the bands trying to keep the same gear mesh roughly.

Moreover, the same test for a used differential, which has been working around 100.000Km, has been done. It was seen that the standard deviation of the three experiments using this differential is little higher than the other differential, however there is still a relationship, which can be shown in a t-paired test.

Here, a decision had to be taken since the test planning would carry out either the new or the used differential (see below for the testing results).

If the new differential was used, there would be some advantages such as:

- Different gears sets (for machining them following the test planning) would be easier to get.

- The spread of the measurements for high torques would be smaller than the used one. So, the results would be more reliable, since the behaviour of the differential would be more even in each experiment.

But there would be a disadvantage that is:

- The new differential is not what the costumer will use and will be able to test and check. A differential is just new the first km, and then the wear appears.

Whereas, if the used differential had been used, it would have been possible to carry out the study with the device that the customer will have during the 90% of its life, but the wear that the differential has was not possible to have it undercontrol.

Finally, the choice was using the new differential in order to have reliable results and fast spare parts for being machined.

New and used differential results

As it is said above, several experiments were done using both differentials until the rig worked well enough. As soon as it did so, the right and final results for these two differentials were got (the data can be found in the Appendix B in the first subchapter of the comparison between new and used differential).

In the following Figure C.4, it can be seen the results from each of the three experiments for both differentials.

It may be observed as well the deviation that exists between every experiment, the lecture got for each input has a certain spread, but small enough in order to still have some relation between the experiments.

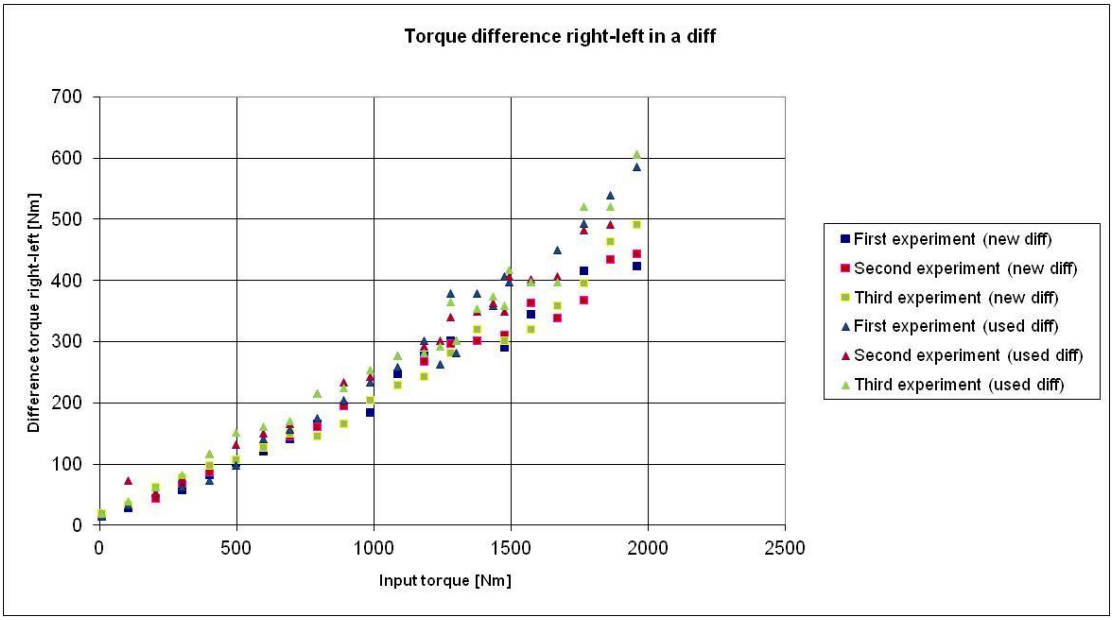

Figure C.4. All experiments for both differentials.

If the average of each of them is done (three different measurements for each input torque), in the Figure C.5 it is possible to see the results.

Thus, it is clear to observe the difference between both differentials.

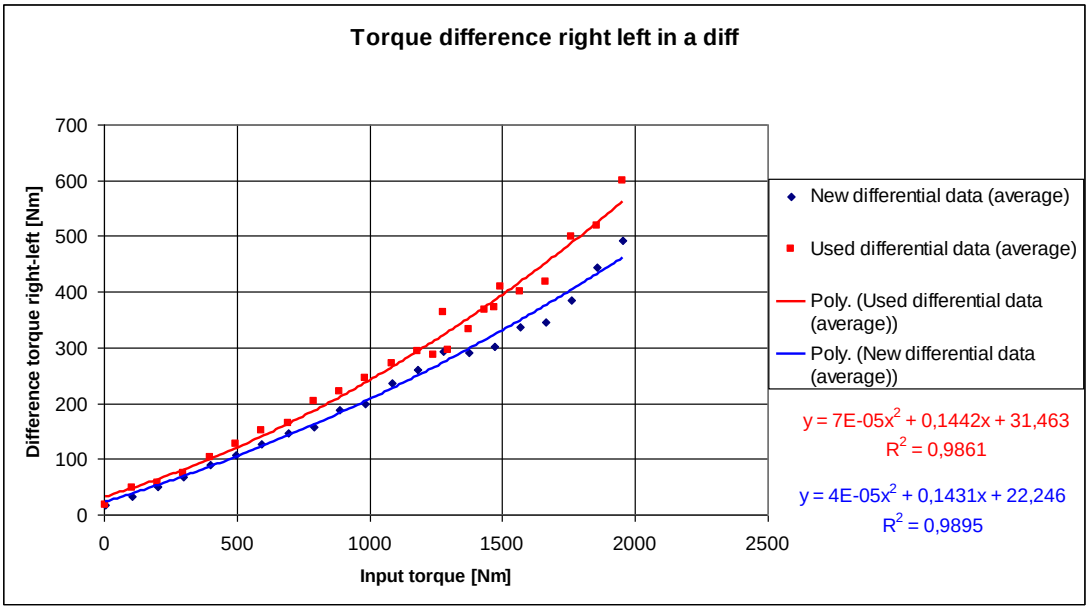

Figure C.5. Average results for both differentials.

In the beginning, for low torques, the slope is quite similar in both, just slightly higher in the used differential which could be explained by the bigger misalignment that it has.

As soon as the torque increases the torque difference between right and left of the used differential starts to increase in a non-linear curve shape. This effect happens not

only before than the new differential, but also stronger (the dependence from the input is more instable).

This could be due to several facts:

- The wear of the housing, bushings and gears is bigger for the used differential which it might change the effective radius a little upwards. So, the friction torque between the housing and the gears increases.

- The wear in the pinion gears (planetary) and in the pin changes the contact points of this contact, so that the effective friction on these surfaces increases.

- Due to bigger misalignment, the contact point between teeth has changed and the gear mesh losses increases.

- Due to the wear, when the housing starts to bend (for torques above 1000 Nm), all the effective friction radius become bigger and so the friction torque does, compared to how the differential without wear behaves (contact and flexion behaves how it was designed and tried to control).

- The shape of the pin when it bends changes due to the wear of the contact surfaces between it and the pinion gears, so the friction torque between these surfaces might be increased because of this bending shape change.

Finally, as far as the adjustable curve is concerned, it can be observed that the result could be approximated with a linear curve in the beginning and a non-linear curve in the end for high torques.

However, there are two other ways to approximate the curve got from the test. Firstly, it could even be approximated with a linear curve (as the model showed in the Chapter 2 is), but then the error becomes too high and it cannot be a reliable model. So, here it is checked how further investigation and simulations of the housing, gears, pin and bushings must be carried out to reach this test model and see the behaviour of all the contacts, frictions and pressures distributions during this middle and high range of torque in order to get a model reliable enough and closer from the real results.

Secondly, there is the possibility to study the full non-linear behaviour for the wide range of torques. Probably, it could be approximated with a polynomial of second order. According to Excel and Minitab, it is the curve which fits the results the best. Nevertheless, it might be not better to get a full non-lineal model and this is the reason why maybe the best choice is getting a lineal model from 0Nm until around 1000Nm and another non-linear model from around 1000Nm until 2000Nm or even approximating the second range of torques with another linear model with a higher slope to get a really good and reliable approximation, so that what happens for no input torque that there are permanent losses and in this change of behaviour must be studied by means of FEM analysis in order to get a clear understanding about what occurs in the reality and why it is due to. This study can be seen in the Chapter 5 and will give the information to understand what really occurs in this system regarding all the deformation and stiffness of each part.

Final setting current new differential results

As soon as the test for new and used differential was done, as well as the decision for using the new differential for the whole test plan, then the differential had to be set again in the rig. After setting it again, the test was done again in order to see how big

the difference of the results was since as it has been said before, it was expected to have a disturbance every time the rig had to be removed and assembled.

The results differed a little from the ones got for the first setting (the non-linear effects became weaker), so it was decided to make the whole test again (three experiments) and then, make the average between both tests (the three experiments for each setting).

Even though, it was tried to fix the differential in the rig as close as possible to the previous setting, there was no fact to show that it was exactly the same, and likely this is the reason why the spread was wider. But also, it was realized that due to some misalignment in the rig during the first tests, the driveshaft got damaged and they had to be grinded in order not to have a tight fitting. Basically, the huge difference torque between left and right that was got before was due to this misalignment. In order to assemble the drive shafts as much concentric as possible with the differential, shims had to be used.

After this fact, it was decided to not remove the differential any more from the rig and do all the changes "*in situ*". Besides, take care every time the driveshafts had to be removed, in order to assemble them again minimizing the misalignment in order to get reliable results.

The following plot shows the final result of the first test with the new differential M66:

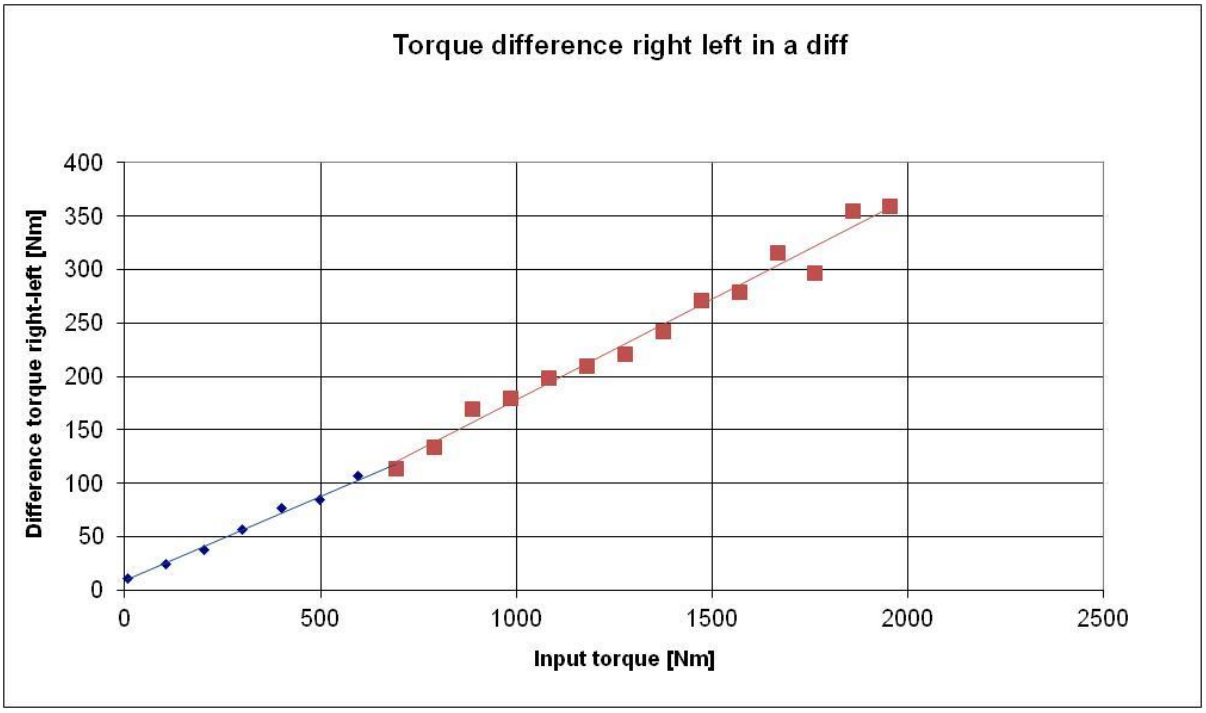

Figure C.6. Final test result with the new current M66 differential.

The results show that the non-linear effects have been reduced so that it is possible to claim that the strong non-linear effects got before during the comparison between new and used differential was caused by the misalignment. However, in these results there is still a slight non-linear effect that seems to occur around 750Nm where the red dots

appear. A second order polynomial is what fits better to the results, but actually, it can be explained splitting the curve in two linear curves (the blue for low torques and the red for high torques).

Moreover, it is seen how there is a permanent loss that exists during the interval of input torque. The permanent loss can be seen from no-input when the difference is already higher than 0Nm. It might be either due to some misalignment in the driveshafts or due to the system itself which has a permanent loss caused by the sitting of the gearset.

It is not possible to claim that this is the real effect, since a fully linear curve also fits the results pretty good, but this will be checked during the Chapter 5 in the FEM analysis.

Rig results and simulation model deviation

Once the results are picked and analysed from the rig, it is seen how much the difference between the linear model that has been done in the Chapter 2 (assuming the data for all the equivalent radius and friction coefficient) and the rig is.

If the curve got in the Figure C.6 is adjusted with two linear curves trying to minimize the square distance between the measurements and the trend line, the green curve is obtained. It has been split in two models, one below and the other above 1000 Nm.

Thus, in the following plot, it can be observed the linear model done so far adding the static loss so as to begin from the same point as the results and the rig results:

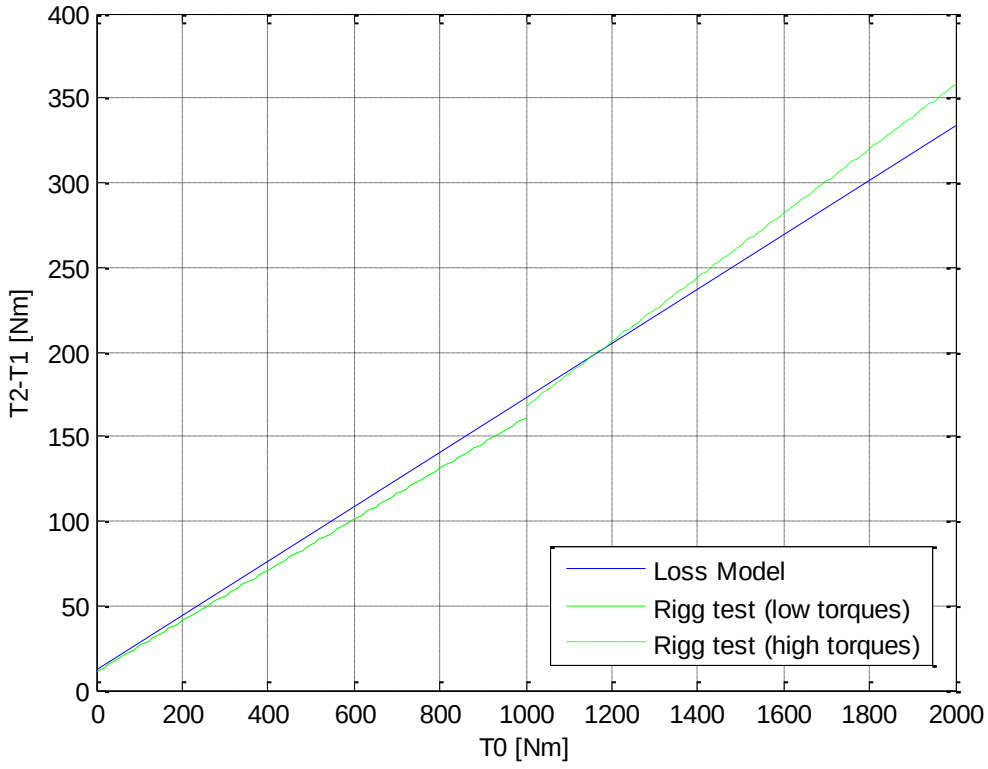

Figure C.7. Loss model vs. Rig results.

It seems that the friction coefficient might be slightly higher than what it really is in the reality (if it is still assumed the consideration of all the equivalent radius and the same friction coefficient on all the contact surfaces in the midpoint in radial direction).

Hence, to approximate the lineal model in order to reach the rig results, a friction coefficient of 0.18 would be needed (see Figure C.8).

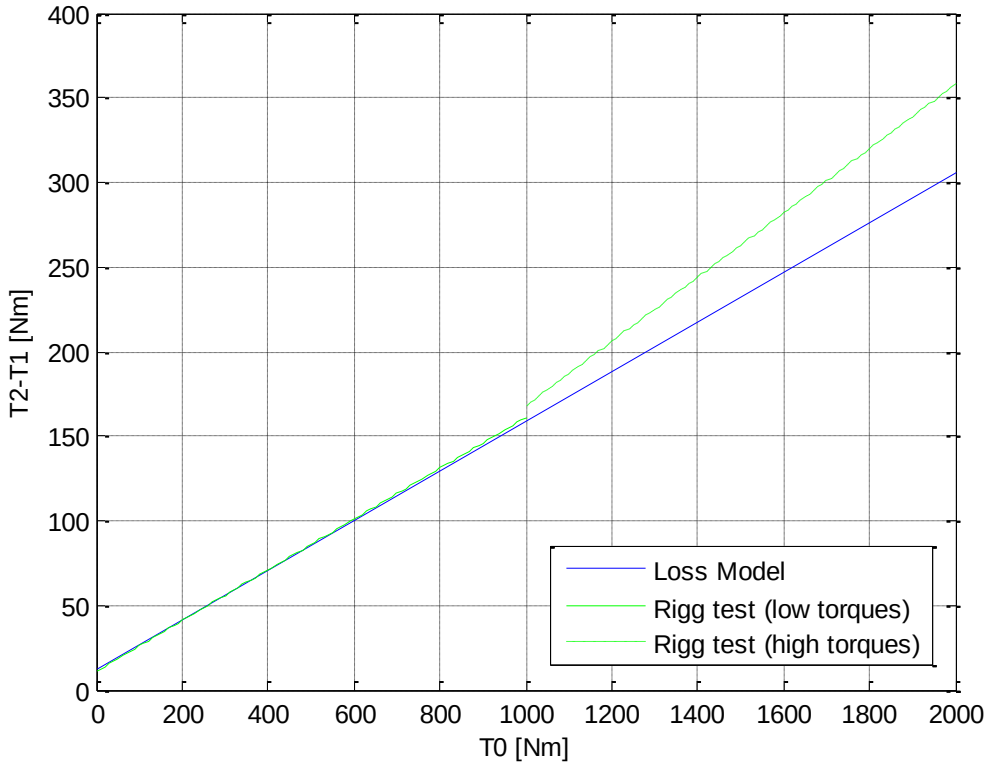

Figure C.8. Loss model vs. Rig results (fitting rig results).

Actually, this value can be even higher since some other effects have not been taken into account. For instance, the losses of the bearings could be taken into account because they are not inside the system, but these are some losses that exist anyway, in the rig and in the vehicle. Nevertheless, these losses are quite small compared to the rest of losses inside the differential, so it is not worth taking them into account.

Furthermore, a loss that will not be possible to be analysed in this study is that since the rig is working in the environment temperature, in static conditions, the differential does not work in the optimal temperature, the oil film thickness is not set (even though the oil is added some often during the test) and also the differential is not running (neglected inertia and centripetal acceleration) as well as it does in the car.

However, there is another kind of loss that would be the cause and explanation of the huge variation between right and left torque. This is the friction existing between the driveshaft and the housing.

As it has been seen in the previous subchapter in this *Appendix C* (Rig design) , the driveshaft is submitted to vertical loads, apart from the torque, which are due to the weights applied on the arms. Instead of applying the torque straight to the carrier

(housing), the torque is applied by means of adding some vertical force in the end of these bars, whereas in the car it is mostly submitted just to torque in its longitudinal axis. That releases a radial force to the driveshaft and a reaction in the shoulder in the differential which provides a friction torque in this surface. This friction torque is proportional to the load and it might be really huge compared to the other parameters that contribute to this fact. All that can be checked in the following figures and equations.

Following the same analysis done in the subchapter above (Rig design), if the right and left driveshaft are studied, the following equations are yield:

Now, if the reactions are set on the shaft the following free body diagram (plane y-z) in the Figure C.9 is got:

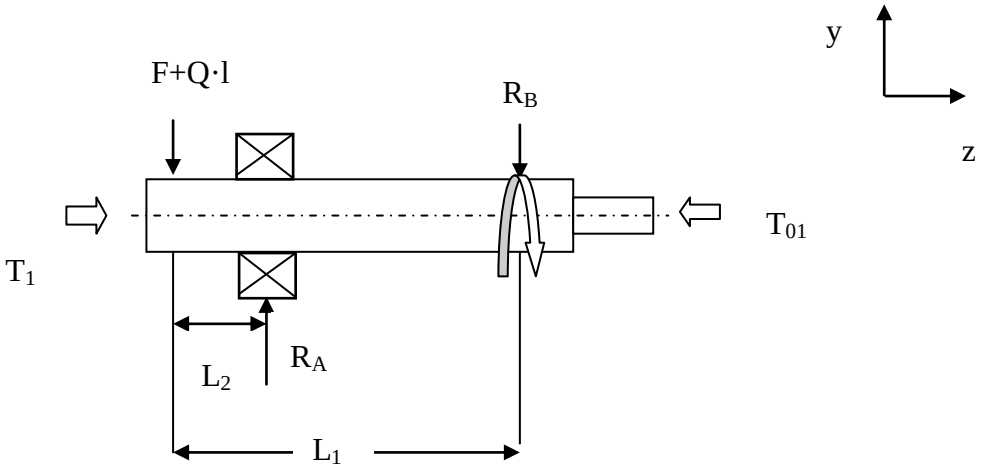

Figure C.9. Free body diagram sketch of the left driveshaft.

$\sum F_y = 0$:

$$R_A - R_B = F + Ql \quad \text{(C.21)}$$

$\sum M_z = 0$:

$$T_1 = T_{01} - R_B\, \mu\, r_{si} \quad \text{(C.22)}$$

$\sum M_x = 0$:

$$FL_2 = R_B(L_1 - L_2) \quad \text{(C.23)}$$

Hence, the reaction in the bearing (A) and the reaction in the housing (B) are:

$$R_A = (F + Ql)(1 + \frac{L_2}{L_1 - L_2}) \quad \text{(C.24)}$$

$$R_B = (F + Ql)\frac{L_2}{(L_1 - L_2)} \quad \text{(C.25)}$$

The friction torque between the shoulder of the differential and the driveshaft can be extracted integrating the pressure distribution around the shaft surface. This shaft surface can be considered to be in contact just on one half, since the bottom part will be lifted. This friction torque can be written as:

$$T = \int\int r(\mu p)dA = \mu p r \int_0^L \int_0^\pi r\, dl\, d\theta = \mu F r \quad \text{(C.26)}$$

That yields to the expression below:

$$T_1 = T_{01} - T_0 \frac{L_2}{(L_1 - L_2)} \mu r_{si} \quad \text{(C.27)}$$

where μ is the friction coefficient between the shaft and the housing and r_{si} is the outer diameter of the shaft (as it is described in the Chapter of Notations).

If the procedure is done equally but for the right shaft, then the results are seen in the Figure C.10 and Equations below:

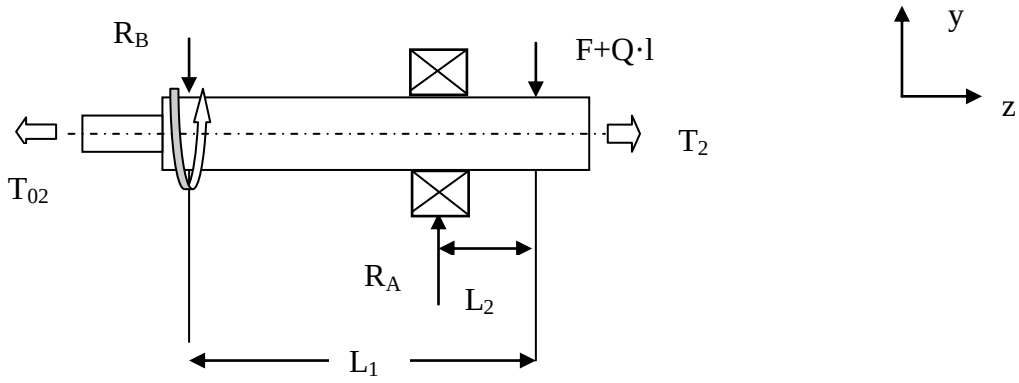

Figure C.10. Free body diagram sketch of the right driveshaft.

Working equally as it has been done with the left driveshaft:

$\sum F_y = 0$:

$$R_A - R_B = F + Ql \quad \text{(C.28)}$$

$\sum M_z = 0$:

$$T_2 = T_{02} + R_B \, \mu \, r_{si} \quad \text{(C.29)}$$

$\sum M_x = 0$:

$$FL_2 = R_B(L_1 - L_2) \quad \text{(C.30)}$$

Hence, the reaction in the bearing (A) and the reaction in the housing (B) are:

$$R_A = (F + Ql)(1 + \frac{L_2}{(L_1 - L_2)}) \quad \text{(C.31)}$$

$$R_B = (F + Ql)\frac{L_2}{(L_1 - L_2)} \quad \text{(C.32)}$$

According to the same expression got for the left drive shaft, the torque becomes:

$$T_2 = T_{02} + T_0 \frac{L_2}{(L_1 - L_2)} \mu r_{si} \quad \text{(C.33)}$$

Then, the difference between shaft becomes:

$$T_2 - T_1 = T_{02} + T_0 \frac{L_2}{(L_1 - L_2)} \mu r_{si} \; - (T_{01} - T_0 \frac{L_2}{(L_1 - L_2)} \mu r_{si}) \quad \text{(C.34)}$$

$$T_2 - T_1 = T_{02} - T_{01} + 2T_0 \frac{L_2}{(L_1 - L_2)} \mu r_{si} \quad \text{(C.35)}$$

Hence, the difference between right and left has been increased by $2T_0 \frac{L_2}{(L_1 - L_2)} \mu r_{si}$

According to this new difference got, it can be plot again the model to check how much it differs from the previous model.

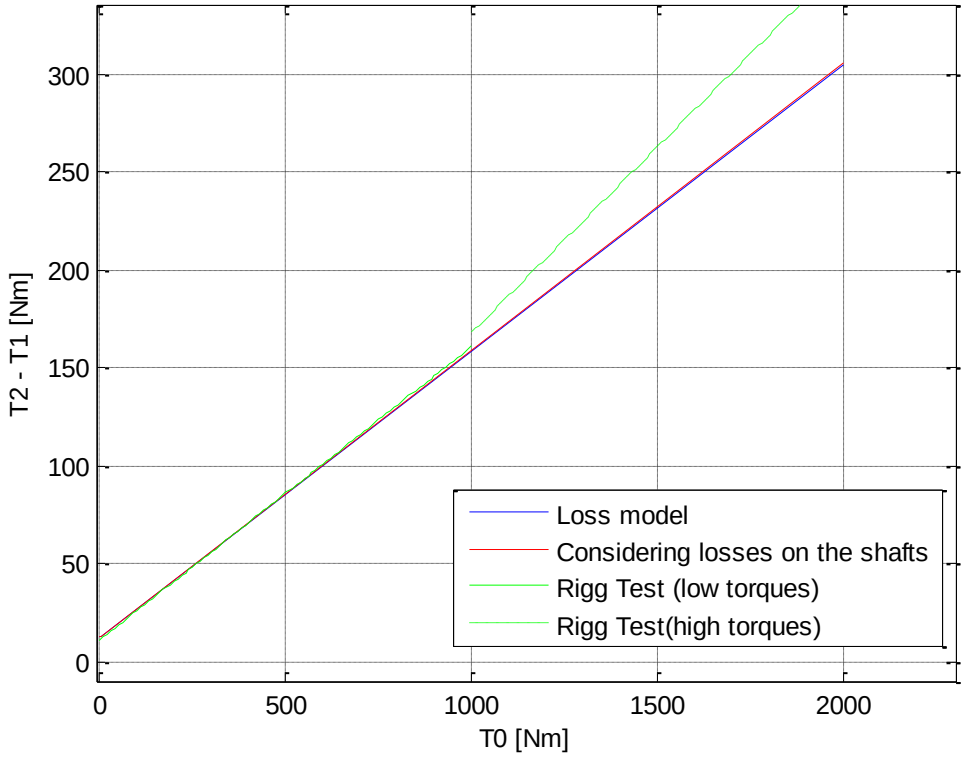

Figure C.11. Difference between rig measurements and the real aimed values.

Once that is done, it can be claimed that these losses are meaningless compared to the other losses so that they can be neglected. Since the bearing support is much closer from the arm than from the differential, it takes the major force, and the vertical reaction which appears on the shaft is really small which releases a low friction torque. For instance, the difference when the input torque applied is 2000 Nm, changes from 305Nm of torque difference to 306 Nm considering torque losses which is equivalent to a 0,05% of the total amount of input torque.

Then, there is no need to extract these losses from the rig. However, this extraction would be done in the vice versa, this extra friction will be added to the simulation model in order to check the results from the rig. By this way, the friction coefficient will be able to be got and the model to be checked for each test. Otherwise the results from the rig are too much manipulated if these losses are extracted from them.

Considering this range, and neglecting these losses, the model must still have a friction coefficient of 0.18 in order to fit the rig results.

Furthermore, the effective friction radius and contact mesh have been considered exactly in the centre of the contact width. The effective gear mesh loss has been set to 99% as VCC claimed according to their design of the differential (*see* [32]).

Hence, the blue curve will allow adjusting the model, and then, it also gets the idea of the behaviour of the differential in the vehicle once the friction between the shaft and the housing has been neglected.

Drawings and rig overview

The rigg had to be designed according to the needs and the goals set. In this Appendix C, there is the explanation of how the rig was set according to not only the limitations such as the workshop that was avaiable (and its limitations) and the possible limitations of the company were all the parts were outsourced to be machined. But also, the factor time which was really important since the goal was mimizing the time consuming as much as possible in order to get a rig reliable and simple.

Thus, in this last part, there is just the summary of all the drawings needed to machine the parts. This drawings were done after designing the assembling concept and the manufacturability of each part. So, below there are the drafts of all the drawings (not in real scale, just fit to the page) in order to have a clearer overview of how the rig assembly is.

On top pf that, there is an overview of the rig assembly both from CAD and real photos after having assembled the rig.

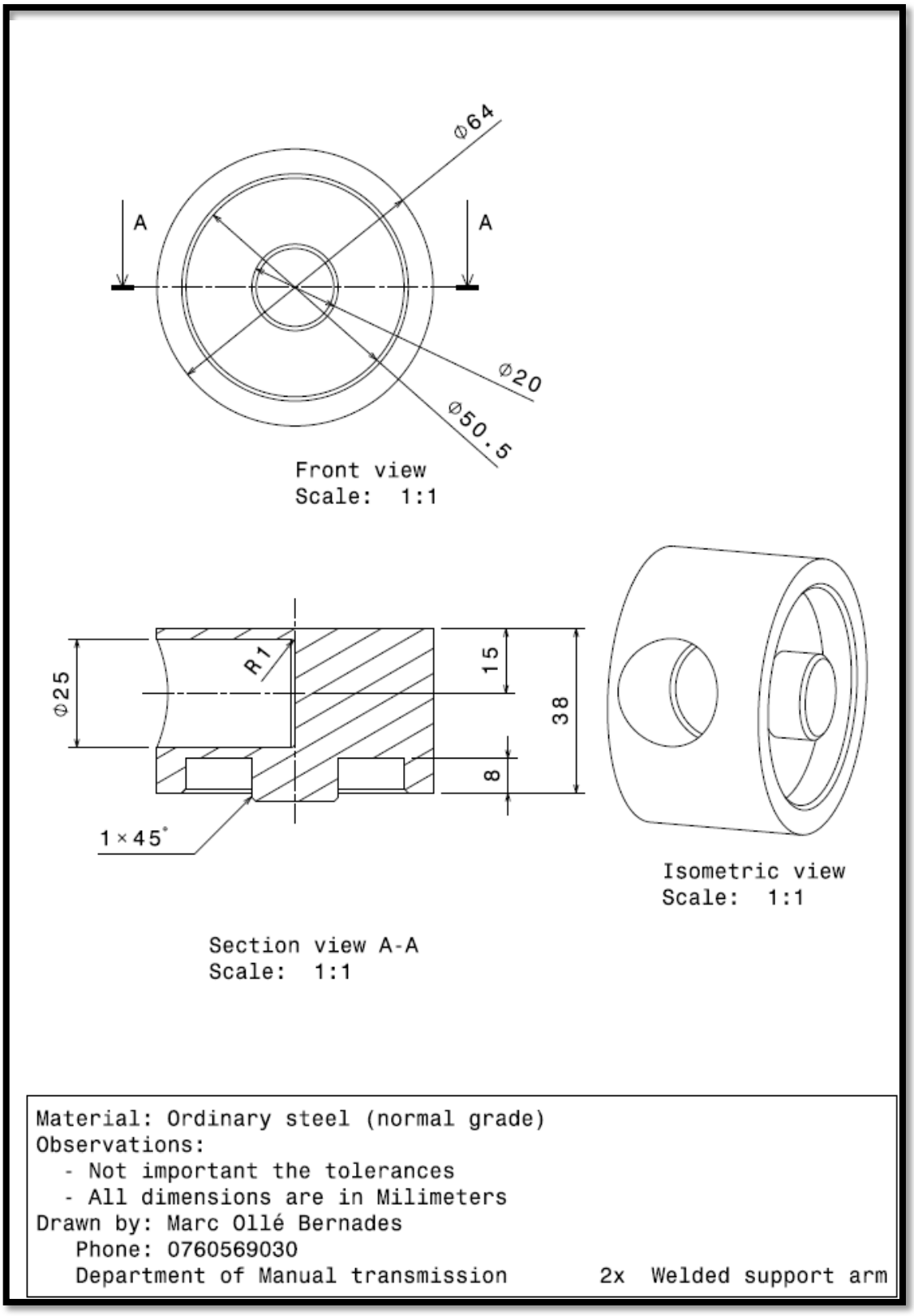

Figure C.12. Drawing of the welded support

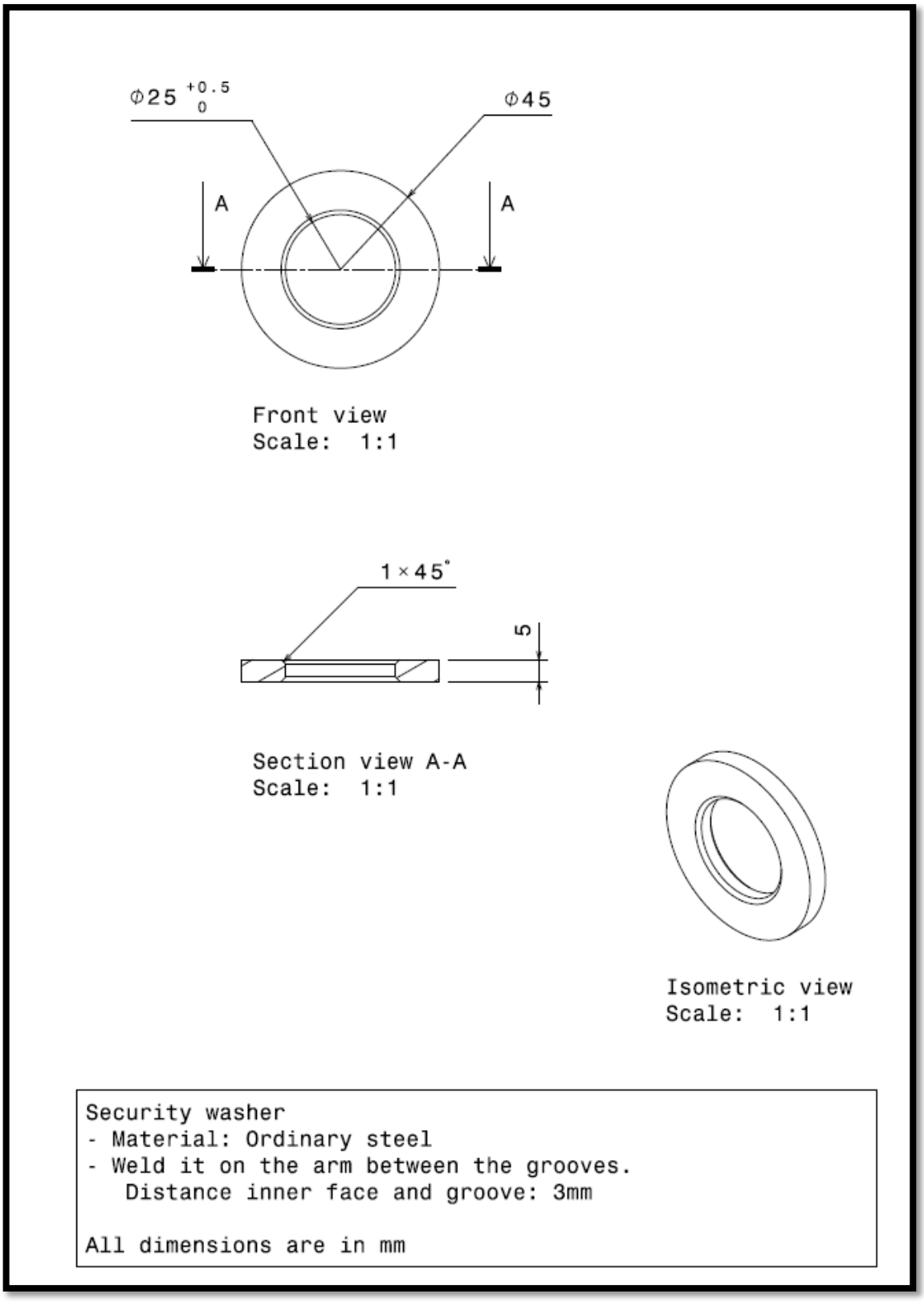

Figure C.13. Drawing of the security washer.

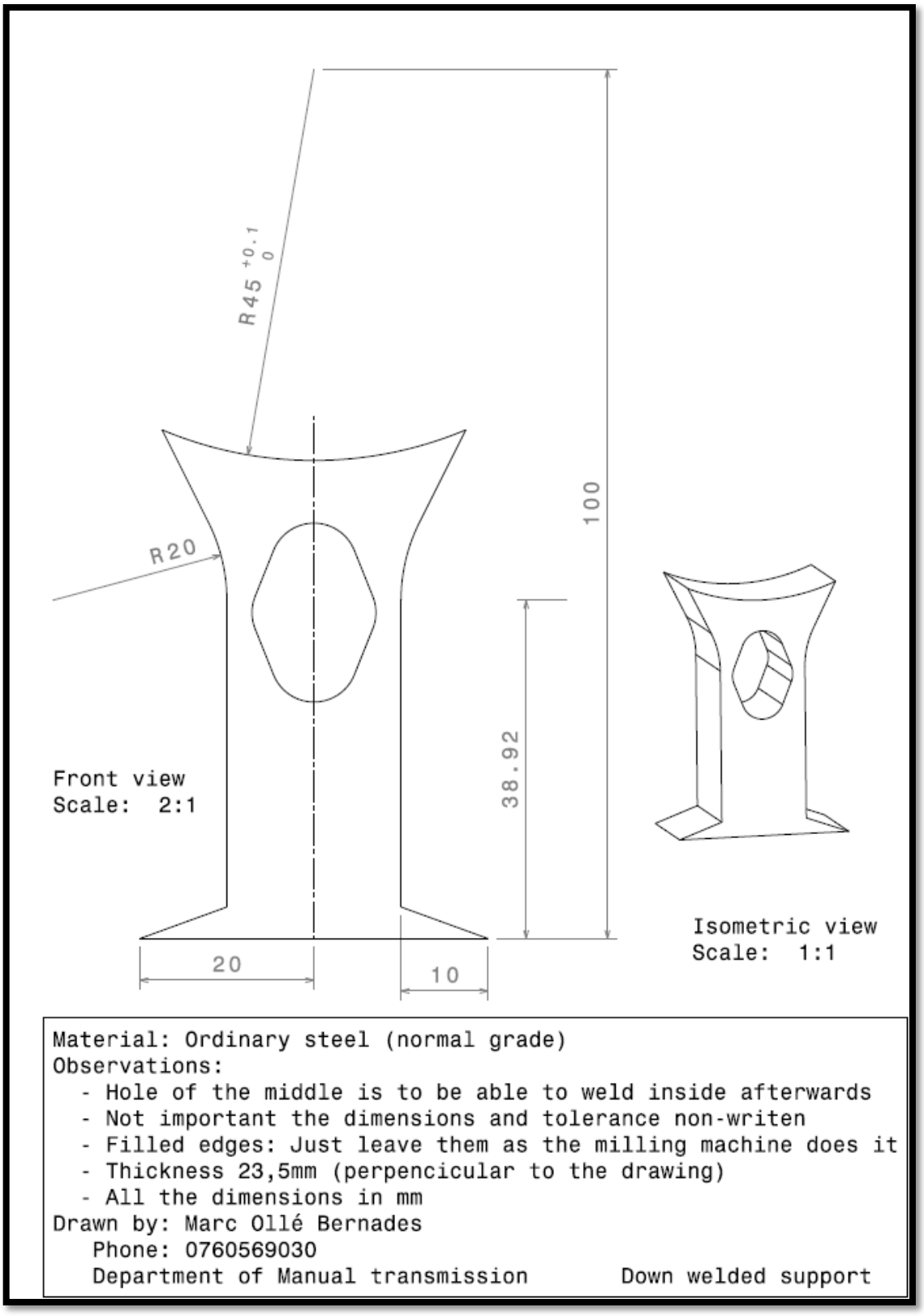

Figure C.14. Drawing of the welded low differential support.

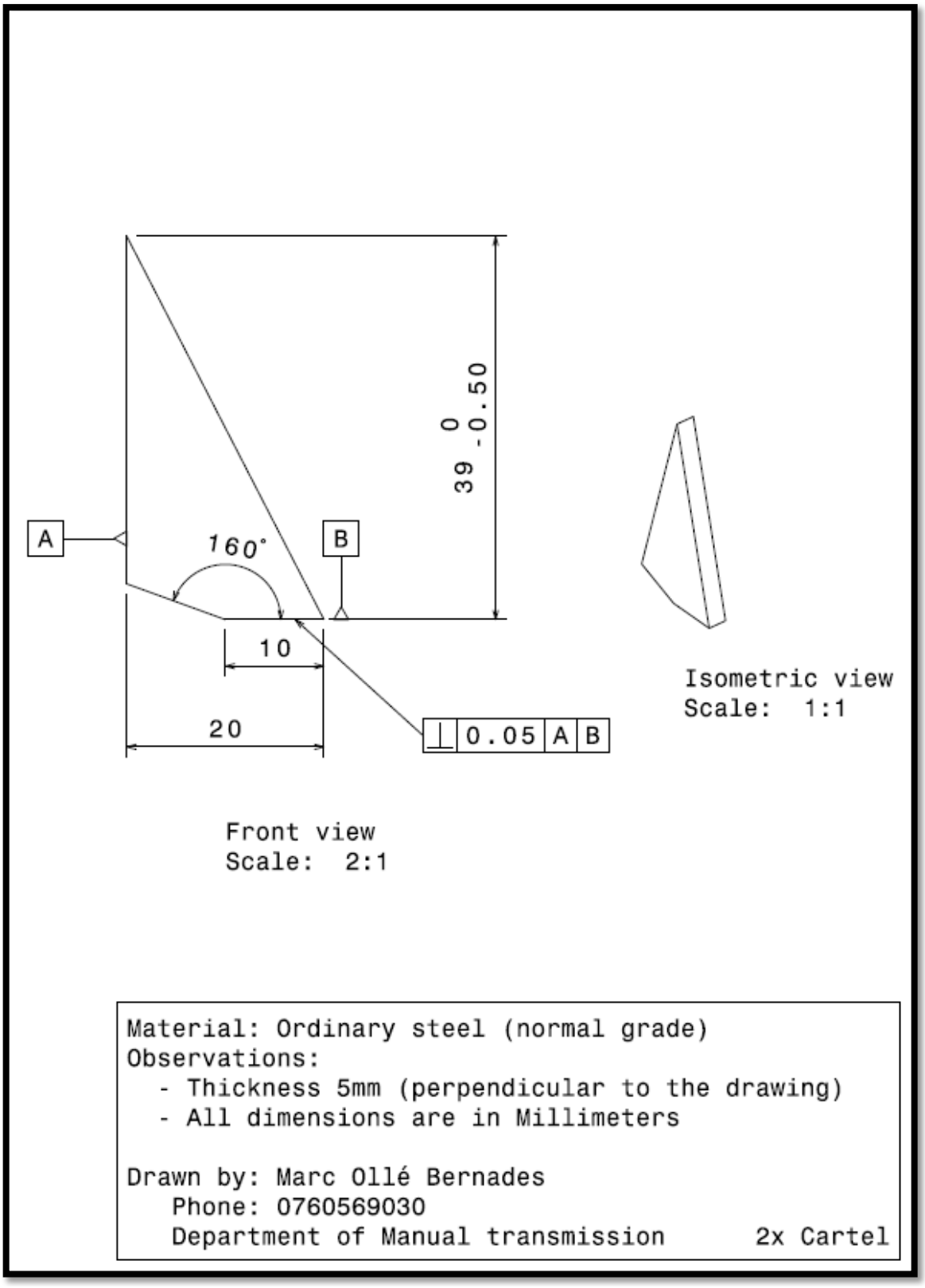

Figure C.15. Drawing of the stiff support.

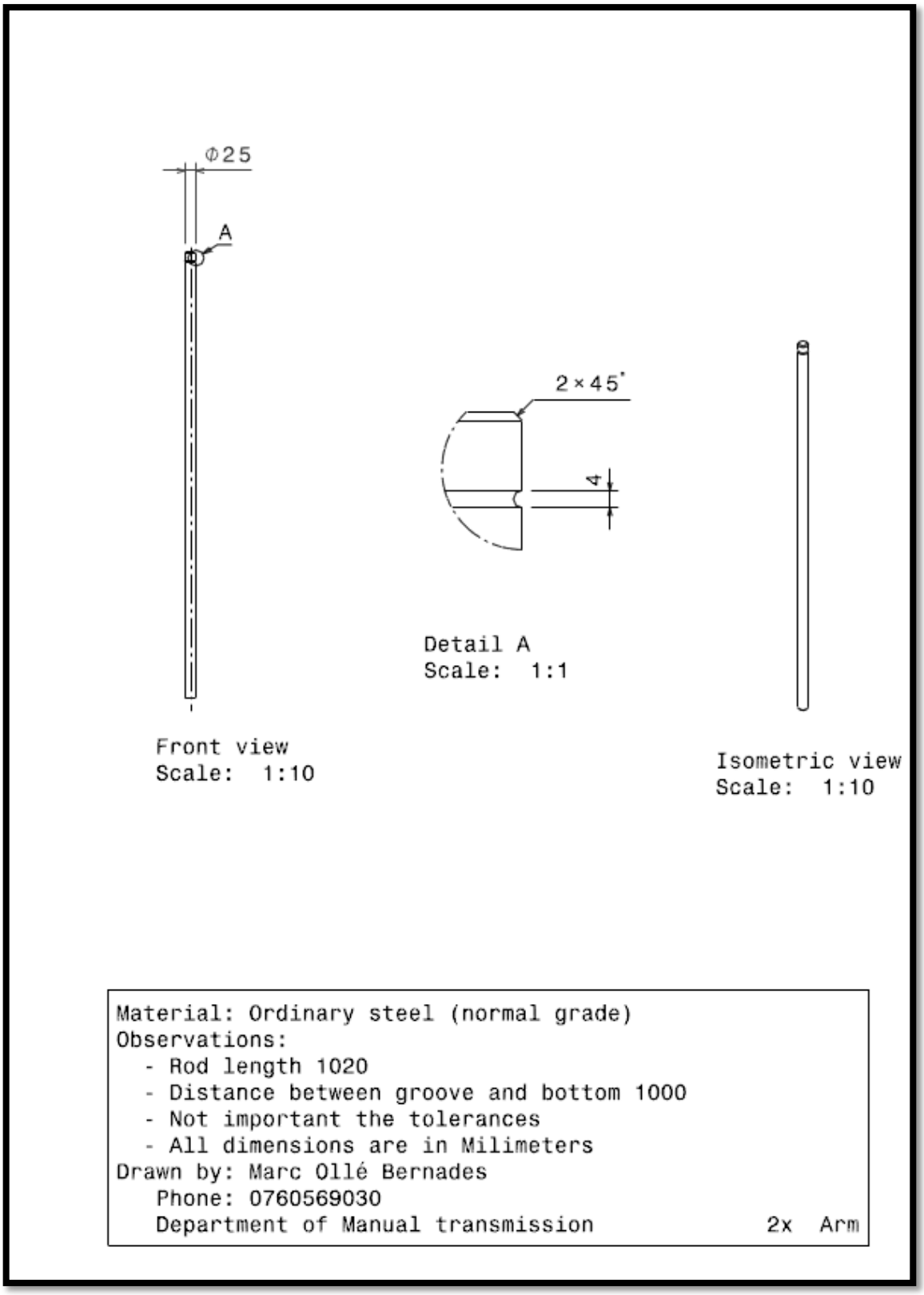

Figure C.16. Drawing of the loaded rod.

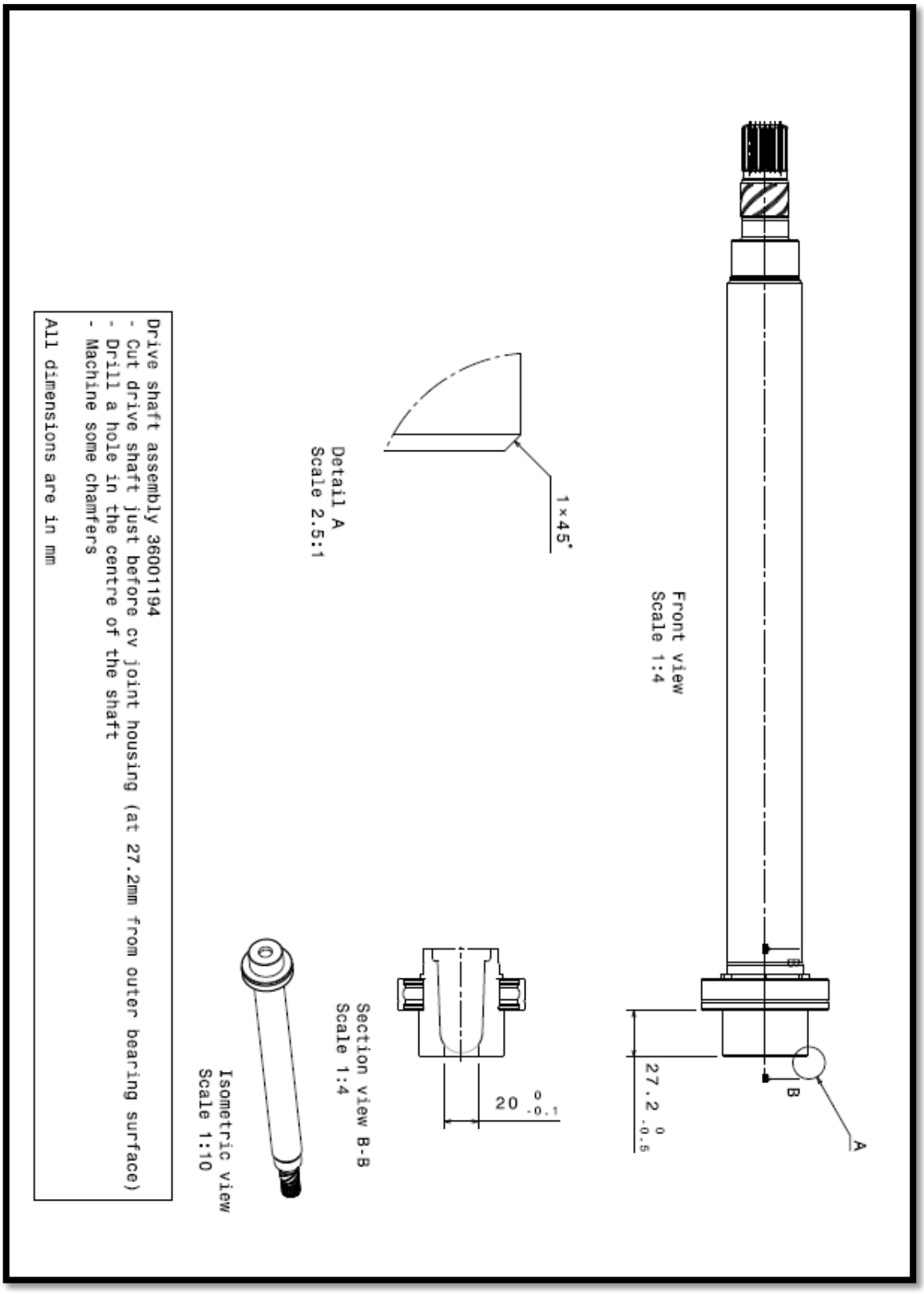

Figure C.17. Drawing of the drive shaft.

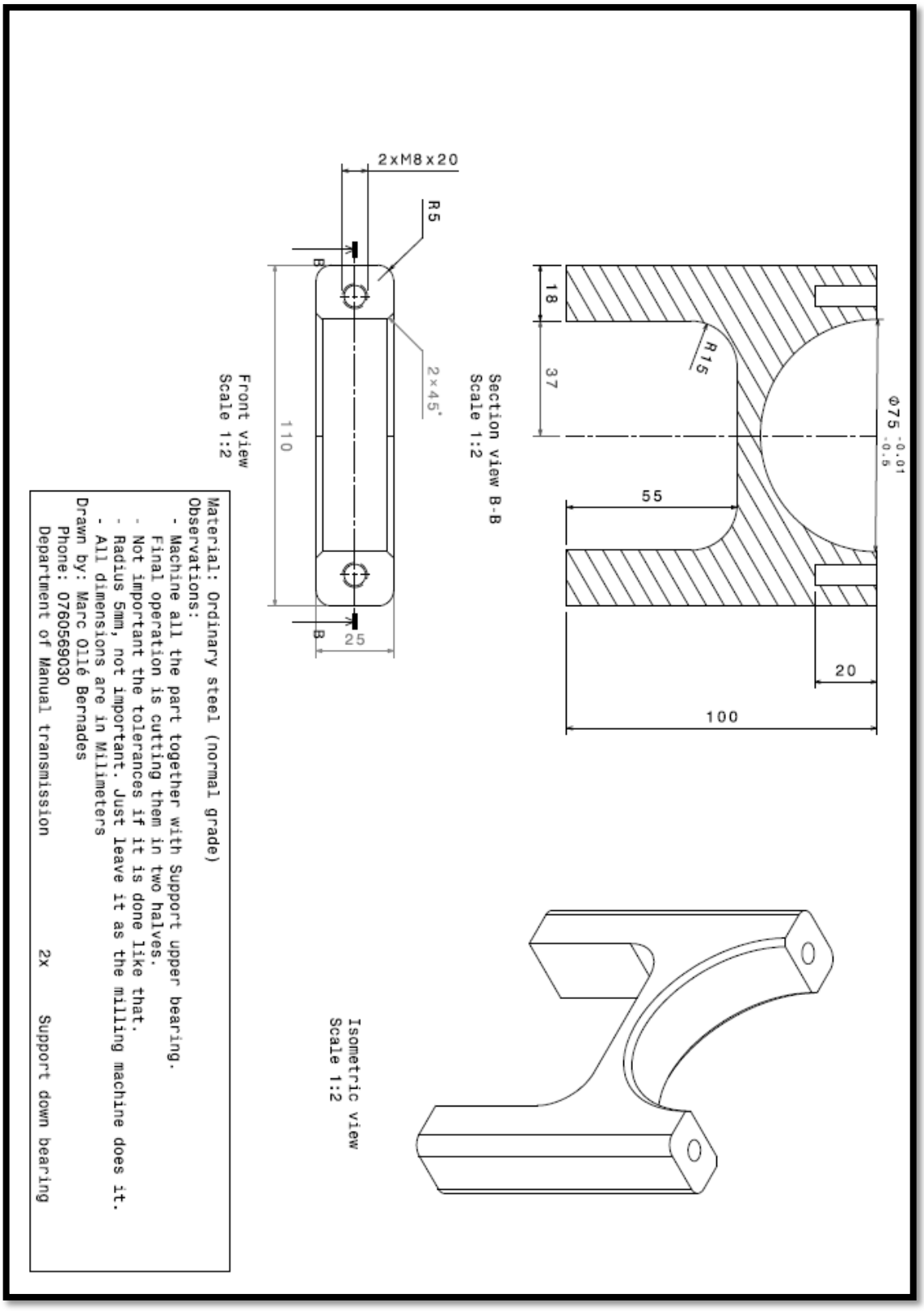

Figure C.18. Drawing of the low bearing support.

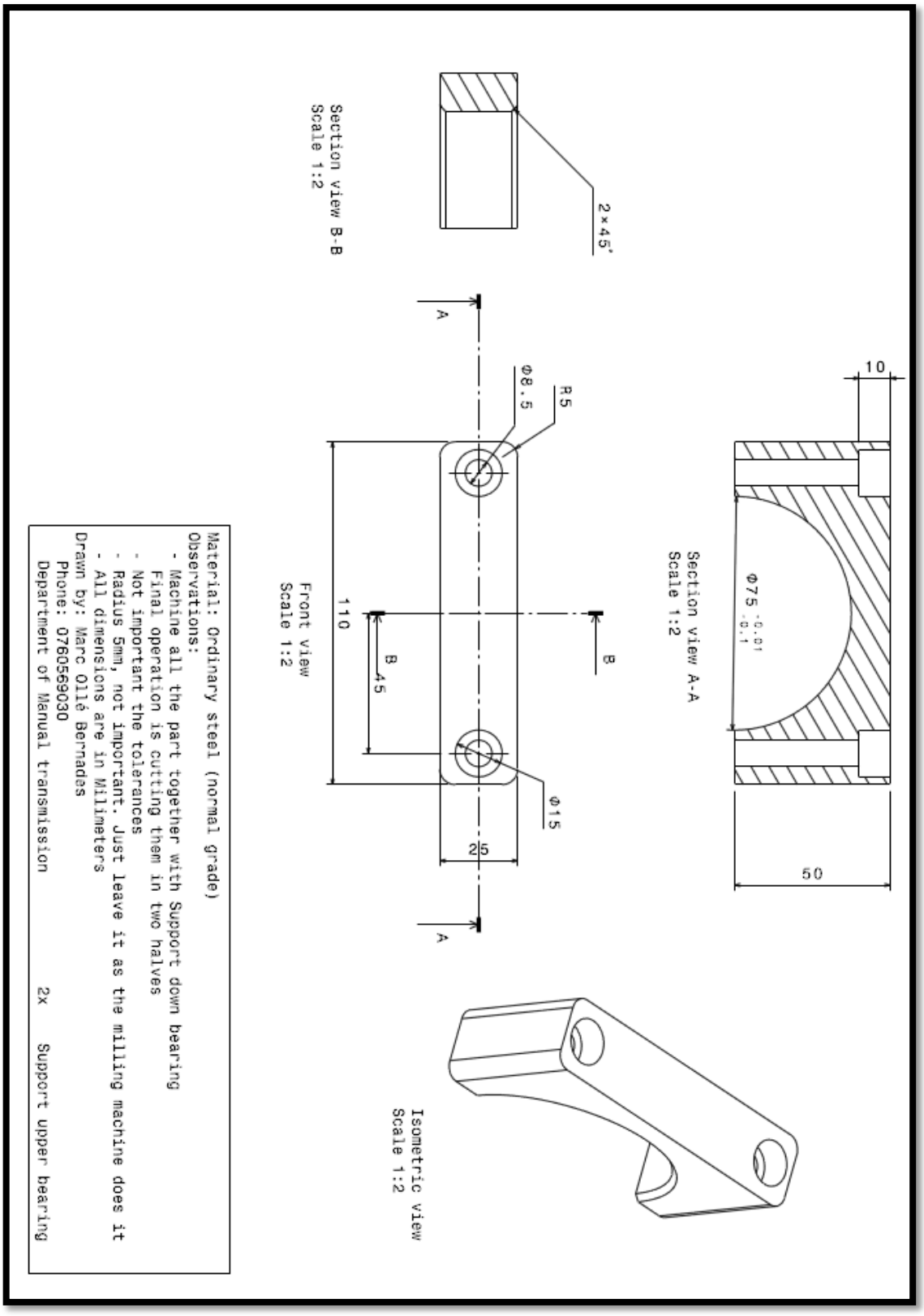

Figure C.19. Drawing of the upper bearing support.

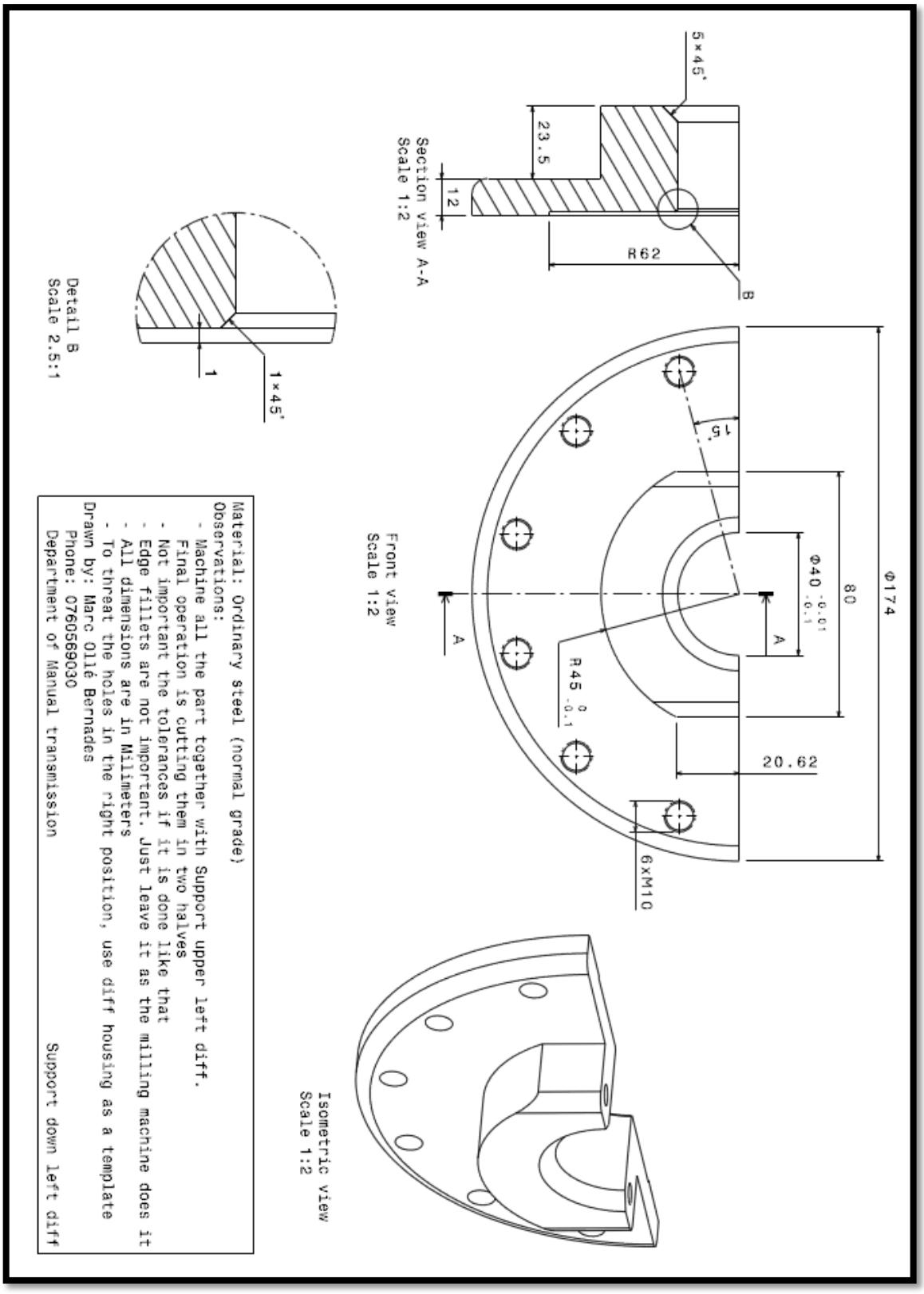

Figure C.20. Drawing of the low left differential support.

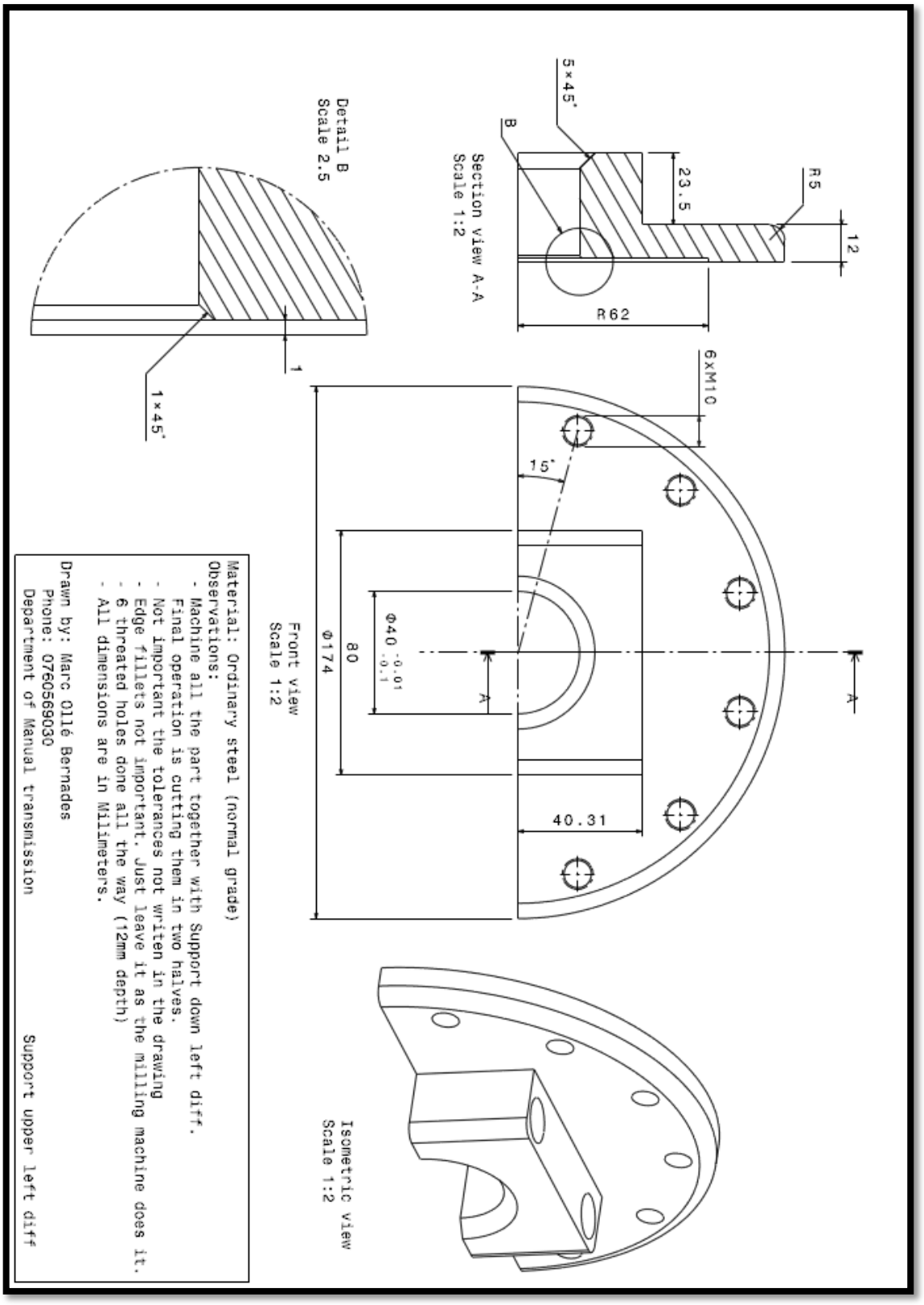

Figure C.21. Drawing of the upper left differential support.

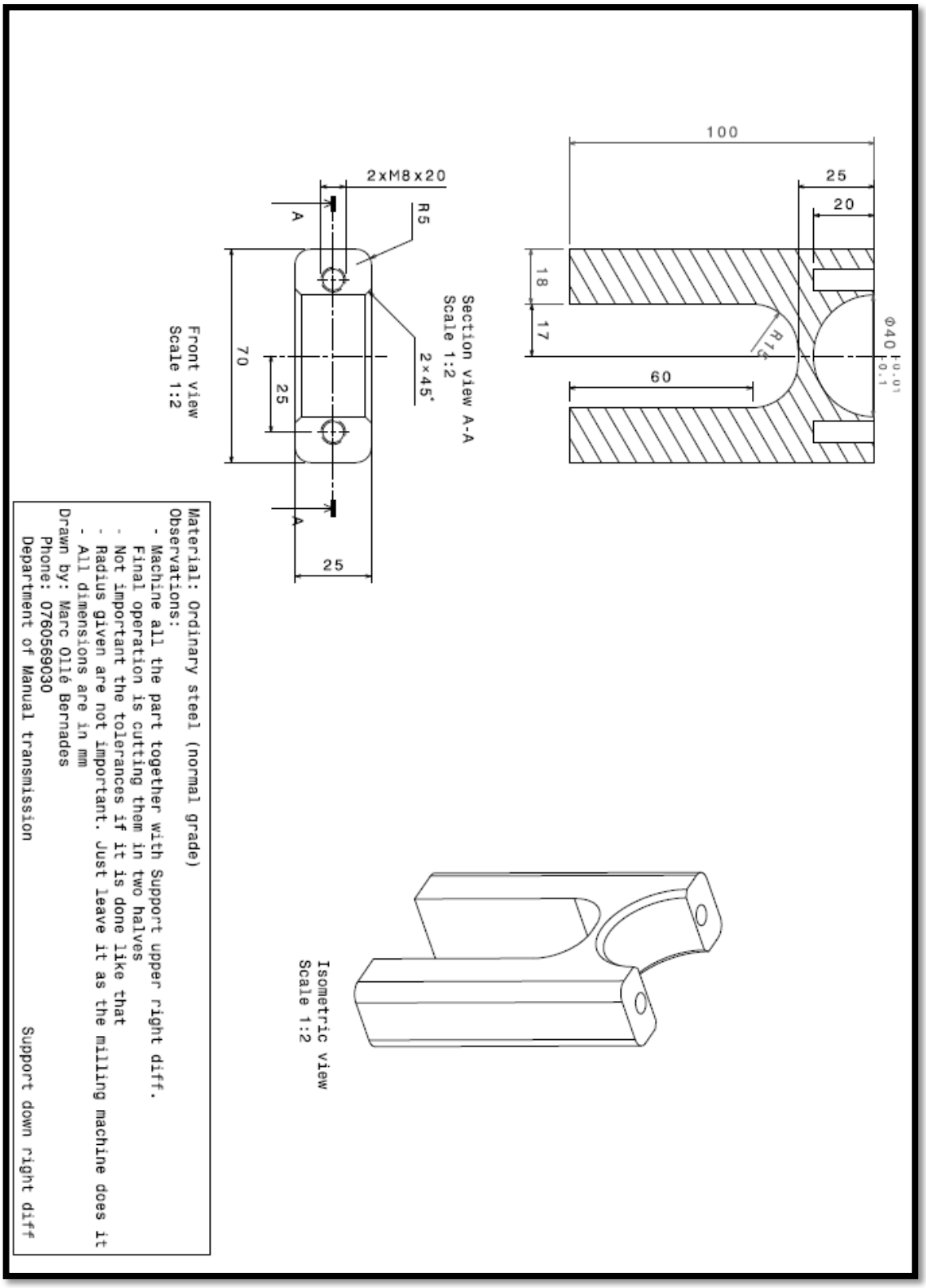

Figure C.22. Drawing of the low right differential support.

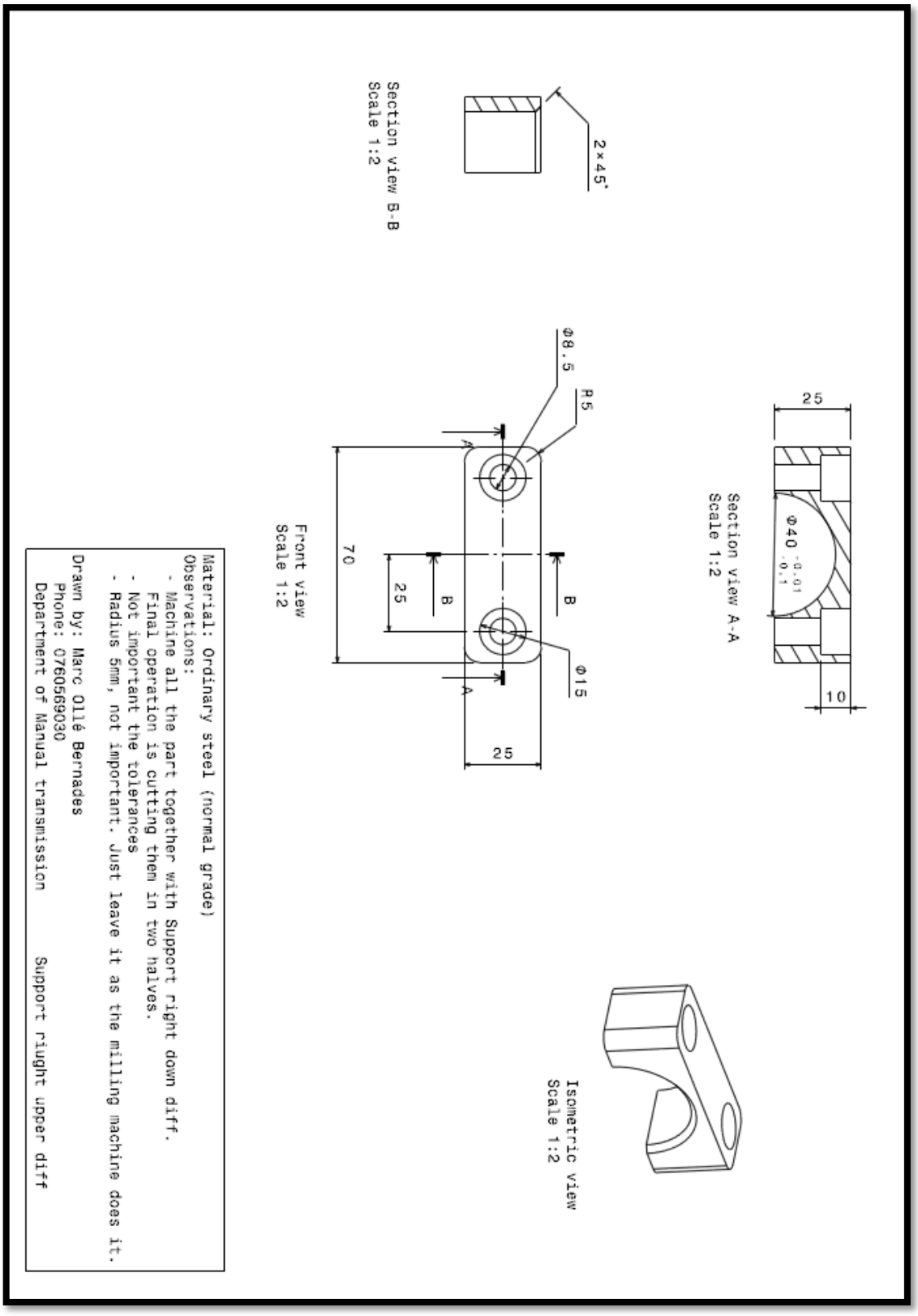

Figure C.23. Drawing of the upper right differential support.

Below, an overview of the rig CAD design can be checked out, both from the front and from the back of the working model.

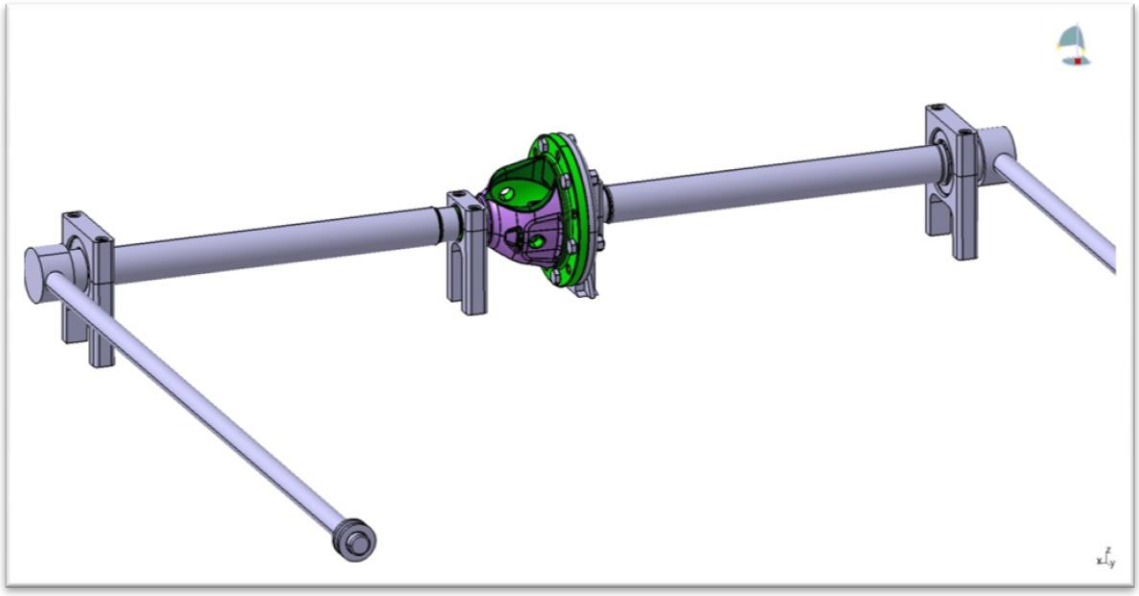

Figure C.24. Front overview rigg CAD design.

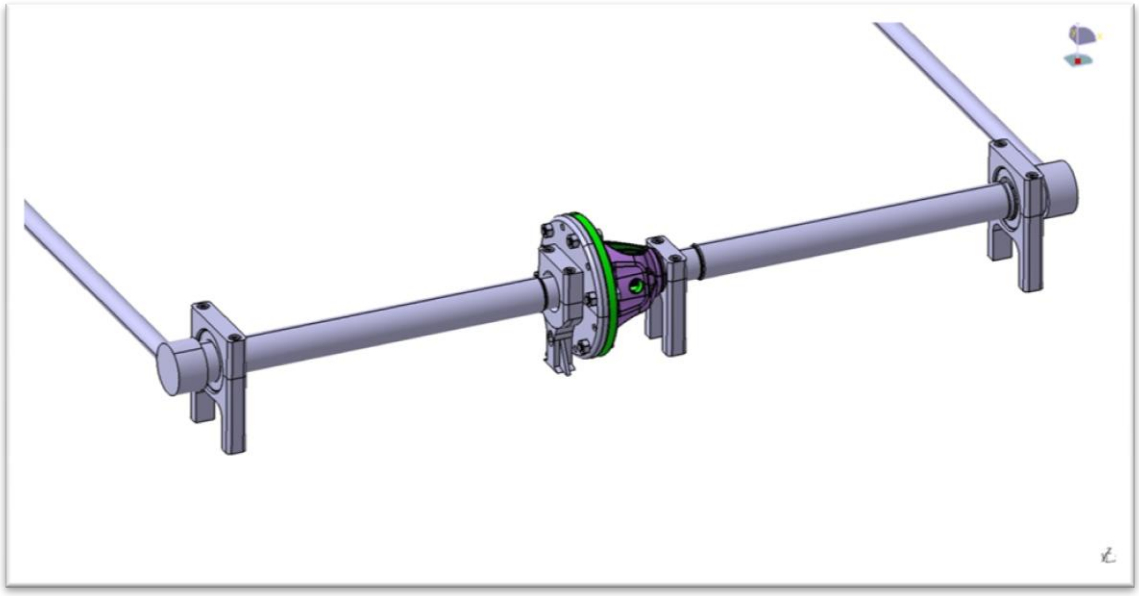

Figure C.25. Rear overview rigg CAD design.

Finally, as it has been said, some pictures taken from the workshop are shown in order to show the final rig design and how it worked.
In the Figure C.26 it is seen the overview of the whole rig. The differential was loaded adding callibrated weights on both sides, once the differential was equal loaded, the left side was extra loaded until the friction was broken away. This extra load was the difference torque between both drive shafts (the losses over the differential). In order to know accurately when the differential started differentiating the speeds, a clock device was set on the right drive shaft. The device setup is seen in the Figure C.27. In addition, the Figure C.28 and C.29 show the differential assembly and left part of the rig respectevely.

Figure C.26. Rig overview 1.

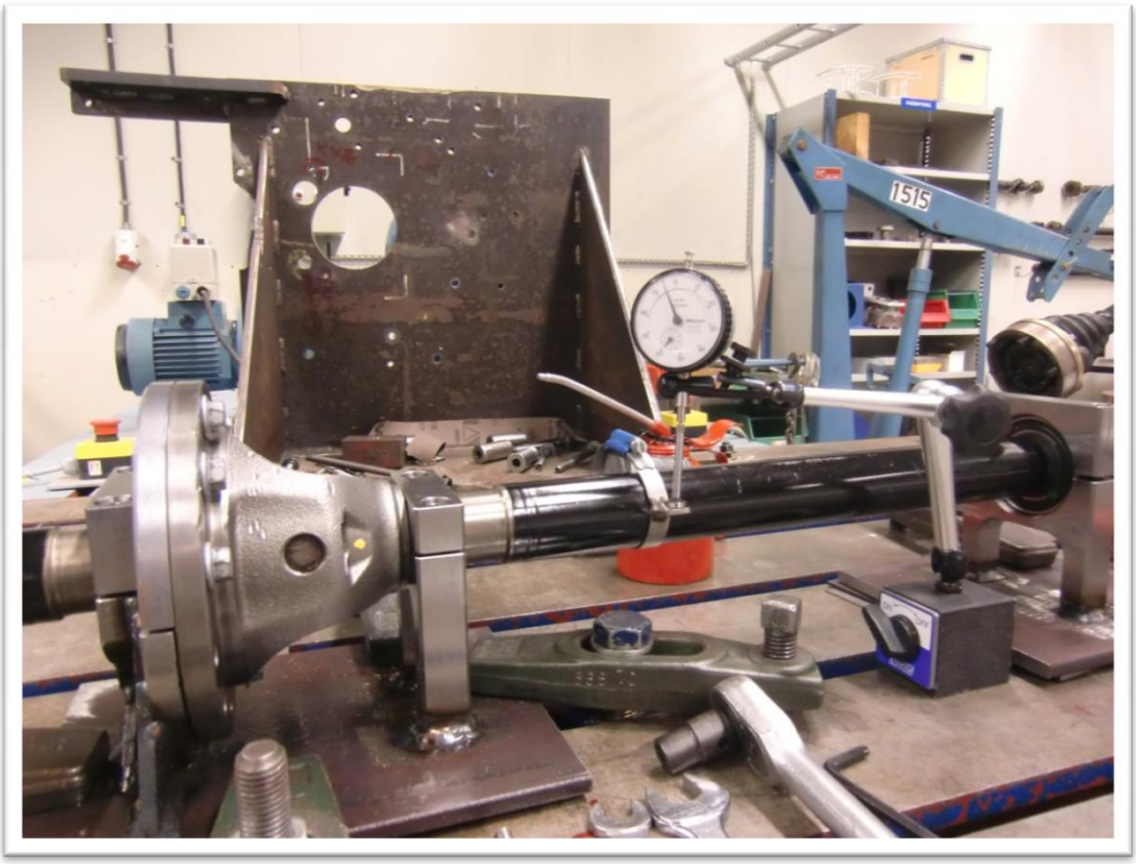

Figure C.27. Rig overview (right side where the measurement device is installed).

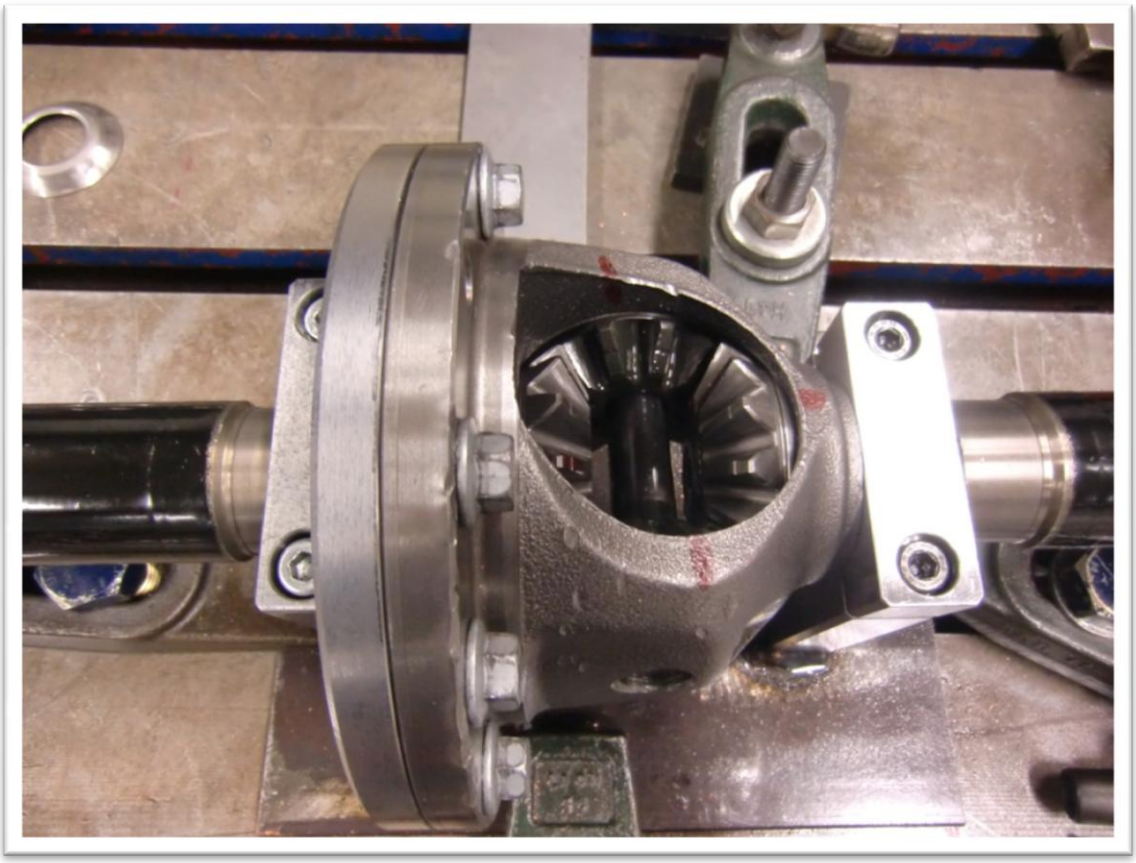

Figure C.28. Rig overviw (differential assembly).

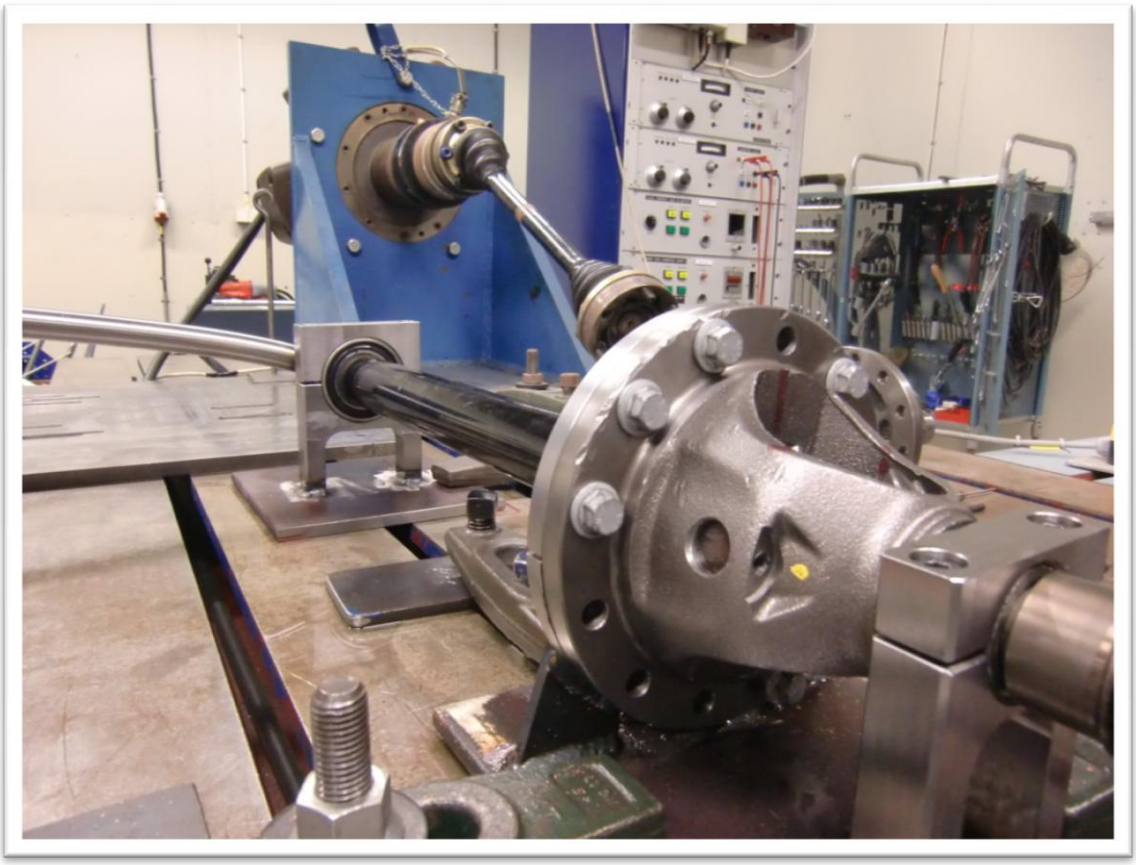

Figure C.29. Rig overview (left side).

Appendix D. FEM Analysis: Complementary plots

As it has been explained in the Chapter 5, in this part of the appendix there are the complementary results of the FEM analysis for the other loads 1000Nm and 2000Nm

Both the translational displacement and the pressure distribution look similar to the case of 500Nm, as the behaviour is linearly dependent on the input torque, in the Chapter 5 it has been just shown the plots got for one load in order to make it shorter and clearer.

Thus, when the input load is 1000 Nm, the results got are:

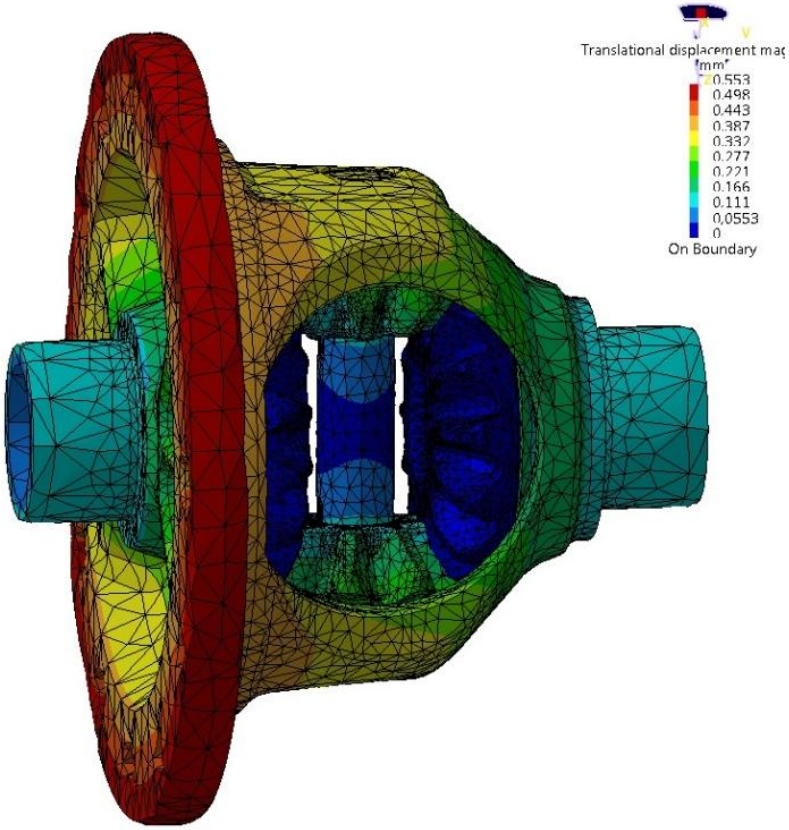

Figure D.1. Total translation deformation of the whole assembly.

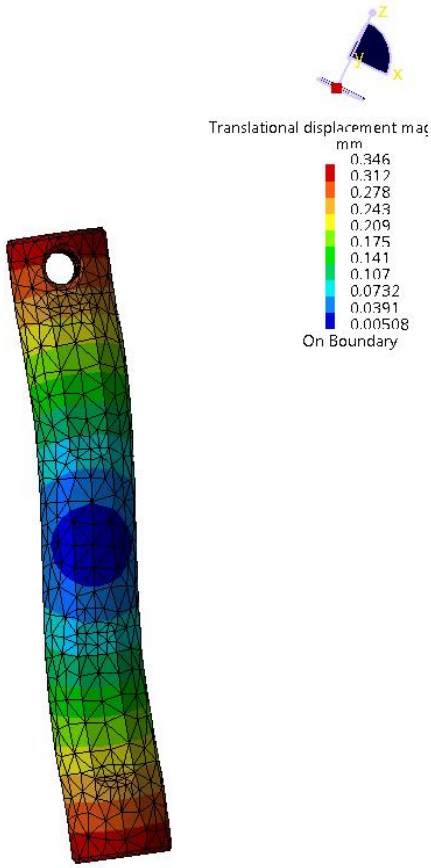

Figure D.2. Total translational deformation of the pinion pin.

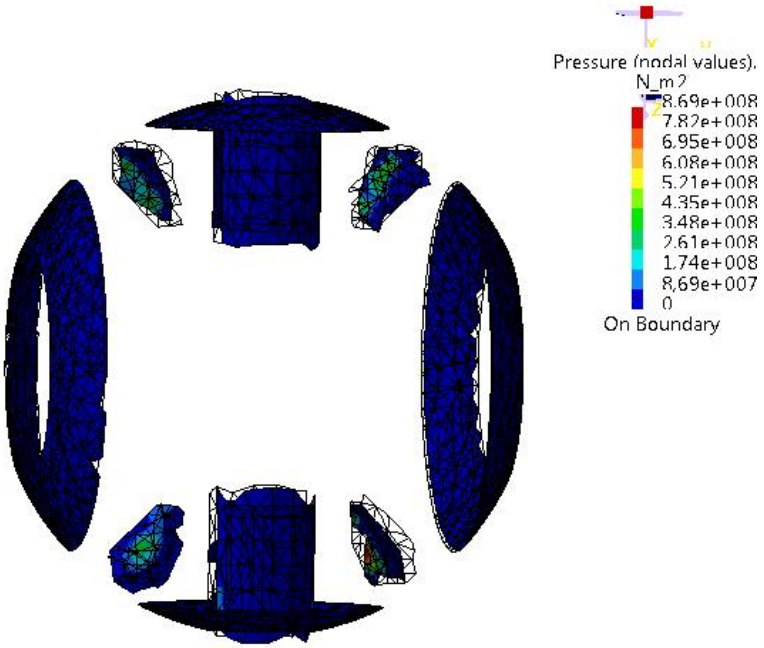

Figure D.3. Contact pressure distribution.

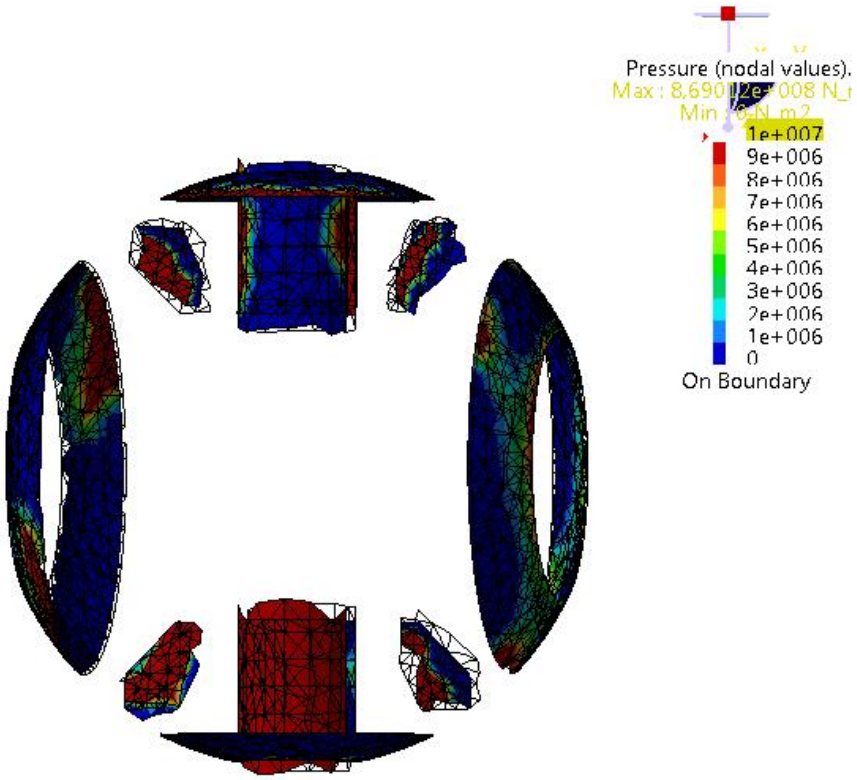

Figure D.4. Contact pressure distribution (scale restricted view 1).

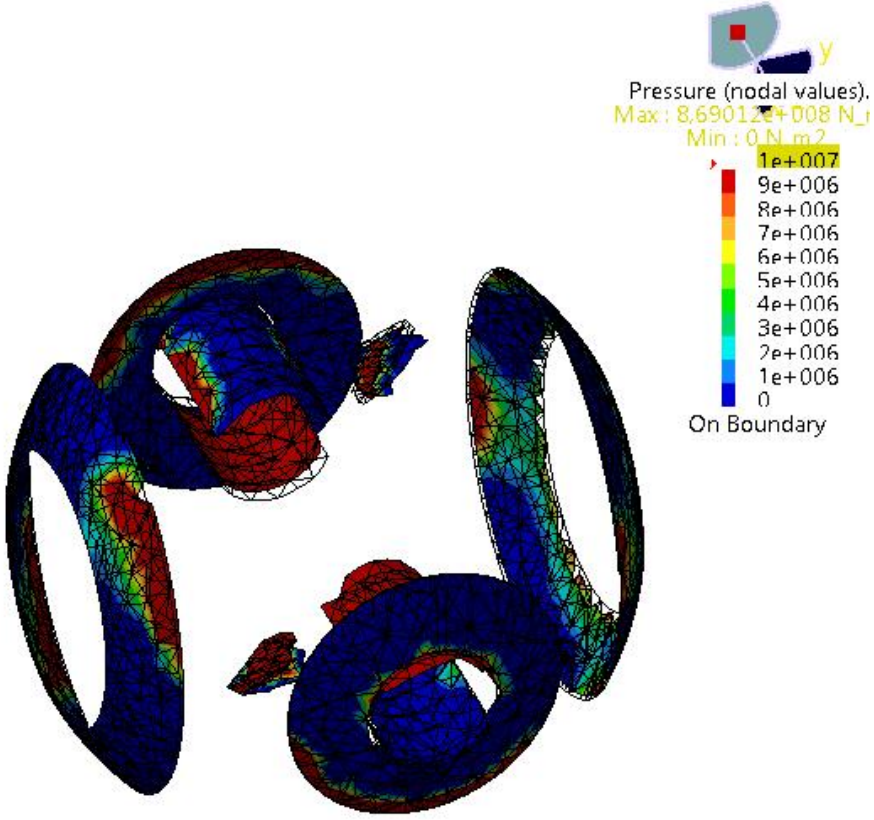

Figure D.5. Contact pressure distribution (scale restricted view 2).

Finally, for the input load of 2000 Nm, it yields to:

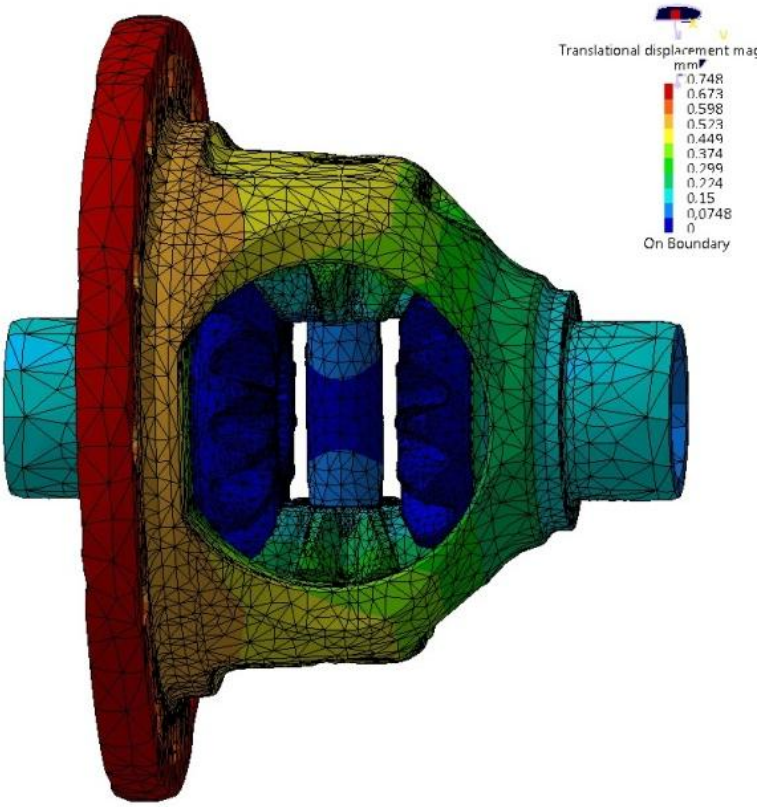

Figure D.6. Total translation deformation of the whole assembly.

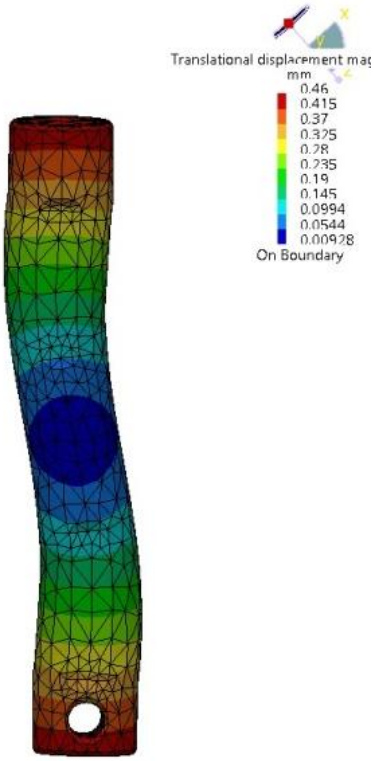

Figure D.7. Total translational deformation of the pinion pin.

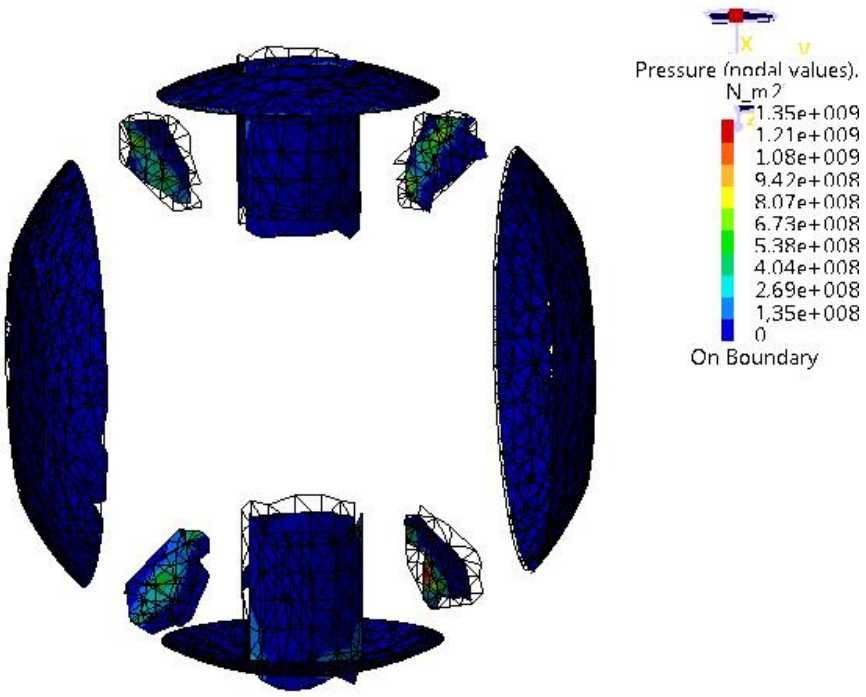

Figure D.8. Contact pressure distribution.

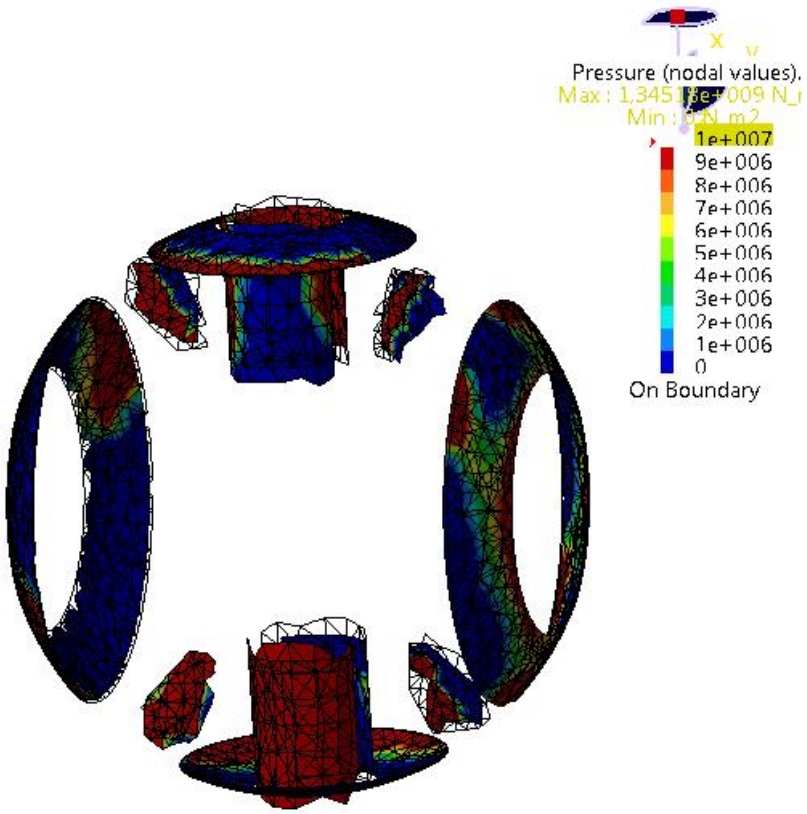

Figure D.9. Contact pressure distribution (scale restricted view 1).

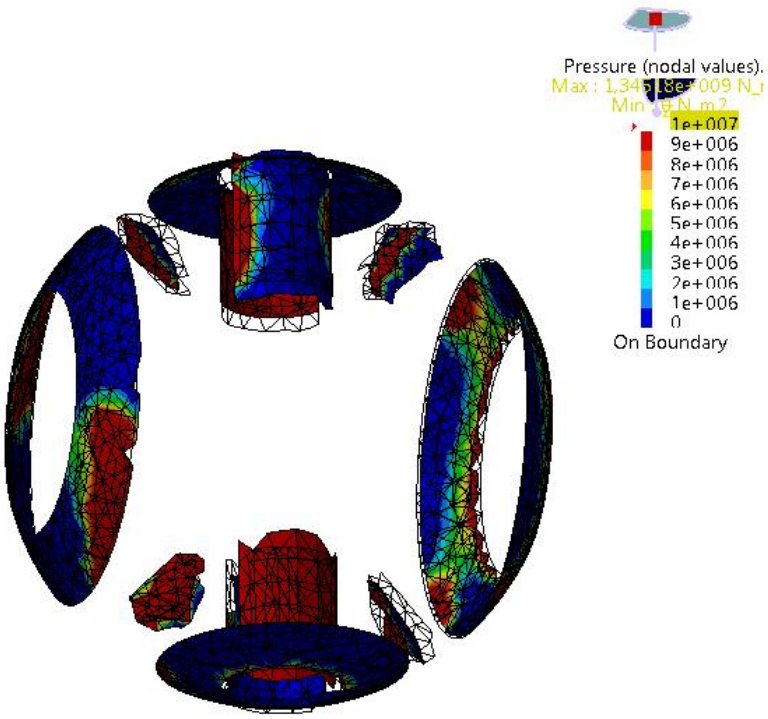

Figure D.10. Contact pressure distribution (scale restricted view 2).

Finally, in the Chapter 5, it has carried out the stiffness analysis for the input load of 500Nm. Below there are some complementary plots of other views of the gear set and housing first component of the strain tensor.

The first Figure D.11 shows the other two gears of the gear set, the maximum strain is reduced here since the gear mesh is asymmetric.

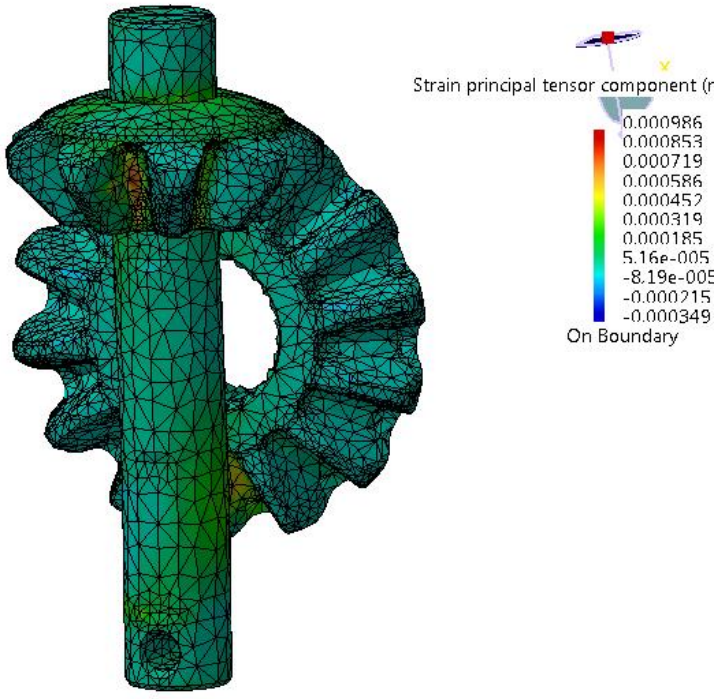

Figure D.11. Principal strain component of the gear set (view 3).

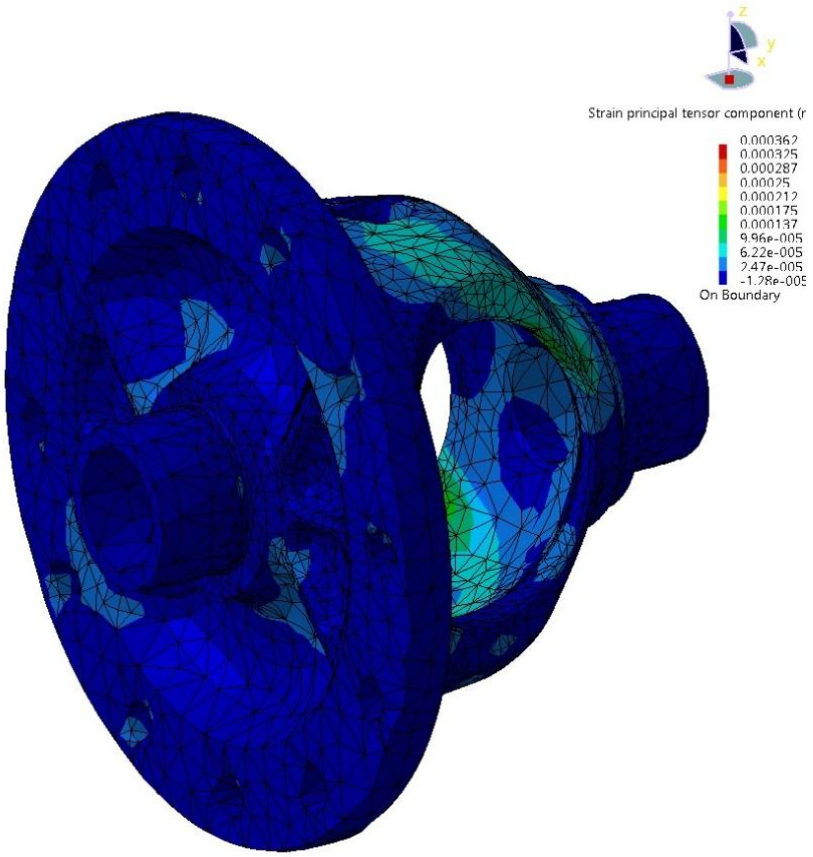

Figure D.12. Principal strain component of the housing (view 2).

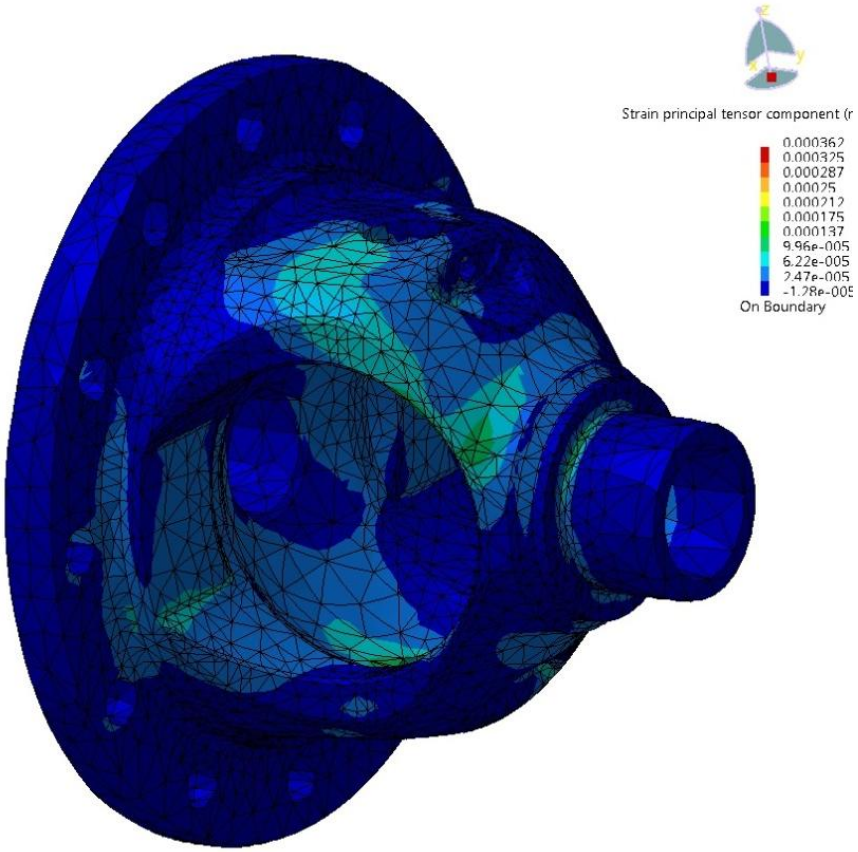

Figure D.13. Principal strain component of the housing (view 3).

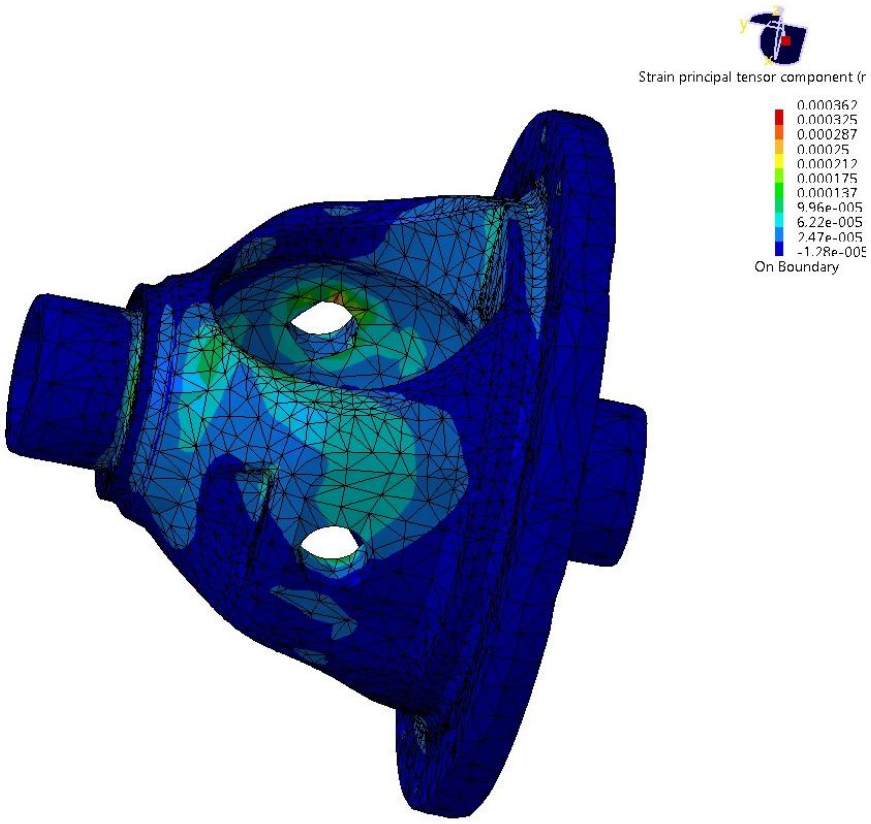

Figure D.14. Principal strain component of the housing (view 4).

Appendix E. Logged Data results

Below, all the other plots got for the driving case scenarios described in the Chapter 7. The results are taken from different vehicle test in order to be able to pick those values that were being looked for, i.e some scenarios driving straight ahead (as it is seen the driving scenarios were just found at high speed, see the rotational speed in the wheels in the first plot of the diagram) with three different torque levels and then another driving scenario to corroborate the vehicle cornering once it has overcome the static losses and there is a relative speed between wheels, which was taken as well in three different torque levels.

The following diagrams not only show the results of the torque that have been used in the Chapter 7, but they also show the wheel speed (first plot), the steering wheel angle (third plot) and the throttle position (forth plot). As it was not got some logged data which showed the friction coefficient, vehicle speed, lateral acceleration, at least with the steering wheel angle and the speed it was shown that the straight ahead driving scenarios were down at high speed and the cornering scenarios were done at low speed with relative high wheel speed difference.

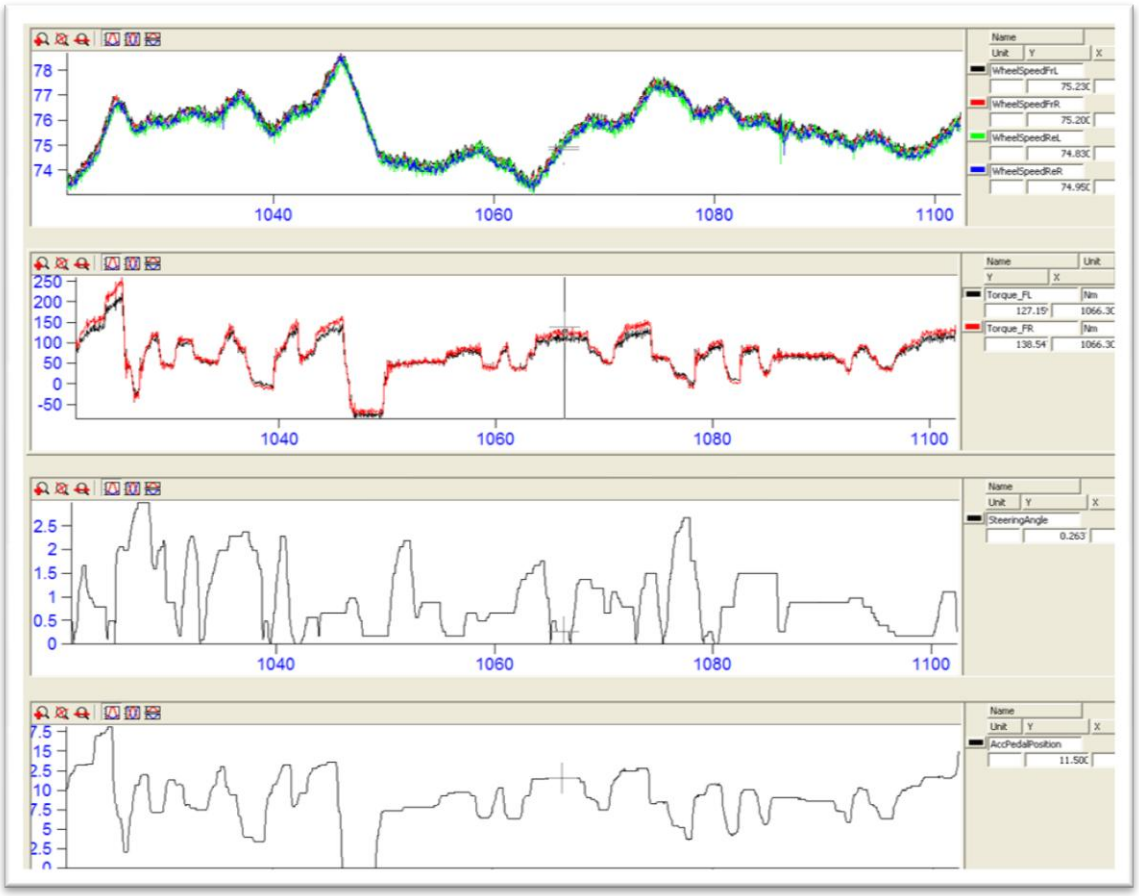

Figure E.1. Vehicle logged data driving scenario 1.

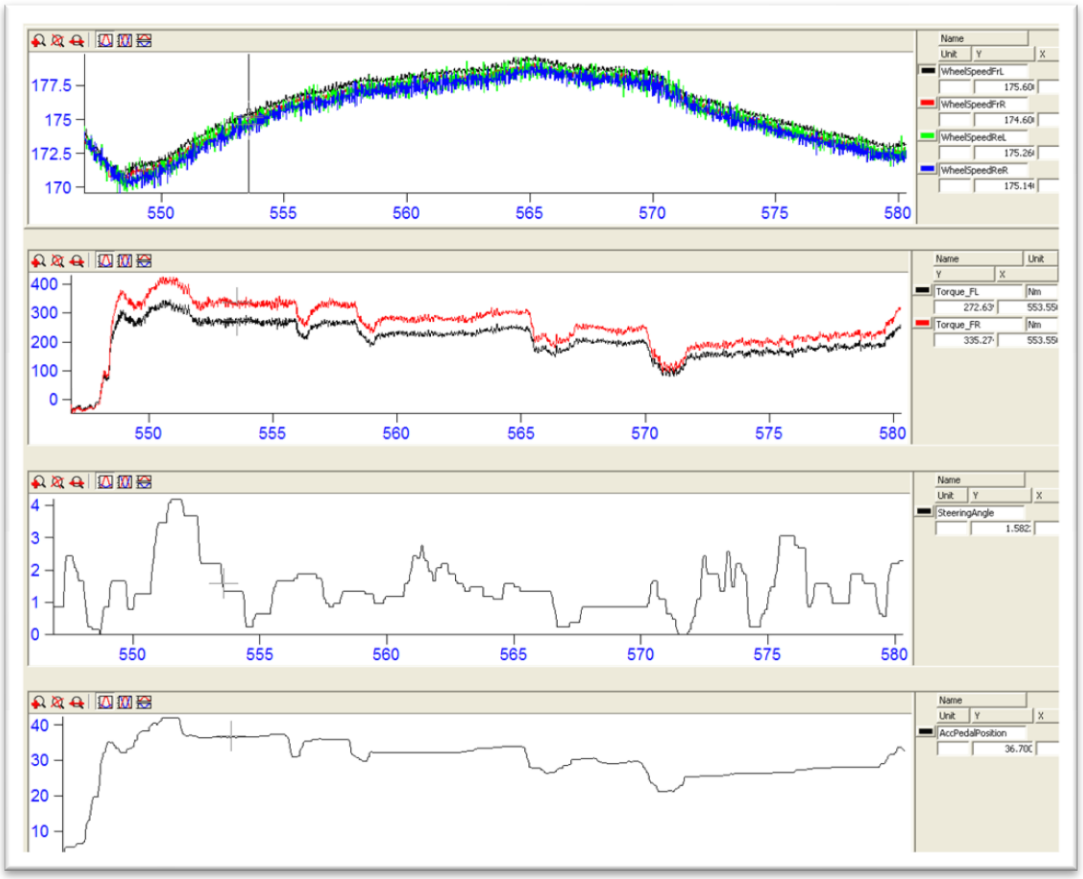

Figure E.2. Vehicle logged data driving scenario 2.

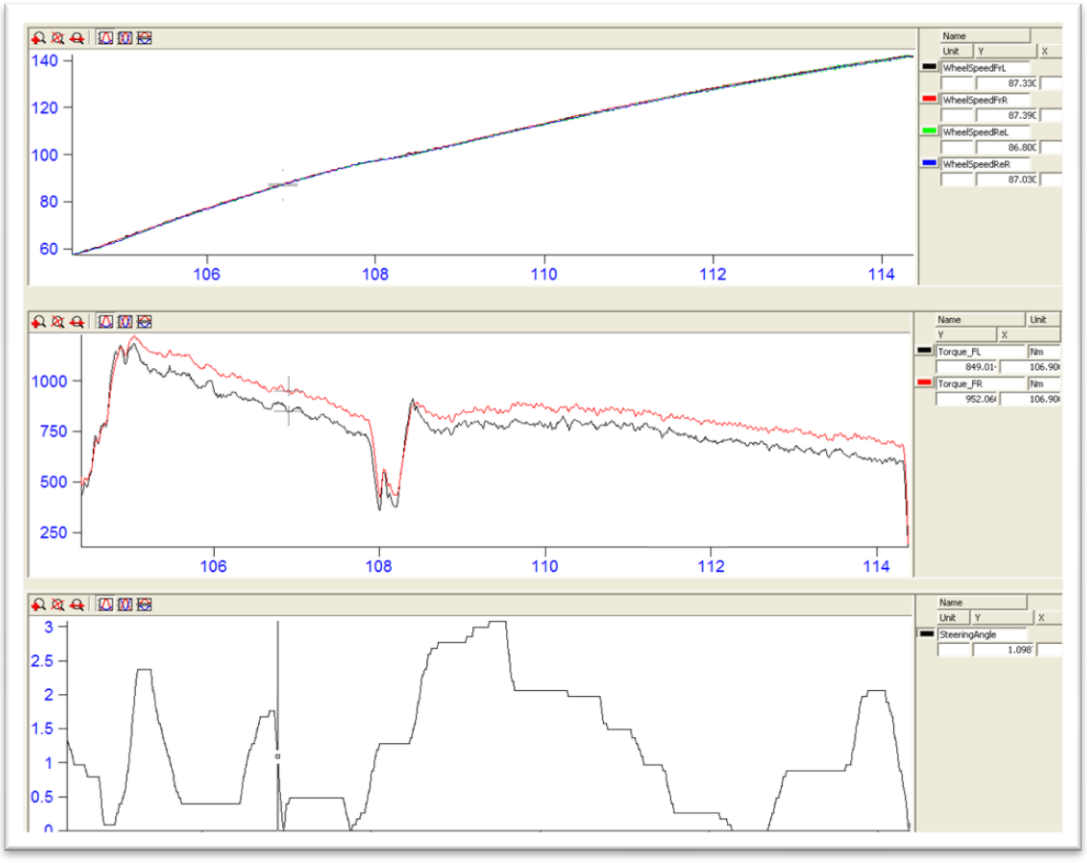

Figure E.3. Vehicle logged data driving scenario 3.

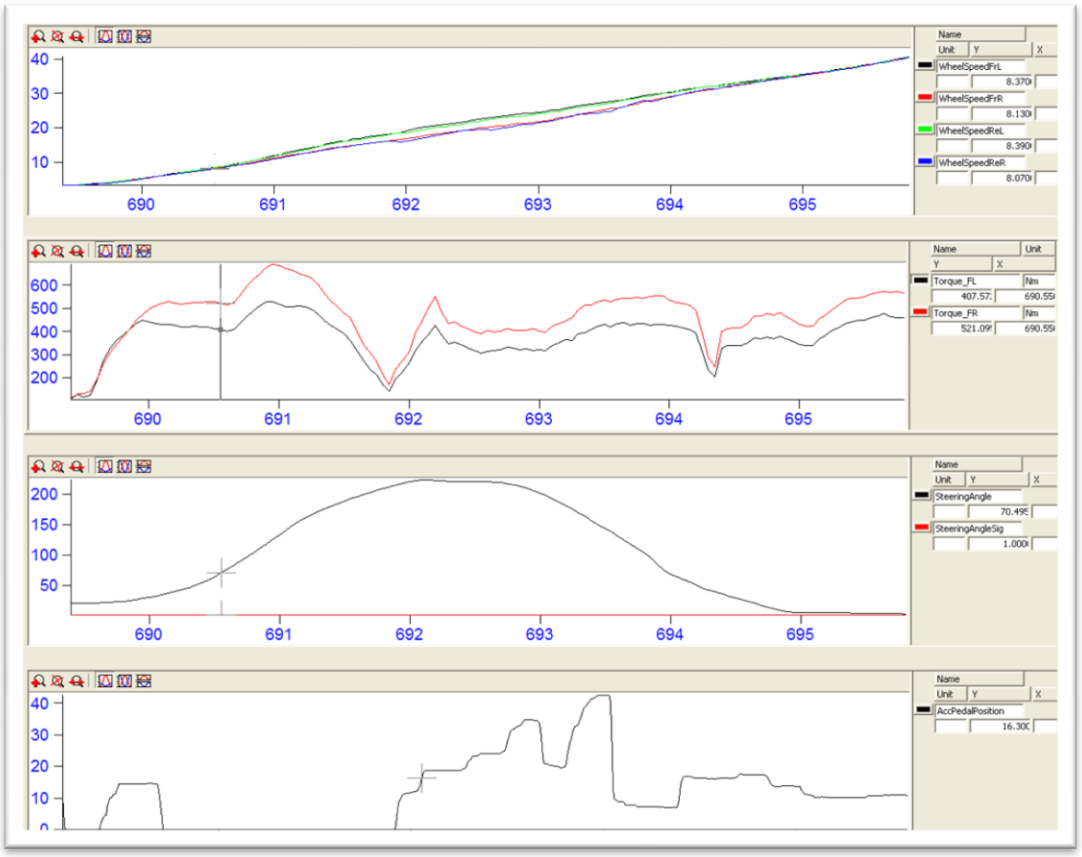

Figure E.4. Vehicle logged data driving scenario 5.

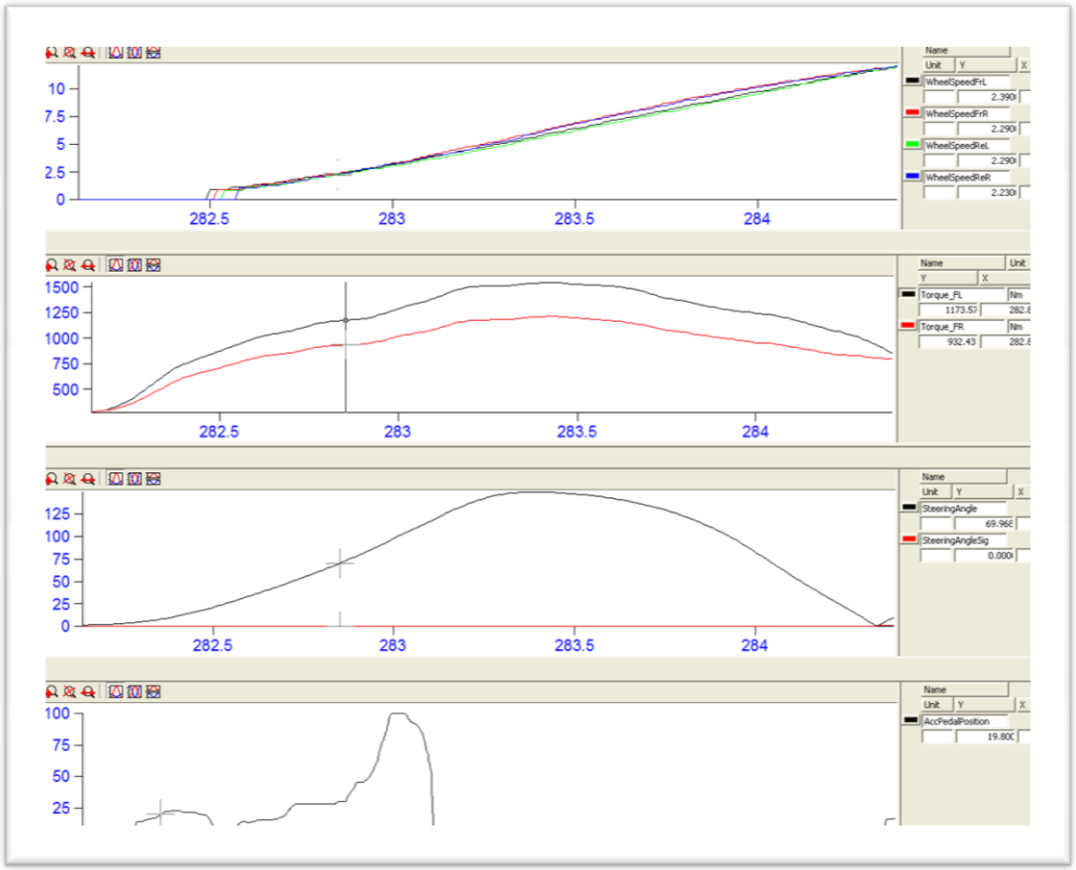

Figure E.5. Vehicle logged data driving scenario 6.

In this last case scenario shown in the Figure E.5, what is possible to check is that apart from having increased the difference between torques. The inner wheel should have the higher torque, but in the sixth driving scenario (as it has already been checked in the Loss Model, where the torque T_2 was higher for the wheel that had the opposite relative speed according to the carrier reference), the effect differs a little. The steering wheel has the signal of 0, which means that it is turning left, and angle around 70º. However, the speed of the inner wheel (left) is 2.39 rad/s which is higher than the outer wheel (right) of 2.29 rad/s. The reason why this has happened would be that the inner wheel has slipped from the ground due to, perhaps, a lower friction coefficient, and it is a transient period where after the relative power should change the sign, or basically as it has just started turning, the wheel speed sensor has not realized about the wheel speed difference, or that the differential has just overcome the breakaway ratio, time when it starts allowing the rotational speed to be different in both wheels (transient from locking to semi locking).

Finally, it should be point out that all the cornering driving scenarios have been taken where the rotational wheel speed differed from left to right in order to be sure that the friction is fully developed and the differential allows the wheel having different speed so that it is semi locked with sliding (dynamic) conditions. In the pictures of the three cornering driving scenarios can be corroborated (see also Chapter 7).

Appendix F. Vehicle Dynamics Simulation

Dymola plots

Drift effects of a semi locked differential

The following plot shows the initial conditions of the lateral displacement when the car is going straight ahead with using the original differential model of the VDL library (equal torque in both shafts).

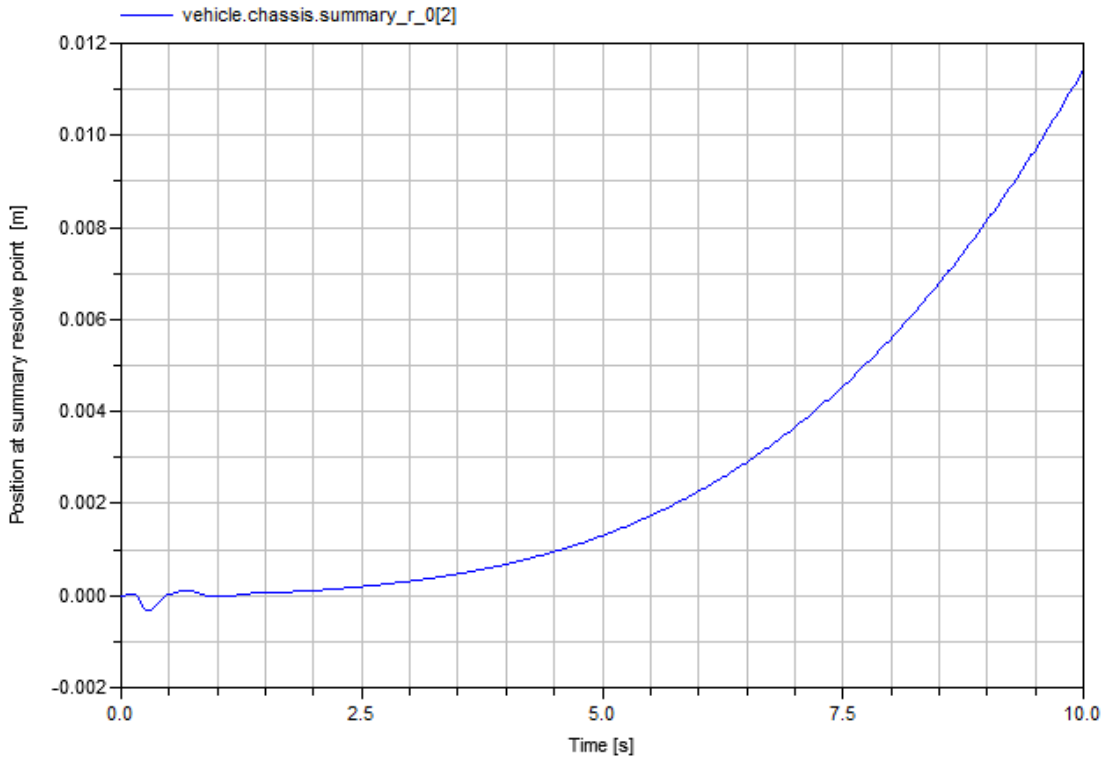

Figure F.1. Lateral displacement vs. Time

Below, the initial conditions can be seen regarding the longitudinal speed and acceleration. Starting from an initial speed of 5km/h, the car is accelerating (around 2 m/s^2) keeping the throttle to the 35% of its position.

Note that for the comparison between having a perfect open differential and a different distribution due to the losses, in the legend it has given the name of VDL model and Diff model respectively (blue and red curve always respectively).

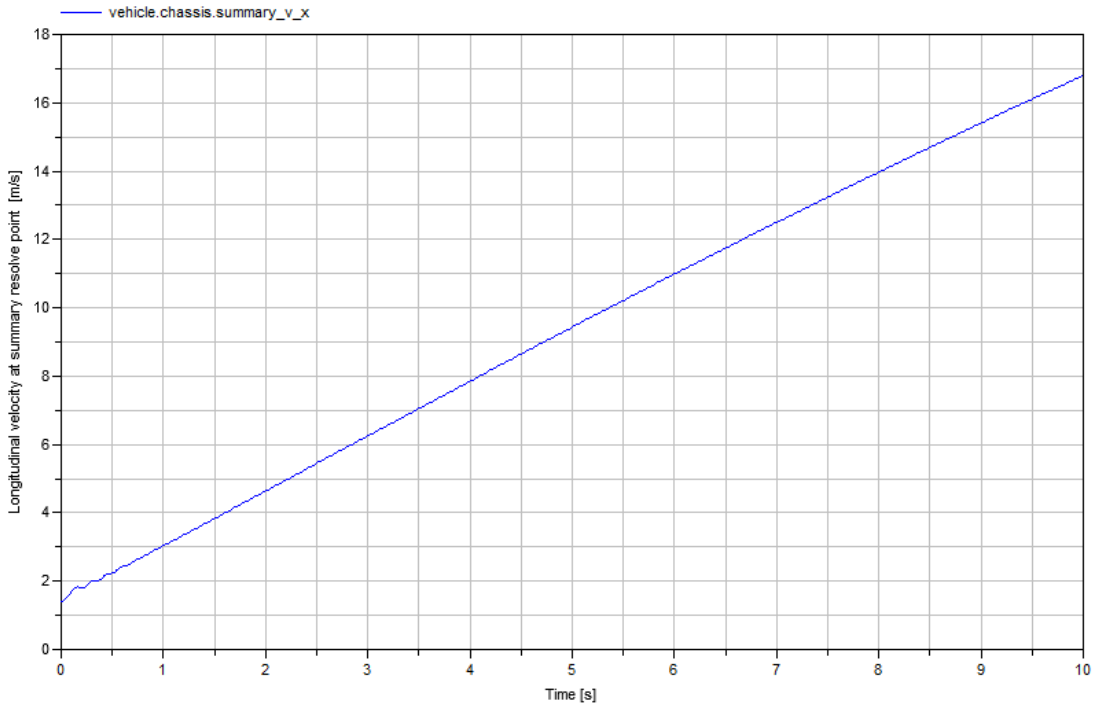

Figure F.2. Longitudinal speed vs. Time

Once the steering wheel is kept to 5º (positive towards the left), there is a difference between the path that the car follows when the torque ratio is unitary (red curve, VDL model) or when the torque split over the differential affects the distribution of torque between wheels (blue curve, Diff model).

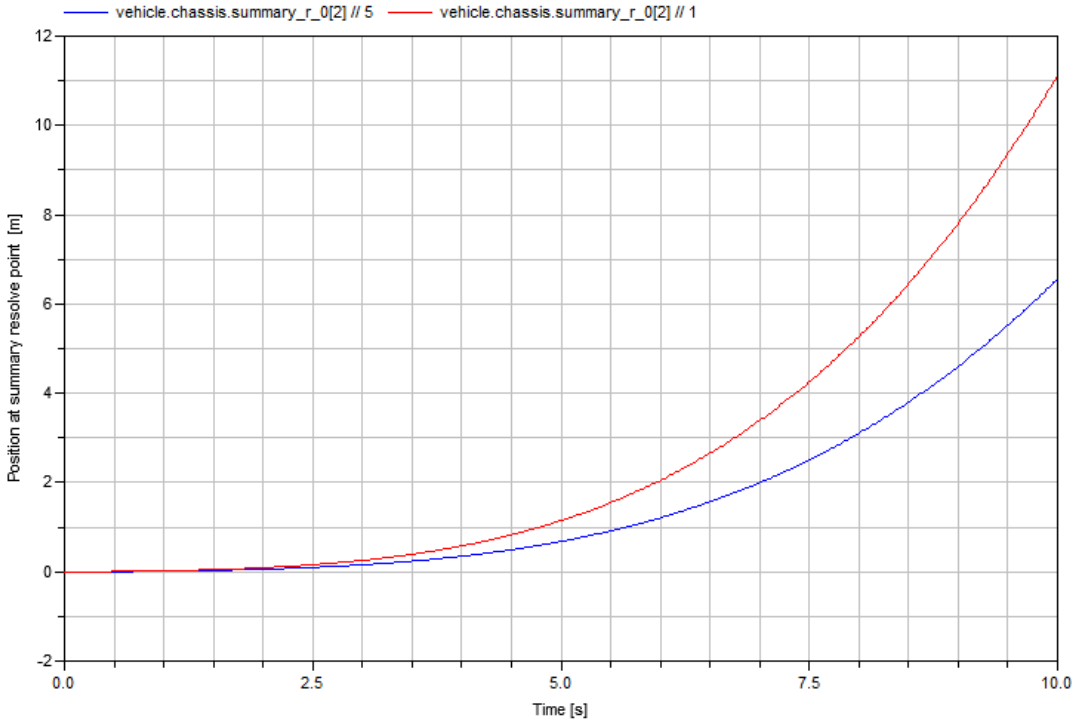

Figure F.3Comparison of Lateral displacement vs. Time

Below, there are all the plots comparing both models:

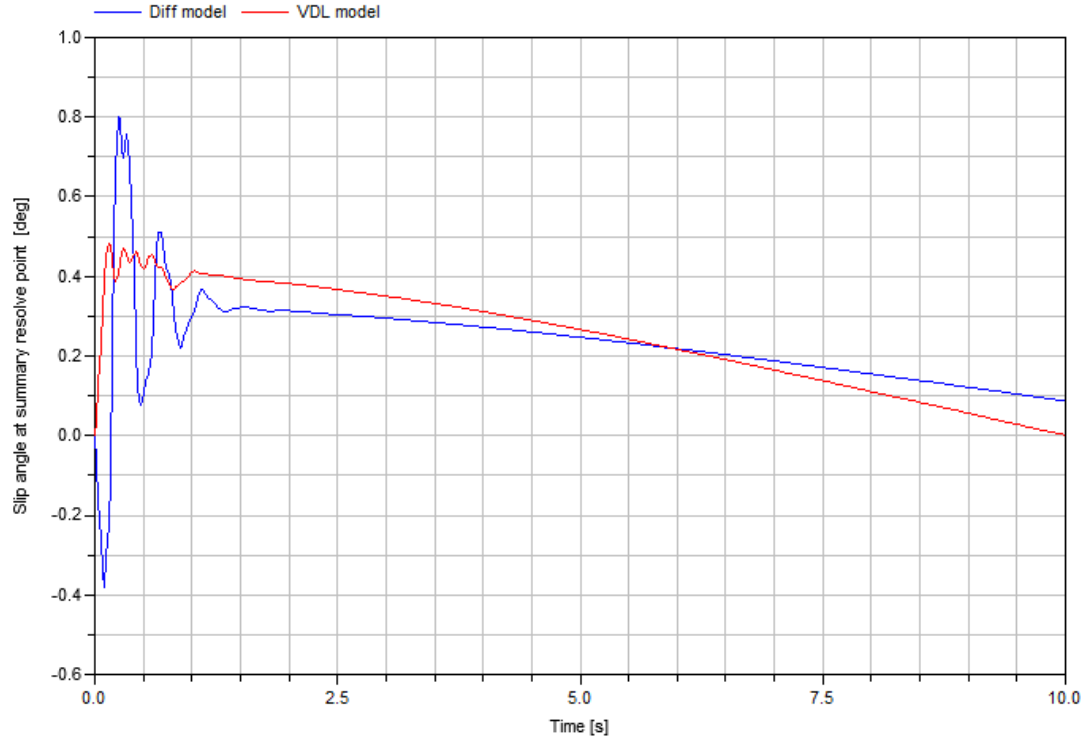

Figure F.4. Side slip angle (body) vs. Time.

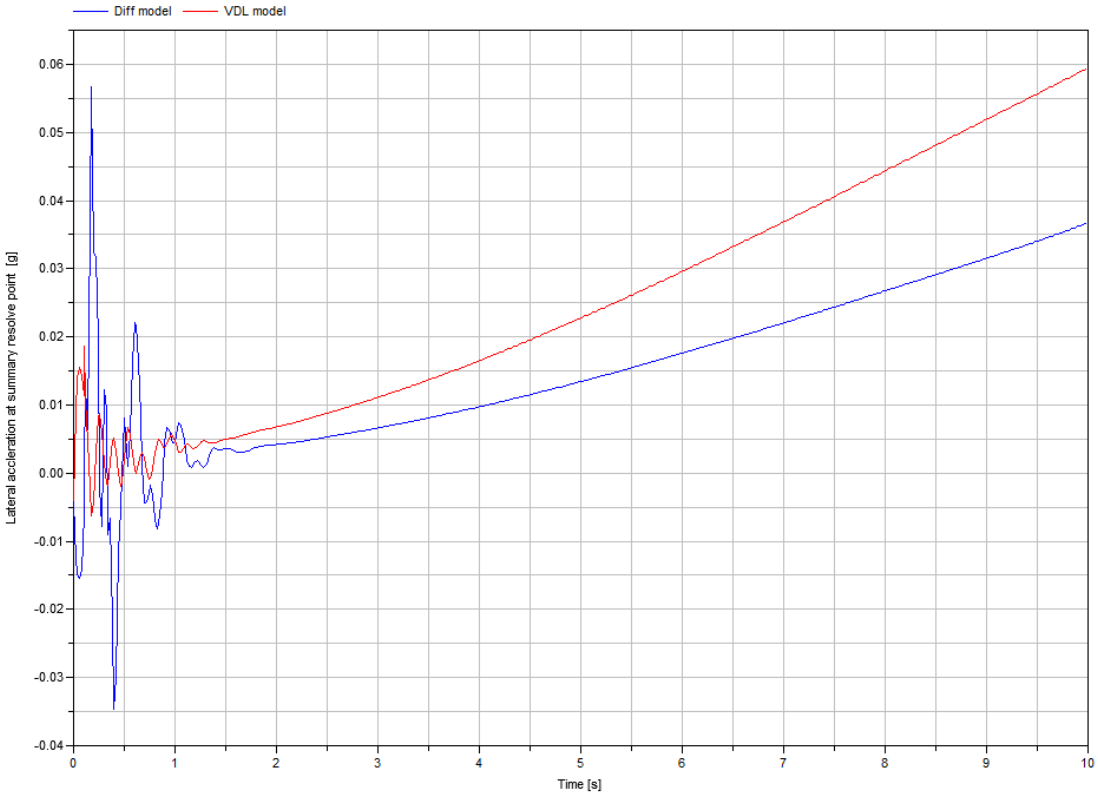

Figure F.5. Lateral acceleration vs. Time.

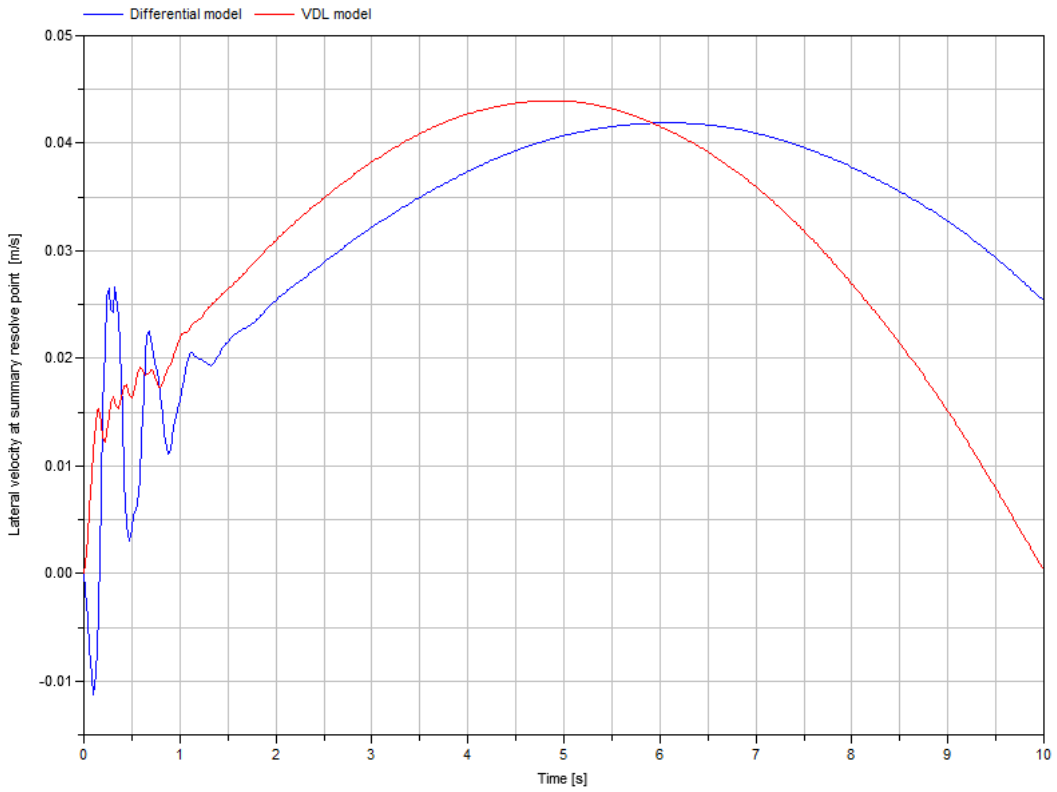

Figure F.6. Lateral speed vs. Time.

In the Figure below, it is seen the difference torque between wheels, and indeed, the VDL model delivers equal torque in each wheel, whereas the Diff model does not.

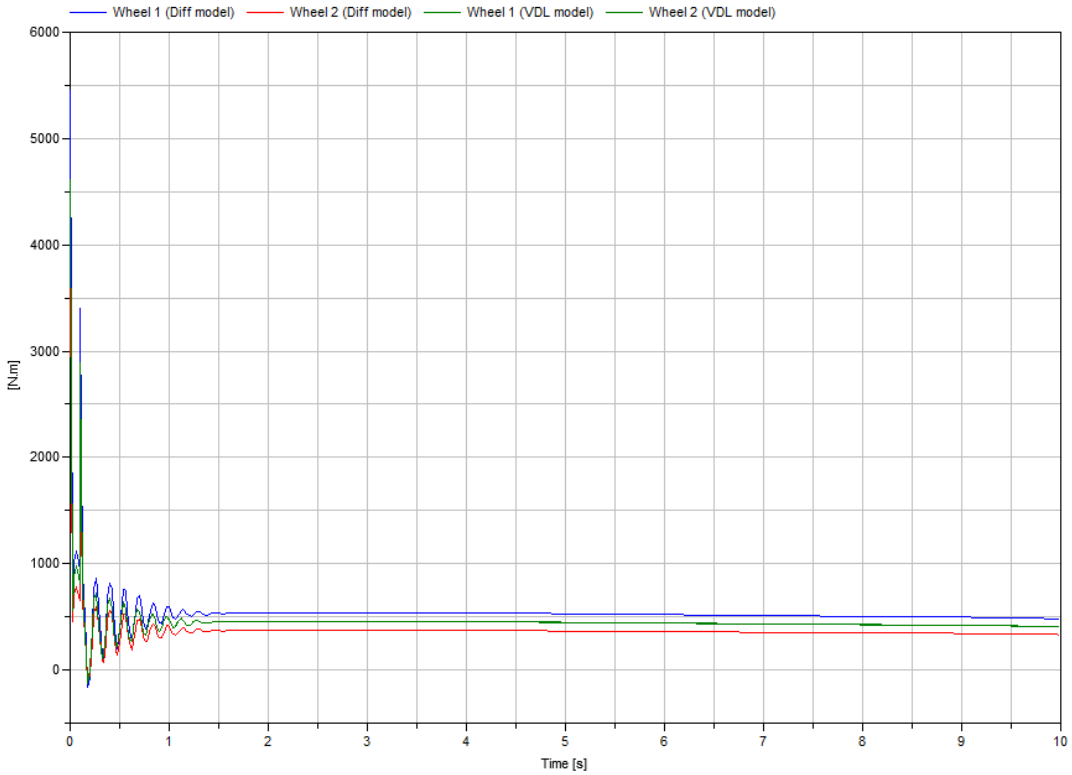

Figure F.7.Front wheel torque vs. Time.

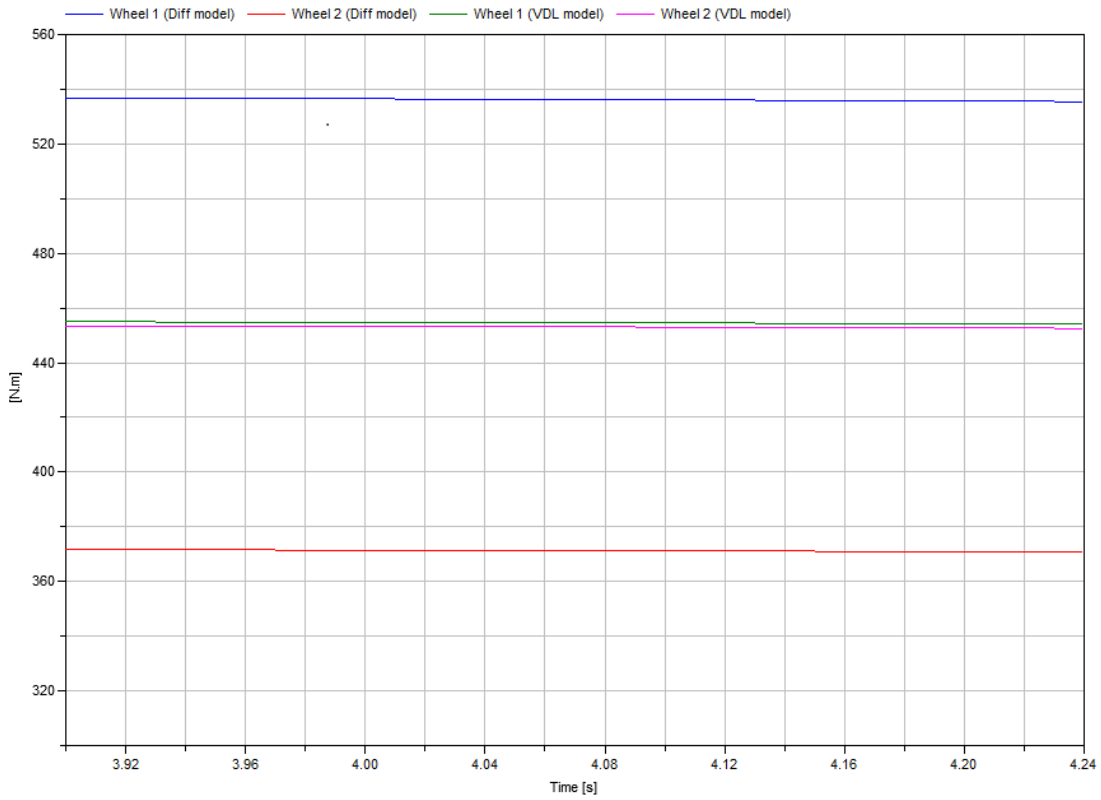

Figure F.8. Zoom in of the front wheel torque vs. Time.

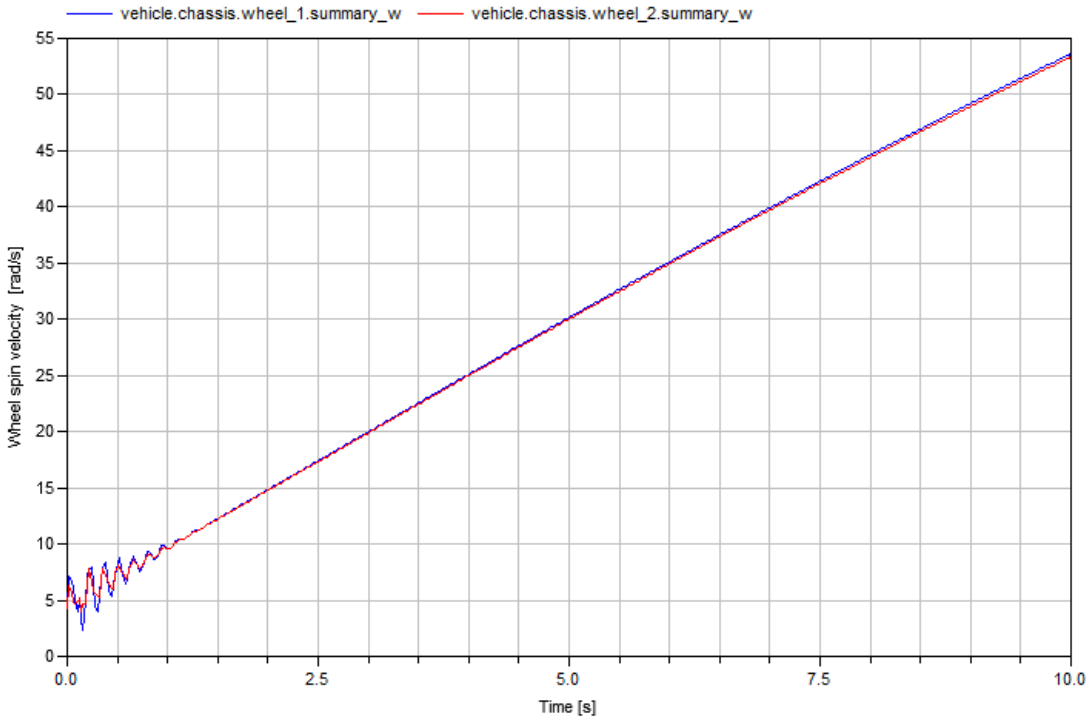

Figure F.9. Wheel speed vs. Time.

Sinusoidal input in steering wheel angle

This first plot describes which state (from the three possible described in Chapter 8) the differential has over all the cycle.

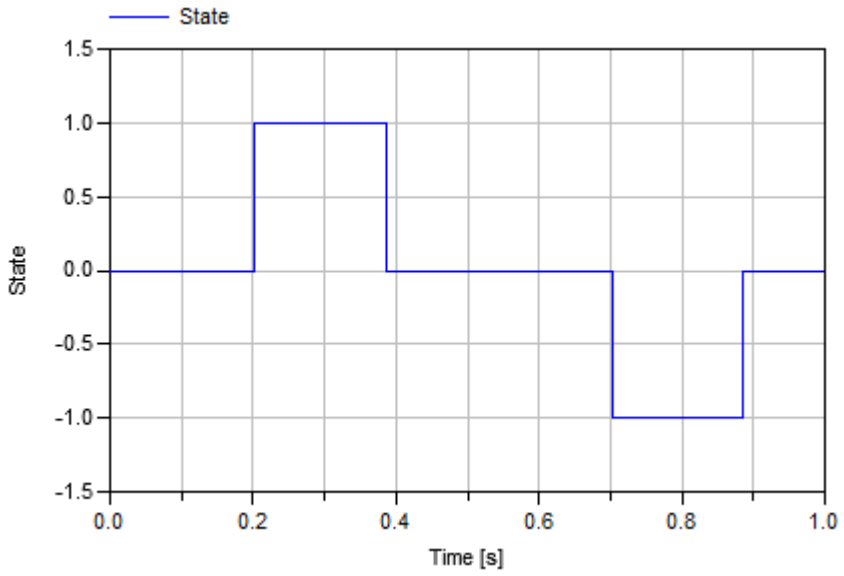

Figure F.10. State vs. Time.

The overall lateral displacement is shown in the figure below. It is not symmetric respect the y-axis because of the scale of the axes of the plot comparing steering wheel and global x and y position.

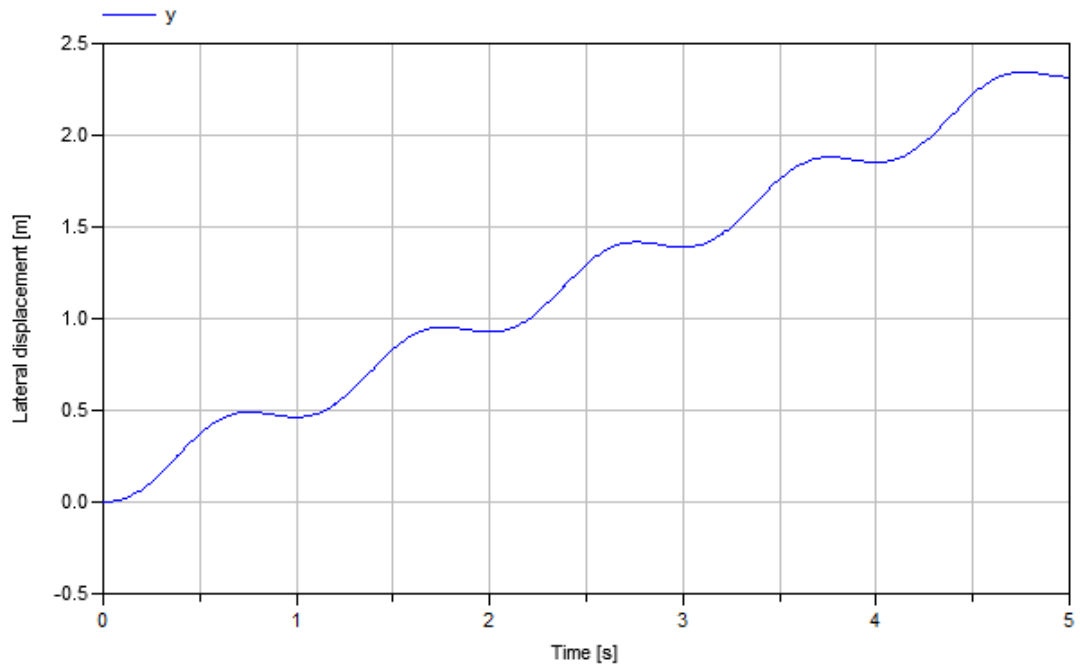

Figure F.11. Lateral displacement vs. Time.

As it has been seen already in the Figure 8.16, when the torque is higher than a certain value for this driving scenario and initial conditions, the system does not reach the breakaway torque ratio, remaining then locked during all the cycle .

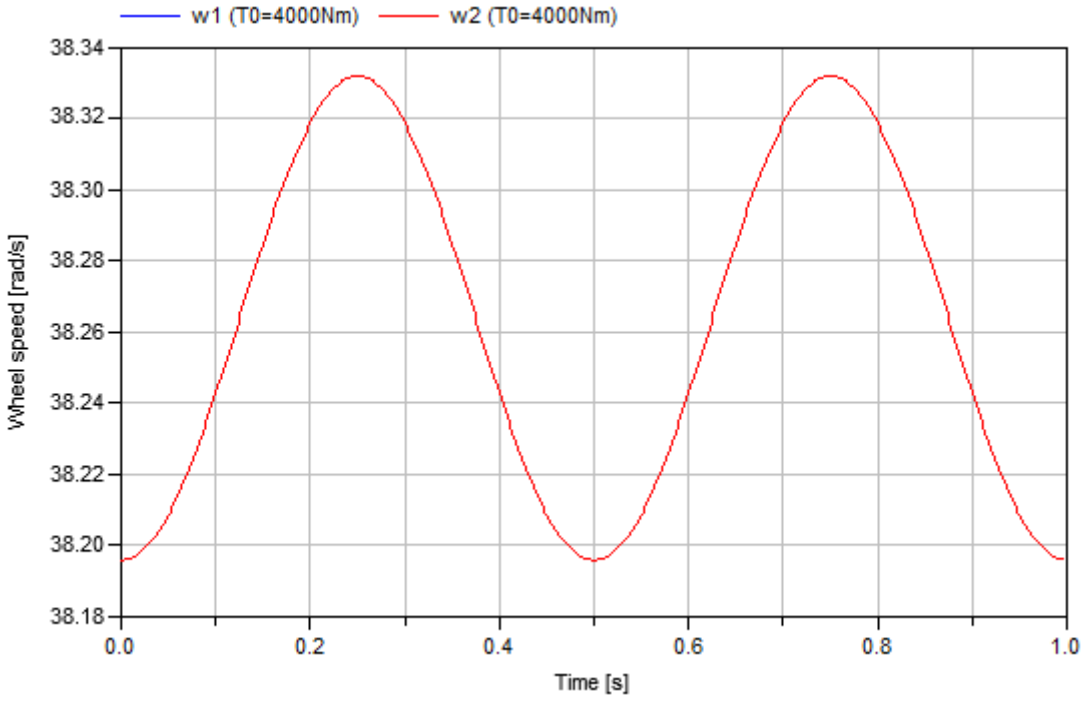

Figure F.12. Wheel speed for higher torque vs. Time.

Thus, if the comparison of doubling the torque lineally 650 Nm every time is done (in Chapter 8.2.5) the result of the traction force yields to be:

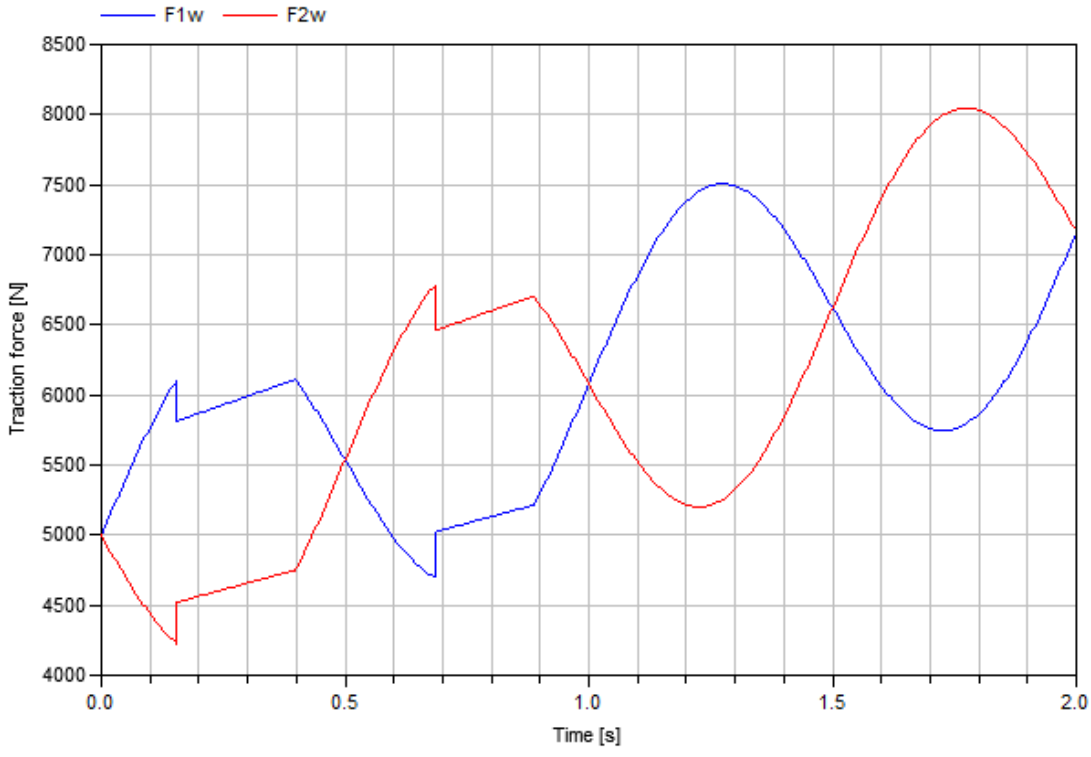

Figure F.13. Longitudinal force for traction torque increasing over time.

As it is has been said in the Chapter 8.2, the lateral forces using a combined slip model might be neglected due to the low contribution in the results.

If the bicycle model (*see* [36]) is used and the equations of the lateral forces are added, it is got:

$$m\left(\frac{dv_y}{dt} + v_x \cdot \omega_z\right) = F_{yf} + F_{yr} \quad \text{(F.1)}$$

$$J\frac{d\omega_z}{dt} = F_{yf} \cdot \frac{L}{2} - F_{yr} \cdot \frac{L}{2} \quad \text{(F.2)}$$

Assuming a typical car weight (m) of 1500Kg and inertia (J) of 3000 kg·m^2.

Note that it has also been assumed small wheel angles (δ) so that the longitudinal forces do not affect the calculations (sinδ≃0).

Then, the following plot shows the results of the lateral forces per axle during the cycle:

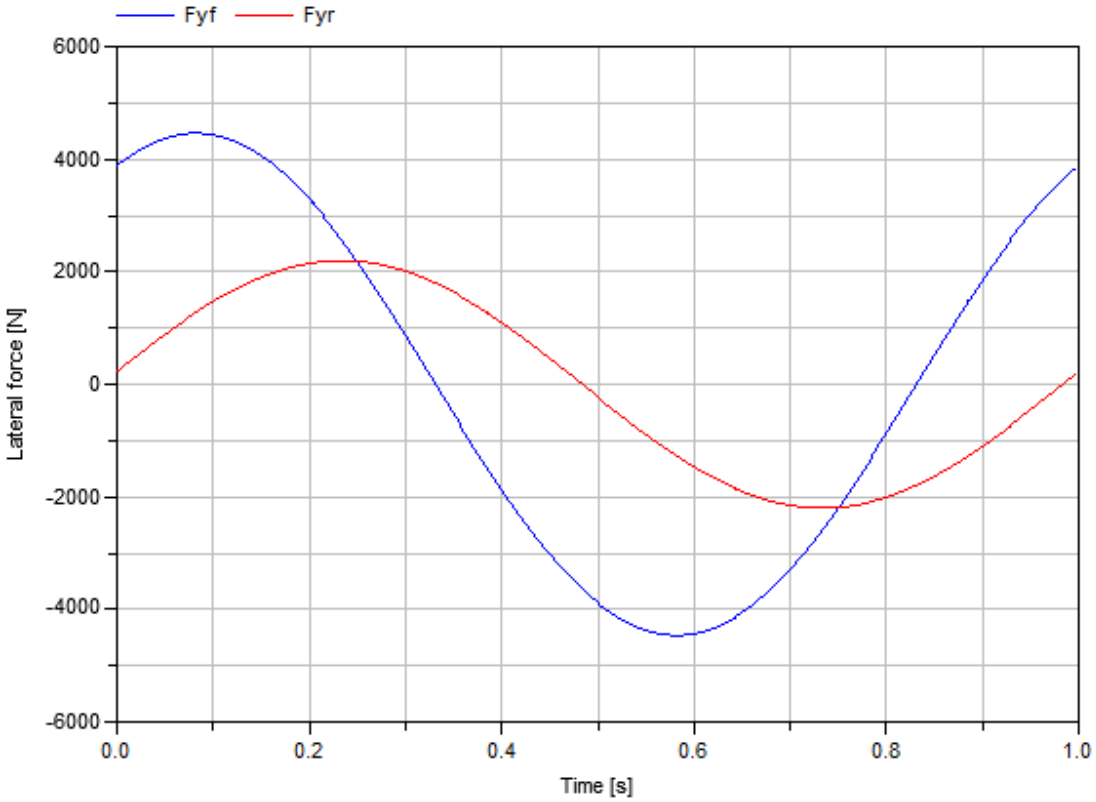

Figure F.14. Lateral force per axle vs. Time.

Thus, it is seen that the maximum lateral force is around 4000N in the front axle. If no weight transfer is taken into account, it yields to a lateral force per wheel around 2000N.

If it is compared to the total amount of longitudinal force that the wheel has in this moment, which is 6000N, it is got that the lateral force is around the 30% of the longitudinal. Perhaps the combined slip model could have been added because a 30% starts to be a boundary value to either include the combined or not. Nevertheless, including a combined slip model gives a more correct model but less understandable regarding the torque steer that it was aimed for. Before including the combined model

with lateral forces in tires, lateral slip angles and so on, it should be study the whole vehicle in real test so as to decide if it is worth including neglected effects so far, or it already explains the behaviour.

Dymola code for Sinusoidal input in steering wheel angle

Main vehicle model

```
model OscillatingSteAn
constant Real pi=4*atan(1);
//Driver
Real SWA;
Real SWA_deg;
parameter Real SWA_ampl_deg=80;
parameter Real SWA_freq_Hz=1;
//EngineAndGearbox
Real T0;
parameter Real T0_param=3600;
parameter Real T0_rate=0; //Nm/s
//Diff & Wheels
parameter Real lossfactor0=1.444;
parameter Real lossfactor1=1.286;
parameter Real Rw=0.3;
Real F1w;
Real F2w;
Real sx1;
Real sx2;
Real w1;
Real w2;
  DiffToWheels_Differentiating DLR(lossfact=lossfactor1, Rw=Rw)
    annotation (Placement(transformation(extent={{-80,78},{18,90}})));
  DiffToWheels_Locking DL(Rw=Rw)
    annotation (Placement(transformation(extent={{-80,48},{18,60}})));
  DiffToWheels_Differentiating DRL(lossfact=1/lossfactor1, Rw=Rw)
    annotation (Placement(transformation(extent={{-80,20},{16,32}})));
//Vehicle
Real d;
Real v1v;
Real v2v;
Real v1w;
Real v2w;
Real vx;
Real wz;
Real w1_NoSlip;
Real w2_NoSlip;
parameter Real tw=1.6;
parameter Real vx_param=10;
parameter Real L=3;
parameter Real m=1500;
parameter Real J=3000;
parameter Real S_ratio=16;
output Real SWT;
Real vy; //in middle between axles
Real ay;
Real Fyf;
Real Fyr;
Real x;
Real y;
Real pz;
//Variables for switching discrete state
output Real T_ratio;
output Real P_rel;
Real State(start=0);
equation
//Driver
SWA=SWA_ampl_deg*(pi/180)*cos(2*pi*SWA_freq_Hz*time+3*pi/2);
SWA_deg=SWA*180/pi;
//EngineAndGearbox
T0=T0_param+T0_rate*time;
DLR.T0=T0;
```

```
DL.T0 =T0;
DRL.T0=T0;
//Diff
DLR.v1w=v1w;
DL.v1w =v1w;
DRL.v1w=v1w;
//
DLR.v2w=v2w;
DL.v2w =v2w;
DRL.v2w=v2w;
//Vehicle
vx=vx_param;
d=SWA/S_ratio;
wz=vx*tan(d)/L;
v1v=vx-wz*tw/2;
v2v=vx+wz*tw/2;
v1w=v1v/cos(d);
v2w=v2v/cos(d);
vy=wz*L/2;
ay=vx*wz;
w1_NoSlip=v1w/Rw;
w2_NoSlip=v2w/Rw;
der(x)=vx*cos(pz)-vy*sin(pz);
der(y)=vy*cos(pz)+vx*sin(pz);
der(pz)=wz;
m*(der(vy)+vx*wz)=Fyf+Fyr;
J*der(wz)= Fyf*L/2-Fyr*L/2;
//Variables for switching discrete state
SWT   =if abs(State)<0.5 then (DL.F1w-DL.F2w)*Rw       else if abs(State-1)<0.5 then (DLR.F1w-
DLR.F2w)*Rw       else (DRL.F1w-DRL.F2w)*Rw;
F1w    =if abs(State)<0.5 then DL.F1w       else if abs(State-1)<0.5 then DLR.F1w       else DRL.F1w;
F2w    =if abs(State)<0.5 then DL.F2w       else if abs(State-1)<0.5 then DLR.F2w       else DRL.F2w;
sx1    =if abs(State)<0.5 then DL.sx1       else if abs(State-1)<0.5 then DLR.sx1       else DRL.sx1;
sx2    =if abs(State)<0.5 then DL.sx2       else if abs(State-1)<0.5 then DLR.sx2       else DRL.sx2;
w1    =if abs(State)<0.5 then DL.w1       else if abs(State-1)<0.5 then DLR.w1       else DRL.w1;
w2    =if abs(State)<0.5 then DL.w2       else if abs(State-1)<0.5 then DLR.w2       else DRL.w2;
T_ratio=if abs(State)<0.5 then DL.T1/DL.T2       else if abs(State-
1)<0.5 then DLR.T1/DLR.T2       else DRL.T1/DRL.T2;
P_rel  =if abs(State)<0.5 then DL.T0*(DL.w1-DL.w2) else if abs(State-1)<0.5 then DLR.T0*(DLR.w1-
DLR.w2) else DRL.T0*(DRL.w1-DRL.w2);
der(State)=0;
 when abs(State)<0.5 and T_ratio>lossfactor0 then
   reinit(State,+1);
 end when;
 when abs(State)<0.5 and T_ratio<1/lossfactor0 then
   reinit(State,-1);
 end when;
 when abs(State-(+1))<0.5 and P_rel>0 then
   reinit(State,0);
 end when;
  when abs(State-(-1))<0.5 and P_rel<0 then
   reinit(State,0);
 end when;
  annotation (uses(Modelica(version="3.2")), Diagram(graphics));
end OscillatingSteAn;
```

Differential submodel (open)

```
model DiffToWheels_Differentiating
constant Real pi=4*atan(1);
//Diff
Real w0;
Real w1;
Real w2;
input Real T0;
Real T1;
Real T2;
parameter Real lossfact=1.286;
//Wheels
```

```
parameter Real Rw=0.3;
parameter Real Cw=1*500*9.80665/0.1;
//Wheel1
Real F1w;
Real sx1;
input Real v1w;
//Wheel2
Real sx2;
input Real v2w;
Real F2w;
equation
//Diff_Differentiating
w0=(w1+w2)/2;
T0=T1+T2;
T1=lossfact*T2;
//Wheel1
T1=F1w*Rw;
sx1=(Rw*w1-v1w)*2/(Rw*w1+v1w);
F1w=Cw*sx1;
//Wheel2
T2=F2w*Rw;
sx2=(Rw*w2-v2w)*2/(Rw*w2+v2w);
F2w=Cw*sx2;
  annotation (uses(Modelica(version="3.2")));
end DiffToWheels_Differentiating;
```

Differential submodel (locked)

```
model DiffToWheels_Locking
constant Real pi=4*atan(1);
//Diff
Real w0;
Real w1;
Real w2;
input Real T0;
Real T1;
Real T2;
//Wheels
parameter Real Rw=0.3;
parameter Real Cw=1*500*9.80665/0.1;
//Wheel1
Real F1w;
Real sx1;
input Real v1w;
//Wheel2
Real sx2;
input Real v2w;
Real F2w;
equation
//Diff in Locking
w0=(w1+w2)/2;
T0=T1+T2;
w1=w2;
//Wheel1
T1=F1w*Rw;
sx1=(Rw*w1-v1w)*2/(Rw*w1+v1w);
F1w=Cw*sx1;
//Wheel2
T2=F2w*Rw;
sx2=(Rw*w2-v2w)*2/(Rw*w2+v2w);
F2w=Cw*sx2;
  annotation (uses(Modelica(version="3.2")));
end DiffToWheels_Locking;
```